AD_____

Award Number: DAMD17-98-1-8260

TITLE: A Novel Apoptotic Protease Activated in Human Breast
Cancer Cells after Poisoning Topoisomerase I

PRINCIPAL INVESTIGATOR: David A. Boothman, Ph.D.

CONTRACTING ORGANIZATION: Case Western Reserve University
                            Cleveland, Ohio   44106-7006

REPORT DATE: October 2001

TYPE OF REPORT: Final

PREPARED FOR: U.S. Army Medical Research and Materiel Command
                Fort Detrick, Maryland   21702-5012

DISTRIBUTION STATEMENT: Approved for Public Release;
                        Distribution Unlimited

The views, opinions and/or findings contained in this report are
those of the author(s) and should not be construed as an official
Department of the Army position, policy or decision unless so
designated by other documentation.

20020131 154

REPORT DOCUMENTATION PAGE		Form Approved OMB No. 074-0188

Public reporting burden for this collection of information is estimated to average 1 hour per response, including the time for reviewing instructions, searching existing data sources, gathering and maintaining the data needed, and completing and reviewing this collection of information. Send comments regarding this burden estimate or any other aspect of this collection of information, including suggestions for reducing this burden to Washington Headquarters Services, Directorate for Information Operations and Reports, 1215 Jefferson Davis Highway, Suite 1204, Arlington, VA 22202-4302, and to the Office of Management and Budget, Paperwork Reduction Project (0704-0188), Washington, DC 20503

1. AGENCY USE ONLY (Leave blank)	2. REPORT DATE October 2001	3. REPORT TYPE AND DATES COVERED Final (15 Sep 98 – 14 Sep 01)	
4. TITLE AND SUBTITLE A Novel Apoptotic Protease Activated in Human Breast Cancer Cells after Poisoning Topoisomerase I			**5. FUNDING NUMBERS** DAMD17-98-1-8260
6. AUTHOR(S) David A. Boothman, Ph.D.			
7. PERFORMING ORGANIZATION NAME(S) AND ADDRESS(ES) Case Western Reserve University Cleveland, Ohio 44106-7006 E-Mail: dab30@po.cwru.edu			**8. PERFORMING ORGANIZATION REPORT NUMBER**
9. SPONSORING / MONITORING AGENCY NAME(S) AND ADDRESS(ES) U.S. Army Medical Research and Materiel Command Fort Detrick, Maryland 21702-5012			**10. SPONSORING / MONITORING AGENCY REPORT NUMBER**

11. SUPPLEMENTARY NOTES
Report contains color

12a. DISTRIBUTION / AVAILABILITY STATEMENT Approved for Public Release; Distribution Unlimited	**12b. DISTRIBUTION CODE**

13. ABSTRACT (Maximum 200 Words)

The goal of this grant was to clone the unknown protease activated by the active anti-breast cancer agent, ß-lapachone (ß-lap). The research team showed for the first time that ß-lap required NQ01, a two-electron reductase elevated in many human breast cancers, for activation. The team then identified the unknown apoptotic protease activated in human breast cancer cells by ß-lap, defining biological endpoints specific for a non-caspase-mediated apoptotic event. The unknown protease: **(a)** is a non-caspase cysteine protease; **(b)** cleaves p53, lamin B, and PARP (atypically) in an NQ01-dependent manner at a time co-incident with calpain activation (appearance of an 18 kDa active form and its movement into the nucleus by confocal microscopy); **(c)** is calcium-dependent (e.g., the proteolytic cleavage of PARP or p53 was blocked by co-administration of EGTA or EDTA), and the drug causes massive NQ01-dependent calcium influx within 3 mins posttreatment with 5-8 µM ß-lap; and **(d)** inhibited by calpastatin, a specific endogenous inhibitor of calpain. We have, therefore, concluded that the unknown protease activated in NQO1-expressing human breast cancer cells is calpain.

14. SUBJECT TERMS Breast Cancer, Apoptosis, ATP loss, B-Lapachone, Calcium, Calpain, NQO1/XIP8, PARP Cleavage			**15. NUMBER OF PAGES** 77
			16. PRICE CODE
17. SECURITY CLASSIFICATION OF REPORT Unclassified	**18. SECURITY CLASSIFICATION OF THIS PAGE** Unclassified	**19. SECURITY CLASSIFICATION OF ABSTRACT** Unclassified	**20. LIMITATION OF ABSTRACT** Unlimited

NSN 7540-01-280-5500

Standard Form 298 (Rev. 2-89)
Prescribed by ANSI Std. Z39-18
298-102

FOREWORD

Opinions, interpretations, conclusions and recommendations are those of the author and are not necessarily endorsed by the U.S. Army.

_X__ Where copyrighted material is quoted, permission has been obtained to use such material.

_X__ Where material from documents designated for limited distribution is quoted, permission has been obtained to use the material.

_X__ Citations of commercial organizations and trade names in this report do not constitute an official Department of Army endorsement or approval of the products or services of these organizations.

_NA__ In conducting research using animals, the investigator(s) adhered to the "Guide for the Care and Use of Laboratory Animals," prepared by the Committee on Care and use of Laboratory Animals of the Institute of Laboratory Resources, national Research Council (NIH Publication No. 86-23, Revised 1985).

_X__ For the protection of human subjects, the investigator(s) adhered to policies of applicable Federal Law 45 CFR 46.

_NA__ In conducting research utilizing recombinant DNA technology, the investigator(s) adhered to current guidelines promulgated by the National Institutes of Health.

_NA__ In the conduct of research utilizing recombinant DNA, the investigator(s) adhered to the NIH Guidelines for Research Involving Recombinant DNA Molecules.

_NA__ In the conduct of research involving hazardous organisms, the investigator(s) adhered to the CDC-NIH Guide for Biosafety in Microbiological and Biomedical Laboratories.

_____
PI - Signature   Date

Boothman, D.A.

TABLE OF CONTENTS: *Type on a separate page. When preparing the Table of Contents, please note the correct spelling of Foreword.*

– manuscripts, abstracts, presentations.
– patents and licenses applied for and/or issued.
– degrees obtained that are supported by this award.
– development of cell lines, tissue or serum repositories.
– informatics such as databases and animal models, etc.
- funding applied for based on work supported by this award.
– employment or research opportunities applied for and/or
    received on experiences/training supported by this award.

          -PUBLICATIONS AND ABSTRACTS

Boothman, D.A.

INTRODUCTION: *Narrative that briefly (one paragraph) describes the subject, purpose, and scope of the research.*

Understanding and exploiting cell death processes in various human breast cancer cells following clinically useful anti-tumor agents is a major focus in breast cancer research. The promise is that a better understanding of apoptotic and anti-apoptotic processes will allow improved anti-breast cancer efficacy of existing chemotherapeutic agents, as well as the development of additional efficacious drugs that elicit programmed cell suicide during treatment without inflammation. Apoptotic processes occurring in human breast cancer cells, particularly noncaspase-mediated cell death, are poorly understood. We discovered that a previously used drug for anti-trypanosomal therapies, ß-lapachone (ß-lap), is an active agent for the initiation and execution of apoptosis in a variety of human breast cancer cells in a p53-independent fashion. In the course of defining the compound's ability to cause cell death, we accomplished the following objectives or defined the following mechanism of action of the drug: (a) the primary intracellular target for ß-lap was NQO1, a two-electron reductase that was previously shown to be ionizing radiation (IR)-inducible; NQO1-containing cells were sensitive, NQO1-deficient cells were resistant; (b) interaction of the drug with NQO1 caused a futile cycling of the compound in which calcium homeostasis was altered within 3 min and intracellular ATP levels decreased to <1% within 30 min; (c) no evidence of caspase activation was detected in NQO1-containing breast cancer cells during ß-lap-mediated apoptosis; (d) an intracellular activation of a non-caspase cysteine protease was activated within 4-8 h, concomitant with the appearance of DNA fragmentation, measured by TUNEL assays; (e) protease activation was concurrent with atypical cleavage of PARP, and apoptotic-related cleavage of lamin B, p53 and degradation of pRb; (f) administration of dicoumarol (an NQO1 inhibitor) or calcium chelators (EGTA or EDTA) was able to prevent ß-lap-mediated apoptosis, and in the case of dicoumarol, cell lethality; (g) calpain activation was noted concomitantly with the intracellular responses in (a) through (f); and (h) an endogenous calpain inhibitor, calpastatin, protected cells from ß-lap-induced apoptosis and suppressed the responses noted in (a) through (f).

The objective of the grant was to clone the unknown cysteine protease activated in NQO1-expressing human breast cancer cells using a variety of strategies, including (1) substrate (PARP, p53 or lamin B) affinity chromatography; (2) previously described calpain isolation techniques; and (3) identification of specific ß-lap-mediated PARP cleavage sites, followed by use of these sites for the isolation of this ß-lap-activated, noncaspase cysteine protease. The studies to date have demonstrated that calpain is activated in an NQO1-dependent fashion and appears to be responsible for ß-lap-induced apoptosis. Progress in the construction of his-tagged PARP has now been achieved and biochemical as well as affinity chromatography experiments are now feasible to isolate the noncaspase cysteine protease activated by ß-lap. We know that calpain is involved, however, the inability of calpain inhibitors to suppress ß-lap-induced cell death leads us to the new hypothesis that calpain is involved, but one enzyme in an entire cascade of enzymes that are activated in this novel noncaspase-mediated cell death process.

4

Boothman, D.A.

BODY OF GRANT UPDATE: *This section shall describe the research accomplishment associated with each Task outlined in the approved Statement of Work. Data presentation shall be comprehensive in providing a complete record of the research findings for the period of the annual/final report. However, appended publications and/or presentations MAY be substituted for a detailed description but MUST be referenced in the BODY of the report. If applicable, for each Task outlined in the Statement of Work, reference appended publications and/or presentations for details of result findings and tables and/or figures. The report shall include negative as well as positive findings, and also shall include any problems in accomplishing any of the tasks. Statistical tests of significance shall be applied to all data whenever possible. Figures and graphs referenced in the text shall be appended. The discussion shall include the relevance to the original hypothesis. Recommended changes or future work to better address the research topic may also be included, although changes to the original statement of work must be approved by the Grants Officer.*

F: **Previous** *Statement of Work and Accomplishments Made.*

<u>Grant Objective</u>: **To test the hypothesis that expression of a novel apoptotic protease in human breast cancer cells directly correlates with the efficacy of β-lap. The objectives of this grant are being accomplished as follows:**

Specific Aim #1: Clone the unknown apoptotic protease, which is activated by ß-lap and whose activity correlates with toxicity after acute drug exposures *(Years 0-2)*.

<u>**ß-Lap activates a noncaspase cysteine protease during apoptotic cell death.**</u> Previous research defined the DNA unwinding enzyme, Topoisomerase I (Topo I), as a potentially important intracellular target for the apoptosis-active drug, ß-lap. However, the efficacy of inhibition or activation of Topo I by ß-lap *in vivo* was **never** established. **In fact, we have now established that the mechanism of action of ß-lap is through the two-electron reductase, NAD(P)H:Quinone oxidoreductase 1 (NQO1) enzyme.**

In order to determine the key enzymatic target for ß-lap, we first established a number of intracellular proteolytic reactions that occur in a temporal sense during ß-lap-mediated apoptosis in MCF-7:WS8 breast cancer cells. Since activation of pre-existing zymogens is common-place during apoptosis and specific apoptotic substrates are known [e.g., poly(ADP-ribosyl) polymerase (PARP), lamin B, the retinoblastoma protein (pRb)], we examined proteolytic cleavage reactions occurring *in vivo* in four human breast cancer cell lines at various times after ß-lap (4-8 µM) treatment (Pink et. al., Exp. Cell Research, 2000). Typical cleavage of pRb and lamin B (Fig. 1) were observed at 8 h posttreatment with 4-8 µM ß-lap (Pink et. al., Exp. Cell Research, 2000). In contrast, an atypical cleavage of PARP (appearance of a ~60 kDa PARP polypeptide) was observed in ß-lap-treated MCF-7 cells (Fig. 2, Pink et. al., Exp. Cell Research, 2000), co-incident with lamin B and pRb cleavage (Fig. 1). Furthermore, cleavage of p53 in T47D human breast cancer cells was also found. The cleavage events described above occurred in ß-lap-treated MCF-7 or T47D cells regardless of cell cycle or p53 status, strongly suggesting that DNA Topoisomerase II-alpha (which is cell cycle regulated, present in G_2/M and S-phases and absent in G_0/G_1 cells) was not a determinant in ß-lap-mediated toxicity. Also, we noted that MDA-MB-468 and MDA-MB-231 cells were fairly resistant to ß-lap treatment and these cells coincidentally lacked expression of the NQO1 enzyme.

5

We next examined the effects of various specific and nonspecific enzyme inhibitors on ß-lap-mediated toxicity using the specific protein cleavage events *in vivo* described above. We discovered that iodoacetamide (I) and N-ethylmaleimide (N), global inhibitors of cysteine proteases, prevented PARP cleavage in ß-lap-treated MCF-7:WS8 cells (see Fig. 7, Pink et. al., Exp. Cell Research, 2000). In contrast, global inhibitors of caspases (i.e., zVAD-fmk, zAAD-fmk, and zFA-fmk) did not block atypical ß-lap-mediated PARP cleavage in MCF-7:WS8 cells. In addition, inhibitors of granzyme B, cathepsins D and L, trypsin and chymotrypsin-like proteases did not prevent ß-lap-mediated atypical PARP cleavage. Furthermore, calpeptin, calpain inhibitor III, and leupeptin (Figs. 2 and 3) also did not block ß-lap-mediated apoptosis and concomitant proteolyses *in vivo*. We concluded from these data that ß-lap treatment of certain sensitive human breast cancer cells caused the activation of a noncaspase cysteine protease during apoptosis; cells were demonstrated to be apoptotic by DNA fragmentation TUNEL assays (Pink et. al., Exp. Cell Research, 2000).

NQ01 is the major intracellular target for ß-lap. We extended our studies using inhibitors to more specific enzymes. The structural similarities between ß-lap and menadione and 1,2-naphthoquinones suggested that either one-electron reduction enzymes (p450 or b5R) or two-electron reductases (e.g., NQ01) may be involved in the detoxification, **or toxification,** of ß-lap. Administration of dicoumarol, a fairly specific inhibitor of NQ01, prevented ß-lap-mediated apoptosis, ß-lap-mediated proteolysis (e.g., atypical PARP cleavage), and ß-lap-induced cell death (see Figs. 1,2 and 4, Pink et. al., J. Biol. Chem., 2000). Furthermore, NQ01 levels appeared to correlate well with overall sensitivity to ß-lap: MCF-7:WS8>T47D>>>MDA-MB-468 cells. MCF-7 cells contained the greatest levels of NQ01, with T47D cells containing significantly lower levels and NQ01 level absent in MDA-MB-468 cells (see Fig. 3, Pink et. al., J. Biol. Chem., 2000). Furthermore, we noticed that MDA-MB-468 cells were fairly resistant to ß-lap and co-administration of dicoumarol with ß-lap did not affect the minimal toxicity caused by this drug in these cells. Similar results were, in fact, found in various human prostate cancer cells, where LNCaP (NQ01-deficient) were resistant to ß-lap and DU-145 and PC-3 (NQ01 over-expressors) were much more sensitive, and dicoumarol prevented toxicity in DU-145 and PC-3 cells, but not in LNCaP cells (Planchon et. al., Exp. Cell Res., 2001).

To further demonstrate that MDA-MB-468 cells were resistant to ß-lap due to their lack of expression of NQ01, we then transfected these cells with CMV-controlled NQ01 (Pink et. al., J. Biol. Chem., 2000). Stable NQ01-expressing human MDA-MB-468 breast cancer transfectants were compared to cells containing pcDNA vector alone to their sensitivity to ß-lap with or without dicoumarol co-administration. As expected, NQ01-containing MDA-MB-468 transfectants were sensitive to ß-lap and this sensitivity was completely prevented by co-administration of dicoumarol. ß-Lap-mediated apoptosis and it's associated proteolyses (e.g., p53 and PARP cleavage events) *in vivo* in MDA-MB-468 transfectants were also prevent by dicoumarol. Surprisingly, the responses of NQ01-containing compared to NQ01-deficient MDA-MB-468 cells to menadione exposures were opposite those of ß-lap. NQ01-expressing MDA-MB-468 cells were extremely resistant to menadione-induced

Boothman, D.A.

apoptosis, PARP cleavage and lethality due to the known detoxification of this drug by NQ01. Dicoumarol co-administration with menadione increased the sensitivity of NQ01-expressing MDA-MB-468 cells to this drug, in direct opposition to the protective effects of dicoumarol on ß-lap-mediated cell death. These data showed that ß-lap targets NQ01 for its lethal effects in human breast cancer cells. Furthermore, NQ01 detoxifies menadione, but enhances ß-lap toxicity. Once again, similar responses were noted in LNCaP cells, where NQO1 transfection rendered these resistant cells sensitive to ß-lap (Planchon et. al., Exp. Cell Res., 2001).

ß-Lap undergoes NQ01-dependent futile cycling to initiate cell death. The opposing lethality data using coadministration of dicoumarol with menadione or ß-lap in NQ01-containing MCF-7:WS8, T47D or transfected MDA-MB-468 cells strongly suggested that NQ01 detoxified menadione, but strongly enhanced ß-lap-mediated apoptosis and lethality. In NQ01 enzyme assays without the addition of cytochrome C, we noticed the continual cycling of ß-lap, as measured by the loss of NAD(P)H over time (Pink et. al., J. Biol. Chem., 2000). Addition of menadione to S100 cell extracts or in purified NQ01 enzymatic assays led to one reaction cycling detoxification of menadione with the utilization of one mole NAD(P)H per one mole of menadione added. In contrast, one mole of ß-lap stimulated the loss of 5-8 moles of NAD(P)H in enzyme assays without the addition of cytochrome C. The activities above were completely prevented by administration of dicoumarol. These data strongly suggest that ß-lap undergoes futile cycling depleting cells of NAD(P)H, causing dramatic loss of energy in ß-lap-treated cells.

ß-Lap-activated proteolyses _in vivo_ is calcium-dependent. The cleavage of p53 in ß-lap-treated, NQ01-containing human breast cancer cells strongly suggested that calpain was activated during apoptosis stimulated by this drug. Ionomycin treatment, which causes massive influx of calcium from the outside of the cell, of human breast cancer cells also induced an identical atypical PARP cleavage independent of NQ01 expression (Planchon et. al., Exp. Cell Res., 2000). These data suggested to us that ß-lap-mediated apoptosis was calcium-dependent. Exposure of ß-lap-treated NQ01-expressing MDA-MB-468 or MCF-7 cells with EGTA or EDTA caused a suppression of ß-lap-mediated atypical PARP cleavage (Tagliarino et. al., J. Biol. Chem., 2001). In addition, EDTA or EGTA co-administration also suppressed ß-lap-mediated p53 cleavage and lamin B in MCF-7 cells. In contrast, treatment of MCF-7 cells with thapsigargin, an inhibitor of the intracellular membrane-bound calcium pump and stimulator of calcium release from ER and mitochondrial stores, caused typical caspase-mediated apoptosis as seen by the typical cleavage of PARP to its 89 kDa cleavage fragment from its full-length 113 kDa peptide (Tagliarino et. al., J. Biol. Chem., 2001). Finally, administration of BAPTA, an intracellular calcium chelator also prevented ß-lap-mediated p53 and atypical PARP cleavage events in MCF-7 or NQ01-expressing MDA-MB-468 cells (Tagliarino et. al., J. Biol. Chem., 2001). EDTA or EGTA treatments of ß-lap-exposed NQ01-expressing cells also prevented the generation of ß-lap-mediated apoptosis (measured as TUNEL positive cells). Administration of EDTA

7

Boothman, D.A.

also prevented ionomycin-induced apoptosis, but not apoptosis induced by staurosporin (STS) or topotecan (TPT) (Tagliarino et. al., J. Biol. Chem., 2001). Thus, the atypical PARP cleavage, as well as p53 cleavage in ß-lap-treated NQO1-expressing human breast cancer cells was mediated by a calcium-dependent noncaspase cysteine protease, which we suspected was calpain.

Accomplishment of Stated Tasks: Although we were delayed a bit with the move of our laboratory to Case Western Reserve University from the University of Wisconsin, we have completed a majority of the stated tasks of Specific Aim #1. Furthermore, we now have genetic models with which to isolate the calcium-dependent, NQO1-dependent, noncaspase cysteine protease, which we now strongly suspect is calpain. We have also recently established activation of calpain *in vivo*, and we have characterized the inhibitory effects of calpastatin, and endogenous inhibitor of calpain, on ß-lap-mediated cell death and survival of exposed cells (see below, Tagliarino et. al., J. Biol. Chem., submitted, 2001).

Task 1: Generation of PARP cDNA bacterial and mammalian expression vectors, and ^{35}S-methionine-labeled PARP protein, plus or minus histidine Tags.

We have generated his- as well as flag-tagged PARP cDNA mammalian expression vectors that can be propagated in bacterial cells. Using either wheat germ or rabbit reticulocyte *in vitro* transcription-translation systems, we have demonstrated that calpain treated, *in vitro* synthesized ^{35}S-methionine PARP protein leads to an identical atypical PARP cleavage fragment, which is prevented by co-administration of calpastatin, addition of EDTA or EGTA, or calpain inhibitors (Tagliarino et. al., J. Biol. Chem., 2001). Furthermore, we have now been able to identify protease activity from whole cell extracts that mimics in vivo PARP cleavage, using 35S-met-labeled PARP protein as a substrate. This activity is only present in ß-lap-exposed cells, and is prevented by coadministered dicoumarol, BAPTA-AM or calpastatin (transfection) treatments (Tagliarino et. al., J. Biol. Chem., submitted). We are now performing these *in vivo* extract protease assays using C-terminal his-tagged PARP to obtain the cleavage site of the proposed calpain or calpain-like protease, for further purification (see below).

Task 2: Initiate ß-lap-activated apoptotic protease isolation using two simultaneous procedures and ß-lap-treated MCF-7:WS8 human breast cancer cells.

As discussed above, we have established stably transfected MCF-7 cells overexpressing N-terminal or C-terminal his-tagged PARP. Treatment of these cells with ß-lap caused the expected appearance of a 60 kDa atypical PARP cleavage fragment from endogenous sources of protein and a slightly larger his-tagged PARP fragment from exogenous sources. These cells will now be used in

8

Boothman, D.A.

Specific Aim #2 as described below. Although we realize this is a final report, the research as described below will be continued via a recently funded NIH grant. We have not accomplished all of the goals of the original grant, but we have sufficient preliminary data to strongly suspect calpain or a calpain-like protease that is activated following ß-lap exposures. Our goal is to now perform a calpain purification using C-terminal his-tagged ^{35}S-met-labeled PARP. This should allow us to complete the specific aims of this grant in less than 6 months. The work by Tagliarino et al., (J. Biol. Chem., 2001 and submitted) has allowed the development of critical biological and biochemical endpoints with which to complete the tasks below. Unfortunately, our funding from the DOD was short by approximately one year. I could not have envisioned that the development of these key assays would take so long, however, work with calpain is tedious and tricky. One major reason is our poor understanding of calpain and its role in apoptosis. Another is the apparent fairly nonspecific and nonconsensus-nature of the protease's cleavage site, which tends to recognize secondary and tertiary structures within a given substrate instead of primary structures as caspases tend to recognize. In any event, we are currently performing the tasks below, and I have indicated the tasks that already have been completed.

2A. Standard Protein Purification Procedure

1. Treat roller bottle-generated MCF-7:WS8 cells with ß-lap. This has been accomplished and extracts are waiting for analyses.
2. Confirm protease activation via endogenous PARP cleavage. This step has been completed, as well as confirming that whole cell extracts retain protease activity using ^{35}S-met-labeled PARP.
3. Ammonium Sulfate Cuts Performed, active fractions pooled.
4. Mono-Q 16/10 FPLC
5. Mono-S 5/5 FPLC
6. Hydroxylapatite column chromatography
7. Superdex 200 26/60 gel filtration
*8. Active fractions pooled, analyzed by SDS-PAGE for atypical
    ^{35}S-PARP cleavage
9. In-gel PARP cleavage assay using cleavage site tetrapeptide fluorescent substrate generated from "Procedure B".

2B. Affinity Chromatographic Purification Procedure

1. PARP cleavage point determination and tetrapeptide syntheses
    1a. Immunoprecipitation of PARP fragments using C-2-10 Antibody. This will not be necessary due to our new reagents, his-tagged N- or C-terminal PARP expressed in MCF-7 cells.
    1b. *In vitro* ^{35}S-PARP cleavage±His tag, immunoprecipitation. Completed.

1c. PARP fragment purification and microsequencing. Completed in vitro, now using transfected MCF-7 cells.

1d. Cleavage site determined by computer analyses. To be completed.

1e. Fluoromethylketone and fluorescent-tetrapeptide cleavage site-specific peptides made by CWRU. Several will be made as positive and negative controls for subsequent enzyme inhibition or activity assays. To be completed.

1f. Confirmation of tetrapeptide-fmk blockage of atypical PARP cleavage and apoptotic protease activity using the tetrapeptide-fluorescent substrate. To be completed.

1g. Mutagenization of PARP cDNA at cleavage site, *in vitro* translate, demonstrate no atypical PARP cleavage. To be completed.

2. Construction of biotin-(streptavidin)-[X]-tetrapeptide-aldehyde. To be completed.

3. DEAE Chromatographic Separation of ß-lap-treated MCF-7 cell
extract, analyses of atypical cleavage activity using ^{35}S-methionine PARP. To be completed.

4. Active fractions from "**Task #2B. 3**" are incubated with biotin-[X]-tetrapeptide-aldehyde and bound to streptavidin-agarose beads and washed. To be completed.

6. Apoptotic protease binding proteins are eluted with biotin. To be completed.

*7. Eluted proteins are analyzed by SDS-PAGE, silver stained
and assayed for ^{35}S-PARP cleavage. To be completed.

The following Tasks may not be needed. The Specific Aims below may not be required should calpain be implicated. Calpain-negative cells, either deficient in calpain expression (mouse knock-out) or cells overexpressing dominant-negative calpain, will be used to explore the specific role of this one protease in ß-lap-sensitivity. These cells are now in-hand and were are currently treating MEFs as well as embryonic stem cells with ß-lap to see the influence of loss of calpain on apoptosis. It is very possible that these results will indicate that calpain is activated after ß-lap exposures, but that, like the caspase cascade, calpain is only one of an entire pathway of proteases whose activities are sufficient to cause apoptosis. Furthermore, using the cell models developed above we will also explore the signaling pathways between ß-lap futile cycling and activation of calpain using calpain-expressing compared to –deficient cells.

Task 3: Production of polyclonal antisera using protein from (2A. *7) or (2B. *6) above. Will probably not be required.

Task 4: Microsequence purified apoptotic protease polypeptides from (2A. *7) or (2B. *6) above. Will be completed for verification using in vitro PARP cleavage reactions that calpain is the active protease stimulated by ß-lap.

Boothman, D.A.

Task 5: Production of degenerative PCR probes corresponding to apoptotic protease amino acid sequences. Will be performed if sequence analyses indicate that the active protease is not calpain.

Task 6: Screen for ß-lap-activated apoptotic protease using antibodies from **Task #3** and PCR probes from **Task #5** in a sequential expression and cDNA hybridization approach. Will most likely not be required.

Task 7: Screen for full-length ß-lap-activated apoptotic protease cDNA. This will be performed if our sequence data above indicate that calpain is not the active protease cleaving PARP in ß-lap-exposed cells.

Task 8: Sequence and analyze the apoptotic protease DNA sequence. Will not be performed if sequence data indicates that the active protease is calpain.

Task 9: Subclone the apoptotic protease into the Tet-on response vector for **Aim #2**. This will be performed in cells from calpain-knockout mice (MEFs or ES cells), or in MCF-7 cells if the protease is not calpain.

Task 10: Examine human breast cancer cells and patient tissue samples for ß-lap-activated apoptotic protease message, protein, and enzymatic activities. This is being completed currently for calpain as well as many of the protein markers (e.g., PARP, pRb, p53) described above.

Specific Aim #2: **Transfect sensitive (i.e., MCF-7) and resistant (i.e., MDA-MB-231) human breast cancer cells with sense and antisense expression vectors encoding the unknown protease to elucidate the role of this apoptotic death enzyme in drug resistance/sensitivities to ß-lap, or other Topo I poisons and DNA damaging agents (Years 2-3).**

These studies have already been completed and the data published (Pink et. al., J. Biol. Chem., 2000 and Planchon et. al., Exp. Cell Res., 2001) for the NQO1 enzyme, which is the primary determinant of ß-lap-mediated apoptosis. The studies described below will first be performed using calpain-deficient cells, followed by transfection of MCF-7 or MDA-MB-231 or MDA-MB-468 cells. We have found that transfection of calpastatin, and endogenous inhibitor of calpain, under the tasks described below protected cells from ß-lap-induced apoptosis and lethality (Tagliarino et al., J. Biol. Chem., submitted), and this provides (a) proof that we can perform the tasks stated below; as well as (b) further indirect evidence that calpain or a calpain-like protease is involved in ß-lap-triggered cell death.

11

Boothman, D.A.

Task 1: Transfect MCF-7:WS8 and MDA-MB-231 cells with Tet-on repressor cDNA and isolate doxycycline-responsive, low basal level subclones.

Task 2: Transfect Tet-on repressor-expressing subclones with doxycycline-responsive, sense- and antisense-oriented ß-lap-activated apoptotic protease expression vectors and double select (hygromycin and neomycin) clones.

Task 3: Examine cells generated in **Tasks #1-3** for apoptotic and survival responses to ß-lap, TPT, and other DNA damaging agents (such as ionizing radiation or Topo II-alpha poisons.

Task 4: Examine treated cells in **Task #4** for apoptotic cell death substrate cleavage and Caspase activities, as well as for the, now known, ß-lap (CPT + PDTC)-activated apoptotic protease.

Evidence for ß-lap-activated apoptosis mediated by calpain. We reasoned that if ß-lap stimulates NQ01-dependent calpain-mediated apoptosis, then the drug must cause significant alterations in calcium homeostasis. In collaboration with Dr. George Dubiak (Dept. Biophysics, CWRU) we demonstrated that ß-lap treatment of NQ01-containing MCF-7:WS8 or MDA-MB-468 transfectants caused dramatic calcium influx within 3 mins as measured by confocal microscopy (Tagliarino et. al., J. Biol. Chem., 2001). Appropriate controls for the release of extracellular (ATP treatment) or intracellular (Thapsigargin) calcium were included. In contrast, calcium release was not evident in NQ01-deficient MDA-MD-468 parental or vector alone cells following ß-lap exposures. Furthermore, treatment of MCF-7:WS8 or NQ01-expressing MDA-MB-468 transfectants with ß-lap caused the cleavage of p53 and atypical cleavage of PARP at the same time as the cleavage-dependent activation of calcium, as monitored by Western blot analyses of the appearance of the 18 kDa active subunit of calpain beginning at 8 hours. Furthermore, the appearance of these cleavage events at 6-12 hours coincided with the initial appearance of TUNEL-positive, condensed-nuclei-containing apoptotic cells (not shown) at ~8 h post-ß-lap-treatment of NQ01 containing (MCF-7 or MDA-MB-468 transfectants) as opposed to parental or vector alone-containing MDA-MB-468 cells. The appearance of all the cleavage fragments described above in NQ01-containing cells was prevented by co-administration of dicoumarol, the NQ01 inhibitor. Furthermore using confocal microscopy, we noted the dramatic movement of cytosolic calpain into the nuclei of ß-lap-treated NQ01-expressing, but not NQ01-deficient, cells (Tagliarino et. al., J. Biol. Chem., 2001). Movement of calpain into the nuclei of ß-lap-treated NQ01-expressing cells was prevented by dicoumoral co-administration, it coincided with the appearance at 6-12 h posttreatment of atypical PARP cleavage, p53 cleavage and the appearance of the 18 kDa small subunit (active) form of calpain, and was not a result of massive breakdown of the nuclear membrane (Tagliarino et. al., J. Biol. Chem., 2001); NQ01 (which is entirely cytosolic) remained cytosolic and the Ku70/Ku80 heterodimer (which is nuclear, not cleaved during apoptosis and was detected by Ab #162) remained nuclear. Furthermore, movement of calpain from the

Boothman, D.A.

cytoplasm to the nucleus was blocked by co-administration of dicoumarol. Finally, we demonstrated that calpastatin over-expression in MCF-7 cells decreased sensitivity to ß-lap in both short-term (apoptosis and appearance of TUNEL-positive cells), as well as long-term survival assays. Collectively, these data strongly suggest that calpain is the apoptotic protease activated during ß-lap-mediated cell death and lethality. These data will be complemented by our current studies using cells from calpain knockout mice. MEF and ES calpain cells (+/+, +/-, and -/-) will be treated with ß-lap +/- dicoumarol and various assays described above performed. These studies should elucidate whether calpain or a calpain-like protease is activated following ß-lap.

Boothman, D.A.

KEY RESEARCH ACCOMPLISHMENTS: Bulleted list of key research accomplishments emanating from this research.

We have accomplished the following objectives of this grant. We have determined that:

- NQO1 is the key determinant in ß-lap-mediated lethality (Pink et al., J. Biol. Chem., 2000 and Planchon et al., Exp. Cell Res., 2001).
- NQO1 is elevated in many human breast cancer cells and should be a useful target for ß-lap and its derivatives (Planchon et al., Oncology Reports, 1999).
- ß-Lap stimulated an unique apoptotic pathway, as measured by TUNEL positive, G0/G1 cells, and specific cleavage of key apoptotic substrates, i.e., PARP, pRb, p53, lamin B and calpain. (Wuerzberger et al., Cancer Res., 1998).
- ß-Lap causes calcium release from endoplasmic reticulum (ER) stores that is sequestered by BAPTA-AM, which subsequently protects cells from ß-lap-induced apoptosis and lethality.
- ß-Lap causes calpain movement from the cytosol to the nucleus at a time concomitant with APRP and p53 cleavage. Apparent movement/activation of calpain is prevented by dicoumarol.
- Atypical PARP and p53 cleavage events are consistent with ß-lap-activated calpain-mediated apoptosis as measured *in vivo* and *in vitro* with whole cell extract, ^{35}S-met-labeled PARP cleavage assays.
- Dicoumarol and calcium chelators protected cells from ß-lap-mediated apoptosis and activation of calpain.
- ß-Lap undergoes NQO1-dependent futile cycling that leads to calcium release and loss of energy (ATP). This combination is thought to prevent ATP-dependent caspase activation and supply the calcium needed to convert the inactive calpain zymogen to the 18 kDa active subunit. Calcium release is responsible for ATP loss, since BAPTA-AM protected cells from ß-lap –mediated ATP loss, as well as lethality.
- Caspases are not activated during NQO1-dependent ß-lap-mediated apoptosis, presumably due to the dramatic loss of ATP within the cell.
- The necessary reagents, C- and N-terminal his- and flag-tagged PARP, have been made and transfected into NQO1-containing cells for the isolation of the ß-lap-activated apoptotic protease.
- Transfection of cells with calpastatin, a specific endogenous calpain protein inhibitor, protected MCF-7 cells from ß-lap-induced apoptosis as well as lethality.

Boothman, D.A.

REPORTABLE OUTCOMES: Provide a list of reportable outcomes to include:

Prior Appendix Items Already Supplied to the DOD In Past Reports:

1. Wuerzberger, S.M., Planchon, S.M., Pink, J.J., Bornmann, W. and Boothman, D.A. ß-Lapachone-induced apoptosis in MCF-7 human breast cancer cells. 1998; Cancer Res. <u>58</u>: 1876-1885.

2. Mendonca, M.S., Howard, K.L., Farrington, D.L., Desmond, L.A., Temples, T.M., Mayhugh, B.M., Pink, J.J. and Boothman, D.A. Delay3ed apoptotic responses associated with radiation-induced neoplastic transformation of human hybrid cells. 1999; Cancer Res. 59: 3972-3979.

3. Separovic, D., Pink, J.J., Oleinick, N.L., Kester, M., Boothman, D.A., McLoughlin, M., Pena, L.A., and Haimovitz-Friedman, A. Nieman-Pick human lymphoblasts are resistant to phthalocyanine 4-photodynamic therapy-induced apoptosis. 1999; Biomed Biophys. Res. Commun., <u>258</u>: 506-512.

CURRENT LIST OF PUBLICATIONS RESULTING FROM THIS AWARD
PAPERS PUBLISHED IN PEER-REVIEWED JOURNALS (Enclosed):

4. Pink, J.J., Planchon, S.M., Tagliarino, C., Wuerzberger-Davis, S.M., Varnes, M.E., Siegel, D., ar Boothman, D.A. NAD(P)H:quinone oxidoreductase (NQO1) activity is the principal determinant (ß-lapachone cytotoxicity. 2000; J. Biol. Chem., <u>275</u> (8): 5416-5422.
5. Pink, J.J., Wuerzberger-Davis, S.M., Tagliarino C., Planchon, S.M., Yang, X-H., Froelich, C.J., ar Boothman, D.A. A novel non-caspase-mediated proteolytic pathway activated in breast cancer cel during ß-lapachone-mediated apoptosis. 2000; Exp. Cell. Res., <u>255</u> (2): 144-155.
6. Huang, T.T., Wuerzberger-Davis, S.M., Seufer, B.J., Shumway, S.D., Kurama, T., Boothman, D.A., ar Miyamoto, S. NF-κB activation by camptothecin: A linkage between nuclear DNA damage ar cytoplasmic signaling events. 2000; J. Biol. Chem., <u>275</u> (13): 9501-9509.
7. Tagliarino, C., Pink, J.J., Dubyak, G.R., Nieminen, A-L., and Boothman, D.A. Calcium is a ke signaling molecule in ß-lapachone-mediated cell death. 2001; J. Biol. Chem. <u>276</u>(22): 19150-19159.
8. Planchon, S.M., Pink, J.J., Tagliarino,, C., Bornmann, W.G., Varnes, M.E., and Boothman, D.A. I Lapachone-induced apoptosis in human prostate cancer cells: involvement of NQO1/xip3. 2001; Ex Cell Res., <u>267</u>: 95-106.

PAPERS PUBLISHED IN NON-PEER-REVIEWED JOURNALS (Not Enclosed).

9. Pink, J.J., Tagliarino, C. Planchon, S., Varnes, M. Simmers, S., and Boothman, D.A. Cell death

pathways triggered by ß-lapachone. Free Radical Biology, In Press, 2001.

10. Miyamoto, S., Huang, T., Wuerzberger-Davis, S., Bornmann, W.,G., Pink, J.J., Tagliarino, C., Kinsella, T.J., and Boothman, D.A. Cellular and Molecular Responses to Topoisomerase I Poisons: Exploiting Synergy For Improved Radiotherapy. 2000; Annals of the New York Academy of Sciences, <u>922</u>: 274-292.

11. Tagliarino, C., Pink, J.J., and Boothman, D.A. Calpains and apoptosis. 2000; Korean Science, In Press.

Abstracts and Presentations Related to this Grant:

1. **Invited Speaker with Abstract,** "Exploitation of and IR-inducible protein (xip3) in human cancer cells using ß-lapachone" C. Tagliarino, J.J. Pink, S.M. Wuerzberger-Davis, S.M. Planchon, and D.A. Boothman. 11th Int Congress of Rad Res., Ireland, July 14-17, 1999. Also paid for by grants from the Radiation Research Society to C.T. and D.A.B.

2. **Invited Speaker,** "Exploiting radiation-inducible proteins for targeted apoptosis" Northern Illinois University, Host: Dr. James B. Mitchel, *Feb. 5, 1999.*

3. **Invited Speaker with Abstract,** Exploiting IR-inducible Proteins For Therapy Against Breast Cancer, Midwest DNA Repair Conference, Ann Arbor, Michigan, *June 13, 1999.*

4. **Invited Speaker with Abstract,** "Exploiting X-ray-inducible proteins for apoptotic chemotherapy" Essen, Germany (C. Streffer, host) *July 14-17, 1999.*

5. **Invited Speaker,** "A novel noncaspase-mediated apoptotic pathway induced by ß-lapachone: involvement of NQO1 Department of Radiation Oncology, University of Maryland, (W.F. Morgan, host) *October 23, 1999.*

6. **Session Chairman, DOE Workshop on Low Dose Irradiation Effects,** "Altered gene expression after low doses ionizing radiation" Germantown, MD, *November 11,1999*

7. **Invited Speaker,** "Exploiting novel apoptotic pathways", Cleveland Clinic Lerner Research Institute. (A. Almasa host) *November, 1999.*

8. **Invited Speaker With Abstract and Accompanying Published Paper,** New York Academy of Sciences Symposiu entitled "The camptothecins: unfolding their anticancer potential", Arlington, Virginia, *March 17-20, 2000.*

9. **Invited Speaker and Session Chairperson with Abstract,** 43rd Annual Meeting of Radiation Research, "Altered ge expression after ionizing radiation", Alburquerque, MN. *April 24-28, 2000.*

10. **Invited Speaker,** DOD Symposium on Breast Cancer Initiative. Seminar entitled "ß-Lapachone triggers NQ0 dependent apoptosis in human breast cancer cells by activating a calcium-dependent noncaspase cysteine protease Atlanta, GA, *June 11-12, 2000.*

11. **Invited Speaker,** "Exploiting IR-inducible responses for chemo- and/or radiotherapy" Department of Pharmacolog University of Pittsburgh, Host:
Dr. Jack Yalowich. *November 9-10, 2000.*

12. **Invited Speaker with Abstract,** Exploiting IR-inducible gene expression for breast cancer therapy, Department Pharmacology, University of Wisconsin-Madison, *December 4, 2001.*

13. **Invited Speaker,** "A novel apoptotic pathway induced by ß-lapachone", Medical College of Wisconsin, *December 5, 2001,*

Patents and licenses applied for and/or issued. None

Degrees Obtained During This Award.

1. Planchon, Sarah, M.   Ph.D., Univ. Wisc.-Madison, Dept. Human Oncology, Dec. 1999.

2. Tagliarino, Colleen   Ph.D., Case Western reserve University, Dept. Pharmacology,

Boothman, D.A.
Oct., 2001.

Development of Cell Lines, Tissue or Serum Repositories:

- -MDA-MB-468 NQ1-6, human NQ01-deficient cells stably transfected with CMV-directed NQ01.
- -vector-alone MDA0-MB-468 cells.
- -Stably transfected MCF-7:WS8 cells expressing caspase 3.
- -Stably transfected MCF-7 cell clones expressing calpastatin.
- -Tetracycline-inducible MCF-7, as well as LNCaP and MDA-MB-231 and MDA-MB-468 cell clones.

Informatics such as databases and animal models, etc.   None

Funding applied for based on work supported by
          this award.

1a. Source and identifying no. **NIH/NCI R01 CA-92250**
          P.I. Boothman, D. A.
b. Title "Exploiting NQO1 for improved therapy of human breast cancers".
c. Dates and costs of entire project   12/01/01 - 11/30/04 $ 825.594
d. Dates and costs of first year   12/01/01 - 11/30/02 $ 200,000
e. Specific aims of project   The goal of this project is to test the hypothesis that ß-lapachone radiosensitizes cells through the inducible enzyme, NQO1 in human breast cancer cells. Another objective of this grant is to further define and clone the apop protease(s) activated by ß-lap in NQO1-expressing human breast cancer cell lines.
f. Describe scientific and budgetary overlap. This grant was funded using the preliminary data developed from a DOD breast cancer g to D.A.B..
g. Describe adjustments you will make if the present application is funded (budget, % effort, aims, etc.).   None.

Employment or research opportunities applied for and/or received on experiences/training supported
          by this award.

Sarah Planchon, Ph.D.   Post-doctoral Fellow, Cleveland Clinic Institutes
John J. Pink, Ph.D.   Instructor, Department of Radiation Oncology
Colleen Tagliarino, Ph.D.   Post-doctoral Fellow, Johnson and Johnson Drug Development
                              Center, Philadelphia, PA.

17

Boothman, D.A.

CONCLUSIONS: Summarize the results to include the importance and/or implications of the completed research and when necessary, recommend changes on future work to better address the problem. A "so what section" which evaluates the knowledge as a scientific or medical product shall also be included in the conclusion of the annual and final reports.

The goal of this grant was to clone the unknown protease activated by the active anti-breast cancer agent, ß-lapachone (ß-lap). The research team showed for the first time that ß-lap required NQ01, a two-electron reduction enzyme elevated in many human breast cancers, for bioactivation. The team then characterized the unknown apoptotic protease activated in human breast cancer cells by ß-lap, defining endpoints that will be essential for the ultimate isolation of this novel apoptotic protease. The unknown protease: (a) is a non-caspase cytsteine protease; (b) cleaves p53, lamin B, and PARP (atypically) in an NQ01-dependent manner at a time co-incident with calpain activation (appearance of an 18 kDa active form and its movement into the nucleus by confocal microscopy); (c) is calcium-dependent (e.g., the proteolytic cleavage of PARP or p53 was blocked by co-administration of EGTA or EDTA), and the drug causes massive NQ01-dependent calcium influx within 3 mins posttreatment with 5-8µM ß-lap; (d) is suppressed by over-expression of calpstatin, a specific endogenous inhibitor of calpain. Furthermore, significant progress has been made in developing reagents that will be required for the cloning of this novel noncaspase cysteine protease. The new hypothesis being tested is that ß-lap activates calpain, which then triggers DNA fragmentation and apoptosis. We have complemented the studies above via the use of MEFs and ES cells from calpain knockout mice, as well as the construction of his-tagged C- and N-terminal PARP reagents that will be useful for novel affinity purification methodology as well as the preparation of a biochemical activity assay, which we have also demonstrated can be used from ß-lap-treated cells.

From work of this DOD grant, we hypothesized that NQ01 could be exploited for breast cancer because (1) the enzyme is elevated in many human breast cancers and tumors can be rapidly assayed for overall levels prior to treatment; (2) the enzyme is induced by cytotoxic agents, such as ionizing radiation (e.g., it was isolated by our laboratory in 1993 as XIP3), and this attribute of the enzyme should be exploitable for improved radiotherapeutic strategies using ß-lapachone; and (3) the data implicates ß-lapachone for chemopreventive therapy against cancer, such as breast cancers, since NQ01 is an early known marker of neoplastic transformation of normal epithelial and other cell types. Based on funding from this DOD award, we were recently able to obtain funding from the National Institutes of Health to explore this hypothesis. We are also currently preparing a grant to be submitted to the NIH for support of the purification of ß-lap-activated calpain or the calpain-like protease.

18

Boothman, D.A.

REFERENCES: List all references pertinent to the report using a standard journal format such as *Science, Military Medicine,* etc.:

1. Planchon, S. M., Wuerzberger, S., Frydman, B., Witiak, D. T., Hutson, P., Church, D. R., Wilding, G., and Boothman, D. A. (1995) *Cancer Res.* **55,** 3706-11

2. Wuerzberger, S. M., Pink, J. J., Planchon, S. M., Byers, K. L., Bornmann, W. G., and Boothman, D. A. (1998) *Cancer Res.* **58,** 1876-85

3. Li, C. J., Averboukh, L., and Pardee, A. B. (1993) *J. Biol. Chem.* **268,** 22463-8

4. Boothman, D. A., Greer, S., and Pardee, A. B. (1987) *Cancer Res.* **47,** 5361-6

5. Schuerch, A. R., and Wehrli, W. (1978) *Eur. J. Biochem.* **84,** 197-205

6. Docampo, R., Cruz, F. S., Boveris, A., Muniz, R. P., and Esquivel, D. M. (1979) *Biochem. Pharmacol.* **28,** 723-8

7. Boorstein, R. J., and Pardee, A. B. (1983) *Biochem. Biophys. Res. Commun.* **117,** 30-6

8. Boothman, D. A., Trask, D. K., and Pardee, A. B. (1989) *Cancer Res.* **49,** 605-12

9. Molina Portela, M. P., and Stoppani, A. O. (1996) *Biochem. Pharmacol.* **51,** 275-83

10. Frydman, B., Marton, L. J., Sun, J. S., Neder, K., Witiak, D. T., Liu, A. A., Wang, H. M., Mao, Y., Wu, H. Y., Sanders, M. M., and Liu, L. F. (1997) *Cancer Res.* **57,** 620-7

11. Vanni, A., Fiore, M., De Salvia, R., Cundari, E., Ricordy, R., Ceccarelli, R., and Degrassi, F. (1998) *Mutat Res* **401,** 55-63

12. Manna, S. K., Gad, Y. P., Mukhopadhyay, A., and Aggarwal, B. B. (1999) *Biochem. Pharmacol.* **57,** 763-74

13. Robertson, N., Haigh, A., Adams, G. E., and Stratford, I. J. (1994) *Eur. J. Cancer* **30A,** 1013-9

14. Cadenas, E. (1995) *Biochem. Pharmacol.* **49,** 127-40

15. Ross, D., Beall, H., Traver, R. D., Siegel, D., Phillips, R. M., and Gibson, N. W. (1994) *Oncol. Res.* **6,** 493-500

16. Rauth, A. M., Goldberg, Z., and Misra, V. (1997) *Oncol. Res.* **9,** 339-49

17. Ross, D., Siegel, D., Beall, H., Prakash, A. S., Mulcahy, R. T., and Gibson, N. W. (1993) *Cancer Met. Rev.* **12,** 83-101

18. Boothman, D. A., Meyers, M., Fukunaga, N., and Lee, S. W. (1993) *Proc. Natl. Acad. Sci. USA* **90,** 7200-4

19. Chen, S., Knox, R., Lewis, A. D., Friedlos, F., Workman, P., Deng, P. S., Fung, M., Ebenstein, D., Wu, K., and Tsai, T. M. (1995) *Mol. Pharmacol.* **47,** 934-9

20. Jaiswal, A. K., McBride, O. W., Adesnik, M., and Nebert, D. W. (1988) *J. Biol. Chem.* **263,** 13572-8

21. Radjendirane, V., Joseph, P., Lee, Y. H., Kimura, S., Klein-Szanto, A. J., Gonzalez, F. J., and Jaiswal, A. K. (1998) *J. Biol. Chem.* **273,** 7382-9

22. Marin, A., Lopez de Cerain, A., Hamilton, E., Lewis, A. D., Martinez-Penuela, J. M., Idoate, M. A., and Bello, J. (1997) *Br. J. Cancer* **76,** 923-9

23. Malkinson, A. M., Siegel, D., Forrest, G. L., Gazdar, A. F., Oie, H. K., Chan, D. C., Bunn, P. A., Mabry, M., Dykes, D. J., Harrison, S. D., and et al. (1992) *Cancer Res.* **52,** 4752-7

24. Belinsky, M., and Jaiswal, A. K. (1993) *Cancer Met. Rev.* **12,** 103-17

25. Joseph, P., Xie, T., Xu, Y., and Jaiswal, A. K. (1994) *Oncol. Res.* **6,** 525-32

26. Buettner, G. R. (1993) *Arch. Biochem. Biophys.* **300,** 535-43

Boothman, D.A.

27. Ross, D., Thor, H., Orrenius, S., and Moldeus, P. (1985) *Chemico-Biological Interactions* **55**, 177-84

28. Riley, R. J., and Workman, P. (1992) *Biochem. Pharmacol.* **43**, 1657-69

29. Siegel, D., Beall, H., Senekowitsch, C., Kasai, M., Arai, H., Gibson, N. W., and Ross, D. (1992) *Biochemistry* **31**, 7879-85

30. Prakash, A. S., Beall, H., Ross, D., and Gibson, N. W. (1993) *Biochemistry* **32**, 5518-25

31. Fitzsimmons, S. A., Workman, P., Grever, M., Paull, K., Camalier, R., and Lewis, A. D. (1996) *J. Natl. Cancer Inst.* **88**, 259-69

32. Beall, H. D., Murphy, A. M., Siegel, D., Hargreaves, R. H., Butler, J., and Ross, D. (1995) *Mol. Pharmacol.* **48**, 499-504

33. Hollander, P. M., and Ernster, L. (1975) *Arch. Biochem. Biophys.* **169**, 560-7

34. Hosoda, S., Nakamura, W., and Hayashi, K. (1974) *J. Biol. Chem.* **249**, 6416-23

35. Duthie, S. J., and Grant, M. H. (1989) *Br. J. Cancer* **60**, 566-71

36. Akman, S. A., Doroshow, J. H., Dietrich, M. F., Chlebowski, R. T., and Block, J. S. (1987) *J. Pharmacol. Exp. Ther.* **240**, 486-91

37. Thor, H., Smith, M. T., Hartzell, P., Bellomo, G., Jewell, S. A., and Orrenius, S. (1982) *J. Biol. Chem.* **257**, 12419-25

38. Siegel, D., McGuinness, S. M., Winski, S. L., and Ross, D. (1999) *Pharmacogenetics* **9**, 113-21

39. Gustafson, D. L., Beall, H. D., Bolton, E. M., Ross, D., and Waldren, C. A. (1996) *Mol. Pharmacol.* **50**, 728-35

40. Sambrook, J., Fritsch, E. F., and Maniatis, T. (1989) *Molecular Cloning-A Laboratory Manual*, Cold Spring Harbor Laboratory Press, Cold Spring Harbor

41. Pink, J. J., Bilimoria, M. M., Assikis, J., and Jordan, V. C. (1996) *Br. J. Cancer* **74**, 1227-36

42. Labarca, C., and Paigen, K. (1980) *Anal. Biochem.* **102**, 344-52

43. Siegel, D., Franklin, W. A., and Ross, D. (1998) *Clin Cancer Res* **4**, 2065-70

44. Hollander, P. M., Bartfai, T., and Gatt, S. (1975) *Arch. Biochem. Biophys.* **169**, 568-76

45. Strobel, H. W., and Dignam, J. D. (1978) *Methods Enzymol* **52**, 89-96

46. Beall, H. D., Mulcahy, R. T., Siegel, D., Traver, R. D., Gibson, N. W., and Ross, D. (1994) *Cancer Res.* **54**, 3196-201

47. Kaufmann, S. H., Desnoyers, S., Ottaviano, Y., Davidson, N. E., and Poirier, G. G. (1993) *Cancer Res.* **53**, 3976-85

48. Preusch, P. C., Siegel, D., Gibson, N. W., and Ross, D. (1991) *Free Radic. Biol. Med.* **11**, 77-80

49. Siegel, D., Gibson, N. W., Preusch, P. C., and Ross, D. (1990) *Cancer Res.* **50**, 7483-9

50. Keyes, S. R., Fracasso, P. M., Heimbrook, D. C., Rockwell, S., Sligar, S. G., and Sartorelli, A. C. (1984) *Cancer Res.* **44**, 5638-43

51. Hess, R., Plaumann, B., Lutum, A. S., Haessler, C., Heinz, B., Fritsche, M., and Brandner, G. (1994) *Toxicol. Lett.* **72**, 43-52

52. Boothman, D. A., and Pardee, A. B. (1989) *Proc. Natl. Acad. Sci. USA* **86**, 4963-7

Boothman, D.A.

53. Boothman, D. A., Wang, M., Schea, R. A., Burrows, H. L., Strickfaden, S., and Owens, J. K. (1992) *Int. J. Radiat. Oncol. Biol. Phys.* **24,** 939-48

54. Nelson, W. G., and Kastan, M. B. (1994) *Mol. Cell. Biol.* **14,** 1815-23

55. Kubbutat, M. H., and Vousden, K. H. (1997) *Mol. Cell. Biol.* **17,** 460-8

56. Squier, M. K., and Cohen, J. J. (1997) *J. Immunol.* **158,** 3690-7

57. Wood, D. E., and Newcomb, E. W. (1999) *J. Biol. Chem.* **274,** 8309-15

58. Squier, M. K., Sehnert, A. J., Sellins, K. S., Malkinson, A. M., Takano, E., and Cohen, J. J. (1999) *J. Cell. Physiol.* **178,** 311-9

59. Wefers, H., and Sies, H. (1983) *Archives of Biochemistry & Biophysics* **224,** 568-78

60. Bellomo, G., Jewell, S. A., and Orrenius, S. (1982) *J. Biol. Chem.* **257,** 11558-62

61. Iyanagi, T. (1990) *Free Radical Research Communications* **8,** 259-68

62. Molina Portela, M. P., Fernandez Villamil, S. H., Perissinotti, L. J., and Stoppani, A. O. (1996) *Biochem. Pharmacol.* **52,** 1875-82

63. Docampo, R., Cruz, F. S., Boveris, A., Muniz, R. P., and Esquivel, D. M. (1978) *Arch Biochem Biophys* **186,** 292-7

64. Chau, Y. P., Shiah, S. G., Don, M. J., and Kuo, M. L. (1998) *Free Radic Biol Med* **24,** 660-70

65. Zhao, Q., Yang, X. L., Holtzclaw, W. D., and Talalay, P. (1997) *Proc. Natl. Acad. Sci. USA* **94,** 1669-74

66. Jaiswal, A. K. (1994) *J. Biol. Chem.* **269,** 14502-8

67. Boorstein, R. J., and Pardee, A. B. (1984) *Biochem. Biophys. Res. Commun.* **118,** 828-34

68. Fornace, A. J., Jr., Alamo, I., Jr., and Hollander, M. C. (1988) *Proc Natl Acad Sci U S A* **85,** 8800-4

69. Williams, J. B., Wang, R., Lu, A. Y., and Pickett, C. B. (1984) *Arch. Biochem. Biophys.* **232,** 408-13

70. Farber, E. (1984) *Can J Biochem Cell Biol* **62,** 486-94

Boothman, D.A.

APPENDICES: Attach all appendices that contain information that supplements, clarifies or supports the text. Examples of appendices include journal articles, reprints of manuscripts and abstracts, a curriculum vitae, patent applications, study questionnaires, and surveys, etc.

Prior Appendix Items Already Supplied to the DOD

Wuerzberger, S.M., Planchon, S.M., Pink, J.J., Bornmann, W. and Boothman, D.A. ß-Lapachone-induced apoptosis in MCF-7 human breast cancer cells. 1998; Cancer Res. 58: 1876-1885.

Mendonca, M.S., Howard, K.L., Farrington, D.L., Desmond, L.A., Temples, T.M., Mayhugh, B.M., Pink, J.J. and Boothman, D.A. Delay3ed apoptotic responses associated with radiation-induced neoplastic transformation of human hybrid cells. 1999; Cancer Res. 59: 3972-3979.

Separovic, D., Pink, J.J., Oleinick, N.L., Kester, M., Boothman, D.A., McLoughlin, M., Pena, L.A., and Haimovitz-Friedman, A. Nieman-Pick human lymphoblasts are resistant to phthalocyanine 4-photodynamic therapy-induced apoptosis. 1999; Biomed Biophys. Res. Commun., 258: 506-512.

CURRENT LIST OF PUBLICATIONS RESULTING FROM THIS AWARD
PAPERS PUBLISHED IN PEER-REVIEWED JOURNALS (Enclosed):

Pink, J.J., Planchon, S.M., Tagliarino, C., Wuerzberger-Davis, S.M., Varnes, M.E., Siegel, D., ar Boothman, D.A. NAD(P)H:quinone oxidoreductase (NQO1) activity is the principal determinant (ß-lapachone cytotoxicity. 2000; J. Biol. Chem., 275 (8): 5416-5422.

Pink, J.J., Wuerzberger-Davis, S.M., Tagliarino C., Planchon, S.M., Yang, X-H., Froelich, C.J., ar Boothman, D.A. A novel non-caspase-mediated proteolytic pathway activated in breast cancer cel during ß-lapachone-mediated apoptosis. 2000; Exp. Cell. Res., 255 (2): 144-155.

Huang, T.T., Wuerzberger-Davis, S.M., Seufer, B.J., Shumway, S.D., Kurama, T., Boothman, D.A., ar Miyamoto, S. NF-κB activation by camptothecin: A linkage between nuclear DNA damage ar cytoplasmic signaling events. 2000; J. Biol. Chem., 275 (13): 9501-9509.

Tagliarino, C., Pink, J.J., Dubyak, G.R., Nieminen, A-L., and Boothman, D.A. Calcium is a key signalir molecule in ß-lapachone-mediated cell death. 2001; J. Biol. Chem. 276(22): 19150-19159.

Planchon, S.M., Pink, J.J., Tagliarino,, C., Bornmann, W.G., Varnes, M.E., and Boothman, D.A. I Lapachone-induced apoptosis in human prostate cancer cells: involvement of NQO1/xip3. 2001; Ex Cell Res., 267: 95-106.

PAPERS PUBLISHED IN NON-PEER-REVIEWED JOURNALS (Not Enclosed).

Pink, J.J., Tagliarino, C. Planchon, S., Varnes, M. Simmers, S., and Boothman, D.A. Cell death pathways triggered by ß-lapachone. Free Radical Biology, In Press, 2001.

22

Boothman, D.A.

Miyamoto, S., Huang, T., Wuerzberger-Davis, S., Bornmann, W.,G., Pink, J.J., Tagliarino, C., Kinsella, T.J., and Boothman, D.A. Cellular and Molecular Responses to Topoisomerase I Poisons: Exploiting Synergy For Improved Radiotherapy. 2000; Annals of the New York Academy of Sciences, 922: 274-292.

Tagliarino, C., Pink, J.J., and Boothman, D.A. Calpains and apoptosis. 2000; Korean Science, In Press.

Boothman, D.A.

BINDING: Because all reports are entered into the Department of Defense Technical Reports Database collection and are microfiched, it is recommended that all reports be bound by stapling the pages together in the upper left hand corner. All reports shall be prepared in camera ready copy (legible print, clear photos/illustrations) for microfiching. Figures should include legends and all figures and tables should be clearly marked.

FINAL REPORTS: All final reports must include a bibliography of all publications and meeting abstracts and a list of personnel (not salaries) receiving pay from the research effort.

SEE ABOVE.

NOTE: IF ALL OF THE ABOVE ELEMENTS ARE NOT MET, THE REPORT WILL BE CONSIDERED UNACCEPTABLE AND WILL BE RETURNED FOR REWRITE.

HELPFUL HINTS:

1. **Please proof all reports for errors.**

2. **Please provide supporting data, i.e. tables, figures, graphs, etc.**

3. **Ensure all publications published as a result of effort acknowledges the work supported by USAMRMC. Copies of all publications supported by the USAMRMC are to be provided with reports.**

■■■

Manuscripts/Reprints, Abstracts

A copy of manuscripts or subsequent reprints resulting from the research shall be submitted to the USAMRMC. An extended abstract suitable for publication in the Proceedings of the Breast Cancer Research Program is required in relation to a DOD BCRP meeting tentatively planned for 2002. The extended abstract shall (1) identify the accomplishments since award and (2) follow instructions to be prepared by the USAMRMC and promulgated at a later date. The extended abstract style will be dependent on the discipline.

An Extended Abstract will be Submitted and the PI will attend the next 2002 Breast Cancer Research Program.

NAD(P)H:Quinone Oxidoreductase Activity Is the Principal Determinant of β-Lapachone Cytotoxicity*

John J. Pink‡, Sarah M. Planchon‡, Colleen Tagliarino‡, Marie E. Varnes‡, David Siegel§, and David A. Boothman‡¶

From the ‡Department of Radiation Oncology, Laboratory of Molecular Stress Responses, Ireland Comprehensive Cancer Center, Case Western Reserve University, Cleveland, Ohio 44106-4942 and the §Department of Pharmaceutical Sciences, School of Pharmacy and Cancer Center, University of Colorado Health Sciences Center, Denver, Colorado 80262

β-Lapachone activates a novel apoptotic response in a number of cell lines. We demonstrate that the enzyme NAD(P)H:quinone oxidoreductase (NQO1) substantially enhances the toxicity of β-lapachone. NQO1 expression directly correlated with sensitivity to a 4-h pulse of β-lapachone in a panel of breast cancer cell lines, and the NQO1 inhibitor, dicoumarol, significantly protected NQO1-expressing cells from all aspects of β-lapachone toxicity. Stable transfection of the NQO1-deficient cell line, MDA-MB-468, with an NQO1 expression plasmid increased apoptotic responses and lethality after β-lapachone exposure. Dicoumarol blocked both the apoptotic responses and lethality. Biochemical studies suggest that reduction of β-lapachone by NQO1 leads to a futile cycling between the quinone and hydroquinone forms, with a concomitant loss of reduced NAD(P)H. In addition, the activation of a cysteine protease, which has characteristics consistent with the neutral calcium-dependent protease, calpain, is observed after β-lapachone treatment. This is the first definitive elucidation of an intracellular target for β-lapachone in tumor cells. NQO1 could be exploited for gene therapy, radiotherapy, and/or chemopreventive interventions, since the enzyme is elevated in a number of tumor types (i.e. breast and lung) and during neoplastic transformation.

β-lap,[1] a novel 1,2-naphthoquinone, is a potent cytotoxic agent that demonstrates activity against various cancer cell lines (1–3). At lower doses, it is a radiosensitizer of a number of human cancer cell lines (4). We previously demonstrated that the primary mode of β-lap cytotoxicity is through the induction of apoptosis (1, 2). However, the clinical efficacy of this drug remains to be explored, and such studies await elucidation of its mechanism of action.

While a number of *in vitro* effects of β-lap have been described, the key intracellular target of β-lap remains unknown.

β-lap has many diverse effects *in vitro*, including (*a*) inhibition of DNA polymerase α (5), (*b*) enhanced lipid peroxidation and free radical accumulation (6), (*c*) inhibition of DNA replication and thymidylate synthase activity (7), (*d*) inhibition of DNA repair (4, 8), (*e*) inhibition or activation of DNA topoisomerase I (1, 3), (*f*) oxidation of dihydrolipoamide (9), (*g*) induction of topoisomerase IIα-mediated DNA breaks (10), (*h*) inhibition of poly(ADP-ribose) polymerase (11), and (*i*) inhibition of NF-κB activity (12). While these effects could be hypothetically linked to the cytotoxicity caused by β-lap administration, most have not been demonstrated *in vivo*, and none have led to elucidation of the drug's intracellular target.

Structural similarities between β-lap and other members of the naphthoquinone family, such as menadione (vitamin K₃; 2-methyl-1,4 naphthoquinone), suggested that the enzyme, DT-diaphorase, quinone oxidoreductase, EC 1.6.99.2 (NQO1), may be involved in the activation or detoxification of β-lap (13–17). The x-ray-inducible nature of NQO1 (*i.e.* it was cloned by our laboratory as x-ray inducible transcript-3 (xip-3)) was also consistent with this compound's ability to sensitize irradiated cells (18).

NQO1 is a ubiquitous flavoprotein found in most eukaryotes. The human NQO1 gene encodes a 30-kDa protein that is expressed in most tissues but does show variable tissue-dependent expression. NQO1 is abundant in the liver of most mammals, except humans, where it is less abundant than in most other tissues (16, 19, 20). NQO1 knock-out mice show no detectable phenotype other than an enhanced sensitivity to menadione, suggesting that the principal function of NQO1 is the detoxification of quinone xenobiotics (21). Importantly, NQO1 is overexpressed in a number of tumors, including breast, colon, and lung cancers, compared with surrounding normal tissue (22–25). This observation, more than any other, suggests that drugs that are activated by NQO1 (*e.g.* MMC, streptonigrin, and EO9; see below) should show significant tumor-specific activity.

NQO1 catalyzes a two-electron reduction of various quinones (*e.g.* menadione), utilizing either NADH or NADPH as electron donors. Unlike most other cellular reductases, NQO1 reduces quinones directly to the hydroquinone, bypassing the unstable and highly reactive semiquinone intermediate. Semiquinones are excellent free radical generators, initiating a redox cycle that results in the generation of superoxide. Superoxide can dismutate to hydrogen peroxide, and hydroxyl radicals can then be formed by the iron-catalyzed reduction of peroxide via the Fenton reaction (26). All of these highly reactive species may directly react with DNA or other cellular macromolecules, such as lipids and proteins, causing damage. NQO1-mediated production of the hydroquinone, which can be readily conjugated and excreted from the cell, constitutes a protective mech-

---

¶ To whom correspondence should be addressed: Tel.: 216-368-0840; Fax: 216-368-1142; E-mail: dab30@po.cwru.edu.

[1] The abbreviations used are: β-lap, β-lapachone (3,4-dihydro-2,2-dimethyl-2H-naphtho[1,2-*b*]pyran-5,6-dione); xip-3, x-ray-inducible transcript-3; NQO1, NAD(P)H:quinone oxidoreductase, DT-diaphorase, xip-3 (EC 1.6.99.2); PARP, poly(ADP-ribose) polymerase; MMC, mitomycin C; TUNEL, terminal deoxynucleotidyl transferase-mediated dUTP nick end labeling.

This paper is available on line at http://www.jbc.org

anism against these types of damage (27). It is thought that the reducing activity of NQO1 protects cells from the toxicity of naturally occurring xenobiotics containing quinone moieties (14).

In addition to its protective effects, NQO1 can also reduce certain quinones to more reactive forms. The most well described of these compounds is MMC. It is through a two-electron reduction by NQO1 or through two separate one electron reductions by other reductases (such as NADH:cytochrome b_5 reductase and NADPH:cytochrome P-450 reductase) that the alkylating activity of MMC is revealed (28–30). A correlation was observed between MMC sensitivity and NQO1 activity in a study using 69 cell lines from the NCI, National Institutes of Health, human tumor cell panel. These data suggested that NQO1 was a critical activator of MMC and probably other quinone-containing antitumor agents (31). Similarly, streptonigrin and EO9 can be activated by NQO1-catalyzed reduction (32).

Dicoumarol (3–3′-methylene-bis(4-hydroxycoumarin)) is a commonly used inhibitor of NQO1, which competes with NADH or NADPH for binding to the oxidized form of NQO1. Dicoumarol thereby prevents reduction of various target quinones (33, 34). Co-administration of dicoumarol significantly enhances the toxicity of a number of quinones, including menadione, presumably by increasing oxidative stress in the cell (35–37).

We demonstrate that NQO1 is an important activating enzyme for β-lap in breast cancer cells. β-lap cytotoxicity was significantly enhanced in breast cancer cells expressing NQO1. Conversely, cells that lacked this enzyme were more resistant to a short term exposure to the drug. Co-administration of dicoumarol protected NQO1-expressing cells from all downstream apoptotic responses and greatly enhanced survival. Stable transfection of NQO1-deficient, MDA-MB-468 cells, homozygous for a proline to serine substitution at amino acid 187, which leads to the synthesis of unstable protein (38), with human NQO1 cDNA sensitized these otherwise resistant cells and re-established apoptotic responses. As seen in other cells expressing endogenous NQO1, cytotoxicity was significantly inhibited by dicoumarol. Our data establish that NQO1 activity is an important determinant of β-lap cytotoxicity in breast cancer cells. A novel downstream apoptotic pathway induced by β-lapachone is also discussed.

EXPERIMENTAL PROCEDURES

Cell Culture—MCF-7:WS8 and T47D:A18 cells were obtained from V. Craig Jordan (Northwestern University, Chicago, IL). MDA-MB-468 cells were obtained from the American Type Culture Collection. All tissue culture components were purchased from Life Technologies, Inc. unless otherwise stated. Cells were grown in RPMI 1640 supplemented with 10% calf serum, 2 mM L-glutamine, 100 units/ml penicillin, and 100 mg/ml streptomycin. Cells were routinely passed at 1:5–1:20 dilutions once per week using 0.1% trypsin. All cells were grown in a 37 °C humidified incubator with 5% CO_2, 95% air atmosphere. Tests for mycoplasma, using the Gen-Probe™ Rapid Detection Kit (Fisher), were performed quarterly, and all cell lines were found to be negative.

Stable Transfection—Cells were seeded into six-well dishes at 2 × 10^5 cells/well and allowed to attach overnight. The following day, 1.0 μg of BE8 plasmid DNA containing the human NQO1 cDNA in the pCDNA3 constitutive expression vector (39) was transfected into each of three wells using standard calcium phosphate methodology (40). After 2 days, cells were selected for growth in 350 μg/ml Geneticin® (G418, Life Technologies, Inc.). A stable, pooled population was established after approximately 3 weeks, and subsequently clones were isolated by limiting dilution cloning, as described (41).

Cell Growth Assays—Cells were seeded into each well of a 96-well plate (1500 cells/well) in 0.2 ml of media on day 0. The following day (day 1), media were removed, and 0.2 ml of medium containing the appropriate compound(s) was added for 4 h. Drugs were then removed, control growth medium was added, and cells were allowed to grow for an additional 7 days. Stock solutions of β-lap (a generous gift from

William Bornmann, Sloan-Kettering Cancer Center, New York, NY) and menadione (Sigma) were dissolved in Me$_2$SO and stored at −80 °C. Drugs were added to medium at a 1:1000 dilution immediately before administration to cells. Dicoumarol (Sigma) was suspended in water and solubilized using a minimal amount of NaOH. Dicoumarol was added at a 1:100 dilution to the appropriate medium. DNA content (a measure of cell growth) was determined by fluorescence of the DNA dye Hoescht 33258 (Sigma), using an adaptation of the method of Labarca and Paigen (42), and read in a Cytofluor fluorescence plate reader. Data were expressed as relative growth, *T/C* (treated/control) from three or more wells per treatment. Each experiment was repeated at least three times, and data were expressed as mean ± S.E. Comparisons were performed using a two-tailed Student's *t* test for paired samples.

Colony-forming Assays—LD$_{50}$ survival determinations were calculated by clonogenic assays (4). Briefly, cells were seeded at various densities on 35-cm^2 tissue culture dishes and allowed 48 h to attach and initiate log phase growth. Drugs were added for 4 h at various concentrations and removed, as described above. Colonies from control or treated conditions were allowed to grow for 10 days. Colonies with 50 or more normal appearing cells were counted, and data were graphed as mean ± S.E. Shown is a compilation of two independent experiments. Comparisons were performed using a two-tailed Student's *t* test for paired samples.

Western Blot Analyses—Whole cell extracts were prepared by direct lysis of scraped, PBS-washed cells (both floating and attached cells were pooled) in buffer composed of 6 M urea, 2% SDS, 10% glycerol, 62.5 mM Tris-HCl, pH 6.8, 5% β-mercaptoethanol, and 5 μg/ml bromphenol blue followed by sonication. Equal amounts of protein were heated at 65 °C for 10 min and loaded into each lane of a 10% polyacrylamide gel with a 5% stacking gel. Following electrophoresis, proteins were transferred to Immobilon-P (Millipore Corp., Bedford, MA) using Multiphor II semi-dry electroblotting (Amersham Pharmacia Biotech) according to the manufacturer's directions. Loading equivalence and transfer efficiency were monitored by Ponceau S staining of the membrane. Standard Western blotting techniques were used, and the proteins of interest were visualized by incubation with Super Signal (Pierce) at 20 °C for 5 min. Membranes were then exposed to x-ray film for an appropriate time and developed. The C-2-10 anti-PARP antibody was purchased from Enzyme Systems Products (Dublin, CA). The anti-p53 antibody (DO-1) was purchased from Santa Cruz Biotechnology, Inc. (Santa Cruz, CA). NQO1 antibody was contained in medium from a mouse hybridoma clone A180 (43) and was used at a 1:4 dilution in 10% serum, 1× PBS, 0.2% Tween 20 for Western blot analysis.

Preparation of S9 Supernatants—Cellular extracts for enzyme assays were prepared from cells in mid-log to late log phase growth. Cells were harvested by trypsinization (0.25% trypsin and 1 mM EDTA), washed twice in ice-cold, phenol red-free Hank's balanced salt solution, and then resuspended in a small volume of PBS, pH 7.2, containing 10 μg/μl aprotinin. The cell suspensions were sonicated on ice four times, using 10-s pulses, and then centrifuged at 14,000 × *g* for 20 min. The S9 supernatants were aliquoted into microcentrifuge tubes and stored at −80 °C until used.

Enzyme Assays—Three enzymes were assayed as described by Fitzsimmons *et al.* (31) and Gustafson *et al.* (39). Reaction medium contained 77 μM cytochrome *c* (practical grade; Sigma) and 0.14% bovine serum albumin in Tris-HCl buffer (50 mM, pH 7.5). NQO1 activity was measured using NADH (200 μM) as the immediate electron donor and menadione (10 μM) as the intermediate electron acceptor. Each assay was repeated in the presence of 10 μM dicoumarol, and activity attributed to NQO1 was that inhibited by dicoumarol (44). NADH:cytochrome b_5 reductase was measured using NADH (200 μM) as the electron donor, and NADPH:cytochrome P-450 reductase was measured using NADPH (200 μM) as electron donor (45) in a Beckman DU 640 spectrophotometer (Beckman Coulter, Fullerton, CA). Reactions were carried out at 37 °C and were initiated by the addition of S9 supernatants. Varying amounts of supernatants, from 10 to 40 μl, were used to ensure linearity of rates with protein concentration. Enzyme activities were calculated as nmol of cytochrome *c* reduced/min/mg of protein, based on the initial rate of change in OD at 550 nm and an extinction coefficient for cytochrome *c* of 21.1 mM/cm. Results shown are the average enzyme activity for three separate cell extractions ± S.D. or both values from duplicate experiments.

NADH Recycling Assays—Assays were performed with either purified NQO1 (46) or S9 extracts from MCF-7:WS8 cells. For the assay using purified NQO1, 1.5 μg of recombinant human NQO1 was mixed with 200–500 μM NADH in 50 mM potassium phosphate buffer, pH 7.0. Reactions were initiated by the addition of 2–20 μM β-lap or menadione, and the change in absorbance at 340 nM was measured over time. For
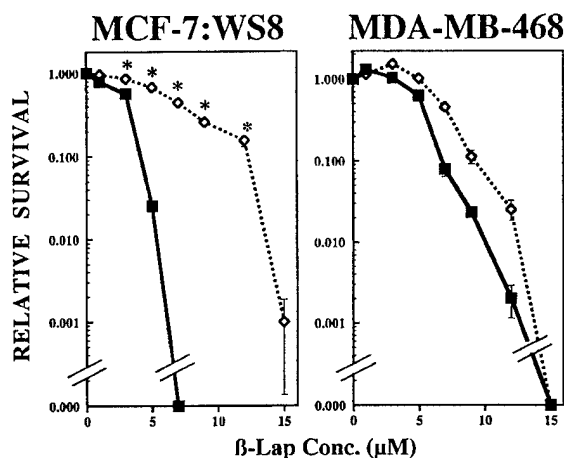
MCF-7:WS8   MDA-MB-468

β-Lap Conc. (µM)

FIG. 1. **Co-administration of dicoumarol protects MCF-7:WS8, but not MDA-MB-468, cells from β-lap-mediated cytotoxicity.** Cells were seeded into 60-mm dishes (10,000 and 1000 cells/dish, in triplicate) and allowed to attach overnight. Cells were then exposed to a 4-h pulse of β-lap either alone (■) or with 50 µM dicoumarol (◇). Media were removed, fresh drug-free media were added, and cells were allowed to grow for 10 days. Plates were then washed and stained with crystal violet in 50% methanol. Colonies of greater than 50 normal-appearing cells were then counted and plotted *versus* β-lap concentration. Shown is the mean ± S.E. of triplicate plates from two independent experiments .

assays using MCF-7:WS8 S9 extracts, 5 µl of extracts containing approximately 2000 units of NQO1/mg of protein were mixed with 200–500 µM NADH in 50 mM Tris-HCl, pH 7.5, containing 0.14% bovine serum albumin. Reactions were initiated by the addition of 5–200 µM β-lap or menadione, and change in absorbance at 340 nM was measured for 10 min. All reactions were also performed in the presence of 10 µM dicoumarol, which inhibited all measurable NQO1 activity.

Flow Cytometry and Apoptotic Measurements—Flow cytometric analyses were performed as described (1, 2). TUNEL assays, to measure DNA fragmentation during apoptosis, were performed using APO-DI-RECT™ as described by the manufacturer (Phoenix Flow Systems, Inc., San Diego, CA). Samples were read in an EPICS Elite ESP flow cytometer using an air-cooled argon laser at 488 nm, 15 milliwatts (Beckman Coulter Electronics, Miami, FL). Propidium iodide was read at 640 nm using a long pass optical filter, and fluorescein isothiocyanate was read at 525 nm using a band pass filter. Analysis was performed using the Elite acquisition software provided with the instrument. All experiments were performed a minimum of three times.

RESULTS

We previously showed that the naturally occurring 1,2-naphthoquinone, β-lap, induced apoptosis in a number of breast cancer cell lines (1, 2). We hypothesized that β-lap, as a member of the naphthoquinone family, may be a substrate for NQO1 and that its toxicity may be influenced by NQO1 expression. We therefore tested the effects of dicoumarol on β-lap-mediated cytotoxicity in MCF-7:WS8 or MDA-MB-468 breast cancer cell lines after a 4-h pulse of drug. Co-administration of 50 µM dicoumarol during a 4-h pulse of β-lap caused a significant survival enhancement in MCF-7:WS8 cells (Fig. 1). While this protection was dramatic at β-lap doses of 4–12 µM, the protective effects of dicoumarol were overcome by >14 µM β-lap. In contrast, MDA-MB-468 cells were relatively resistant (LD$_{50}$ ~ 8 µM, compared with MCF-7:WS8, LD$_{50}$ ~ 4 µM) to β-lap alone and were not significantly protected by dicoumarol (Fig. 1). Since MDA-MB-468 cells do not express NQO1 (Table I and Fig. 3) and dicoumarol significantly protected NQO1-expressing MCF-7:WS8 cells (Table I and Fig. 3), these data suggested that NQO1 expression was a critical determining factor in β-lap-mediated cytotoxicity.

We then extended these studies to compare the relative toxicity of menadione (2-methyl-1,4-naphthoquinone) to β-lap, either alone or in the presence of dicoumarol. Three breast

TABLE I
Endogenous reductase levels in breast cancer cell lines

Values represent averages for three or more separate S9 preparations ± S.D. except as noted in Footnote c.

Cell line	Enzyme activities[a]		
	NQO1	NADH:cytochrome b_5 reductase	NADPH:cytochrome P-450 reductase
	nmol/min/mg		
MCF-7:WS8	2641 ± 555	81 ± 18	27 ± 5.0
T47D:A18	82 ± 17	131 ± 35	31 ± 1.0
MDA-MB-468	<10.0[b]	93/108[c]	26/36[c]

[a] Units are nanomoles of cytochrome c reduced per min per mg of protein.
[b] <10.0**, NQO1 activity not detected. The difference in the rate of cytochrome c reduction with and without dicoumarol was not statistically significant, based on Student's t test.
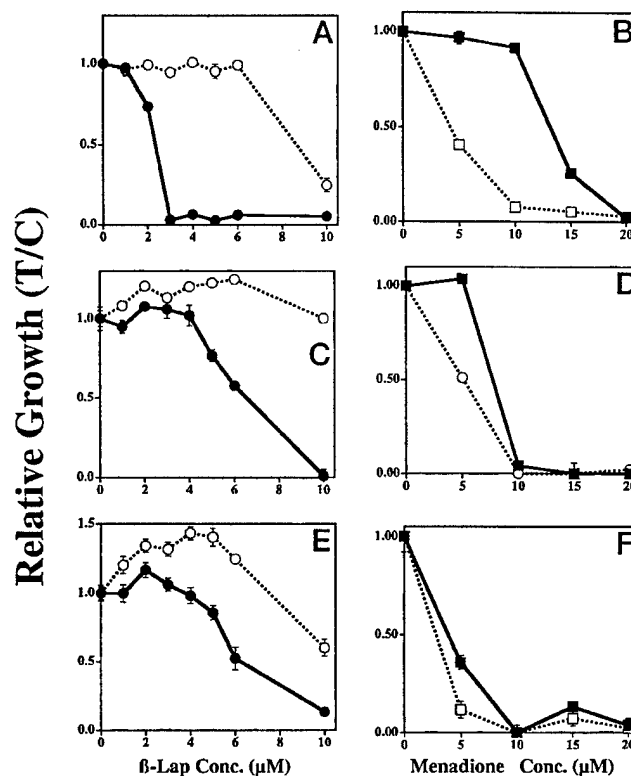[c] Both values from separate S9 preparations are shown.

β-Lap Conc. (µM)   Menadione Conc. (µM)

FIG. 2. **Relative growth inhibition of various breast cancer cell lines by β-lap or menadione.** Cells (MCF-7:WS8 (*A* and *B*), T47D:A18 (*C* and *D*) and MDA-MB-468 (*E* and *F*) were seeded into 96-well plates (1500 cells/well) and allowed to attach overnight. Media containing drugs (β-lap in *A*, *C*, and *E*; menadione in *B*, *D*, and *F*), either alone (β-lap (●) or menadione (■)) or in the presence of 50 µM dicoumarol (β-lap (○) or menadione (□)), were then added for 4 h. Media were then removed, fresh drug-free media were added, and the cells were allowed to grow for an additional 7 days. Relative DNA per well was then determined by Hoescht 33258 fluorescence, and relative growth (treated/control DNA) was plotted. Each point represents the mean of four independent wells ± S.E.

cancer cell lines (T47D:A18, MDA-MB-468, and MCF-7:WS8) were treated with a 4-h pulse of drugs, and relative growth was measured 7 days later (Fig. 2). Dicoumarol significantly inhibited β-lap toxicity in MCF-7:WS8 and T47D:A18 cells. In contrast, dicoumarol showed little or no protective effect in MDA-MB-468 cells (compare *graphs A, C*, and *E* in Fig. 2).

In a parallel experiment using menadione, alone or with dicoumarol, the relative sensitivities of the cell lines to menadione were opposite those found with β-lap; MCF-7:WS8 cells were the most resistant to menadione, and MDA-MB-468 cells
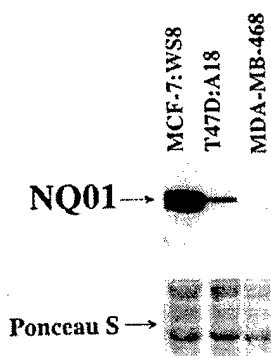
FIG. 3. NQO1 expression in various breast cancer cell lines. Whole cell extracts were prepared from exponentially growing cell lines. Equal protein was loaded into each lane and confirmed by Ponceau S staining. Proteins were separated by standard 10% SDS-polyacrylamide gel electrophoresis, transferred to Immobilon P, and probed with medium from an anti-NQO1 hybridoma followed by horseradish peroxidase-conjugated anti-mouse secondary antibody. Signals were visualized using Super Signal reagent as described under "Experimental Procedures." Shown is a representative blot from experiments performed at least three times.

were the most sensitive. Co-administration of dicoumarol caused a significant sensitization of MCF-7:WS8 cells to menadione toxicity, with a decrease in the relative IC_{50} from 12 to 3 μM. MDA-MB-468 cells, which were inherently more sensitive to menadione, were unaffected by dicoumarol co-administration. T47D:A18 cells were only minimally sensitized to menadione exposure when dicoumarol was co-administered (compare *graphs B, D*, and *F*; Fig. 2). These data were consistent with NQO1 expression (Fig. 3), where NQO1 protein levels were high in MCF-7:WS8 cells, moderate in T47D:A18 cells, and undetectable in MDA-MB-468 cells. NQO1 enzyme activities were consistent with protein levels (compare Fig. 3 and Table I). Using these cell extracts, we showed that β-lap could substitute for menadione in this *in vitro* assay, demonstrating that the compound was a suitable NQO1 substrate in intact cells (Fig. 9 and data not shown). These data demonstrated that both menadione and β-lap could serve as substrates for NQO1-mediated reduction and suggested that the end results of these reductions were opposite (*i.e.* menadione was inactivated by reduction, and β-lap was activated by reduction).

We previously showed that apoptosis in various human breast cancer cell lines induced by β-lap administration was unique, in that it caused a pattern of PARP and p53 cleavages distinct from that induced by other caspase-activating agents. After β-lap treatment, we observed a 60-kDa PARP fragment, which was probably due to the activation of a neutral, calcium-dependent protease with similar properties as calpain.[2] To investigate the effect of dicoumarol on this cleavage pattern in MCF-7:WS8 cells, we treated cells with a 4-h pulse of 8 μM β-lap alone or in the presence of 50 μM dicoumarol. Cells were lysed 20 h later, and PARP cleavage was monitored. We also investigated the effects of 1 μM staurosporine treatment, in order to determine if dicoumarol could block classic apoptotic proteolysis or if it was specific for β-lap-induced apoptosis. As seen in Fig. 4, dicoumarol completely abrogated atypical PARP cleavage after β-lap exposure but had no effect on staurosporine-induced classic PARP cleavage (*i.e.* formation of an 89-kDa PARP fragment (47)) in MCF-7:WS8 cells. The fact that dicoumarol significantly protected NQO1-expressing cells from β-lap-mediated apoptosis strongly suggested a role for NQO1 in β-lap toxicity. However, previous studies indicated that dicou-
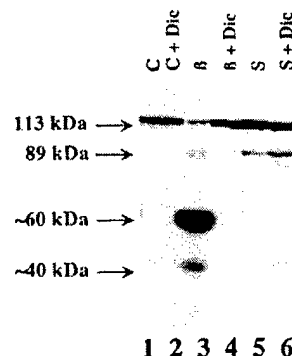
---

[2] J. J. Pink, S. Wuerzberger-Davis, C. Tagliarino, S. M. Planchon, X. Yang, C. J. Froelich, and D. A. Boothman (2000) *Exp. Cell Res.*, in press.

1 2 3 4 5 6

FIG. 4. Dicoumarol inhibition of β-lap-induced atypical PARP cleavage. MCF-7:WS8 cells were treated with a 4-h pulse of 8 μM β-lap (β, *lanes 3* and *4*) or a 24-h pulse of 1 μM staurosporine (*S, lanes 5* and *6*) either alone or with 50 μM dicoumarol during the time of drug exposure. Untreated cells (*C, lane 1*) or cells treated only with 50 μM dicoumarol (*C + Dic, lane 2*) were included as controls. Whole cell extracts were prepared at 24 h and analyzed using standard Western blot techniques as described for Fig. 3. The blot was probed with the C-2-10 anti-PARP monoclonal antibody followed by horseradish peroxidase-conjugated anti-mouse secondary antibody and visualized with Super Signal reagent. Shown is a representative blot from experiments performed at least three times.
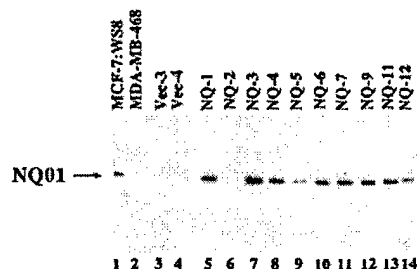

1 2 3 4 5 6 7 8 9 10 11 12 13 14

FIG. 5. NQO1 protein expression in MDA-MB-468 transfectants. Whole cell extracts were prepared from exponentially growing parental MCF-7:WS8 and MDA-MB-468 cells, two control vector alone MDA-MB-468 transfectants, and 10 NQO1 expression vector MDA-MB-468 transfectants. Equal amounts of protein were analyzed by standard Western blot techniques as described above using anti-NQO1 as described for Fig. 4. Shown is a representative blot from experiments performed at least three times.

marol may also inhibit other cellular enzymes (48).

In order to definitively demonstrate the role of NQO1 in β-lap toxicity, we utilized the NQO1-negative, β-lap-resistant, MDA-MB-468 cell line to determine if exogenous expression of NQO1 could sensitize these cells to β-lap. We stably transfected MDA-MB-468 cells with a constitutive NQO1 expression vector under the control of a cytomegalovirus promoter. We also performed a parallel transfection using the empty vector, pcDNA3. Following selection of a pooled population of G418-resistant cells, we isolated a number of clones by limiting dilution subcloning, as described under "Experimental Procedures." NQO1 expression in isolated clones was then determined by Western blot analyses (Fig. 5) and enzyme assays (Table II). In all cases, enzyme activity correlated with protein expression. As shown in Fig. 5 and Table II, the empty vector-containing clones did not demonstrate measurable NQO1 expression, as observed with parental, nontransfected cells (see *lanes 2, 3*, and *4*). Of the 10 clones isolated from the NQO1 transfections, nine exhibited NQO1 expression. Clone NQ-2 (*lane 6*) showed no measurable NQO1 expression.

We tested a number of the clones for β-lap and menadione sensitivity. Growth inhibition was measured after a 4-h pulse of drugs, either alone or in the presence of 50 μM dicoumarol. Relative growth of β-lap-treated compared with control cells (*T/C*) was determined 7 days after drug exposures, using DNA

TABLE II
NQO1 expression in MDA-MB-468 transfectants

Clone	NQO1 activity[a]
	nmol/min/mg
Vec-3	$<10^b$
NQ-1	$6555/8264^c$
NQ-2	$<10^b$
NQ-3	9276 ± 491^d
NQ-6	$14,684/18,511^c$
NQ-7	$11,341/12,332^c$

[a] Units are nmol of cytochrome *c* reduced per min per mg of protein.

[b] $<10_1$, NQO1 not detected. The difference in the rate of cytochrome *c* reduction with and without dicoumarol was not statistically significant, based on Student's *t* test.

[c] Both values from two separate S9 preparations.

[d] Average for three separate S9 preparations ± S.D.

FIG. 7. **Acute β-lap-mediated apoptosis requires NQO1 activity.** DNA fragmentation was assessed using the TUNEL assay, as described under "Experimental Procedures." Cells were exposed to a 4-h pulse of β-lap alone or in combination with 50 μM dicoumarol, and TUNEL assays were performed to monitor apoptosis 44 h later using the APO-DIRECT™ kit. Data were analyzed using an EPICS Elite ESP flow cytometer. Shown are the results of one experiment representative of at least three independent assays.

FIG. 6. **NQO1 expression sensitizes cells to acute β-lap cytotoxicity.** *A*, acute β-lap toxicity was determined using the control vector MDA-MB-468 transfectant (clone Vec-3) and five NQO1 vector-containing MDA-MB-468 transfectants, as described in Fig. 2. Note that clone NQ-2 showed no measurable NQO1 expression (Fig. 5 and Table II). Cells were exposed to a 4-h pulse of a range of β-lap doses either alone (●) or with 50 μM dicoumarol (○) and then allowed to grow for an additional 7 days, at which time DNA content for treated (*T*) cells was measured and plotted relative to control (*C*) cells. *B*, Vec-3 (■, □), NQ-1 (▲, △), and NQ-3 (●, ○) cells were treated with a 4-h pulse of a range of β-lap doses alone (■, ▲, ●) or with 50 μM dicoumarol (□, △, ○). Overall survival, as assessed by colony-forming ability, was measured after 10 days growth in control media. Shown is a representative graph from experiments performed at least three times with each group consisting of at least triplicate determinations. Differences between treatments were compared using a two-tailed Student's *t* test for paired samples and groups having *p* < 0.01 compared with β-lap or dicoumarol alone are indicated by an *asterisk*.

amount per well as an indicator of cell growth. In all cases, expression of NQO1 led to a marked increase in sensitivity to β-lap (see Fig. 6*A*). Co-administration of 50 μM dicoumarol selectively inhibited β-lap toxicity in all clones that expressed NQO1. Dicoumarol did not affect the relatively more β-lap-resistant Vec-3 or NQ-2 clones, which did not express NQO1.

Opposite results were observed after menadione treatments. Cells expressing NQO1 were more resistant to menadione than NQO1-negative clones, and resistance could be ameliorated by dicoumarol co-administration (data not shown). To demonstrate that this effect was not due simply to transient growth inhibition, we also measured clonogenic survival of the Vec-3, NQ-3, and NQ-7 clones after a 4-h treatment with β-lap alone or in the presence of 50 μM dicoumarol (Fig. 6*B*). Relative survival closely mimicked growth inhibition, demonstrating the sensitizing effect of NQO1 expression on β-lap cytotoxicity. These data clearly established that NQO1 activity was critical for the acute toxicity of β-lap.

To confirm that cell death occurred due to the induction of apoptosis in the NQO1 transfectants, we used TUNEL assays to measure DNA fragmentation due to apoptosis after β-lap treatment. Cells were treated with a 4-h pulse of 8 μM β-lap alone or in combination with 50 μM dicoumarol, harvested 48 h later, and monitored for apoptosis using TUNEL assays, where terminal deoxynucleotide transferase-mediated FITC-dUTP incorporation was measured. As shown in Fig. 7, Vec-3 cells showed less than 2% TUNEL-positive (apoptotic) cells after β-lap treatment. All NQO1-expressing clones showed between 30 and 70% TUNEL-positive cells. Dicoumarol co-administration completely blocked apoptosis-related DNA fragmentation in all of the NQO1-expressing MDA-MB-468 clones. These findings further demonstrated that while certain aspects of β-lap cytotoxicity were unique (*e.g.* atypical PARP cleavage), other aspects conform to the classic apoptotic pathway (*e.g.* DNA fragmentation, as measured by TUNEL assays and the presence of a sub-G_0/G_1 cell population (2)).

We next utilized a number of the NQO1-expressing MDA-MB-468 clones to determine if cytotoxicity equated with corresponding increases in atypical apoptotic proteolysis, as measured by PARP and p53 cleavage. NQO1-expressing clones were exposed to 8 μM β-lap for 4 h, and cell lysates were prepared 48 h later. As observed in Fig. 8*A*, clones with NQO1 expression (*i.e.* NQ-1, NQ-3, NQ-6, and NQ-7) demonstrated a prevalent 60-kDa PARP cleavage fragment after exposure to 8 μM β-lap. The NQO1-negative clone, Vec-3, exhibited no PARP cleavage
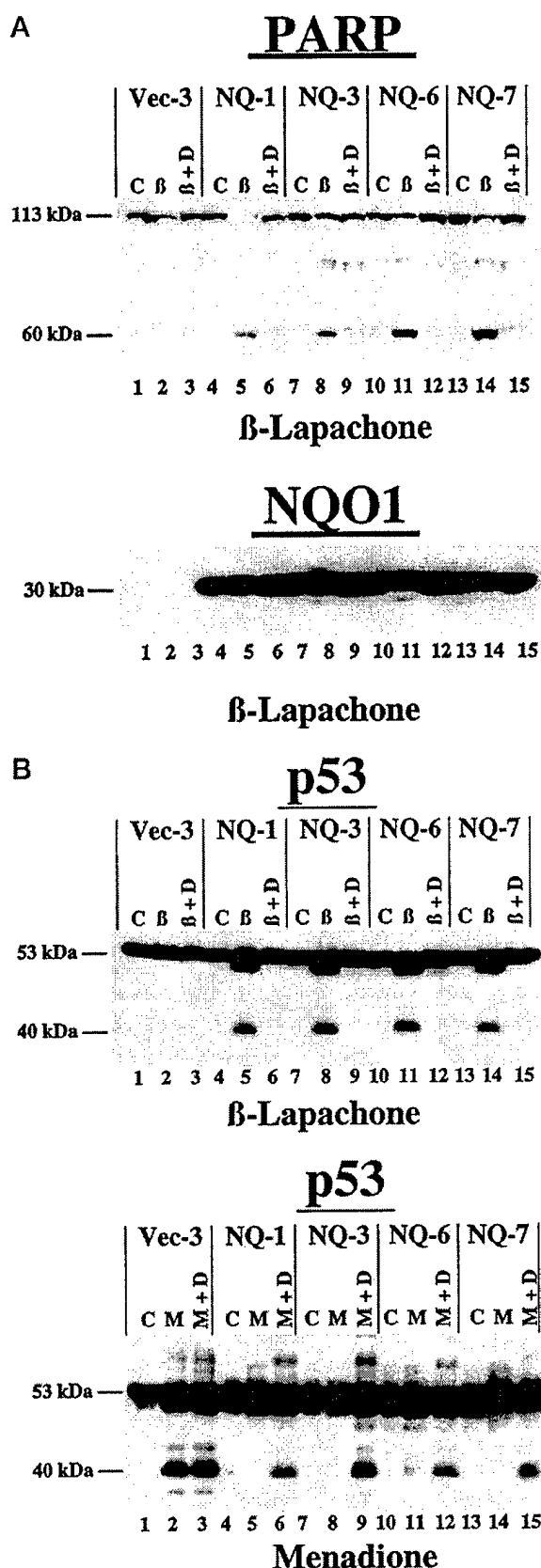
A

PARP

113 kDa —

60 kDa —

1 2 3 4 5 6 7 8 9 10 11 12 13 14 15

ß-Lapachone

NQO1

30 kDa —

1 2 3 4 5 6 7 8 9 10 11 12 13 14 15

ß-Lapachone

B

p53

53 kDa —

40 kDa —

1 2 3 4 5 6 7 8 9 10 11 12 13 14 15

ß-Lapachone

p53

53 kDa —

40 kDa —

1 2 3 4 5 6 7 8 9 10 11 12 13 14 15

Menadione

FIG. 8. **NQO1 expression sensitizes cells to β-lap-mediated apoptotic proteolysis and inhibits menadione-mediated apoptotic proteolysis.** Apoptotic proteolysis was measured in cells exposed to a 4-h pulse of 8 μM β-lap alone (β) or 8 μM menadione alone (M) or in combination with 50 μM dicoumarol (β + D and M + D, respectively). Whole cell extracts were prepared 44 h after drug treatment and ana-

at this β-lap dose. We noted cleavage of p53 (resulting in an ~40-kDa fragment) at the same β-lap dose that gave rise to the 60-kDa PARP fragment. Cells exposed to 10 μM menadione with or without dicoumarol showed an opposite pattern, as monitored by p53 and PARP cleavage (Fig. 8B and data not shown). Dicoumarol enhanced p53 cleavage after menadione exposure. Importantly, NQO1 expression also led to resistance to menadione-induced p53 cleavage, which could be reversed by co-administration of dicoumarol. Previous studies from our laboratory suggested that both the PARP and p53 cleavage events were the result of activation of the calcium-dependent protease, calpain.[2]

To further characterize the nature by which β-lap could serve as a substrate for NQO1, we measured NADH oxidation using a modified *in vitro* assay. Using purified recombinant human NQO1 or cell extracts containing NQO1, we measured the oxidation of NADH in the presence of either menadione or β-lap. This assay was different from that used to measure NQO1 activity in cell lysates (described in Tables I and II), in that a terminal electron acceptor (*i.e.* cytochrome c) was not included in the reaction. If the substrates (menadione or β-lap) were utilized once in the enzyme reaction, the compounds could not reduce a terminal electron acceptor and would thereby presumably accumulate in their respective hydroquinone forms. This would result in oxidation of 1 mol of NADH/mol of quinone reduced. As expected, menadione reduction resulted in the oxidation of 1–3 mol of NADH/mol of menadione in 2 min and 3–4 mol of NADH/mol of menadione in 3 min using S9 extracts from MCF-7:WS8 or NQ-3 cells (Fig. 9 and data not shown). β-lap resulted in the oxidation of 10–20 mol of NADH/ mol of β-lap in 2 min and 50–60 mol of NADH/mol of β-lap in 3 min (Fig. 9). The relative NADH oxidation with β-lap may be an underestimate of β-lap-mediated NADH oxidation, due to exhaustion of reduced NADH at later time points. Using purified NQO1, this effect was even more pronounced, giving rise to oxidation of 10 mol of NADH/mol of β-lap in 10 s and 100 mol of NADH/mol of β-lap in 10 min (data not shown). These results strongly suggest that the hydroquinone form of β-lap is unstable and rapidly undergoes autoxidation to the parent quinone, which can again serve as substrate for reduction by NQO1.

DISCUSSION

We demonstrated that β-lap cytotoxicity is dependent upon the expression of the obligate two-electron reductase, NQO1. Dicoumarol, an NQO1 inhibitor, significantly protected NQO1-expressing breast cancer cell lines against all tested aspects of β-lap toxicity, including cell death. Overall, NQO1 expression correlated well with sensitivity of various breast cancer cell lines to the effects of β-lap. Use of the redox cycling compound menadione, which is detoxified by NQO1, demonstrated that the protection offered by dicoumarol is not the result of a global apoptotic inhibition, since dicoumarol significantly enhanced the cytotoxicity of menadione, in cells that expressed NQO1 (Fig. 2). Dicoumarol also did not protect against staurosporine-induced apoptosis, instead demonstrating a very modest enhancement of PARP cleavage. The nature of this response is unknown but may involve signaling through the MEKK1 pathway, as recently described by Cross *et al.* (49). In addition, the relative sensitivities of the cell lines to menadione were oppo-

lyzed using standard Western blot techniques. *A*, PARP cleavage was assessed using the C-2-10 monoclonal antibody, the blots were then stripped and reprobed with the anti-NQO1 antibody. *B*, cells were treated with either β-lap or menadione for 4 h and then probed with a p53 antibody (DO-1). Equal protein loading was assessed by Ponceau S staining as described under "Experimental Procedures." Shown is a representative blot from experiments performed at least three times.
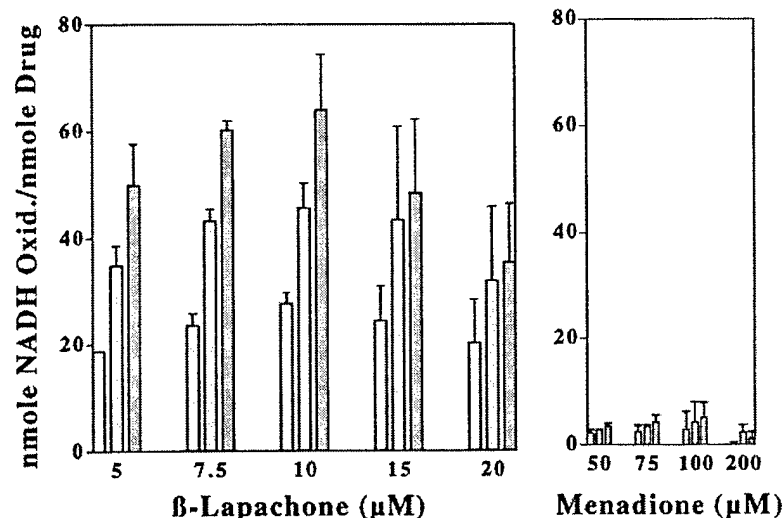
FIG. 9. **β-lap-mediated NADH oxidation and futile cycling by NQO1-containing cell extracts.** S9 extracts prepared from MCF-7:WS8 cells served as a source for NQO1 and were mixed with 500 μM NADH in 50 mM Tris-HCl, pH 7.5, as described under "Experimental Procedures." Reactions were initiated by adding β-lap or menadione, and changes in absorbance at 340 nm (NADH absorbs at 340; NAD+ does not) were measured over time for 3 min. Total loss of NADH was then calculated and divided by the concentration of β-lap or menadione used. This ratio was then plotted as a function of β-lap or menadione concentration after 1 (*light bars*), 2 (*darker bars*), and 3 (*darkest bars*) min. Shown is a representative graph from experiments repeated at least two times.

site those of β-lap, demonstrating that the β-lap-sensitive cells were not merely sensitive to unrelated cytotoxic compounds. Exogenous expression of NQO1, in NQO1-deficient MDA-MB-468 cells, shifted the LD_{99} from >10 μM to less than 4 μM. While this shift may appear modest, the dose-response curves for both growth inhibition and survival after β-lap treatment were extremely steep. At 4 μM β-lap, 60% of the NQO1-negative cells survived, whereas less than 0.05% survival was noted in cells transfected with NQO1. A similarly steep curve was noted with growth inhibition, where treatment with 4 μM β-lap led to greater than 90% growth in the NQO1-negative cells and undetectable growth in the NQO1-expressing cells. In both survival and growth measurements, addition of 50 μM dicoumarol protected NQO1-expressing cells completely and resulted in values nearly equal to that observed in untreated cells. While these findings suggest that β-lap should show considerable activity against NQO1 expressing tumors, the dose-response curves indicate that the overall drug exposure will undoubtedly need to be closely monitored if this drug is to prove clinically useful.

β-lap may be activated by NQO1 in a manner analogous to that of MMC or EO9 (50, 51). However, unlike MMC (52), there is no indication of direct DNA damage by β-lap as assessed by p53 induction, alkaline or neutral filter elution, or covalent complex protein-DNA formation (2, 53, 54). Most specific demonstrations of β-lap activity have come from *in vitro* assays. For example, topoisomerase IIα-mediated DNA damage has been observed *in vitro* after treatment with either β-lap or menadione (10). However, the expected downstream effects of this damage (*e.g.* p53 induction, DNA-topoisomerase IIα complexes, etc.) have not been observed (1, 2). In addition, we previously showed that topoisomerase I could be inhibited or activated *in vitro* in a manner distinct from that of the classic topoisomerase I inhibitor, camptothecin (1). Neither "cleavable complex" formation (8) nor increases in the steady state levels of wild-type p53 were observed following β-lap treatment. In contrast, camptothecin or topoisomerase IIα inhibitors caused a dramatic increase in p53, as previously reported (1, 55). The observations reported here suggest that β-lap must either be activated (reduced) to inhibit topoisomerases I or IIα or that topoisomerase inhibition is not a necessary component of β-lap-mediated cytotoxicity.

One particularly unique aspect of β-lap toxicity is the apparent activation of a novel protease, which we first discerned by observation of an atypical cleavage pattern of the DNA repair protein and apoptotic substrate, PARP.[2] This pattern (giving rise to an ~60-kDa fragment instead of the classic 89-kDa fragment) was unique to β-lap-mediated apoptosis and correlated well with lethality. In addition, investigation of p53 proteolysis after β-lap treatment showed a fragment of ~40 kDa (Fig. 7B), which was similar to that previously attributed to calpain activation (56). Calpain has been implicated in apoptosis in a number of systems (57–59), and we hypothesize that calpain is the primary protease activated in β-lap-mediated cell death.[2] The data regarding the role of calpain as an inducer of apoptosis or simply a component of the execution phase of apoptosis appear to depend upon the cell type and method of apoptosis induction. The demonstration of menadione-induced p53 cleavage (Fig. 8) suggests that this proteolytic pathway is not unique to β-lap. Enhancement of menadione-mediated proteolysis by dicoumarol suggests that the hydroquinone form of menadione is a nontoxic species or is rapidly conjugated and excreted from the cell and does not activate this cell death pathway (60). However, when menadione is reduced to the semiquinone, in the absence of NQO1 activity, it can also undergo a futile cycle, leading to the loss of reduced NAD(P)H (61). This futile cycle is less potent than the β-lap futile cycling but can be activated by high concentrations of menadione in NQO1 expressing cells and lower menadione concentrations in cells lacking NQO1 activity.

While reduction of β-lap appears to be important for its cytotoxic effects against breast cancer cells, the mechanism by which reduction of β-lap leads to toxicity is still unresolved. Our findings regarding the futile cycling of β-lap suggest a possible component of the cytotoxic mechanism. β-lap-mediated exhaustion of NADH in the *in vitro* studies (Fig. 8) suggests that the hydroquinone form of β-lap is unstable and autoxidizes back to the parent compound. In an intact cell, this futile cycle would be expected to continue until one of the critical components of the reaction is exhausted (Fig. 10). Since NQO1 can utilize either NADH or NADPH as electron donors, this futile cycle could lead to a substantial loss of NADH and NADPH with a concomitant rise in NAD+ and NADP+ levels. This would have a dramatic effect on any cellular process
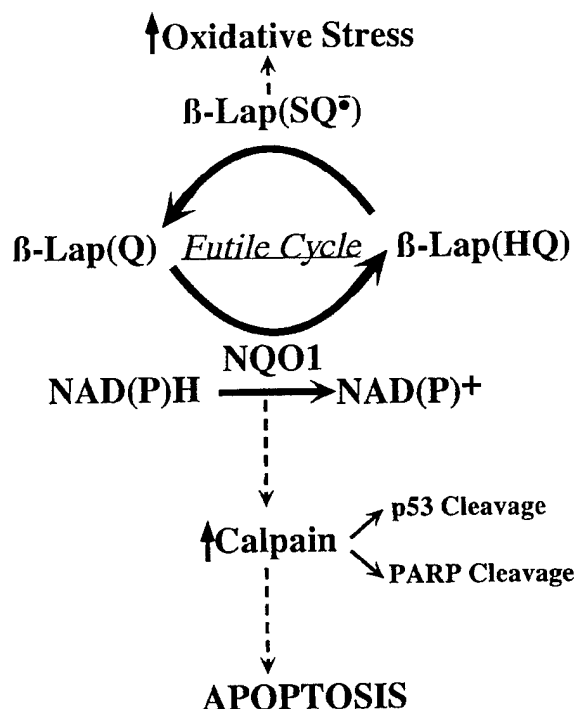
↑Oxidative Stress

ß-Lap(SQ•)

ß-Lap(Q) *Futile Cycle* **ß-Lap(HQ)**

NQO1
NAD(P)H ────→**NAD(P)+**

↑Calpain ⟨ p53 Cleavage
⟨ PARP Cleavage

APOPTOSIS

FIG. 10. **Proposed model for β-lapachone-mediated cytotoxicity in cells expressing NQO1.** In cells that express NQO1, the 1,2-naphthoquinone β-lap(Q) is reduced to the hydroquinone form (β-lap(HQ)) using one molecule of NADH per reaction. The hydroquinone form of β-lap is presumably unstable and spontaneously autoxidizes to its original parent form, probably through a semiquinone intermediate (β-lap (SQ⁻), which can cause redox cycling and oxidative stress. The regenerated parent compound can then serve as substrate for another round of reduction. This futile cycle causes a rapid and severe loss in reduced NAD(P)H, which ultimately activates calpain by mechanisms that are not completely understood at present.

requiring NADH or NADPH. It is likely that this exhaustion of reduced enzyme co-factors may be a critical factor for the activation of the apoptotic pathway after β-lap treatment. The downstream consequences of this futile cycle are currently under investigation in our laboratory.

At higher doses of β-lap (>10 μM), NQO1-negative cells and NQO1-expressing cells treated with dicoumarol were killed by β-lap. This may be due to the production of oxidative stress, as a result of one electron reduction of β-lap by other enzymes, such as cytochrome b_5 reductase and/or cytochrome P-450 reductase (62). One electron reduction of β-lap to the semiquinone would be expected to cause extensive redox cycling with the formation of various reactive oxygen species, and previous studies showed that β-lap caused oxygen radical formation in trypanosomes (63, 64). We speculate that β-lap-mediated free radical formation can be lethal to NQO1-deficient cells, as we previously reported with HL60 cells. The result in these studies was stimulation of a caspase-mediated death pathway (1). This hypothesis is supported by a recent study that showed that β-lap can induce apoptosis in HL-60 cells through peroxide production (65). Alternatively, other members of the NQO1 family that are insensitive to dicoumarol, such as NQO2 (66, 67), may be present and reduce (i.e. activate) β-lap when administered at high doses. However, we hypothesize that the production of cytosolic free radicals is not a primary mode of cell death in NQO1-expressing cells, since free radical scavengers (e.g. α-tocopherol, N-acetyl-L-cysteine, or pyrrolidinedithiocarbamate) did not significantly affect lethality caused by β-lap exposure (data not shown). The free radical-driven path-

ways may predominate in NQO1-negative cells or in cells with inactivated NQO1. We propose that when active NQO1 is present, the pathway described in Fig. 10 is primarily responsible for cell death.

Our data identifying the intracellular target of β-lap as NQO1 may explain the myriad of *in vitro* and *in vivo* responses reported for this compound. β-lap exposure synergizes with MMS, ionizing radiation, and ultraviolet light irradiation damage (68). We speculate that the synergy between this compound and these DNA damaging agents is related to the induction of NQO1 (cloned as xip-3, an x-ray-inducible protein by our laboratory (18) and that of Fornace *et al.* (69)). This is further supported by the fact that only posttreatments of 4–5 h, and not pretreatments, with β-lap caused synergistic cell killing. Induction of β-lap's target may have been required for synergy, and the induction kinetics of NQO1/XIP3 after ultraviolet light or ionizing radiation exposures (*i.e.* ~2 h) appear to fit this mechanism (18). β-lap exposure also prevented the formation of ionizing radiation-inducible secondary neoplastic transformants in Chinese hamster embryo fibroblasts (53). Since NQO1 expression is thought to increase during early stages of neoplastic initiation (possibly due to the permanent induction of a normal stress response, *i.e.* induction of NQO1) (70, 71), it is possible that β-lap administration selectively eliminates genetically damaged cells that constitutively overexpress this preneoplasic marker (*i.e.* NQO1). These data suggest that it may be possible to exploit this IR-inducible NQO1 target protein for improved radiochemotherapy, which would also result in a significantly lower level of IR-induced secondary carcinogenesis, as previously reported (53).

Thus, our data strongly suggest that NQO1 expression is an important determinant of β-lap-mediated apoptosis and lethality. The connection between the futile cycle of oxidation and reduction of β-lap by NQO1 and the activation of calpain-mediated apoptosis (Fig. 10) is currently under investigation in our laboratory. Investigation of this drug should shed light on calpain-mediated cell death processes and yield clinical regimens using β-lap or more efficient drugs in combination with DNA-damaging agents (*e.g.* radiotherapy). Use of this drug against tumors that overexpress NQO1, such as breast, colon, or lung cancers, is indicated. Identification of NQO1 as the intracellular target of β-lap also suggests the use of this compound for chemoprevention, since NQO1 is commonly elevated during neoplastic progression (43).

REFERENCES

1. Planchon, S. M., Wuerzberger, S., Frydman, B., Witiak, D. T., Hutson, P., Church, D. R., Wilding, G., and Boothman, D. A. (1995) *Cancer Res.* **55**, 3706–3711
2. Wuerzberger, S. M., Pink, J. J., Planchon, S. M., Byers, K. L., Bornmann, W. G., and Boothman, D. A. (1998) *Cancer Res.* **58**, 1876–1885
3. Li, C. J., Averboukh, L., and Pardee, A. B. (1993) *J. Biol. Chem.* **268**, 22463–22468
4. Boothman, D. A., Greer, S., and Pardee, A. B. (1987) *Cancer Res.* **47**, 5361–5366
5. Schuerch, A. R., and Wehrli, W. (1978) *Eur. J. Biochem.* **84**, 197–205
6. Docampo, R., Cruz, F. S., Boveris, A., Muniz, R. P., and Esquivel, D. M. (1979) *Biochem. Pharmacol.* **28**, 723–728
7. Boorstein, R. J., and Pardee, A. B. (1983) *Biochem. Biophys. Res. Commun.* **117**, 30–36
8. Boothman, D. A., Trask, D. K., and Pardee, A. B. (1989) *Cancer Res.* **49**, 605–612
9. Molina Portela, M. P., and Stoppani, A. O. (1996) *Biochem. Pharmacol.* **51**, 275–283
10. Frydman, B., Marton, L. J., Sun, J. S., Neder, K., Witiak, D. T., Liu, A. A., Wang, H. M., Mao, Y., Wu, H. Y., Sanders, M. M., and Liu, L. F. (1997) *Cancer Res.* **57**, 620–627
11. Vanni, A., Fiore, M., De Salvia, R., Cundari, E., Ricordy, R., Ceccarelli, R., and Degrassi, F. (1998) *Mutat. Res.* **401**, 55–63
12. Manna, S. K., Gad, Y. P., Mukhopadhyay, A., and Aggarwal, B. B. (1999)

Biochem. Pharmacol. **57**, 763–774

13. Robertson, N., Haigh, A., Adams, G. E., and Stratford, I. J. (1994) *Eur. J. Cancer* **30A**, 1013–1019

14. Cadenas, E. (1995) *Biochem. Pharmacol.* **49**, 127–140

15. Ross, D., Beall, H., Traver, R. D., Siegel, D., Phillips, R. M., and Gibson, N. W. (1994) *Oncol. Res.* **6**, 493–500

16. Rauth, A. M., Goldberg, Z., and Misra, V. (1997) *Oncol. Res.* **9**, 339–349

17. Ross, D., Siegel, D., Beall, H., Prakash, A. S., Mulcahy, R. T., and Gibson, N. W. (1993) *Cancer Metastasis Rev.* **12**, 83–101

18. Boothman, D. A., Meyers, M., Fukunaga, N., and Lee, S. W. (1993) *Proc. Natl. Acad. Sci. U. S. A.* **90**, 7200–7204

19. Chen, S., Knox, R., Lewis, A. D., Friedlos, F., Workman, P., Deng, P. S., Fung, M., Ebenstein, D., Wu, K., and Tsai, T. M. (1995) *Mol. Pharmacol.* **47**, 934–939

20. Jaiswal, A. K., McBride, O. W., Adesnik, M., and Nebert, D. W. (1988) *J. Biol. Chem.* **263**, 13572–13578

21. Radjendirane, V., Joseph, P., Lee, Y. H., Kimura, S., Klein-Szanto, A. J. P., Gonzalez, F. J., and Jaiswal, A. K. (1998) *J. Biol. Chem.* **273**, 7382–7389

22. Marin, A., Lopez de Cerain, A., Hamilton, E., Lewis, A. D., Martinez-Penuela, J. M., Idoate, M. A., and Bello, J. (1997) *Br. J. Cancer* **76**, 923–929

23. Malkinson, A. M., Siegel, D., Forrest, G. L., Gazdar, A. F., Oie, H. K., Chan, D. C., Bunn, P. A., Mabry, M., Dykes, D. J., Harrison, S. D., and Ross, D. (1992) *Cancer Res.* **52**, 4752–4757

24. Belinsky, M., and Jaiswal, A. K. (1993) *Cancer Metastasis Rev.* **12**, 103–117

25. Joseph, P., Xie, T., Xu, Y., and Jaiswal, A. K. (1994) *Oncol. Res.* **6**, 525–532

26. Buettner, G. R. (1993) *Arch. Biochem. Biophys.* **300**, 535–543

27. Ross, D., Thor, H., Orrenius, S., and Moldeus, P. (1985) *Chem. Biol. Interact.* **55**, 177–184

28. Riley, R. J., and Workman, P. (1992) *Biochem. Pharmacol.* **43**, 1657–1669

29. Siegel, D., Beall, H., Senekowitsch, C., Kasai, M., Arai, H., Gibson, N. W., and Ross, D. (1992) *Biochemistry* **31**, 7879–7885

30. Prakash, A. S., Beall, H., Ross, D., and Gibson, N. W. (1993) *Biochemistry* **32**, 5518–5525

31. Fitzsimmons, S. A., Workman, P., Grever, M., Paull, K., Camalier, R., and Lewis, A. D. (1996) *J. Natl. Cancer Inst.* **88**, 259–269

32. Beall, H. D., Murphy, A. M., Siegel, D., Hargreaves, R. H., Butler, J., and Ross, D. (1995) *Mol. Pharmacol.* **48**, 499–504

33. Hollander, P. M., and Ernster, L. (1975) *Arch. Biochem. Biophys.* **169**, 560–567

34. Hosoda, S., Nakamura, W., and Hayashi, K. (1974) *J. Biol. Chem.* **249**, 6416–6423

35. Duthie, S. J., and Grant, M. H. (1989) *Br. J. Cancer* **60**, 566–571

36. Akman, S. A., Doroshow, J. H., Dietrich, M. F., Chlebowski, R. T., and Block, J. S. (1987) *J. Pharmacol. Exp. Ther.* **240**, 486–491

37. Thor, H., Smith, M. T., Hartzell, P., Bellomo, G., Jewell, S. A., and Orrenius, S. (1982) *J. Biol. Chem.* **257**, 12419–12425

38. Siegel, D., McGuinness, S. M., Winski, S. L., and Ross, D. (1999) *Pharmacogenetics* **9**, 113–121

39. Gustafson, D. L., Beall, H. D., Bolton, E. M., Ross, D., and Waldren, C. A. (1996) *Mol. Pharmacol.* **50**, 728–735

40. Sambrook, J., Fritsch, E. F., and Maniatis, T. (1989) *Molecular Cloning: A Laboratory Manual*, pp. 16.33–16.36, Cold Spring Harbor Laboratory, Cold Spring Harbor, NY

41. Pink, J. J., Bilimoria, M. M., Assikis, J., and Jordan, V. C. (1996) *Br. J. Cancer* **74**, 1227–1236

42. Labarca, C., and Paigen, K. (1980) *Anal. Biochem.* **102**, 344–352

43. Siegel, D., Franklin, W. A., and Ross, D. (1998) *Clin. Cancer Res.* **4**, 2065–2070

44. Hollander, P. M., Bartfai, T., and Gatt, S. (1975) *Arch. Biochem. Biophys.* **169**, 568–576

45. Strobel, H. W., and Dignam, J. D. (1978) *Methods Enzymol.* **52**, 89–96

46. Beall, H. D., Mulcahy, R. T., Siegel, D., Traver, R. D., Gibson, N. W., and Ross, D. (1994) *Cancer Res.* **54**, 3196–3201

47. Kaufmann, S. H., Desnoyers, S., Ottaviano, Y., Davidson, N. E., and Poirier, G. G. (1993) *Cancer Res.* **53**, 3976–3985

48. Preusch, P. C., Siegel, D., Gibson, N. W., and Ross, D. (1991) *Free Radical Biol. Med.* **11**, 77–80

49. Cross, J. V., Deak, J. C., Rich, E. A., Qian, Y., Lewis, M., Parrott, L. A., Mochida, K., Gustafson, D., Vande Pol, S., and Templeton, D. J. (1999) *J. Biol. Chem.* **274**, 31150–31154

50. Siegel, D., Gibson, N. W., Preusch, P. C., and Ross, D. (1990) *Cancer Res.* **50**, 7483–7489

51. Keyes, S. R., Fracasso, P. M., Heimbrook, D. C., Rockwell, S., Sligar, S. G., and Sartorelli, A. C. (1984) *Cancer Res.* **44**, 5638–5643

52. Hess, R., Plaumann, B., Lutum, A. S., Haessler, C., Heinz, B., Fritsche, M., and Brandner, G. (1994) *Toxicol. Lett.* **72**, 43–52

53. Boothman, D. A., and Pardee, A. B. (1989) *Proc. Natl. Acad. Sci. U. S. A.* **86**, 4963–4967

54. Boothman, D. A., Wang, M., Schea, R. A., Burrows, H. L., Strickfaden, S., and Owens, J. K. (1992) *Int. J. Radiat. Oncol. Biol. Phys.* **24**, 939–948

55. Nelson, W. G., and Kastan, M. B. (1994) *Mol. Cell. Biol.* **14**, 1815–1823

56. Kubbutat, M. H., and Vousden, K. H. (1997) *Mol. Cell. Biol.* **17**, 460–468

57. Squier, M. K., and Cohen, J. J. (1997) *J. Immunol.* **158**, 3690–3697

58. Wood, D. E., and Newcomb, E. W. (1999) *J. Biol. Chem.* **274**, 8309–8315

59. Squier, M. K., Sehnert, A. J., Sellins, K. S., Malkinson, A. M., Takano, E., and Cohen, J. J. (1999) *J. Cell. Physiol.* **178**, 311–319

60. Wefers, H., and Sies, H. (1983) *Arch. Biochem. Biophys.* **224**, 568–578

61. Bellomo, G., Jewell, S. A., and Orrenius, S. (1982) *J. Biol. Chem.* **257**, 11558–11562

62. Iyanagi, T. (1990) *Free Radical Res. Commun.* **8**, 259–268

63. Molina Portela, M. P., Fernandez Villamil, S. H., Perissinotti, L. J., and Stoppani, A. O. (1996) *Biochem. Pharmacol.* **52**, 1875–1882

64. Docampo, R., Cruz, F. S., Boveris, A., Muniz, R. P., and Esquivel, D. M. (1978) *Arch. Biochem. Biophys.* **186**, 292–297

65. Chau, Y. P., Shiah, S. G., Don, M. J., and Kuo, M. L. (1998) *Free Radical Biol. Med.* **24**, 660–670

66. Zhao, Q., Yang, X. L., Holtzclaw, W. D., and Talalay, P. (1997) *Proc. Natl. Acad. Sci. U. S. A.* **94**, 1669–1674

67. Jaiswal, A. K. (1994) *J. Biol. Chem.* **269**, 14502–14508

68. Boorstein, R. J., and Pardee, A. B. (1984) *Biochem. Biophys. Res. Commun.* **118**, 828–834

69. Fornace, A. J., Jr., Alamo, I., Jr., and Hollander, M. C. (1988) *Proc. Natl. Acad. Sci. U. S. A.* **85**, 8800–8804

70. Williams, J. B., Wang, R., Lu, A. Y., and Pickett, C. B. (1984) *Arch. Biochem. Biophys.* **232**, 408–413

71. Farber, E. (1984) *Can. J. Biochem. Cell Biol.* **62**, 486–494

Activation of a Cysteine Protease in MCF-7 and T47D Breast Cancer Cells during β-Lapachone-Mediated Apoptosis

John J. Pink,*,1 Shelly Wuerzberger-Davis,*,1 Colleen Tagliarino,* Sarah M. Planchon,* XiaoHe Yang,†
Christopher J. Froelich,† and David A. Boothman*,2

*Laboratory of Molecular Stress Responses, Department of Radiation Oncology, Case Western Reserve University, Cleveland, Ohio 44106;
and †Evanston Northwestern Healthcare Research Institute, Evanston, Illinois 60201

β-Lapachone (β-lap) effectively killed MCF-7 and T47D cell lines via apoptosis in a cell-cycle-independent manner. However, the mechanism by which this compound activated downstream proteolytic execution processes were studied. At low concentrations, β-lap activated the caspase-mediated pathway, similar to the topoisomerase I poison, topotecan; apoptotic reactions caused by both agents at these doses were inhibited by zVAD-fmk. However at higher doses of β-lap, a novel non-caspase-mediated "atypical" cleavage of PARP (i.e., an ~60-kDa cleavage fragment) was observed. Atypical PARP cleavage directly correlated with apoptosis in MCF-7 cells and was inhibited by the global cysteine protease inhibitors iodoacetamide and N-ethylmaleimide. This cleavage was insensitive to inhibitors of caspases, granzyme B, cathepsins B and L, trypsin, and chymotrypsin-like proteases. The protease responsible appears to be calcium-dependent and the concomitant cleavage of PARP and p53 was consistent with a β-lap-mediated activation of calpain. β-Lap exposure also stimulated the cleavage of lamin B, a putative caspase 6 substrate. Reexpression of procaspase-3 into caspase-3-null MCF-7 cells did not affect this atypical PARP proteolytic pathway. These findings demonstrate that β-lap kills cells through the cell-cycle-independent activation of a noncaspase proteolytic pathway.   © 2000 Academic Press

Key Words: apoptosis; β-lapachone; caspase; breast cancer; poly(ADP)-ribose polymerase; PARP; calpain; topotecan.

INTRODUCTION

The execution phase of apoptosis culminates in the activation of a cascade of specific cysteine proteases which cleave following aspartate residues in target proteins. These proteases, named caspases [1], comprise a family of zymogens that are converted to activated proteases by specific cleavage reactions. Substrate cleavage products include the 89-kDa fragment of poly(ADP-ribose) polymerase (PARP), the 46-kDa polypeptide of lamin B, the ~100-kDa C-terminally or ~68-kDa internally cleaved polypeptides of retinoblastoma protein (pRb), and the ~68-kDa fragment derived from Sp1 [2–5]. The cleavage sites within some apoptotic death substrates have been precisely mapped and used to design inhibitors of the caspases, such as zVAD-fmk and DEVD-fmk, which were developed using the recognition sites for caspases-1 and -3, respectively [6]. In contrast, the global cysteine protease inhibitors iodoacetamide and N-ethylmaleimide react directly with active site cysteines and thereby inhibit all cysteine proteases, as well as other enzymes that contain accessible –SH groups [7, 8].

While a great deal of information regarding the action of caspases during apoptosis has been generated, less is known about alternate apoptotic proteolytic pathways that are activated after treatment with various cytotoxic agents. A number of reports have shown that the neutral calcium-dependent protease calpain can be activated during apoptosis [9–11]; a key *in vivo* target of calpain appears to be p53. Other reports have demonstrated the activation of noncaspase proteases, such as the nuclear scaffold protease [12, 13] and unknown serine proteases during apoptosis [14, 15]. The serine protease(s) described in these studies appeared to be distinct from granzyme B, which induces apoptosis through caspase activation [16].

β-Lapachone (β-lap) is a naturally occurring 1,2-naphthoquinone initially isolated from the bark of the lapacho tree, native to South America. We previously demonstrated that this drug is a radiosensitizing agent against human laryngeal carcinoma and melanoma cell lines [17]. Using cell-free assays, β-lap inhibited topoisomerase I (Topo I) by a mechanism quite different from that of camptothecin (CPT) or the related compounds topotecan (TPT), 9-aminocamptothecin, or

(T) by that of untreated cells (C) at identical times. Data points represent the means ± SEM of at least four replicate wells. All experiments were performed at least three times.

Western immunoblot analyses. Whole-cell extracts were prepared by direct lysis of PBS-washed cells (both floating and attached cells were pooled) in PARP extraction buffer [6 M urea, 2% SDS, 10% glycerol, 62.5 mM Tris–HCl (pH 6.8), 5% β-mercaptoethanol, and 5 mg/ml bromphenol blue]. Samples were then sonicated with a 15-s burst using a Fisher 550 sonic dismembrator. Equal amounts of protein were heated at 65°C for 10 min and separated by 10% SDS–PAGE. Separated proteins were transferred to Immobilon-P (Millipore Corp., Bedford, MA) membranes using a Multiphor II semidry electroblotting device (Pharmacia Biotech Inc., Piscataway, NJ) according to the manufacturer's instructions. Loading equivalence and transfer efficiency were monitored by Ponceau S staining of transferred membranes. Standard Western immunoblotting techniques were used to probe for various steady-state protein levels as indicated and previously described [18, 24]. Proteins of interest were visualized with ECL using the Super Signal chemiluminescence reagent (Pierce Chemical Co., Rockford, IL) at 20°C for 5 min. Membranes were exposed to X-ray film and developed. Gels shown represent results of experiments repeated at least three times.

Flow cytometry. Flow cytometric analyses of breast cancer cell lines before and after β-lap or TPT treatments were performed as previously described [18, 24]. TUNEL assays were performed using the APO-DIRECT kit (Phoenix Flow Systems, Inc., San Diego, CA). The samples were read in a EPICS Elite ESP flow cytometer using an air-cooled argon laser at 488 nm, 15 mW (Beckman Coulter Electronics, Miami, FL). Propidium iodide was read at 640 nm using a long-pass optical filter and FITC was read at 525 nm using a band-pass filter. Analyses were performed using the Elite acquisition software provided with the instrument.

Retroviral-mediated stable expression of caspase 3 in MCF-7 cells. The pBabe/puro/cpp32 plasmid was constructed by treating the *Bam*HI/*Pst*I cpp32 cDNA insert from the pBS/cpp32 plasmid (a generous gift from Dr. Vishva Dixit, Genentech, Inc.) with T4 DNA polymerase and then subcloning into the blunt-ended pBabe/puro vector.

MCF-7 cells (3×10^5 cells/plate) were seeded and allowed to grow overnight. The pBabe/puro retroviral vector (a generous gift from Dr. T. Sladek, Chicago Medical School) (2 μg/plate) encoding cpp32 (caspase-3) cDNA or empty vector was mixed with 10 μl of LipofectAMINE (Life Technologies, Gaithersburg, MD) and transfected into cells according to the manufacturer's instructions. After transfection (24 h), cells were split, diluted, and inoculated into 96-well plates. Transfected cells were selected with 2 μg/ml puromycin. Individual clones were screened by immunoblot analysis of caspase-3 expression and positive clones (5 of 12) were pooled for further characterization. A single caspase-3-expressing clone was selected for investigation.

RESULTS

Relative drug sensitivities. Log-phase MCF-7 and T47D breast cancer cells were exposed to a range of β-lap or TPT doses for 48 h and cell numbers were compared (using DNA content measurements) to untreated, log-phase growing control cells as described under Materials and Methods (Fig. 1). At higher doses, MCF-7 cells were more sensitive to β-lap ($IC_{75} = 3.5$ μM) than were T47D cells ($IC_{75} = 7.0$ μM); however, the IC_{50} dose was very similar in both cell lines. In contrast, T47D cells were more sensitive to TPT at all doses tested, with IC_{50} and IC_{75} values of 20 and 500
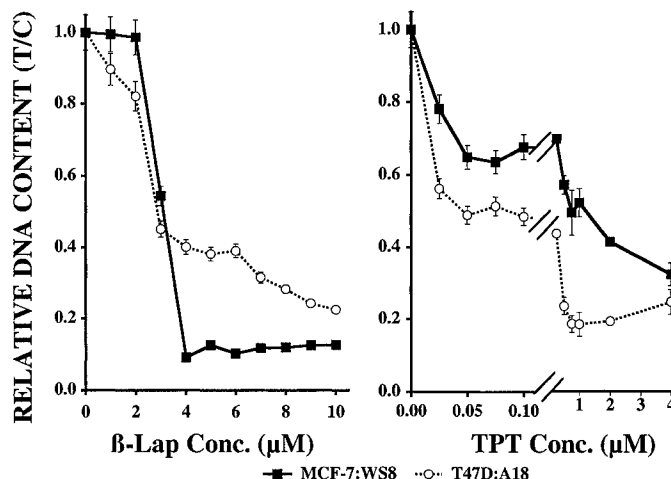

FIG. 1. Sensitivities of breast cancer cells to β-lap or TPT. Cells were seeded into 96-well tissue culture plates (1.5×10^3 cells/well) and allowed to attach overnight. Drugs were then added and cells were allowed to grow for an additional 48 h, as described under Materials and Methods. Cell number was assessed using Hoechst 33258 fluorescence, and relative growth inhibition (Relative DNA Content T/C) was calculated. Shown are toxicities for MCF-7 (■) and T47D (○) cell lines exposed to various concentrations of β-lap or TPT. Data shown are representative of at least two experiments expressed as means ± SEM of at least four replicate wells.

nM, respectively, compared with MCF-7 cells IC_{50} and IC_{75} values of 350 nM and 4.0 μM, respectively. Differences in relative sensitivities to TPT compared to β-lap suggested a disparate mechanism(s) of growth inhibition or cell death (possibly due to apoptosis).

Cell cycle-independent cytotoxicity. Since Topo I poisons are thought to kill cycling, but not arrested, cells (presumably due to DNA synthesis past Topo I–DNA "cleavable complexes"), we assessed the influence of cell cycle progression on β-lap compared to TPT cytotoxicity using DNA content assays. In addition, these studies would address the relative role of topoisomerase IIα inhibition in β-lap-mediated cytotoxicity, due to the cell-cycle-dependent expression of this protein. These studies utilized the estrogen-dependent MCF-7 and T47D breast cancer cell lines, since their growth in estrogen-deprived, phenol red-free culture medium has been well defined [33]. Cells were deprived of estrogen for 6 days, which caused a significant G_1 delay at a predetermined point in the cell cycle [33, 35, 36], prior to addition of either β-lap or TPT. Cells were then exposed to various concentrations of β-lap or TPT in estrogen-deprived (control) medium, control medium containing E_2 (10 nM), or medium containing whole serum alone or in the presence of inhibitory concentrations of the anti-estrogens 4-OHT or ICI for 48 h (Fig. 2). Both cell lines were stimulated to enter the cell cycle and begin log-phase growth after addition of medium containing 17β-estradiol or whole serum. Addition of anti-estrogens specifically inhibited

irinotecan [18]. For example, β-lap administration did not stabilize Topo I–DNA cleavable complexes *in vivo* [19] or *in vitro* [20]. In contrast, the CPT family members stabilized cleavable complexes [19], resulting in the formation of DNA single-strand nicks [21] and induction of wild-type p53 [22]. The fact that β-lap did not produce DNA single-strand nicks in human or hamster cancer cells [21, 23] was indirectly confirmed by the absence of wild-type p53 induction in breast or prostate cancer cells [18, 24]. While *in vitro* assays indirectly suggested that Topo I may be an intracellular target of β-lap, it seemed likely that it was not the only mechanism through which this compound acted [24, 25]. We recently reported that the cytotoxicity caused by β-lap in MCF-7 breast cancer cells could be solely accounted for by apoptotic responses [24].

Recent results have suggested that β-lap can lead to Topo IIα-mediated DNA breaks [25]. In contrast to Topo I, topoisomerase IIα causes ATP-dependent, double-strand DNA unwinding [26]. Topo IIα also shares another important distinction from Topo I, in its cell cycle regulation. Topo I is consistently expressed throughout the cell cycle while Topo IIα is poorly expressed during G_0/G_1 and expression increases during S phase, reaching a peak during late S and G_2 [27]. Drugs which primarily target Topo IIα are, therefore, cell cycle specific [28], while Topo I-specific drugs can kill cells in all phases of the cell cycle [29]. Variation in sensitivity to either β-lap or TPT during different cell-cycle stages was measured to address the relative importance of Topo I and Topo IIα activity for the cytotoxicity of these drugs.

Interestingly, β-lap-mediated apoptosis in MCF-7 cells was accompanied by a dramatic decrease in p53 steady-state levels, prior to the appearance of apoptotic morphologic changes [24]. We were, therefore, interested to see if this relationship between loss of survival and apoptosis held true for other breast cancer cells. We describe the activation of a noncaspase, cysteine protease, which shares some characteristics with the neutral calcium-dependent protease, calpain, during β-lap-mediated apoptosis. β-Lap-mediated cell death and proteolysis are induced in all phases of the cell cycle, suggesting that topoisomerase IIα was not the critical target for this death pathway.

MATERIALS AND METHODS

Chemicals and tissue culture reagents. Estradiol (E_2), 4-hydroxytamoxifen (4-OHT) (Sigma Chemical Co., St. Louis, MO), or ICI 182,780 (a generous gift from Dr. V. Craig Jordan, Northwestern University) were dissolved in 100% ethanol as 1000× stocks and maintained at −20°C. β-Lap (MW 242, ε = 25790), generously supplied by Dr. William G. Bornmann (Memorial Sloan Kettering, New York, NY), and TPT (Smith Kline Beecham, Philadelphia, PA) were dissolved in DMSO and concentrations confirmed by spectrophotometric analyses [24, 30]. Nocodazole was purchased from Sigma Chemical Co., and a 2 mg/ml stock solution was made in DMSO immediately before use. All tissue culture reagents were purchased

TABLE 1

Characteristics of Breast Cancer Cell Lines

Cell line	ER	p53	pRb
MCF-7:WS8	++++	WT	+
T47D:A18	++	Mutant	+

from GIBCO Laboratories (Grand Island, NY), unless otherwise stated. Charcoal-stripped serum was prepared by treating fetal bovine serum (FBS) three times with dextran-coated charcoal as described [31].

Antibodies and protease inhibitors. The C-2-10 PARP monoclonal antibody was purchased from Enzyme Systems Products (Dublin, CA). An N-terminal PARP (clone N-20), an Sp1 polyclonal, a p53 monoclonal (clone DO-1), and all horseradish peroxidase-conjugated secondary antibodies were obtained from Santa Cruz Biotechnologies (Santa Cruz, CA). Monoclonal antibodies to pRb (clone G3-245) and underphosphorylated pRb (clone G99-549) were obtained from PharMingen (San Diego, CA). A polyclonal antibody specific to phosphorylated serine 780 of the pRb protein was obtained from Medical and Biological Laboratories Co. Ltd. (Boston, MA). Antibody to caspase-3 was obtained from Transduction Laboratories (Lexington, KY). Antibody to lamin B was obtained from Matritech, Inc. (Cambridge, MA). zVAD-fmk, DEVD-fmk, zFA-fmk, and zAAD-fmk were obtained from Enzyme Systems Products (Dublin, CA), diluted in DMSO, and used at 25 μM unless otherwise stated. TPCK, TLCK, iodoacetamide, and N-ethylmaleimide were purchased from Sigma Chemical Co. and diluted in DMSO (TPCK and TLCK), ethanol (N-ethylmaleimide), or water (iodoacetamide). The pBabe/puro vector was a generous gift from Dr. Todd Sladek.

Tissue culture and growth conditions. MCF-7:WS8, T47D:A18 (clones of the standard MCF-7 and T47D cell lines, selected by limiting dilution cloning of the parental cell lines in whole serum [31–33], referred to as MCF-7 and T47D in the text) were obtained from Dr. V. Craig Jordan (Northwestern University, Chicago, IL). The ER, p53, and pRb statuses of these cell lines are outlined in Table 1. Cells were grown in RPMI 1640 medium supplemented with 10% FBS, 6 ng/ml bovine insulin, 2 mM L-glutamine, 100 U/ml penicillin, and 100 mg/ml streptomycin. For estrogen-free tissue culture medium, phenol red-free RPMI and charcoal-stripped FBS were used as previously described [31]. Cells were routinely passed at 1:5 to 1:20 dilutions once per week using 0.1% trypsin. All cells were mycoplasma free and grown at 37°C in a humidified incubator with 5% CO_2–95% air atmosphere.

Growth assays and estrogen-deprivation studies. Forty-eight-hour or 6-day growth assays were used to assess the relative sensitivities of breast cancer cells to various drug treatments as previously described [31–33]. For estrogen-deprivation studies, cells were grown in estrogen-free medium for at least 4 days prior to the start of experiments. Cells were seeded into 96-well plates (1.5 × 10^3 or 1 × 10^4 cells/well) in 0.2 ml of medium on day 0 and allowed to attach for 24 h. On day 1, fresh medium containing the indicated drug(s) was added to the appropriate wells. E_2, 4-OHT, or ICI 182,780 (ICI) were added to cells at 1:1000 dilutions from appropriate stock solutions. Estrogen-deprivation significantly retarded cell growth and dramatically increased the proportion of MCF-7 and T47D cells in G_1. For MCF-7, 83% G_1 cells were observed after 6 days of growth in estrogen-free medium compared to 53% in log-phase cultures. Changes in cell number, measured as DNA content, were then determined in untreated or drug-treated cells by an adaptation of the method of Labarca and Paigen [34] and analyzed using a Molecular Dynamics Biolumin 960 plate reader with an excitation wavelength of 360 and emission wavelength of 450 nm. Data were expressed as relative growth (T/C) by dividing the DNA content of treated cells
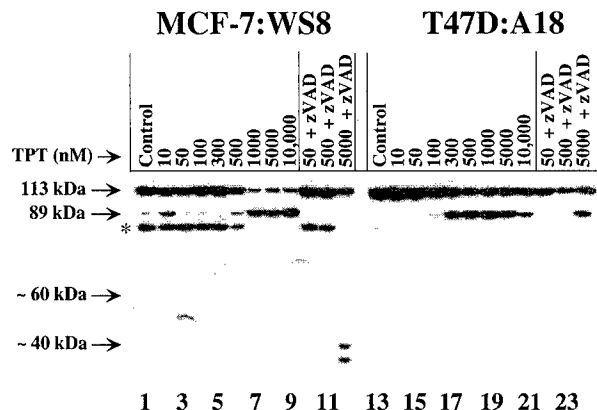
MCF-7:WS8   T47D:A18

FIG. 4. Caspase-mediated, classical PARP cleavage in breast cancer cells following TPT treatment. Log-phase MCF-7 and T47D cells were treated with 10 nM to 10 μM TPT for 48 h. Three doses of TPT (50, 500, and 5000 nM, lanes 10–12 and 22–24, top and bottom) also included the caspase inhibitor zVAD-fmk (25 μM). An unknown ~80-kDa cross-reacting protein is present in MCF-7 lysates as indicated by an asterisk. Cells were then harvested and analyzed by Western immunoblotting using the C-2-10 monoclonal PARP antibody as described for Fig. 3.

89-kDa PARP cleavage fragment observed in untreated MCF-7 cells was due to slight overgrowth of control cells, which activated a basal level of apoptosis and classic PARP cleavage. This basal, caspase-mediated PARP cleavage was completely inhibited by zVAD-fmk in both cell lines (compare the minor 89-kDa PARP cleavage fragment in lane 1 to the absence of this fragment in lane 2 for MCF-7 in Fig. 5).

As shown in Fig. 3, T47D cells exposed to 8 μM β-lap for 48 h showed classic PARP cleavage. As expected, this apoptotic cleavage reaction was completely blocked by coadministration of zVAD-fmk at 25 μM. β-Lap-treated T47D cells also showed cleavage of Sp1, giving rise to the previously described 68-kDa fragment [2]. In addition, T47D cells treated with β-lap showed a loss of phosphorylated pRb and appearance of an ~100-kDa cleavage fragment, previously described by Janicke et al. [4] (compare lanes 13 and 19, Fig. 5). All cleavage reactions observed in T47D cells after β-lap treatment were completely prevented by 25 μM zVAD-fmk. However, accumulation of hypophosphory-
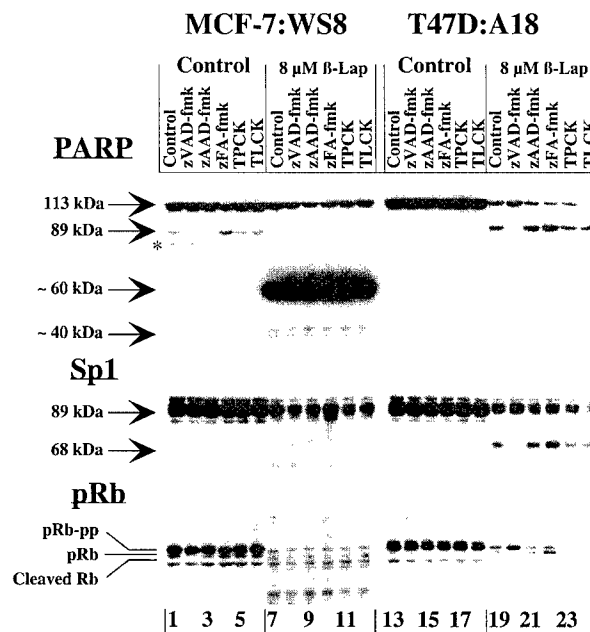
mine if PARP cleavage was caused by caspase activation after three doses of TPT (50, 500, and 5000 nM) (Fig. 4). As observed following β-lap exposures, the relative sensitivity of MCF-7 and T47D cells to the growth inhibitory effects of TPT was reflected to some degree in PARP cleavage (Fig. 4). However, the doses of TPT required to elicit PARP cleavage *in vivo* were significantly above the apparent IC_{50} values for each cell line (see Fig. 1); this was not the case for cells exposed to β-lap. These data are consistent with previous data demonstrating that β-lap is a much more effective inducer of apoptosis than CPT or its derivatives [20]. Coadministration of zVAD-fmk inhibited TPT-mediated PARP cleavage in both MCF-7 (lanes 10–12) and T47D cells (lanes 22 and 23 with 50 and 500 nM, but not 5000 nM, TPT). These data suggested that TPT exposure led to the activation of the classic caspase pathway. Importantly, no dose of TPT gave rise to the atypical PARP cleavage fragment, even when 10 μM TPT was used (lanes 9 and 21, Fig. 4).

Evidence for two apoptotic proteolytic pathways activated by β-lap. In order to determine whether atypical PARP cleavage observed after β-lap treatment was the result of an activated caspase family member, or another class of cysteine proteases, cells were exposed for 48 h to 8 μM β-lap in the presence of a battery of known protease inhibitors (Fig. 5). Included were general chemical inhibitors and more specific cleavage site inhibitors [38]. Exposure of MCF-7 cells to 8 μM β-lap caused apoptotic responses (measured by PARP, pRb, and Sp1 cleavage) that were insensitive to any of the inhibitors, simultaneously administered at previously determined efficacious doses [38]. The modest level of

MCF-7:WS8   T47D:A18

FIG. 5. Effect of global or specific cleavage site protease inhibitors on β-lap-mediated atypical PARP cleavage. Log-phase MCF-7 and T47D cells were grown for 48 h in RPMI medium alone or in medium containing 8 μM β-lap. Protease inhibitors were coadministered with β-lap. The protease inhibitors used were 25 μM zVAD-fmk (a caspase family inhibitor), 25 μM zAAD-fmk (an inhibitor of granzyme B), 25 μM zFA-fmk (an inhibitor of cathepsins B and L), 1.0 μM TPCK (a trypsin inhibitor), or 10 μM TLCK (a chymotrypsin inhibitor). Control cells received RPMI medium alone (lanes 1 and 13) or RPMI medium containing 8 μM β-lap (lanes 7 and 19). Whole-cell extracts were then analyzed by Western immunoblotting as described under Materials and Methods for PARP cleavage, pRb dephosphorylation and cleavage, and cleavage of the Sp1 transcription factor by repeated probing of the same blots. The Western blot shown is representative of at least three separate experiments.
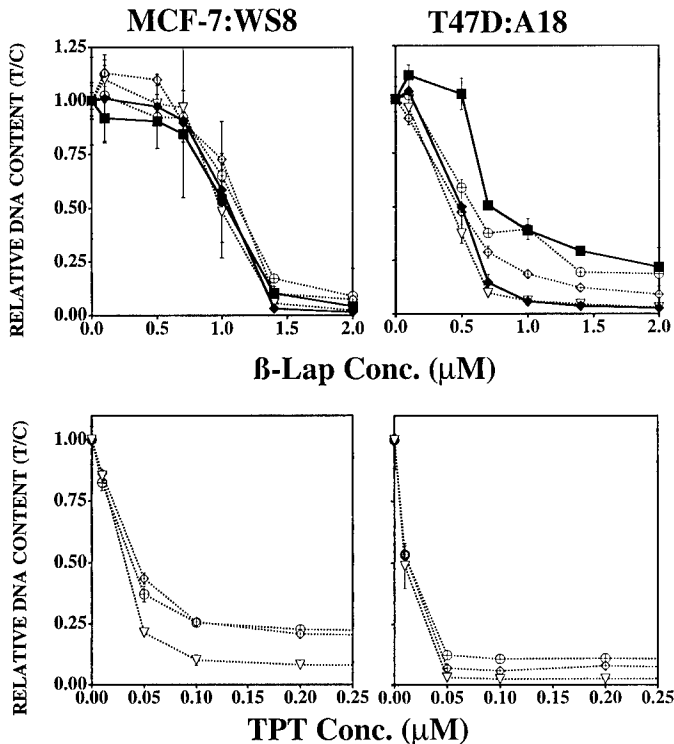
FIG. 2. β-Lap- or TPT-mediated cytotoxicity of G_1-arrested cells. MCF-7 and T47D estrogen-dependent cell lines were grown for 6 days in estrogen-depleted, phenol red-free medium and exposed to varying concentrations of β-lap or TPT for 6 days, as indicated. Drugs were included in RPMI 1640 medium containing estrogen-deprived calf serum (control, ■), estrogen-replenished, stripped calf serum (10 nM E_2, ◆), whole serum alone (▽), or whole serum treated with the anti-estrogens 4-hydroxytamoxifen (100 nM, ◇) or ICI 182,780 (100 nM, ○). Cell number was then assessed after 6 days using DNA content as in Fig. 1. Relative cell growth of treatment was determined using the DNA content of cells grown in comparable medium without β-lap or TPT. Data shown are representative of at least two experiments expressed as means ± SEM of at least four replicate wells.

estrogen-mediated cell growth. Estrogen deprivation and/or anti-estrogen administration led to a cytostatic growth inhibition of 75–85% compared with cells grown in medium containing E_2 or whole serum (data not shown and [32, 37]). Additional β-lap or TPT treatments led to a complete loss of cells, demonstrating a similar cytotoxic response in both log-phase (+E_2) and arrested (−E_2 or plus antiestrogens) cells (Fig. 2).

Apoptotic protease activation after β-lap or TPT treatment. To investigate caspase activation in MCF-7 and T47D breast cancer cells following TPT or β-lap exposures, we examined PARP cleavage using Western immunoblot analyses as described under Materials and Methods. Cells were treated continuously with 5 to 10 μM β-lap and PARP cleavage was assessed 48 h later. Treatment with 5 μM β-lap induced classic PARP cleavage, resulting in the appearance of an 89-kDa fragment in both cell lines (Fig. 3). In MCF-7 cells,

a cross-reacting protein of ~80 kDa (indicated by an asterisk in Figs. 3, 4, and 5) was present even in untreated cells. The identity of this protein is unknown; however, it does appear to be degraded during apoptosis.

At higher doses of β-lap we observed an atypical ~60-kDa PARP fragment. This atypical cleavage of PARP was most apparent in MCF-7 cells (Fig. 3, lanes 4–6), which were more sensitive to β-lap (Figs. 1 and 2). In general, PARP cleavage reflected the relative sensitivity of each cell line to β-lap, by which MCF-7 cells demonstrated primarily the atypical cleavage pattern and T47D predominantly showed typical caspase-mediated PARP cleavage at lower doses and atypical PARP cleavage following treatment with 10 μM β-lap (see lane 12, Fig. 3). A minor PARP cleavage fragment of ~40 kDa was also observed in MCF-7 cells, which display maximal amounts of the 60-kDa PARP fragment (Fig. 3). It is currently unclear whether this is a unique fragment or the result of further cleavage of the original 60-kDa fragment. Interestingly, the apparent amount of the 60-kDa fragment was much greater than that of full-length PARP protein. Loading equivalence, as assessed by Ponceau S staining, showed that all lanes contained equal amounts of protein. This apparent incongruity may be the result of either more efficient extraction of the fragment from the nuclear matrix or increased accessibility of the epitope to the antibody, after β-lap-induced cleavage (Fig. 3).

MCF-7 and T47D cells were treated with a range of TPT doses (10 nM to 10 μM) for 48 h. We coadministered 25 μM zVAD-fmk, a caspase inhibitor, to deter-
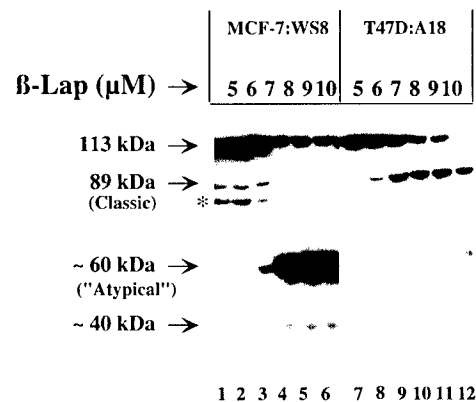

FIG. 3. Atypical and classic PARP cleavage in breast cancer cells following β-lap exposure. Breast cancer cell lines were treated with β-lap (5–10 μM) for 48 h and whole-cell lysates prepared at various times posttreatment from pooled (attached and floating) cells and assessed for cleavage of PARP using standard Western immunoblot procedures and the C-2-10 monoclonal PARP antibody, described under Materials and Methods. An unknown ~80-kDa cross-reacting protein was present in MCF-7 lysates as indicated by an asterisk. The Western blot shown is representative of at least three separate experiments.
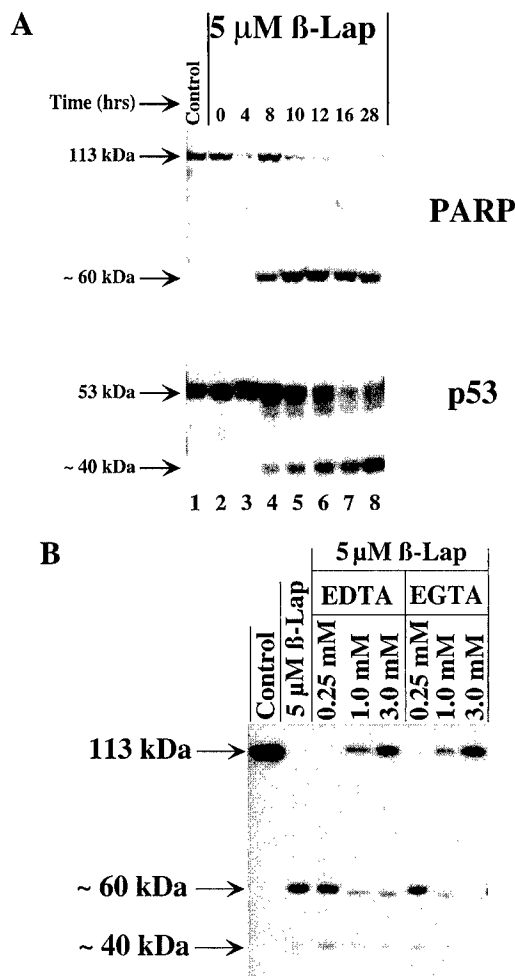
A

PARP

p53

1 2 3 4 5 6 7 8

B

FIG. 7. Implication of calpain in atypical PARP cleavage. (A) MCF-7 cells were treated with 5 μM β-lap for 4 h and whole-cell extracts were prepared 20 h later. Western blots were probed with anti-PARP antibody, then stripped and reprobed with anti-p53 antibody. (B) MCF-7 cells were pretreated for 30 min with the designated concentrations of EDTA or EGTA in complete medium. Medium containing 5 μM β-lap was then added for 4 h in the continued presence of EDTA or EGTA. After β-lap exposure cells were treated with medium containing only the designated concentrations of EDTA or EGTA for an additional 20 h. Whole-cell extracts were prepared and probed for PARP as described above. The blots shown are representative of at least two independent experiments.

fragments. Both EDTA and EGTA showed a dose-dependent inhibition of β-lap-mediated atypical PARP cleavage and p53 cleavage in MCF-7 cells (Fig. 7B and data not shown). These data suggest that extracellular calcium is a necessary component for β-lap-mediated atypical PARP and p53 cleavage, an attribute consistent with activation of a calcium-dependent, non-caspase cysteine protease, such as calpain.

Loss of hypophosphorylated pRb and apoptosis induced by β-lap is independent of cell cycle status. To investigate the effects of cell cycle position on β-lap-induced accumulation of hypophosphorylated pRb and

apoptosis, estrogen-dependent MCF-7 cells were cultured in estrogen-free medium for 6 days as described under Materials and Methods. To ensure a complete estrogen block, the pure anti-estrogen ICI 182,780 (1 nM) [44, 45] was added to cells growing in estrogen-free medium 2 days prior to the beginning of each experiment. Increases in G_1 cells (up to 85%) were noted, as described [46]. Arrested cells were compared to MCF-7 cells that were subsequently restimulated to enter the cell cycle by addition of 10 nM E_2 at the time of β-lap or TPT exposure (i.e., a 4-h pulse of either 8 μM β-lap or 5 μM TPT). Drugs were administered as short pulse treatments in order to determine if the rapid accumulation of hypophosphorylated pRb could be reversed after removal of β-lap or TPT. When used, ICI or E_2 was maintained in the medium.

MCF-7 cells treated with β-lap showed a dramatic loss of phosphorylated pRb within 6 h (compare lanes 3 and 4, Fig. 8), followed by general loss of the protein by 18 h after treatment (see lanes 10 and 13, Fig. 8); these data are consistent with earlier findings [24]. A similar loss of phosphorylated pRb was noted in MCF-7 cells after 5 μM TPT; however, significant accumulation of hypophosphorylated pRb was not observed until 12 h after treatment (not shown), and complete loss was not noted until more than 18 h posttreatment (Fig. 8 and data not shown). In control cells, stimulation of arrested cells with estradiol led to an increase in the relative level of hyperphosphorylated pRb (by 6 to 18 h) compared to estrogen-deprived and/or ICI-treated cells (compare hypophosphorylated retinoblastoma protein (pRb) to hyperphosphorylated retinoblastoma protein (pRb-pp) levels in lanes 6, 9, and 12 to lane 3, Fig. 8). The change in phosphorylation status of pRb was accompanied by a dramatic increase in the proportion of cells in S phase by 18 h after E_2 stimulation (43% S phase with E_2, 10% S phase without E_2, compare lanes 12 and 9, Fig. 8). In both the E_2- and the ICI-treated groups, β-lap exposure led to a complete loss of hyperphosphorylated pRb followed by an overall loss of all forms of pRb. Since estrogen-deprivation can cause an arrest in the cell cycle ~6 h from the restriction point in MCF-7 cells [47–49], possibly past the first cyclin D1–cdk2-dependent phosphorylation of pRb, the levels of hyperphosphorylated pRb in estrogen-deprived, anti-estrogen-treated MCF-7 cells were rather high (Fig. 8). In MCF-7 cells treated with either β-lap or TPT, PARP cleavage (atypical for β-lap, classic for TPT) was not apparent until 12–18 h after treatment (Fig. 8 for 18 h, and data not shown). Addition of E_2, or maintenance of MCF-7 cells in estrogen-deprived medium (including ICI), had no effect on the appearance of PARP cleavage (see lanes 10 and 13, Fig. 8).

We performed a similar series of experiments using nocodazole to arrest cells during M phase. All MCF-7 groups examined showed a similar pattern of PARP

lated pRb in T47D cells following β-lap treatment was unaffected by the administration of 25 μM zVAD (lanes 19 to 20, Fig. 5). These data are consistent with the activation of a caspase-mediated apoptotic pathway in T47D cells after β-lap treatment, which may be downstream of changes in pRb phosphorylation state.

MCF-7 cells, which showed only atypical PARP cleavage after 8 μM β-lap exposure, also demonstrated an overall decline in Sp1 steady-state levels. However, apoptotic cleavage fragments (as observed in T47D cells) were not observed after extended exposures of the Western blots in Fig. 5 (not shown). MCF-7 cells treated with β-lap showed an overall loss of pRb, with the presence of a modest amount of a 60-kDa pRb fragment (visible after extended exposure, data not shown), similar to that described by An and Dou [5]. pRb cleavage in MCF-7 cells caused by β-lap exposure was not affected by coadministered protease inhibitors (Fig. 5, lanes 8–12).

To confirm that β-lap cytotoxicity was primarily mediated by the induction of apoptosis and not necrosis, we utilized the TUNEL assay, which measures DNA breaks created by apoptotic endonucleases [39]. MCF-7 cells were exposed to a 4-h pulse of 8 μM β-lap and analyzed for terminal deoxynucleotide transferase-mediated incorporation of FITC-labeled dUTP, 20 h later. Greater than 90% of the β-lap-treated MCF-7 cells were TUNEL positive (Fig. 6). This finding, in addition to the dramatic nuclear condensation reported previously [24], confirms that cytotoxicity caused by β-lap is primarily apoptotic and not due to necrosis.

The global cysteine protease inhibitors iodoacetamide and N-ethylmaleimide [7, 40, 41] were used to determine if a cysteine protease was responsible for the formation of atypical PARP cleavage fragments in MCF-7 cells (Figs. 3 and 5). MCF-7 cells were treated with 5 μM β-lap in medium with or without 10 mM iodoacetamide or 10 mM N-ethylmaleimide (data not shown). Cleavage of PARP was prevented by both inhibitors, but was not inhibited by the caspase inhibitors zVAD-fmk or DEVD-fmk (Fig. 5 and data not shown), suggesting that a noncaspase, cysteine protease was primarily responsible for the atypical PARP cleavage observed after β-lap treatment. Administration of N-ethylmaleimide caused a mobility shift of the full-length PARP band, possibly due to methylation of cysteine and methionine groups in the protein [40]. Neither iodoacetamide nor N-ethylmaleimide prevented β-lap-mediated apoptosis in MCF-7 cells.

Simultaneous cleavage of PARP and p53. The inhibition of PARP cleavage by cysteine-alkylating agents suggested that a noncaspase cysteine protease may be responsible for the atypical PARP cleavage observed in cells after treatment with β-lap. One protease which may fit these data would be the neutral calcium-depen-
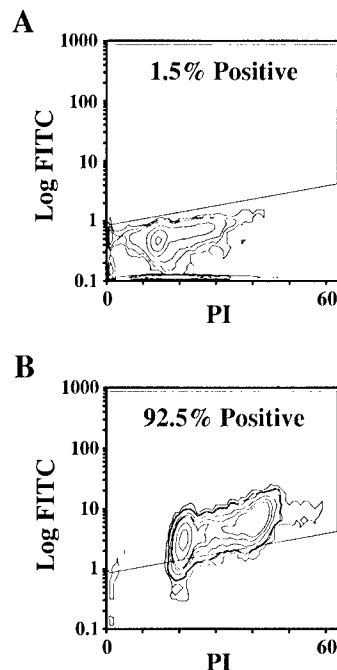

FIG. 6. β-Lapachone induced DNA fragmentation. MCF-7 cells were treated with 8 μM β-lap for 4 h and harvested 20 h later. Cells were analyzed for DNA fragmentation using the TUNEL assay. Cells which have significant DNA fragmentation incorporate FITC–dUTP and are shown above the line in both graphs. Shown are representative examples of experiments repeated at least three times.

dent protease calpain [9]. Calpain has a wide substrate specificity and has been shown to specifically cleave p53 during apoptosis [42, 43]. We treated MCF-7 cells with a 4-h pulse of 5 μM β-lap and isolated whole-cell extracts at various times, up to 28 h after drug exposure. Extracts were probed for PARP and subsequently stripped and reprobed for p53 steady-state expression (Fig. 7A). As expected, PARP cleavage was observed by 8 h after drug administration. Importantly, cleavage of p53, giving rise to an ~40-kDa fragment, accompanied this PARP cleavage. The p53 cleavage pattern resembled that observed by Pariat *et al.* [43] and Kubbutat *et al.* [42], which was the result of calpain activation.

Since calpain activity is dependent upon changes in Ca^{+2} homeostasis, we utilized the calcium chelators EDTA and EGTA to determine if removal of extracellular calcium influenced the appearance of atypical PARP cleavage in MCF-7 cells after β-lap treatment. MCF-7 cells were pretreated with 0.25, 1.0, or 3.0 mM EGTA or EDTA in complete medium for 30 min. After treatment, medium containing 5 μM β-lap or DMSO (control medium), including the corresponding concentration of EDTA or EGTA used in the pretreatment, was added for an additional 4 h. All cells were then treated with medium alone containing EGTA or EDTA for an additional 20 h. Whole-cell extracts were then prepared and analyzed for PARP and p53 cleavage
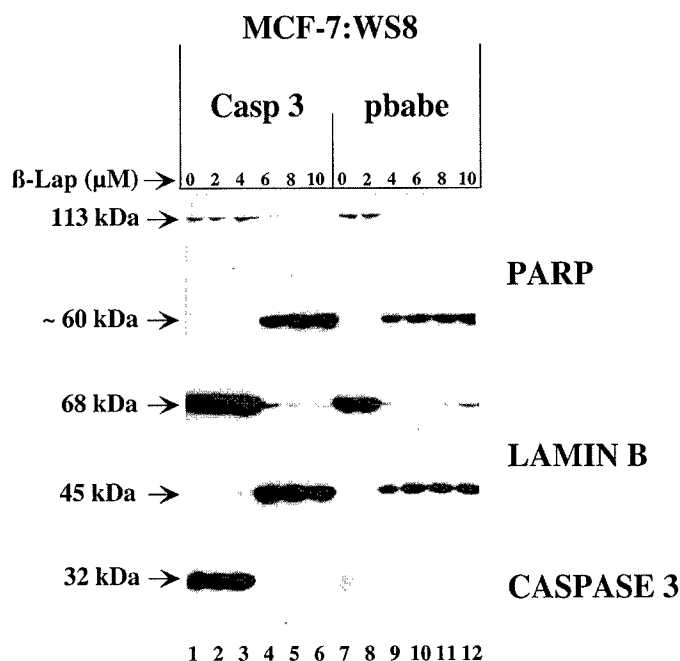
FIG. 9. Effect of caspase-3 expression on β-lap-mediated proteolysis. Caspase-3-negative MCF-7 cells were infected with a retroviral construct expressing full-length procaspase-3 (Casp 3) or vector alone (pbabe). Caspase 3 (full length is 32 kDa) expression is shown at the bottom. Cells were then treated with the designated concentrations of β-lap for 4 h, fresh medium was added, and whole-cell extracts were prepared 20 h later. Western immunoblots were then probed with the C-2-10 anti-PARP antibody, stripped, and reprobed with lamin B and later with caspase-3 antibodies. The Western blot shown is representative of at least three separate experiments.

study, we expanded our investigations to include the T47D cell line which has significant phenotypic and genotypic differences (Table 1). Using these cell lines (and others not shown here), we demonstrated that β-lap-mediated apoptosis did not require active ER and we confirmed that cell death was not dependent on wild-type p53 or cell-cycle status.

Our previous studies could not discern a cell cycle phase-specific apoptotic mechanism following β-lap exposure. In these studies, we utilized the estrogen-dependent G_1 arrest characteristics of MCF-7 and T47D cells (~80% growth inhibition in E_2-deprived, compared to log-phase cells) to show that both cell lines were equally sensitive to β-lap or TPT, irrespective of their progression through the cell cycle (Fig. 2). When arrested cells were treated with either β-lap or TPT, the relative cytotoxicity was identical to that of log-phase cells. This result is in apparent conflict with the current paradigm for the mechanism of action of Topo I poisons, which suggested that the primary lethal event was the creation of DNA double-strand breaks following movement of the replication fork through the "cleavable complex." This mechanism has been used to describe the S-phase-specific killing of cancer cells by

TPT. Morris and Geller [53] also showed that CPT could induce apoptosis in postmitotic rat cortical neurons. Our data indicate that DNA synthesis may not be required for lethality or the stimulation of apoptosis in G_1-arrested breast cancer cells by β-lap or TPT. These data suggest that DNA–Topo I lesions caused by treatment may activate a nuclear signal (possibly originating from inhibited transcription) that triggers pRb dephosphorylation (see below) and downstream apoptotic reactions. Taken together, these results demonstrate that while actively growing cells may be killed more efficiently in some systems, arrested cells may also be sensitive to the toxic (i.e., apoptotic) effects of Topo I poisons. In comparison with β-lap, TPT was a less effective inducer of apoptosis, stimulating apoptotic reactions only at concentrations 20- to 100-fold over its IC_{50}. β-Lap killed cells by apoptosis at concentrations near its IC_{50}, as previously reported [24].

Using two methods of cell cycle arrest, estrogen deprivation (Figs. 2 and 9) and nocodazole administration (data not shown), we demonstrated that β-lap kills MCF-7 cells equally in all phases of the cell cycle. This would suggest that Topo IIα does not play a central role in β-lap toxicity. Unlike Topo I, the expression of Topo IIα is clearly cell cycle dependent ([26] and data not shown), and stages of the cell cycle in which Topo IIα was not expressed (i.e., G_0/G_1) would be expected to be protected from β-lap toxicity, if Topo IIα was a critical target. Conversely, stages of the cell cycle with highest Topo IIα expression (i.e., G_2/M) would be expected to be more sensitive to β-lap. It is important to note that the β-lap/Topo IIα-mediated cleavage has been observed using only *in vitro* assays, and β-lap/Topo IIα-mediated DNA breaks have not been demonstrated in intact cells. Importantly, downstream consequences of DNA damage, such as p53 induction, have not been observed after β-lap treatment [24]. These data are in apparent conflict with the suggested role of Topo IIα in β-lap-mediated toxicity as proposed by Frydman *et al.* [25].

β-Lap induces a novel apoptotic protease. Exposure to β-lap gave rise to a unique pattern of proteolysis. At lower doses, β-lap treatment caused classic PARP cleavage. At higher doses, an ~60-kDa atypical PARP fragment was observed. The dose range over which this novel fragment appeared was quite sharp and correlated well with the notably sharp growth inhibition responses noted in Figs. 1 and 2 and previously described cytotoxicity [24]. Atypical PARP fragmentation was not simply the result of supralethal drug exposure, since cells treated with TPT at doses 200-fold greater than the IC_{50} of the drug did not show the same atypical cleavage pattern. Doses of β-lap necessary to induce atypical PARP cleavage were generally less than 5-fold over the IC_{50} for β-lap, depending upon the cell line examined and the method of treatment (i.e., continuous exposure or 4-h pulse). The lack of
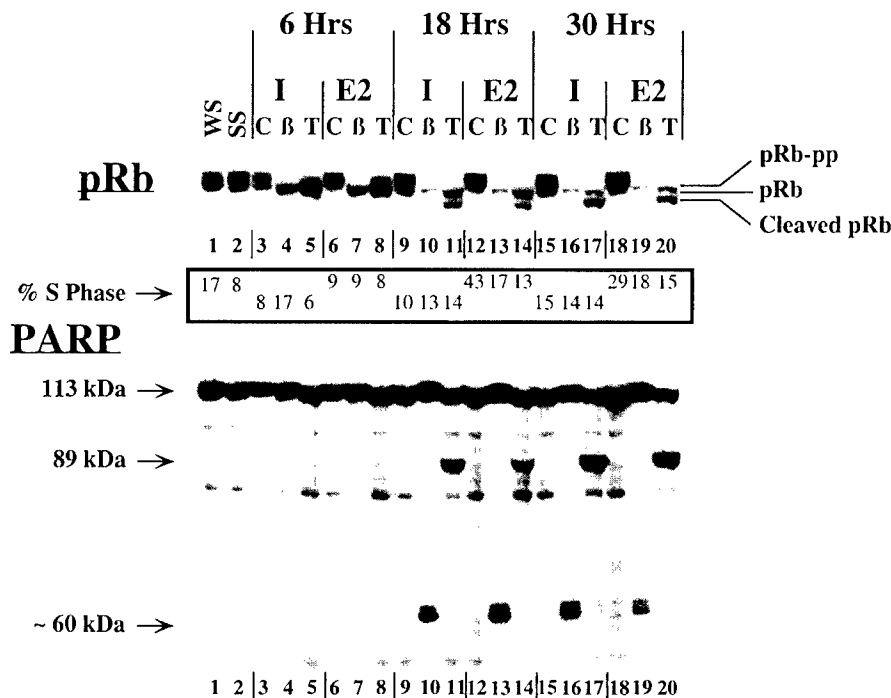
FIG. 8. Effect of β-lap or TPT on logarithmically growing or anti-estrogen-arrested MCF-7 cells. MCF-7 cells were estrogen-deprived for 6 days prior to seeding in estrogen-deprived medium containing 10 nM ICI 182,780 to ensure complete blockage of estrogen-stimulated growth. Cells were then treated with no drug (C), 5 μM β-lap (β), or 5 μM TPT (T), in estrogen-free RPMI media supplemented with either 100 nM ICI (I) or 10 nM E_2 (E_2). Whole-cell extracts were prepared at 6 and 18 h after treatment and changes in cell cycle distribution were monitored by flow cytometry, as described under Materials and Methods. For Western analyses, immunoblots were first probed with the C-2-10 anti-PARP monoclonal antibody, then stripped and reprobed with an anti-pRb monoclonal antibody which detected all forms of pRb. For controls, log-phase MCF-7 cells were grown continuously in medium containing whole serum (WS) or in medium containing estrogen-deprived serum (SS, for stripped serum) as described under Materials and Methods. Shown are three separate forms of the pRb protein: (a) pRb-pp, hyperphosphorylated pRb; (b) pRb, hypophosphorylated (nonphosphorylated) pRb; and (c) the cleaved form of pRb, in which 4 kDa of the C-terminus has been removed (Cleaved pRb). PARP protein forms included (a) the full-length PARP polypeptide of 113 kDa, (b) a caspase-mediated 89-kDa PARP fragment, and (c) an ~60-kDa atypical PARP cleavage polypeptide, which sometimes appears as a doublet at ~60 kDa. The Western blot shown is representative of at least three separate experiments.

cleavage after β-lap treatment (data not shown), supporting a cell-cycle-independent activation of apoptosis.

We [16], as well as others [50], showed that MCF-7 cells were devoid of caspase-3, due to a deletion in exon 3. To determine whether caspase-3 deficiency was responsible for atypical PARP cleavage, we isolated an MCF-7 clone that stably expressed full-length proform caspase-3 (Casp 3) (see Materials and Methods). A puromycin-resistant clone expressing empty vector (pBabe) was also analyzed. PARP, lamin B, and caspase-3 expression was monitored before or 24 h after β-lap treatment (2–10 μM). Cells were treated for 4 h with 2–10 μM β-lap and harvested 20 h later. As expected, Casp 3 cells expressed the 32-kDa proform of caspase-3, unlike MCF-7 cells transfected with the vector alone (Fig. 9, compare lanes 1 and 7). Atypical PARP cleavage was noted following β-lap treatment at similar levels in both transfected cell lines. Classic lamin B cleavage, presumably the result of caspase-6 activation [51, 52], was also observed. These data suggest that expression of caspase-3 had no effect on apoptotic cleavage events in MCF-7 cells following various doses of β-lap. Interestingly, loss of procaspase-3 protein, in Casp 3 cells, mirrored cleavage of both PARP and lamin B. Importantly, the active p12 and p20 fragments of caspase-3 were not observed due to the lower affinity of this antibody to the processed forms of caspase-3. In contrast to β-lap treatments, Casp 3 cells showed an increased rate of apoptosis after exposure to TNF-α or granzyme B compared to MCF-7 cells transfected with pBabe/puro alone [16].

DISCUSSION

We previously showed that β-lap killed a variety of cells by apoptosis. However, the mechanisms of specific proteolytic execution cascades that were activated by this compound remained unexplored. β-Lap induced apoptosis independent of p53 status and cell cycle distribution [18, 24]. In MCF-7 cells, the lethal effects of β-lap were accounted for solely by apoptosis. In this

β-lap was observed. Sensitivity to this agent was very different from the cytotoxic responses observed following TPT treatment. In MCF-7 cells, the primary proteolytic events, which correlate directly with apoptosis induction and loss of survival, appear to be the result of this novel calcium-dependent noncaspase protease. Activation of this protease was not affected by inhibitors of a variety of proteases, most importantly the caspase inhibitors zVAD-fmk and DEVD-fmk. We hypothesize that this calcium-dependent, noncaspase cysteine protease is calpain. When this protease is activated, its novel apoptotic pathway may be a specific target for manipulation in the clinical treatment of breast cancer.

REFERENCES

1. Alnemri, E. S., Livingston, D. J., Nicholson, D. W., Salvesen, G., Thornberry, N. A., Wong, W. W., and Yuan, J. Y. (1996). Human Ice/Ced-3 protease nomenclature. *Cell* **87,** 171.

2. Piedrafita, F. J., and Pfahl, M. (1997). Retinoid-induced apoptosis and Sp1 cleavage occur independently of transcription and require caspase activation. *Mol. Cell. Biol.* **17,** 6348–6358.

3. Patel, T., Gores, G. J., and Kaufmann, S. H. (1996). The role of proteases during apoptosis. *FASEB J.* **10,** 587–597.

4. Janicke, R. U., Walker, P. A., Lin, X. Y., and Porter, A. G. (1996). Specific cleavage of the retinoblastoma protein by an ICE-like protease in apoptosis. *EMBO J.* **15,** 6969–6978.

5. An, B., and Dou, Q. P. (1996). Cleavage of retinoblastoma protein during apoptosis: An interleukin 1 beta-converting enzyme-like protease as candidate. *Cancer Res.* **56,** 438–442.

6. Talanian, R. V., Quinlan, C., Trautz, S., Hackett, M. C., Mankovich, J. A., Banach, D., Ghayur, T., Brady, K. D., and Wong, W. W. (1997). Substrate specificities of caspase family proteases. *J. Biol. Chem.* **272,** 9677–9682.

7. Kaufmann, S. H., Desnoyers, S., Ottaviano, Y., Davidson, N. E., and Poirier, G. G. (1993). Specific proteolytic cleavage of poly-(ADP-ribose) polymerase: An early marker of chemotherapy-induced apoptosis. *Cancer Res.* **53,** 3976–3985.

8. Wang, X., Pai, J. T., Wiedenfeld, E. A., Medina, J. C., Slaughter, C. A., Goldstein, J. L., and Brown, M. S. (1995). Purification of an interleukin-1 beta converting enzyme-related cysteine protease that cleaves sterol regulatory element-binding proteins between the leucine zipper and transmembrane domains. *J. Biol. Chem.* **270,** 18044–18050.

9. Squier, M. K., Miller, A. C., Malkinson, A. M., and Cohen, J. J. (1994). Calpain activation in apoptosis. *J. Cell. Physiol.* **159,** 229–237.

10. Wood, D. E., Thomas, A., Devi, L. A., Berman, Y., Beavis, R. C., Reed, J. C., and Newcomb, E. W. (1998). Bax cleavage is mediated by calpain during drug-induced apoptosis. *Oncogene* **17,** 1069–1078.

11. Porn-Ares, M. I., Samali, A., and Orrenius, S. (1998). Cleavage of the calpain inhibitor, calpastatin, during apoptosis. *Cell Death Differ.* **5,** 1028–1033.

12. Chandra, J., Niemer, I., Gilbreath, J., Kliche, K. O., Andreeff, M., Freireich, E. J., Keating, M., and McConkey, D. J. (1998). Proteasome inhibitors induce apoptosis in glucocorticoid-resistant chronic lymphocytic leukemic lymphocytes. *Blood* **92,** 4220–4229.

13. McConkey, D. J. (1996). Calcium-dependent, interleukin 1-converting enzyme inhibitor-insensitive degradation of lamin B1 and DNA fragmentation in isolated thymocyte nuclei. *J. Biol. Chem.* **271,** 22398–22406.

14. Shimizu, T., and Pommier, Y. (1997). Camptothecin-induced apoptosis in p53-null human leukemia HL60 cells and their isolated nuclei: Effects of the protease inhibitors Z-VAD-fmk and dichloroisocoumarin suggest an involvement of both caspases and serine proteases. *Leukemia* **11,** 1238–1244.

15. Marthinuss, J., Andrade-Gordon, P., and Seiberg, M. (1995). A secreted serine protease can induce apoptosis in Pam212 keratinocytes. *Cell Growth Differ.* **6,** 807–816.

16. Yang, X., Stennicke, H. R., Wang, B., Green, D. R., Janicke, R. U., Srinivasan, A., Seth, P., Salvesen, G. S., and Froelich, C. J. (1998). Granzyme B mimics apical caspases. Description of a unified pathway for trans-activation of executioner caspase-3 and -7. *J. Biol. Chem.* **273,** 34278–34283.

17. Boothman, D. A., Trask, D. K., and Pardee, A. B. (1989). Inhibition of potentially lethal DNA damage repair in human tumor cells by beta-lapachone, an activator of topoisomerase I. *Cancer Res.* **49,** 605–612.

18. Planchon, S. M., Wuerzberger, S., Frydman, B., Witiak, D. T., Hutson, P., Church, D. R., Wilding, G., and Boothman, D. A. (1995). Beta-lapachone-mediated apoptosis in human promyelocytic leukemia (HL-60) and human prostate cancer cells: A p53-independent response. *Cancer Res.* **55,** 3706–3711.

19. Boothman, D. A., Wang, M., Schea, R. A., Burrows, H. L., Strickfaden, S., and Owens, J. K. (1992). Posttreatment exposure to camptothecin enhances the lethal effects of x-rays on radioresistant human malignant melanoma cells. *Int. J. Radiat. Oncol. Biol. Phys.* **24,** 939–948.

20. Li, C. J., Averboukh, L., and Pardee, A. B. (1993). beta-Lapachone, a novel DNA topoisomerase I inhibitor with a mode of action different from camptothecin. *J. Biol. Chem.* **268,** 22463–22468.

21. Boothman, D. A., and Pardee, A. B. (1989). Inhibition of radiation-induced neoplastic transformation by beta-lapachone. *Proc. Natl. Acad. Sci. USA* **86,** 4963–4967.

22. Nelson, W. G., and Kastan, M. B. (1994). DNA strand breaks: The DNA template alterations that trigger p53-dependent DNA damage response pathways. *Mol. Cell. Biol.* **14,** 1815–1823.

23. Boothman, D. A. (1994). Enhanced malignant transformation is accompanied by increased survival recovery after ionizing radiation in Chinese hamster embryo fibroblasts. *Radiat. Res.* **138,** S121–S125.

24. Wuerzberger, S. M., Pink, J. J., Planchon, S. M., Byers, K. L., Bornmann, W. G., and Boothman, D. A. (1998). Induction of apoptosis in MCF-7:WS8 breast cancer cells by beta-lapachone. *Cancer Res.* **58,** 1876–1885.

25. Frydman, B., Marton, L. J., Sun, J. S., Neder, K., Witiak, D. T., Liu, A. A., Wang, H. M., Mao, Y., Wu, H. Y., Sanders, M. M., and Liu, L. F. (1997). Induction of DNA topoisomerase II-mediated

observable atypical PARP cleavage at the IC_{50} dose was likely due to a relatively modest, but constant, loss of cells through apoptosis that does not result in the accumulation of enough cells containing cleaved PARP to be observed in Western analyses.

Previous reports have shown cleavage of PARP during necrosis, giving rise to a 50-kDa fragment [54]. However, the atypical PARP fragment observed in β-lap treated cells was ~60 kDa (Fig. 4). The demonstration of nuclear condensation, appearance of sub-G_0/G_1 cells [24], >90% TUNEL-positive cells (Fig. 6), and inhibition of apoptosis by EDTA and EGTA (Fig. 7B) leave little doubt that this response was apoptotic. Interestingly, in β-lap-treated cells, we have noted some unique characteristics that do not fit the "classic" definition of apoptosis. Further study of the action of this novel apoptosis-inducing agent may allow for elucidation of cell death processes which contain characteristics of apoptotic as well as necrotic proteolytic cascades. This agent may induce a heretofore uncharacterized apoptotic pathway that may be exploited for improved treatment of breast cancer. For example, this agent may be useful for treatment of breast cancer which has lost classic caspase-mediated apoptotic responses.

Atypical PARP cleavage observed in MCF-7 cells was not likely the result of caspase, granzyme B, cathepsins B or L, trypsin, or chymotrypsin-like proteases (see Fig. 5) [38]. However, the classic cleavage pattern observed in T47D cells after low-level β-lap exposures was prevented by 25 μM zVAD-fmk, a general caspase inhibitor. Classic PARP cleavage induced by low-dose β-lap exposure was unaffected by other protease inhibitors, suggesting that a different member of the caspase family was responsible for apoptotic proteolysis in T47D cells. At higher doses of β-lap, T47D cells responded like MCF-7 cells, undergoing apoptosis and atypical PARP cleavage. Lack of inhibition of atypical PARP cleavage by zVAD-fmk in MCF-7 cells treated with β-lap strongly suggests that activation of the caspase pathway was not necessary for atypical PARP cleavage.

In β-lap-treated MCF-7 cells, atypical PARP fragmentation was blocked by iodoacetamide or N-ethylmaleimide, both cysteine-alkylating agents (data not shown). Additionally, atypical PARP cleavage was not inhibited by a battery of inhibitors (Fig. 5), each used at previously determined effective doses. These data suggest that atypical fragmentation of PARP in vivo was due to the activation of a cysteine protease which is apparently not a member of the caspase family of proteases. However, the nonspecific reactivity of iodoacetamide and N-ethylmaleimide does allow the possibility that the unknown protease may be indirectly activated after β-lap treatment by a factor which contains critical –SH groups. One protease which fits the available data could be the neutral calcium-dependent protease calpain. This possibility is further supported by the fact that p53 was cleaved in β-lap-treated MCF-7 cells, giving rise to fragments (Fig.

7A) which match those previously described as being the result of calpain activity [42, 43]. Furthermore, the time course of p53 cleavage was concomitant with the appearance of atypically cleaved PARP. Additionally, we provide evidence showing that the cysteine protease is Ca^{+2} dependent, since its activity (as measured by atypical PARP or p53 cleavage) was prevented by coadministration of EDTA or EGTA (Fig. 8B and data not shown). While these findings do not conclusively prove that calpain is responsible for this cleavage, they are suggestive. Our laboratory is currently in the process of definitively identifying the protease responsible for this cleavage of PARP. The use of caspase-3-expressing MCF-7 cells demonstrated that reexpression of caspase-3 did not lead to enhanced apoptosis or appearance of the caspase-mediated 89-kDa PARP fragmentation after β-lap exposure. In contrast, other studies have demonstrated enhanced apoptotic reactions in caspase-3-expressing MCF-7 cells after granzyme B or TNF-α treatments, compared to cells infected with the empty vector [16].

While β-lap treatment of MCF-7 cells appeared to activate a novel apoptotic pathway, classic lamin B cleavage (primarily due to the activation of caspase-6) was also observed ([24, 51] and Fig. 9). While caspase-6 is thought to be activated directly by caspase-3 [55, 56], our data suggest that either a distinct upstream protease can activate caspase-6 after β-lap treatment or an unknown, β-lap-activated protease can directly cleave lamin B, giving rise to fragments of size similar to those observed after caspase-6 cleavage. Our data suggest that once the apoptotic protease is activated, it dominates proteolysis in β-lap-treated MCF-7 cells, since visible classic PARP cleavage fragments were not observed. Interestingly, overexpression of caspase-3 in MCF-7 cells did not affect β-lap cytotoxicity, while increasing sensitivity to granzyme B or TNF-α [16].

Our studies demonstrate that β-lap can induce at least two independent apoptotic pathways in breast cancer cells. The apoptotic response seems to be independent of the in vitro observed β-lap/Topo IIα-mediated DNA cleavage [25], since G_1-arrested cells (which contain very low Topo IIα enzyme activity) were as effectively killed by β-lap as log-phase or G_2/M-arrested cells (which express high levels of Topo IIα enzyme activity). Furthermore, the in vivo pathway activated by β-lap leading to apoptosis may also be independent of the Topo I inhibition observed in vitro. In some cells, β-lap mediates typical caspase activation, leading to the formation of the classic 89 kDa PARP cleavage fragment in vivo [57]. In other cells (specifically, MCF-7), β-lap activates a calcium-dependent, noncaspase cysteine protease. Interestingly, activation of this pathway of apoptosis (which may also result in midprotein cleavage of pRb) eventually occurred in MCF-7 and T47D breast cancer cells. An interesting profile of sensitivity of breast cancer cells to

DNA cleavage by beta-lapachone and related naphthoquinones. *Cancer Res.* **57,** 620–627.

26. Larsen, A. K., Skladanowski, A., and Bojanowski, K. (1996). The roles of DNA topoisomerase II during the cell cycle. *Prog. Cell. Cycle. Res.* **2,** 229–239.

27. D'Arpa, P., and Liu, L. F. (1989). Topoisomerase-targeting antitumor drugs. *Biochim. Biophys. Acta* **989,** 163–177.

28. Slevin, M. L. (1991). The clinical pharmacology of etoposide. *Cancer* **67,** 319–329.

29. Jonsson, E., Fridborg, H., Csoka, K., Dhar, S., Sundstrom, C., Nygren, P., and Larsson, R. (1997). Cytotoxic activity of topotecan in human tumour cell lines and primary cultures of human tumour cells from patients. *Br. J. Cancer* **76,** 211–219.

30. Lamond, J. P., Wang, M., Kinsella, T. J., and Boothman, D. A. (1996). Radiation lethality enhancement with 9-aminocamptothecin: Comparison to other topoisomerase I inhibitors. *Int. J. Radiat. Oncol. Biol. Phys.* **36,** 369–376.

31. Pink, J. J., Bilimoria, M. M., Assikis, J., and Jordan, V. C. (1996). Irreversible loss of the oestrogen receptor in T47D breast cancer cells following prolonged oestrogen deprivation. *Br. J. Cancer* **74,** 1227–1236.

32. Pink, J. J., Jiang, S. Y., Fritsch, M., and Jordan, V. C. (1995). An estrogen-independent MCF-7 breast cancer cell line which contains a novel 80-kilodalton estrogen receptor-related protein. *Cancer Res.* **55,** 2583–2590.

33. Pink, J. J., and Jordan, V. C. (1996). Models of estrogen receptor regulation by estrogens and antiestrogens in breast cancer cell lines. *Cancer Res.* **56,** 2321–2330.

34. Labarca, C., and Paigen, K. (1980). A simple, rapid, and sensitive DNA assay procedure. *Anal. Biochem.* **102,** 344–352.

35. Musgrove, E. A., and Sutherland, R. L. (1993). Acute effects of growth factors on T-47D breast cancer cell cycle progression. *Eur. J. Cancer* **29A,** 2273–2279.

36. Musgrove, E. A., and Sutherland, R. L. (1991). Steroids, growth factors, and cell cycle controls in breast cancer. *Cancer Treat. Res.* **53,** 305–331.

37. Pink, J. J., Fritsch, M., Bilimoria, M. M., Assikis, V. J., and Jordan, V. C. (1997). Cloning and characterization of a 77-kDa oestrogen receptor isolated from a human breast cancer cell line. *Br. J. Cancer* **75,** 17–27.

38. Lotem, J., and Sachs, L. (1996). Differential suppression by protease inhibitors and cytokines of apoptosis induced by wild-type p53 and cytotoxic agents. *Proc. Natl. Acad. Sci. USA* **93,** 12507–12512.

39. Li, X., Traganos, F., Melamed, M. R., and Darzynkiewicz, Z. (1995). Single-step procedure for labeling DNA strand breaks with fluorescein- or BODIPY-conjugated deoxynucleotides: Detection of apoptosis and bromodeoxyuridine incorporation. *Cytometry* **20,** 172–180.

40. Zollner, H. (1993). "Handbook of Enzyme Inhibitors," pp. 728–730, VCH, Weinheim/New York.

41. Waxman, L. (1981). Calcium-activated proteases in mammalian tissues. *Methods Enzymol.* **80,** 664–680.

42. Kubbutat, M. H., and Vousden, K. H. (1997). Proteolytic cleavage of human p53 by calpain: A potential regulator of protein stability. *Mol. Cell. Biol.* **17,** 460–468.

43. Pariat, M., Carillo, S., Molinari, M., Salvat, C., Debussche, L., Bracco, L., Milner, J., and Piechaczyk, M. (1997). Proteolysis by calpains: A possible contribution to degradation of p53. *Mol. Cell. Biol.* **17,** 2806–2815.

44. Wakeling, A. E., and Bowler, J. (1992). ICI 182,780, a new antioestrogen with clinical potential. *J. Steroid Biochem. Mol. Biol.* **43,** 173–177.

45. Pink, J. J., and Jordan, V. C. (1995). Molecular mechanisms of antiestrogen resistance. *In* "Drug and Hormonal Resistance in Breast Cancer: Cellular and Molecular Mechanisms" (R. B. Dickson and M. E. Lippman, Eds.), Ellis Horwood, Hemel Hempstead, UK.

46. Musgrove, E. A., Sarcevic, B., and Sutherland, R. L. (1996). Inducible expression of cyclin D1 in T-47D human breast cancer cells is sufficient for Cdk2 activation and pRB hyperphosphorylation. *J. Cell. Biochem.* **60,** 363–378.

47. Musgrove, E. A., and Sutherland, R. L. (1994). Cell cycle control by steroid hormones. *Semin. Cancer Biol.* **5,** 381–389.

48. Musgrove, E. A., Wakeling, A. E., and Sutherland, R. L. (1989). Points of action of estrogen antagonists and a calmodulin antagonist within the MCF-7 human breast cancer cell cycle. *Cancer Res.* **49,** 2398–2404.

49. Foster, J. S., and Wimalasena, J. (1996). Estrogen regulates activity of cyclin-dependent kinases and retinoblastoma protein phosphorylation in breast cancer cells. *Mol. Endocrinol.* **10,** 488–498.

50. Li, F., Srinivasan, A., Wang, Y., Armstrong, R. C., Tomaselli, K. J., and Fritz, L. C. (1997). Cell-specific induction of apoptosis by microinjection of cytochrome c. Bcl-xL has activity independent of cytochrome c release. *J. Biol. Chem.* **272,** 30299–30305.

51. Orth, K., Chinnaiyan, A. M., Garg, M., Froelich, C. J., and Dixit, V. M. (1996). The CED-3/ICE-like protease Mch2 is activated during apoptosis and cleaves the death substrate lamin A. *J. Biol. Chem.* **271,** 16443–16446.

52. Takahashi, A., Alnemri, E. S., Lazebnik, Y. A., Fernandes-Alnemri, T., Litwack, G., Moir, R. D., Goldman, R. D., Poirier, G. G., Kaufmann, S. H., and Earnshaw, W. C. (1996). Cleavage of lamin A by Mch2 alpha but not CPP32: Multiple interleukin 1 beta-converting enzyme-related proteases with distinct substrate recognition properties are active in apoptosis. *Proc. Natl. Acad. Sci. USA* **93,** 8395–8400.

53. Morris, E. J., and Geller, H. M. (1996). Induction of neuronal apoptosis by camptothecin, an inhibitor of DNA topoisomerase-I: Evidence for cell cycle-independent toxicity. *J. Cell Biol.* **134,** 757–770.

54. Shah, G. M., Shah, R. G., and Poirier, G. G. (1996). Different cleavage pattern for poly(ADP-ribose) polymerase during necrosis and apoptosis in HL-60 cells. *Biochem. Biophys. Res. Commun.* **229,** 838–844.

55. Faleiro, L., Kobayashi, R., Fearnhead, H., and Lazebnik, Y. (1997). Multiple species of CPP32 and Mch2 are the major active caspases present in apoptotic cells. *EMBO J.* **16,** 2271–2281.

56. Hirata, H., Takahashi, A., Kobayashi, S., Yonehara, S., Sawai, H., Okazaki, T., Yamamoto, K., and Sasada, M. (1998). Caspases are activated in a branched protease cascade and control distinct downstream processes in Fas-induced apoptosis. *J. Exp. Med.* **187,** 587–600.

57. Planchon, S. M., Wuerzberger-Davis, S. M., Pink, J. J., Robertson, K. A., Bornmann, W. G., and Boothman, D. A. (1999). Bcl-2 protects against β-lapachone-mediated caspase 3 activation and apoptosis in human myeloid leukemia (HL-60) cells. *Oncol. Rep.* **6,** 485–492.

NF-κB Activation by Camptothecin

A LINKAGE BETWEEN NUCLEAR DNA DAMAGE AND CYTOPLASMIC SIGNALING EVENTS*

Tony T. Huang‡§, Shelly M. Wuerzberger-Davis¶, Bradley J. Seufzer§, Stuart D. Shumway§‖,
Takeshi Kurama§, David A. Boothman¶**, and Shigeki Miyamoto‡§¶‖‡‡

From the ‡Program in Molecular and Cellular Pharmacology, the ¶Human Cancer Biology Program, the ‖Program in
Cellular and Molecular Biology, and the §Department of Pharmacology University of Wisconsin, Madison, Wisconsin
53792 and the **Departments of Radiation Oncology and Pharmacology, Laboratory of Molecular Stress Responses, Case
Western Reserve University, Cleveland, Ohio 44106-4942

Activation of the transcription factor NF-κB by extracellular signals involves its release from the inhibitor protein IκBα in the cytoplasm and subsequent nuclear translocation. NF-κB can also be activated by the anticancer agent camptothecin (CPT), which inhibits DNA topoisomerase (Topo) I activity and causes DNA double-strand breaks during DNA replication to induce S phase-dependent cytotoxicity. Here we show that CPT activates NF-κB by a mechanism that is dependent on initial nuclear DNA damage followed by cytoplasmic signaling events. NF-κB activation by CPT is dramatically diminished in cytoplasts and in CEM/C2 cells expressing a mutant Topo I protein that fails to bind CPT. This response is intensified in S phase cell populations and is prevented by the DNA polymerase inhibitor aphidicolin. In addition, CPT activation of NF-κB involves degradation of cytoplasmic IκBα by the ubiquitin-proteasome pathway in a manner that depends on the IκB kinase complex. Finally, inhibition of NF-κB activation augments CPT-induced apoptosis. These findings elucidate the progression of signaling events that initiates in the nucleus with CPT-Topo I interaction and continues in the cytoplasm resulting in degradation of IκBα and nuclear translocation of NF-κB to attenuate the apoptotic response.

The NF-κB/Rel family of transcription factors regulates expression of genes critical for multiple biological processes, including immune responses, inflammatory reactions, and apoptosis (1–3). In mammalian cells, NF-κB exists as dimeric complexes composed of p50, p65 (RelA), c-Rel, RelB, or p52. These proteins share a conserved Rel homology domain that encodes dimerization, DNA binding, and nuclear localization functions. NF-κB associates with members of the IκB family of proteins, most notably IκBα, which masks the nuclear localiza-

tion sequence of NF-κB and retains it in the cytoplasm (4, 5). Dissociation from IκBα is essential for NF-κB to enter the nucleus and to activate gene expression. Several signaling cascades that control NF-κB activation converge at an IκB kinase (IKK)[1] complex, responsible for site-specific phosphorylation of IκBα at serines 32 and 36 (6–10). Phosphorylation of IκBα induces multiubiquitination of IκBα and its subsequent degradation by the ubiquitin-dependent 26 S proteasome (11, 12). This sequence of events can be induced without de novo protein synthesis by multiple extracellular stimuli, including tumor necrosis factor α (TNFα), interleukin-1, phorbol ester (PMA), bacterial lipopolysaccharide (LPS), and others. However, NF-κB activation can also be achieved through mechanisms that are distinct from the above IKK-dependent model. These include phosphorylation-independent yet proteasome-mediated IκBα degradation induced by ultraviolet irradiation (13, 14), calpain-dependent degradation of IκBα by silica and TNFα (15, 16), and tyrosine phosphorylation-induced dissociation of IκBα from NF-κB following hypoxia and reoxygenation (17). Thus, depending on the stimuli, NF-κB can be activated through multiple distinct regulatory pathways.

Activation pathways of NF-κB typically originate from ligand-receptor interactions on the cell membrane. However, NF-κB can also be activated by a group of agents that damage DNA in the nucleus. A paradox confounding our current understanding of the mechanism of NF-κB activation by agents that damage DNA is that the major source of damaged DNA is in the nucleus, whereas latent NF-κB complex is in the cytoplasm. It was previously hypothesized that a signal may transfer from the nucleus to the cytoplasm (18). In support of this model, a recent study by Piette and Piret (19) provides evidence that NF-κB activation by DNA-damaging agents correlates with their capacity to induce DNA breaks. However, the requirement of damaged DNA in the nucleus has not been directly demonstrated. In contrast, Devary et al. (20) showed that enucleated cells (i.e. cytoplasts) retained full capacity to activate NF-κB following UV irradiation, indicating that nuclear DNA damage is not necessary for NF-κB activation by UV irradiation. There is now substantial evidence to support the notion that UV activation of NF-κB involves activation of cell surface receptors by ligand-independent oligomerization (14,

[1] The abbreviations used are: IKK, IκB kinase; TNFα, tumor necrosis factor α; PMA, phorbol myristyl acetate; LPS, lipopolysaccharide; CPT, camptothecin; Topo I, DNA topoisomerase I; SSB, DNA single-strand break; DSB, DNA double-strand break; TPT, topotecan; ALLN, acetyl-leucinyl-leucinyl-norleucinal; EMSA, electrophoretic mobility shift assay; HA, hemagglutinin; GFP, green fluorescent protein; WT, wild type; FACS, fluorescence-activated cell sorter; X-gal, 5-bromo-4-chloro-3-indolyl β-D-galactopyranoside.

21–24) and/or oxidative stress-mediated inactivation of receptor tyrosine phosphatases, which ultimately leads to ligand-independent activation of receptor tyrosine kinases (25). Whether nuclear DNA damage can directly activate an intracellular NF-κB signaling pathway without involving cell surface receptors remains an important question yet to be resolved.

We and others have observed that an anti-cancer agent, camptothecin (CPT), can activate NF-κB in pre-B or T cell lines (19, 26). CPT inhibits the activity of DNA topoisomerase (Topo) I (27–29). Topo I changes the supercoiling of DNA and therefore plays critical roles in DNA replication, in RNA transcription, and, indirectly, in DNA damage repair (30). CPT selectively binds to and stabilizes a covalent Topo I-DNA reaction intermediate, referred to as the cleavable complex, which contains a single-strand DNA break (SSB) (31, 32). DNA double-strand breaks (DSBs) are then generated during DNA replication when the replication fork collides with the cleavable complex (33). In the present study, our objective was to determine whether or not nuclear events associated with the DNA-damaging action of CPT and a clinically utilized derivative of CPT, topotecan (TPT) (34, 35) were required for activation of cytoplasmically localized NF-κB complexes. We also examined whether CPT activation of NF-κB modulated an apoptotic response. Our findings elucidate a series of nuclear events induced by CPT/TPT that converge with cytoplasmic signaling events responsible for the activation of NF-κB, which can provide anti-apoptotic function.

EXPERIMENTAL PROCEDURES

Cell Culture—Culture conditions for 70Z/3 and 70Z/3-CD14 murine pre-B cells have been described (36). CEMp and CEM/C2 human T cell lines were kindly provided by Dr. Y. Pommier (National Institutes of Health) and maintained in RPMI 1640 medium (Cellgro, Mediatech) supplemented with 10% fetal bovine serum (HyClone Laboratory, Inc.), 1000 units of penicillin G (Sigma), and 0.5 mg/ml streptomycin sulfate (Sigma) in an humidified 5% CO_2-95% air incubator (Forma Scientific). HeLa human cervical carcinoma cells and PC-3 human prostate carcinoma cells were maintained in Dulbecco's modified Eagle's medium (Cellgro) supplemented with 10% fetal bovine serum and antibiotics as above in a 10% CO_2-90% air incubator. The human kidney embryonic fibroblast 293 (HEK293) was maintained in the latter medium on 0.1% (w/v) gelatin-coated plastic culture dishes.

Reagents—CPT, VP16, calpain inhibitor I (ALLN), Me₂SO, bacterial LPS, PMA, cycloheximide, aphidicolin, and cytochalasin B were purchased from Sigma. TPT was a gift from SmithKline Beecham. Lactacystin was generously provided by Dr. E. J. Corey (Harvard University). Stock solutions were prepared in Me₂SO at 10 mM (CPT), 10 mM (VP16), 30 mM (aphidicolin), cytochalsin B (10 mg/ml), and 25 mM (lactacystin, 25% Me₂SO-75% H_2O). TPT stock was made in water at 30 mM. LPS was prepared in RPMI growth medium at 1 or 10 mg/ml. Human recombinant TNFα was from CalBiochem and resuspended in phosphate-buffered saline containing 0.1% bovine serum albumin (fraction V, Sigma). A 50 μM PMA stock was made in 100% ethanol. A cycloheximide stock solution was made in water at 50 mg/ml. In each experiment, all samples received the same amounts of Me₂SO to control for potential Me₂SO effects. All stock solutions were stored in aliquots at either −70 °C or −20 °C. IgGs against IκBα (C21), c-Rel (C), p65 (A and C20), Rel-B (C-19), p52 (I-18), and p50 (NLS) were purchased from Santa Cruz Biotechnology. A monoclonal anti-FLAG antibody was purchased from Kodak, and horseradish peroxidase-conjugated anti-rabbit and anti-mouse antibodies and protein A were obtained from Amersham Pharmacia Biotech. Prestained protein molecular weight markers were purchased from Life Technologies, Inc. Cell preparation and Western immunoblots were performed as described (36) and developed using the ECL procedure according to the manufacturer (Amersham Pharmacia Biotech). Blots were then exposed to x-ray film (Kodak).

Electrophoretic Mobility Shift and Supershift Assays—The Igκ-κB oligonucleotide probe and conditions for EMSA were previously described (36). For supershift assays, 1 μg of IgG antibodies specific to members of the NF-κB proteins (Santa Cruz Biotechnology) were added to nuclear extracts for 20 min on ice prior to addition of radiolabeled probe. The AP-1 site used for control EMSA reactions was obtained from Promega.

Enucleation Procedure—Enucleation was performed as described (37) with the following modifications. PC3 or HeLa cells were seeded in 30-mm dishes, grown overnight, and exposed to cytochalasin B (10 μg/ml) for a total of 30 min at 37 °C. Plates were placed upside down in 400-ml centrifuge bottles and bathed in growth medium containing cytochalasin B at the same concentration. Plates were secured at the bottom of the centrifuge bottles by appropriately sized styrofoam. Samples were then centrifuged at 10,000 rpm for 15 min at 37 °C using a Beckman JA-14 rotor. The rotor and centrifuge chamber were prewarmed to ~37 °C by prior centrifugation without samples. Plates with enucleated cells (*i.e.* cytoplasts) were then removed from the centrifuge bottle, gently rinsed with phosphate-buffered saline, and incubated with prewarmed growth medium for 30 min at 37 °C. Samples of enucleated cells were fixed in 3:1 methanol/acetic acid, stained with Hoechst dye 33258, and photographed under a fluorescent microscope equipped with a 4'6,-diamidino-2-phenylindole-specific filter. The enucleation efficiency varied from ~75 to 95% for PC-3 and HeLa cells.

Transient Transfection Assay—Cells (HEK293, HeLa, or PC-3) were transiently transfected using a standard calcium phosphate precipitation method (38). CEMp and CEM/C2 cells were transfected with DEAE-Dextran method (39). An NF-κB-dependent luciferase reporter (3xκB-Luc) was constructed by inserting a *Hind*III-*Bgl*II fragment of 3xκB-CAT into the *Hind*III-*Bgl*II sites of the tk-Luc plasmid (kindly provided by Dr. R. Evans, Salk Institutite). 3xMκB-Luc was constructed using a similar cloning strategy starting with the 3xMκB-CAT (40). 24 h following transfection, cells were treated with TPT (30 μM) or CPT (10 μM) for 2 h, rinsed twice with growth medium, and further incubated without drugs for 6 h before termination of the cultures. Positive control samples were treated with TNFα (10 ng/ml) for a total of 8 h. Control samples were transfected with the LacZ cDNA under the control of the cytomegalovirus promoter in the pCMX vector (CMV-LacZ). For CEMp and CEM/C2 cells, total proteins were used for normalization.

Full-length human IKKα cDNA was provided by Dr. I. M. Verma (Salk Institute). Full-length human IKKβ cDNA was cloned by screening a human kidney cDNA library in λZAPII with a polymerase chain reaction-amplified DNA fragment using a HeLa cDNA library (CLONTECH) and TO237 (5-CTCAGCAGCTCAAGGCCAAG-3') and TO240 (5'-CCAGAGCTCCTTCTGCCGC-3') primers. IKKα and IKKβ with a Lys-to-Ala substitution at the conserved ATP binding site were generated by polymerase chain reaction mutagenesis and confirmed by DNA sequencing. The mutant genes were placed under the control of the cytomegalovirus promoter in the pcDNA3.1(+) expression vector (CLONTECH). HEK293 cells were transfected with these constructs by calcium phosphate precipitation and then treated with either TNFα (10 ng/ml) or TPT (30 μM) for 2 h. Nuclear extracts were analyzed by EMSA as described above. Cytoplasmic extracts were analyzed by Western blotting using the anti-FLAG monoclonal antibody (Kodak) to determine expression levels of respective dominant-negative mutants in each condition. An horseradish peroxidase-conjugated donkey anti-mouse antibody (Amersham Pharmacia Biotech) was used for secondary antibody followed by ECL development.

Retrovirus Construction and Infection—Production and infection of HA-tagged wild-type and HA-tagged S32A/S36A mutant IκBα expression constructs were described (36). Other IκBα deletion mutants were generated by polymerase chain reaction-mediated mutagenesis and confirmed by sequencing. Stable pools were selected with hygromycin (1 mg/ml, Roche Molecular Biochemicals), and the expression levels of the corresponding proteins were examined by either anti-IκBα (C21, a C-terminal epitope) or anti-HA antibodies. For experiments shown in Figs. 7*B* and 9, HA-S32A/S36A clone 5 that expressed a relatively high level of the mutant protein was used. Similar but less pronounced effects were also seen with pooled cultures and in five isolated clones expressing varying levels of mutant protein (not shown).

Generation of a Green Fluorescent Protein-IκBα Fusion Construct—N-terminally fused GFP-IκBα was generated by subcloning polymerase chain reaction amplified human IκBα (MAD3) into *Hind*III-*Bam*HI sites of the pEGFP vector (CLONTECH), such that the entire MAD3 coding sequence was in-frame with the GFP coding sequence. Stable HEK293 cell clones were generated by G418 selection and subsequent FACS sorting. Cells were photographed using a Zeiss Axioplan microscope equipped for fluorescence with the aid of a fluorescein-specific filter.

FACS Analyses—For FACS sorting of G_1, S, and total cell fractions for EMSA analyses, 70Z/3 cells untreated or treated with CPT, TPT, or LPS for appropriate durations were stained with Hoechst 33342 (stock at 10 mg/ml in water) at the final concentration of 10 μg/ml for 15 min
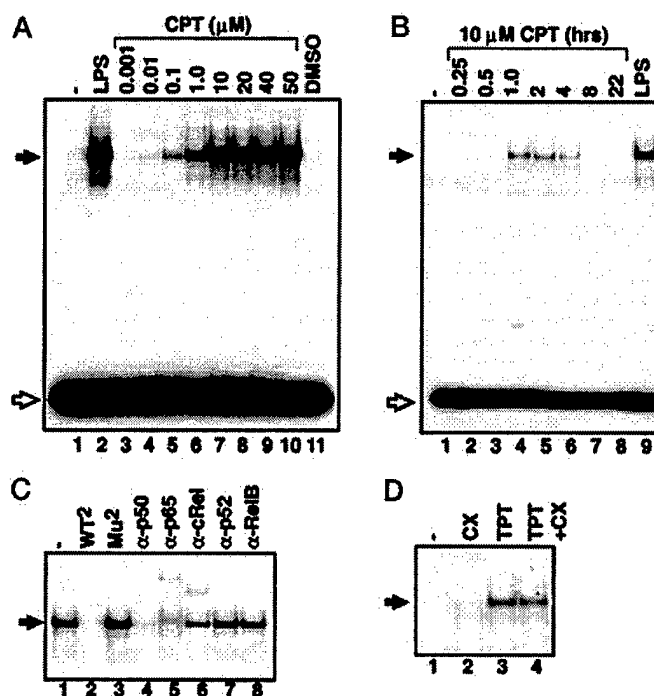
FIG. 1. **NF-κB activation by CPT is transient and does not require *de novo* protein synthesis.** *A*, dose response of CPT-induced NF-κB activation. Exponentially growing 70Z/3-CD14 murine pre-B cells were treated with various doses of CPT shown in μM for 2 h (*lanes 4–11*). Nuclear extracts (10 μg) were analyzed by EMSA using the Igκ-κB probe as in Ref. 36. Stimulation of NF-κB activation by LPS was for 15 min at 1 μg/ml final concentration. All samples, except for untreated cell extracts, were adjusted to 0.5% Me$_2$SO, a solvent for CPT. NF-κB complex and free probe were indicated by *closed* and *open arrows*, respectively. *B*, time course of CPT-induced NF-κB activation. 70Z/3-CD14 cells were treated with 10 μM CPT, terminated at various times and analyzed as described above. The LPS positive control (*lane 9*) was as described above. *C*, specificity of NF-κB complexes induced by CPT. A nuclear extract isolated from cells exposed to 10 μM CPT for 2 h was incubated with 50-fold excess wild-type or mutated oligonucleotides or with antibodies specific to p50 (NLS), p65/RelA (A), c-Rel (C), p52 (I-18), or RelB (C-19). Supershifted bands for anti-p65 and anti-c-Rel can be seen as slower migrating bands. Antibody against p50 causes reduced DNA binding. *D*, NF-κB activation by CPT occurs in the absence of *de novo* protein synthesis. Cells were treated with or without 20 μg/ml cycloheximide (*CX*) for 30 min to block *de novo* protein synthesis and treated with TPT (30 μM) for 1 h and analyzed as described above. The above data are representative of experiments performed at least three times.

at 37 °C in RPMI growth medium, followed by cell isolation using FACStar^{PLUS} (Becton Dickinson) at 4 °C. 10^6 cells each were purified, and total cell extracts were prepared for EMSA analyses. The status of the cell cycle of purified fractions was confirmed by propidium iodide staining followed by analysis with FACSCalibur (Becton Dickinson). Detailed protocols for apoptosis analyses using FACS have been published (41). Briefly, cells were fixed in ethanol, treated with a citric acid buffer to release fragmented DNA out of the cells, stained with propidium iodide, and analyzed using FACSCalibur.

RESULTS

CPT Induces Transient NF-κB Activation in the Absence of de Novo Protein Synthesis—NF-κB activity is dictated by its ability to bind cognate κB sites present in responsive genes. We utilized a κB site from the immunoglobulin κ intronic enhancer in EMSA analyses to evaluate NF-κB activation by CPT or TPT treatments. CPT induces dose-dependent (Fig. 1*A*, saturating at 10 μM) and transient (Fig. 1*B*, peaking at 1–2 h) NF-κB binding activity in 70Z/3-CD14 pre-B cells. Addition of 50-fold excess specific and nonspecific oligonucleotides (Fig. 1*C*, *lanes 1–3*) shows that the binding activity is specific to NF-κB. Specificity is further demonstrated by the interaction of binding complex with antibodies to p50, RelA, and c-Rel (Fig. 1*C*). Antibodies to other NF-κB family members, p52 and RelB, did not alter binding, indicating that these proteins are not components of the NF-κB complex induced by CPT in 70Z/3-CD14 cells. Pretreatment with cycloheximide (Fig. 1*D*, *lanes 3* and *4*) did not interfere with this pathway, which shows that CPT action does not require *de novo* protein synthesis. This activation is not limited to lymphoid cells because it was also induced
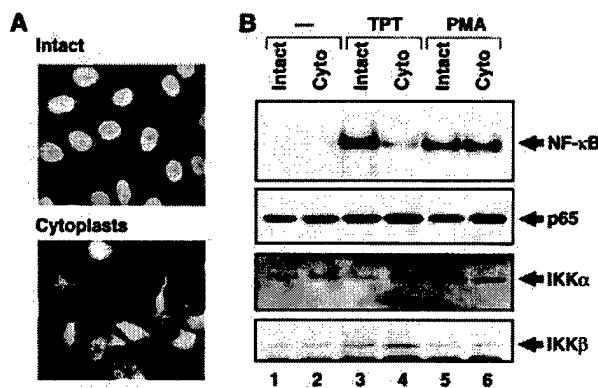

FIG. 2. **Intact nucleus is necessary for NF-κB activation by TPT.** *A*, Hoechst dye staining of intact and enucleated PC-3 cells. PC-3 cells were enucleated as described under "Experimental Procedures." Cells were fixed and stained with Hoechst DNA dye and visualized under a fluorescent microscope and photographed. The exposure time for the cytoplasts was longer than that for the intact cells to aid visualization of otherwise faint cytoplast staining. *B*, EMSA of intact cells and cytoplasts treated with TPT or PMA. Intact cells or cytoplasts were treated with TPT (30 μM) or PMA (50 nM) for 1 h, and equal amount of total cell extracts (2.5 μg) were analyzed by EMSA (NF-κB) or Western blots (p65, IKKα, and IKKβ). The data are representative of three independent experiments.

by both CPT and TPT in CEM T leukemic, PC-3 prostate cancer, HEK293 embryonic kidney fibroblast, and HeLa cervical cancer cell lines (see below, others not shown). Induction of

NF-κB DNA binding activity by CPT or TPT treatment resulted in increased NF-κB-dependent transcription of a luciferase reporter gene (see below). Thus, CPT or TPT activation of NF-κB occurs without *de novo* protein synthesis and may utilize pre-existing regulatory component(s).

Interaction of CPT with Nuclear Topo I Is Necessary for NF-κB Activation—The primary molecular target of CPT or TPT is nuclear Topo I enzyme (27, 32). However, mitochondria also contain CPT-sensitive Topo I (42). It is also possible that CPT activation of NF-κB may involve molecular target(s) other than nuclear Topo I. To evaluate the requirement of a nuclear event in NF-κB activation by CPT, we enucleated PC-3 and HeLa cells by the cytochalasin B-mediated enucleation procedure (37). This protocol produced enucleated cells with approximately 90% efficiency as determined by nuclear staining with Hoechst dye (Fig. 2A). Consistent with a previous report (43), EMSA of total cell extracts prepared from intact and enucleated cells demonstrated that NF-κB activation by activators, such as PMA (Fig. 2B) or TNF (80), does not require an intact nucleus. By contrast, the NF-κB response by CPT and TPT was dramatically diminished in the enucleated cells (Fig. 2B). Modest activation by TPT in enucleated cells is likely due to low numbers of intact cells present in the enucleated cell population (Fig. 2B). NF-κB (p65), and upstream kinases in the signaling pathway, IKKα and IKKβ, are still present in the cytoplasts (Fig. 2B, lanes 2, 4, and 6), demonstrating that the lack of NF-κB activation response in certain enucleated samples (lane 4) is not due to potential leakage of these signaling components. Thus, these results are consistent with the hypothesis that a nuclear event is necessary for NF-κB activation by CPT-related compounds.

Although the above data are consistent with the notion that an intact nucleus is required for NF-κB activation by CPT, it is unknown whether Topo I-induced DNA damage is also required for this process. Its DNA-damaging function requires CPT to interact with Topo I-DNA cleavable complexes (33). To address whether direct interaction of CPT and a Topo I-DNA complex is necessary for activation of NF-κB, we examined human CEM/C2 cells, which exclusively express a mutant Topo I enzyme (44). This mutant Topo I enzyme contains two amino acid substitutions, Met[370] to Thr and Asp[722] to Ser. The latter mutation alone makes Topo I enzyme ~1000-fold more resistant to CPT (or TPT)-mediated inhibition of the religation of DNA nicks, making it incapable of efficiently inducing DNA damage by CPT treatment *in vivo* (45). We compared CPT-induced NF-κB activity in CEM/C2 and the parental CEMp cells by EMSA. Time course and dose response studies (Fig. 3, A and B, respectively), as well as κB-dependent luciferase reporter assay (Fig. 3C), clearly demonstrated that CEM/C2 cells could not mount the NF-κB response by CPT treatment, whereas the parental cell line retained the ability to activate NF-κB. Efficient activation of NF-κB in CEM/C2 cells by TNF (Fig. 3B) or other DNA-damaging agents, such as VP16 and ionizing radiation (Fig. 3D, others not shown), revealed that the lack of NF-κB activation was specific to CPT treatment. Thus, these results together provide strong evidence that Topo I-mediated nuclear DNA damage is necessary for NF-κB activation by CPT treatment.

NF-κB Activation by CPT Depends on DNA Replication and Is Concentrated in S phase of the Cell Cycle—CPT inhibition of the religation step during the Topo I reaction induces stabilization of the cleavable complexes, resulting in generation of SSB. These SSB are reversible but can be converted into lethal DSB during S phase, when the replication fork collides with the cleavable complex (33). It has been suggested that aphidicolin-induced inhibition of DNA polymerase activity prevents DSB
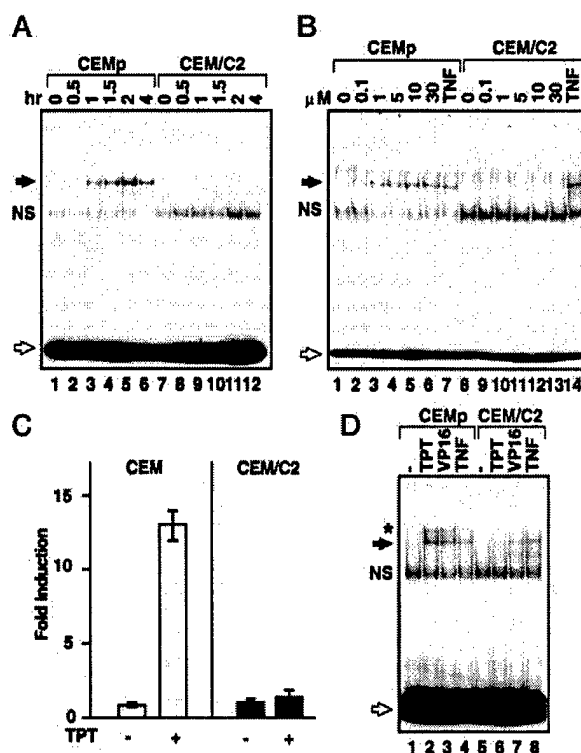
FIG. 3. **Interaction of CPT with Topo I is necessary for NF-κB activation.** A, time course of NF-κB activation by CPT treatment in CEMp and CEM/C2 cells. Asynchronous cultures of CEMp and CEM/C2 cells were treated with 10 μM CPT for the periods indicated, and nuclear extracts were analyzed by EMSA as in Fig. 1A. The *filled arrow* points to NF-κB, and the *open arrow* points to free probe. *NS* refers to nonspecific band. B, CPT dose response of NF-κB activation in CEMp and CEM/C2 cells. These cells were treated for 2 h with various doses of CPT in μM or TNFα (10 ng/ml) and analyzed as above. C, NF-κB-dependent luciferase activation in CEMp and CEM/C2 cells. These cells were transiently transfected with the 3xκB-Luc reporter construct treated with 30 μM TPT for 2 h at 24 h after transfection. After medium change, cells were further incubated in the absence of TPT for 6 additional hours before analysis for luciferase activity. Luciferase activity in untreated cells were set as an arbitrary unit of one. *Error bars* are standard deviation from three experiments. D, NF-κB activation by VP16 in CEMp and CEM/C2 cells. CEMp and CEM/C2 cells were treated with TPT (30 μM), VP16 (20 μM), or TNFα (20 ng/ml) for 2 h and analyzed by EMSA. The optimum dose of VP16 and exposure time was determined by dose response and time course experiments (not shown). The *asterisk* indicates an NF-κB complex whose appearance was not consistently seen. The above data are representative of three independent experiments.

liberation (34). Aphidicolin prevents S phase-specific toxicity of CPT (46). To evaluate whether a SSB or DSB is critical for NF-κB activation by CPT, we examined the influence of aphidicolin on CPT induction of NF-κB. FACS analysis confirmed that ~50% 70Z/3-CD14 cells were in S phase of the cell cycle at the time of CPT treatment (see below). The EMSA demonstrated that CPT activation of NF-κB was efficiently blocked by this treatment (Fig. 4A, lanes 3–5). Aphidicolin, however, did not block NF-κB activation by bacterial LPS (lanes 10–12). Aphidicolin also did not directly block NF-κB DNA binding activity (lanes 6–8). These results are consistent with the hypothesis that the generation of DSB, not SSB, is necessary for efficient NF-κB activation by CPT treatment (19). These data also imply that this activation pathway may occur only in the S phase of the cell cycle. We therefore enriched 70Z/3-CD14 cells in the S phase by FACS sorting after cells were stimulated with CPT or LPS for 2 h (Fig. 4B). Compared with a similarly obtained G_1 cell population, NF-κB activation was 2.8-fold higher in the S phase
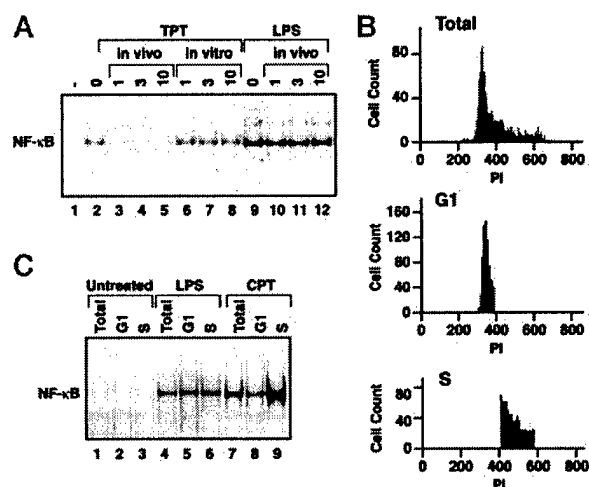
FIG. 4. **CPT activation of NF-κB requires S phase-dependent generation of DSB.** *A*, DNA replication is required for NF-κB activation by CPT treatment. 70Z/3-CD14 cells were treated with 30 μM TPT or 1 μg/ml LPS in the presence or absence of the indicated concentration of aphidicolin (*in vivo* treatments) and nuclear extracts were analyzed by EMSA. *In vitro* refers to addition of the drug direct to cell extracts as in *lane 2* prior to electrophoresis. *B*, FACS enrichment of G_1 and S phase cell population. Exponentially growing 70Z/3-CD14 cells were FACS purified based on DNA content as measured by Hoechst staining into total, G_1, and S populations. *C*, NF-κB activation by CPT treatment is concentrated in S phase of the cell cycle. NF-κB activation in cell fractions isolated as in *B* was analyzed by EMSA using equal protein loading. Phosphorimage analysis showed that CPT activation was 2.8-fold higher in S fraction than in G_1. The data are representative of at least two independent experiments.

population when equivalent amounts of cell extracts were analyzed by EMSA (Fig. 4C). LPS stimulation did not show any significant differences between S and G_1 cells. These findings demonstrate that CPT activation of NF-κB is cell cycle coupled and predominantly takes place during the S phase of the cell cycle in a DNA-polymerase-dependent fashion. This also can explain why NF-κB activation by CPT or TPT is relatively lower in virtually all cell types examined when compared with LPS or TNFα. NF-κB activation by CPT or TPT is dependent on the percentage of replicating cells in S phase, whereas activation by either LPS or TNFα is not cell cycle coupled.

CPT Induces Degradation of IκBα by a Ubiquitin-Proteasome Pathway—The regulatory events governing NF-κB activity induced by cytokines and LPS are well characterized and involve activation of cytoplasmic signaling cascades (2). The primary regulator is the inhibitory protein, IκBα, which maintains NF-κB in the cytoplasm. Release of NF-κB to the nucleus depends on degradation of IκBα. To determine whether CPT activation of NF-κB is solely dependent on nuclear events or whether cytoplasmic events are also required, IκBα protein levels were monitored following treatment with CPT by Western immunoblot analyses. CPT treatment caused a reduction in IκBα protein levels (Fig. 5A, compare *lanes 6* and *7*), consistent with induction of IκBα degradation. This degradation was prevented by the proteasome inhibitors, ALLN and lactacystin (Fig. 5A, *lanes 8* and *9*). A longer exposure of the film (Fig. 5B, *lanes 8* and *9*) revealed an accumulation of characteristic high molecular mass multiubiquitinated IκBα ladders (11, 12). Proteasome inhibitors not only prevented IκBα degradation but also NF-κB activation by CPT treatment (Fig. 5C, compare *lanes 2* and *3*). TPT induced similar IκBα degradation (Fig. 6A). Inhibition of IκBα degradation by ALLN resulted in accumulation of IκBα in the cytoplasm, as visualized by an IκBα protein N-terminally tagged with the green fluorescent protein
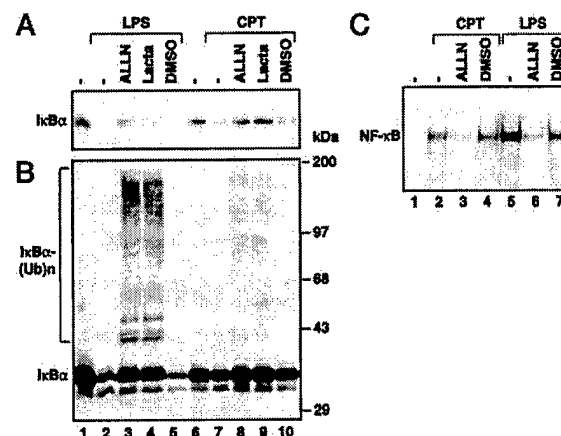

FIG. 5. **CPT induces degradation of IκBα by the ubiquitin-proteasome pathway.** *A*, IκBα degradation induced by CPT is blocked by proteasome inhibitors. 70Z/3-CD14 cells were pretreated for 30 min with ALLN (50 μg/ml), lactacystin (*Lacta*; 20 μM), or Me_2SO solvent (*DMSO*; 0.1%) and then treated with 1 μg/ml LPS (*lanes 2–6*) for 15 min or 10 μM CPT (*lanes 8–12*) for 1 h. Samples were analyzed by Western immunoblot using an IκBα-specific antibody (C21). *B*, inhibition of IκBα degradation by proteasome inhibitors induces accumulation of high molecular mass IκBα-ubiquitin ladders. A longer exposure of the blot in *A*. The positions of the IκBα band and multiubiquitinated IκBα ladders (IκBα-(Ub)n) are shown on the *left* of the figure. Relative molecular mass (in kDa) is shown on the *right*. *C*, NF-κB activation induced by CPT is blocked by proteasome inhibitors. Nuclear extracts prepared from cells that were treated as in *A* were analyzed by EMSA for NF-κB binding activity as in Fig. 1A. The data are representative of two or more independent experiments.

(GFP-IκBα) (Fig. 6B, *right panel*). Control coimmunoprecipitation experiments with RelA-specific antibodies confirmed that the addition of the GFP tag did not interfere with its association with NF-κB (80). The GFP tag also did not affect TPT-induced proteolysis (Fig. 6A, *lanes 2–5*). Thus, induction of IκBα degradation by CPT or TPT is similar to that induced by LPS in 70Z/3 cells or TNFα in multiple cell types (1, 2), which utilizes a ubiquitin-proteasome pathway. Moreover, we also found that IκBα degradation by TPT was markedly reduced in enucleated PC3 cells (not shown). These data demonstrate that the progression of events initiated in the nucleus by TPT or CPT treatment is continued in the cytoplasm.

IκBα Degradation Induced by CPT or TPT Is Ser[32/36]-dependent—Although cytokines and LPS cause IκBα degradation by a ubiquitin-proteasome pathway that requires intact Ser[32] and Ser[36] residues, UV irradiation causes IκBα degradation by a ubiquitin-proteasome pathway independent of these Ser residues (13, 14). To evaluate whether CPT or TPT-induced IκBα degradation requires intact Ser[32/36] residues, the S32A/S36A mutant protein was N-terminally tagged with an HA epitope (HA-S32A/S36A) (36), stably introduced in 70Z/3-CD14 cells, and analyzed for sensitivity to degradation by TPT treatment. The S32A/S36A mutant protein was completely resistant to degradation induced by TPT treatment (Fig. 7A). This was not due to the presence of the HA tag because the control HA-WT IκBα protein was efficiently degraded. Moreover, a Ser[32/36] deletion mutant without the HA tag also failed to be efficiently degraded (Fig. 7A, Δ30–40). Stable expression of the HA-S32A/S36A mutant, but not HA-WT, selectively eliminated the appearance of NF-κB DNA binding in the nucleus after treatment with CPT or TPT (Fig. 7B, *lanes 9* and *10*). Consistent with the formation of multiubiquitinated IκBα ladders (Fig. 5B, *lanes 8* and *9*), substitution of the primary ubiquitination sites Lys[21] and Lys[22] (11, 50), with Arg resulted in retardation of degradation following TPT treatments (Fig. 7A, *HA-K21/22R*). These results are similar to those obtained with LPS (Fig. 7, *A*,
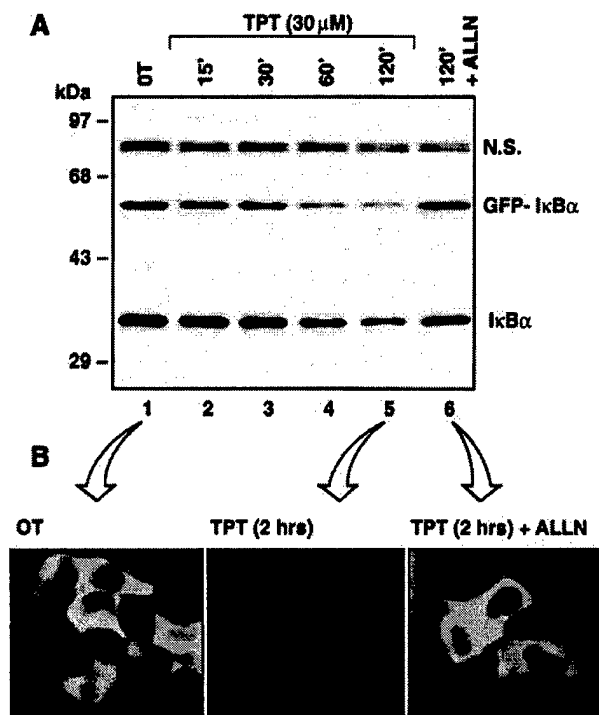
FIG. 6. **Inhibition of IκBα degradation induced by TPT results in accumulation of IκBα in the cytoplasm.** *A*, GFP-IκBα degraded in a similar manner to the endogenous IκBα protein following TPT treatment. Human IκBα (MAD-3), N-terminally fused to GFP, was stably transfected into the HEK293 cells and brighter GFP-IκBα expressing pools were isolated by fluorescent activated cell sorting. These cells were treated with TPT (30 μM) for the indicated times without (*lanes 2–5*) or with 100 μM ALLN (*lane 6*) and analyzed by Western blot using an anti-IκBα antibody (C21) as above. GFP-IκBα, but not IκBα, was also detected using GFP-specific antibody (CLONTECH; not shown). *B*, degradation of GFP-IκBα protein is largely cytoplasmic. *Left panel*, HEK293 stably expressing the GFP-IκBα protein was left untreated and visualized under fluorescein-aided fluorescent microscopy. *Middle panel*, parallel cultures as in the left panel were treated with TPT (30 μM) for 2 h as in A and visualized as above. There were decline of GFP signals in ~50% of the cell population (those showing reduced fluorescence are shown), potentially corresponding to replicating cells as suggested from results in Fig. 4. *Right panel*, parallel cultures were treated with 100 μM ALLN and 30 μM TPT and visualized as above. The exposure settings for all three panels were identical. The above data are representative of two independent experiments.

FIG. 7. **IκBα degradation induced by CPT or TPT requires intact Ser$^{32/36}$ and Lys$^{21/22}$ sites.** *A*, mutation or deletion of Ser$^{32/36}$ or Lys$^{21/22}$ abrogates IκBα degradation induced by TPT or CPT. *Left figures* show schematic presentation of IκBα mutants analyzed. Pools of 70Z/3-CD14 cells stably expressing HA-WT, HA-S32A/S36A, or Δ30–40 IκBα were treated with TPT (3, 10 or 30 μM) for 1 h (*lanes 2–4*). The cells were also treated with LPS (1 μg/ml) for 15 min (*lane 5*). Total cell extracts were analyzed by Western blot analysis using the C21 anti-IκBα antibody. A pool of 70Z/3-CD14 cells stably expressing HA-K21/22R IκBα mutant protein was treated with 1 μg/ml LPS for 15 min (*lane 2*), 10 μM CPT for 1 h (*lane 3*), or 0.1% Me₂SO for 1 h (*lane 4*) and analyzed as above. *Filled arrows* point to the exogenously introduced IκBα proteins, and *open arrows* point to the endogenous IκBα proteins. *B*, HA-S32A/S36A mutant prevents NF-κB activation. EMSA was performed as described in the legend to Fig. 1A using nuclear extracts from a 70Z/3-CD14 cell clone stably expressing either HA-WT (*lanes 1–5*) or HA-S32A/S36A (*lanes 6–10*) and treated with LPS (1 μg/ml for 15 min or 2 h—marked LPS*), CPT (10 μM for 2 h), or TPT (30 μM for 2 h). Positions of NF-κB and p50 homodimeric complexes are indicated on the *left*. The data are representative of two or more independent experiments.

lane 5, and *B*, *lanes 7* and *8*) or TNFα (1, 2) but distinct from data obtained with UV irradiation (13, 14). Of note, LPS caused efficient degradation of HA-K21/22R (Fig. 7A, *K21/22R, lane 2*), which is consistent with the observations that other Lys residue(s) can compensate for the lack of Lys$^{21/22}$ sites when cells are exposed to potent NF-κB inducers (50).

The IKK Complex Is Essential for NF-κB Activation by CPT—To further elucidate the events upstream of IκBα degradation that are involved in CPT activation of NF-κB, we evaluated the NF-κB response by EMSA in HEK293 cells transiently expressing dominant-negative IKKα and β proteins. The use of EMSA analysis to investigate potential inhibitory responses was possible because transfection efficiency was consistently >90% in this cell type (Fig. 8A), and thus almost all cells in the transfected population expressed the IKK mutant proteins. Both IKK mutants (N-terminally tagged with a FLAG epitope) reduced the level of NF-κB activation by TPT in a dose-dependent manner (Fig. 8B, *upper panel*). By contrast, these mutants did not appreciably alter the DNA binding levels of AP-1 complex (Fig. 8B, *lower panel*). Dose-dependent expression of IKK mutant proteins is shown by Western blot analysis
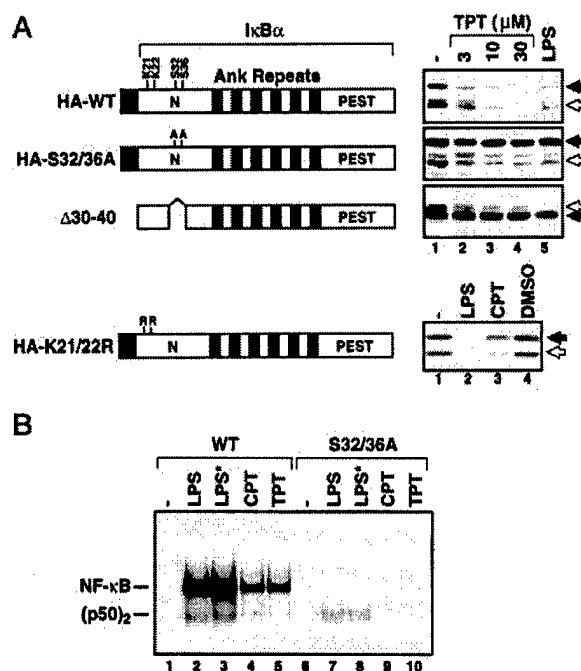
of cell extracts using monoclonal anti-FLAG antibody (Fig. 8C).

To independently determine the requirement of IKKα and IKKβ in NF-κB activation by CPT, embryonic fibroblast lines derived from IKKα and IKKβ knockout mice (51, 52) were treated with TNFα or CPT. Consistent with published observations (51–55), TNF activation of NF-κB was much weaker in IKKβ knockout cells than in IKKα knockout cells (Fig. 8D). However, NF-κB activation by CPT treatment was undetectable in both IKKα- and IKKβ-deficient cells (Fig. 8D, *lanes 12* and *8*, respectively). In addition, CPT activation of NF-κB was also undetectable in IKKγ-deficient 1.3E2 cells (56) (Fig. 8E, *lane 6*). Thus, key components of the IKK complex (IKKα/β/γ) are essential for NF-κB activation by CPT.

NF-κB Activation by CPT or TPT Is an Anti-apoptotic Cell Survival Response—Recent studies demonstrated that NF-κB activation by certain death inducing agents can provide an anti-apoptotic function (57–59). To evaluate whether NF-κB activation affects CPT induced apoptotic responses, the levels of apoptosis were estimated by FACS analysis based on sub-G₀/G₁ DNA content in WT and S32A/S36A expressing 70Z/3-CD14 cells. Untreated cells showed an expected pattern of cell cycle distribution for these cells with more than half of the cell
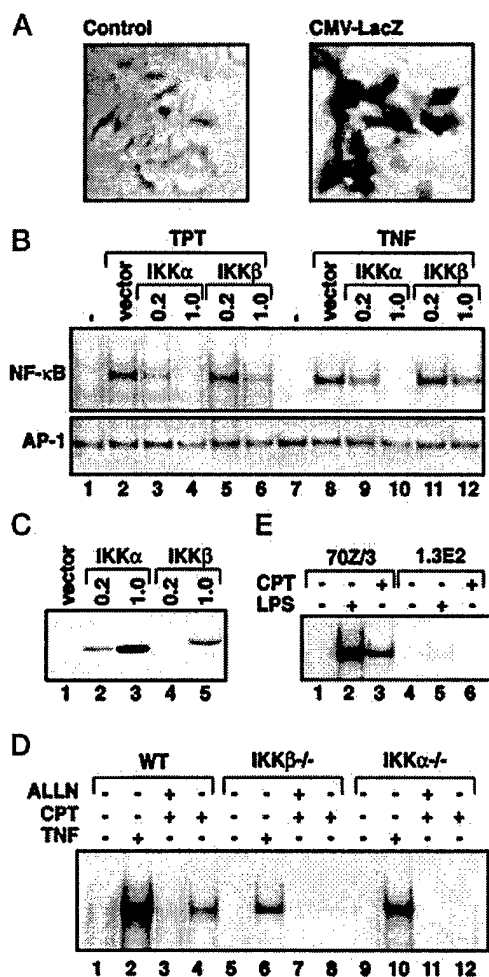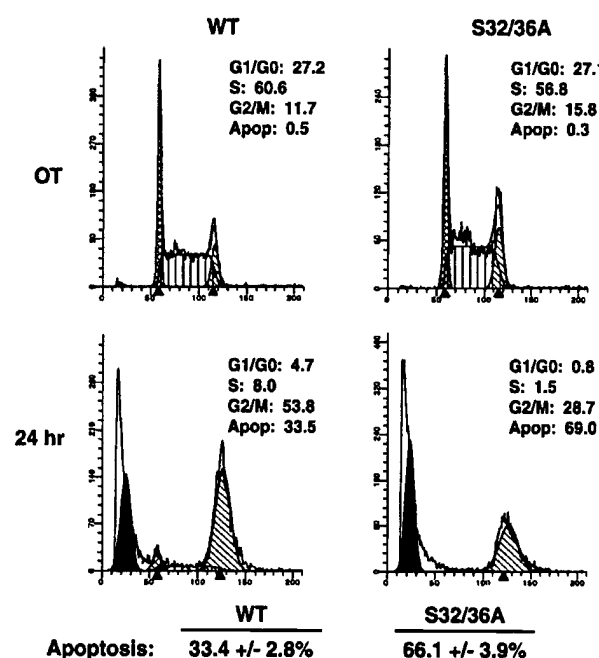
FIG. 9. **Inhibition of CPT activation of NF-κB results in an increased apoptotic response.** 70Z/3-CD14 cell clones expressing either WT or S32A/S36A IκBα were exposed to 1 μM CPT for 24 h. These cells were fixed, stained with propidium iodide, and analyzed by FACS for relative DNA content. Each panel shows the relative levels of cells in each of the cell cycle phases as well as in sub-G_1/G_0 apoptotic peaks. Average levels of apoptosis ± S.D. from three independent experiments are shown below the figure.

FIG. 8. **IKKα, β, and γ are essential for CPT activation of NF-κB.** *A*, X-gal staining of transiently transfected HEK293 cells. HEK293 cells were transfected with the empty vector (*left panel*) or the CMV-LacZ construct (*right panel*) and 36 h following transfection they were stained with X-gal. No X-gal-positive cells are visible in the *left panel*, whereas most cells are strongly X-gal-positive in the *right panel*. *B*, EMSA analysis of HEK293 cells transfected with dominant-negative IKKα and IKKβ constructs and treated with TPT. HEK293 cells were transfected with expression vectors (pcDNA, 0.2 or 1.0 μg/sample) for either a FLAG-tagged IKKα or IKKβ dominant-negative mutant (a Lys-to-Ala mutation at the putative ATP binding site as in Refs. 7–10 and 74) for 36 h and then treated with 30 μM TPT (2 h) or 10 ng/ml TNFα (20 min). Equivalent total cell extracts were analyzed by EMSA using Igκ-κB site (*upper panel*) or an AP-1 site (*lower panel*). Vector refers to empty pcDNA transfected cells. *C*, Western blot analysis of transfected dominant-negative IKKα and IKKβ proteins. Cell extracts prepared as above in *B* were analyzed by Western blot analysis using an anti-FLAG antibody. *D*, CPT activation of NF-κB requires IKKα and IKKβ. Mouse embryonic fibroblast lines generated from IKKα−/−, IKKβ−/−, or control mice were treated with 10 μM CPT in the presence or absence of 100 μM ALLN or 10 ng/ml TNFα for 1 h, and nuclear extracts were analyzed by EMSA. *E*, CPT activation of NF-κB requires IKKγ. 1.3E2 (IKKγ-deficient) or parental 70Z/3 cells were treated with 10 μM CPT or 10 μg/ml LPS for 1 h, and nuclear extracts were analyzed by EMSA. The above data are representative of two to three independent experiments.

population in S phase of the cell cycle (Fig. 9, *OT*, *WT*). Expression of S32A/S36A mutant protein did not significantly affect the cell cycle status of untreated cells (OT, S32A/S36A). After treatment with 1 μM CPT for 24 h, however, most of the cells appeared in either a G_2/M or sub-G_0/G_1 apoptotic peak (Fig. 9, *24 h, WT*). The fraction of apoptotic peak was approximately

twice as great in S32A/S36A expressing cells as WT expressing cells (24 h, S32A/S36A). Similar results were obtained with higher CPT doses or TPT treatments (not shown). Thus, these observations indicate that activation of NF-κB retards some cancer cells from undergoing apoptosis. These findings demonstrate that CPT activation of NF-κB can provide an anti-apoptotic activity.

DISCUSSION

The activity of NF-κB depends on a series of reactions that releases it from an inhibitory complex in the cytoplasm and allows it to migrate to the nucleus. The elucidation of the individual steps within NF-κB signaling cascades induced by a variety of structurally and functionally unrelated stimuli has revealed the use of both shared and unique components that may contribute to the diverse functions of this ubiquitous transcription factor (38, 60–68). DNA-damaging agents represent a unique group of NF-κB activators because their primary site of action is in the nucleus. In this study, we demonstrate that nuclear events arising from the DNA-damaging function of CPT and TPT are components of a NF-κB signaling pathway that converges in the cytoplasm with events associated with signaling pathways induced by cytokines or LPS stimulation.

The DNA-damaging function of CPT in replicating cells is a multi-step process that initiates with intercalation of CPT into a covalent Topo I-DNA reaction intermediate. CPT stabilizes this transient intermediate, forming the cleavable complex with a SSB. The cleavable complexes and associated SSBs are mostly reversible until the cell undergoes replication, during which the replication fork collides with the cleavable complex and yields a DSB. Our results obtained by utilizing mutant CEM/C2 cells, pharmacological agents, and FACS enrichment of S phase cells indicate that S phase-dependent generation of DSB is essential for NF-κB activation. Of note, however, is that

CPT or TPT activation of NF-κB is transient in all cell lines tested thus far. Similar dose-dependent and time course responses in lymphoid, fibroblastic, and epithelial cell lines suggest that a conserved activation mechanism may be involved. It has been demonstrated that CPT can induce degradation of Topo I enzyme by the ubiquitin-proteasome pathway causing marked reduction of Topo I enzyme within 2–4 h (69). Although this correlates well with the reduction of NF-κB activation in the continual presence of CPT in the present study, substantial levels of DSBs induced by CPT can persist for as long as 24 h in SV40-transformed human skin fibroblast cells (SV40MRC5VI) and EJ30/8D human bladder carcinoma cells (70). Because the critical DNA lesion (*i.e.* DSBs) may remain despite declining levels of Topo I enzyme, it is unlikely that the reduction of Topo I enzyme is solely responsible for transient NF-κB activation. It further implies that the mere presence of DSBs is insufficient to maintain NF-κB activation. It is thus possible that event(s) downstream of DSBs or those coupled to cell cycle may be responsible for transient NF-κB activation by CPT-related compounds. A recent study has implicated the involvement of the ataxia telangiectasia mutant protein in sustained activation of NF-κB by CPT (81).

Enucleation studies demonstrated that the process of NF-κB activation induced by CPT or TPT requires an intact nucleus. To our knowledge, this is the first demonstration of the lack of NF-κB activation in enucleated cells. Although this may be implied from the demonstration that events associated with DNA damage are required for NF-κB activation, mitochondria also contain DNA and CPT-sensitive Topo I enzyme (42). Studies utilizing L929 fibrosarcoma cells deficient for mitochondrial (DNA) and antimycin A, which increases the generation of reactive oxygen intermediates by inhibiting the electron transport chain, indicate that NF-κB activation by TNFα requires reactive oxygen intermediates derived from mitochondria (71). Because NF-κB is implicated as an important mammalian oxidative stress-responsive transcription factor (72), determination of the contribution of nuclear *versus* potential mitochondrial events was crucial for elucidating the NF-κB activation mechanism induced by CPT and TPT. Our findings provide direct evidence that CPT- or TPT-induced DNA damage in the nucleus is a primary component of the signaling events required for NF-κB activation. Although recent studies that utilized UV-C treatment of Xeroderma pigmentosa group A fibroblasts suggested the involvement of DNA damage in late stage NF-κB activation (14), whether or not an intact nucleus is required for this late activation was not investigated. Previous studies demonstrated that UV activation of NF-κB could efficiently take place in enucleated cells (20).

CPT induction of DNA damage translates into activation of a cytoplasmic signaling cascade that liberates active NF-κB from the inhibitor protein, IκBα. We utilized well characterized mutants of signaling components within the cytokine-inducible NF-κB signaling pathway to dissect the signaling cascade activated by CPT and TPT. Ser-to-Ala mutations at positions 32 and 36 of IκBα disrupt inducible phosphorylation and prevent subsequent ubiquitination and degradation by the proteasome pathway (47–49). We showed that these mutants also prevent IκBα degradation and activation of NF-κB induced by CPT and TPT. We additionally demonstrated that dominant-negative IKK mutants that inhibit phosphorylation of IκBα at these sites also prevent NF-κB activation by TPT. IKKα-, β-, or γ-deficient cells fail to activate NF-κB by CPT treatment. Mutation of Lys residues critical for the attachment of ubiquitin moieties further disrupts CPT-inducible IκBα degradation. Together with pharmacological evidence using proteasome inhibitors, our findings show that CPT and TPT induction of IκBα

degradation is similar to that induced by cytokines, LPS, and several other signals (7, 8, 10, 11, 47–50, 73, 74). Our findings therefore demonstrate that nuclear DNA damage causes IKK-dependent degradation of IκBα in the cytoplasm. This activation may involve signal transfer from the nucleus to the cytoplasm. This type of nuclear-to-cytoplasmic signaling has also been suggested for the late stage NF-κB activation induced by UV irradiation, which involves the production of an autocrine/paracrine factor, interleukin-1α (14). A recent study has also implicated the involvment of the DNA-dependent protein kinase in NF-κB activation by certain DNA damaging agents (82). Further definition of signaling components and reactions will help to determine whether NF-κB activation by CPT indeed involves a nuclear-to-cytoplasmic signal transduction pathway.

CPT derivatives, including TPT, are utilized clinically as part of cancer therapy regimes (34, 35). Recently, several studies have reported that NF-κB may control expression of genes involved in the regulation of apoptosis (57–59, 75–78). In particular, Wang *et al.* (58) have shown that NF-κB activation by ionizing radiation and daunarubicin may have anti-apoptotic effects in HT1080 human fibrosarcoma cells. The same group recently showed that NF-κB activation by CPT-11 can display similar anti-apoptotic effects in the above cell line (79). We have also shown that CPT activation of NF-κB provides an anti-apoptotic function. NF-κB-dependent survival of even a fraction of cancer cells after treatment with DNA-damaging agents, such as TPT or ionizing radiation, will likely lead to increased mutation rates and accelerated manifestation of malignancy. Moreover, it may also contribute to transformation of normal cells during the therapy. Understanding the mechanism(s) of NF-κB activation, therefore, may help improve the current methods of cancer therapy by defining a resistance mechanism to Topo I inhibitors and potentially other clinically important DNA-damaging and NF-κB-activating agents, such as ionizing radiation and Topo II inhibitors.

REFERENCES

1. Baeuerle, P. A., and Baltimore, D. (1996) *Cell* **87**, 13–20
2. Verma, I. M., Stevenson, J. K., Schwarz, E. M., Van Antwerp, D., and Miyamoto, S. (1995) *Genes Dev.* **9**, 2723–2735
3. Sonenshein, G. E. (1997) *Semin. Cancer Biol.* **8**, 113–119
4. Beg, A. A., Ruben, S. M., Scheinman, R. I., Haskill, S., Rosen, C. A., and Baldwin, A. S. J. (1992) *Genes Dev.* **6**, 1899–1913
5. Ganchi, P. A., Sun, S. C., Greene, W. C., and Ballard, D. W. (1992) *Mol. Biol. Cell* **3**, 1339–1352
6. Chen, Z. J., Parent, L., and Maniatis, T. (1996) *Cell* **84**, 853–862
7. DiDonato, J. A., Hayakawa, M., Rothwarf, D. M., Zandi, E., and Karin, M. (1997) *Nature* **388**, 548–554
8. Mercurio, F., Zhu, H., Murray, B. W., Shevchenko, A., Bennett, B. L., Li, J. W., Young, D. B., Barbosa, M., Mann, M., Manning, A., and Rao, A. (1997) *Science* **278**, 860–866
9. Woronicz, J. D., Gao, X., Cao, Z., Rothe, M., and Goeddel, D. V. (1997) *Science* **278**, 866–869
10. Zandi, E., Rothwarf, D. M., Delhase, M., Hayakawa, M., and Karin, M. (1997) *Cell* **91**, 243–252
11. Alkalay, I., Yaron, A., Hatzubai, A., Orian, A., Ciechanover, A., and Ben-Neriah, Y. (1995) *Proc. Natl. Acad. Sci. U. S. A.* **92**, 10599–10603
12. Chen, Z., Hagler, J., Palombella, V. J., Melandri, F., Scherer, D., Ballard, D., and Maniatis, T. (1995) *Genes Dev.* **9**, 1586–1597
13. Li, N., and Karin, M. (1998) *Proc. Natl. Acad. Sci. U. S. A.* **95**, 13012–13017
14. Bender, K., Gottlicher, M., Whiteside, S., Rahmsdorf, H. J., and Herrlich, P. (1998) *EMBO J.* **17**, 5170–5181
15. Han, Y., Weinman, S., Boldogh, I., Walker, R. K., and Brasier, A. R. (1999) *J. Biol. Chem.* **274**, 787–794
16. Chen, F., Lu, Y., Kuhn, D. C., Maki, M., Shi, X., Sun, S. C., and Demers, L. M. (1997) *Arch. Biochem. Biophys.* **342**, 383–388
17. Imbert, V., Rupec, R. A., Livolsi, A., Pahl, H. L., Traenckner, E. B. M., Mueller-Dieckmann, C., Farahifar, D., Rossi, B., Auberger, P., Baeuerle, P. A., and Peyron, J. F. (1996) *Cell* **86**, 787–798
18. Stein, B., Kramer, M., Rahmsdorf, H. J., Ponta, H., and Herrlich, P. (1989) *J. Virol.* **63**, 4540–4544
19. Piret, B., and Piette, J. (1996) *Nucleic Acids Res.* **24**, 4242–4248

20. Devary, Y., Rosette, C., DiDonato, J. A., and Karin, M. (1993) *Science* **261,** 1442–1445
21. Coffer, P. J., Burgering, B. M., Peppelenbosch, M. P., Bos, J. L., and Kruijer, W. (1995) *Oncogene* **11,** 561–569
22. Herrlich, P., Blattner, C., Knebel, A., Bender, K., and Rahmsdorf, H. J. (1997) *Biol. Chem.* **378,** 1217–1229
23. Rosette, C., and Karin, M. (1996) *Science* **274,** 1194–1197
24. Tobin, D., van Hogerlindern, M., and Toftgard, R. (1998) *Proc. Natl. Acad. Sci. U. S. A.* **95,** 565–569
25. Knebel, A., Rahmsdorf, H. J., Ullrich, A., and Herrlich, P. (1996) *EMBO J.* **15,** 5314–5325
26. Miyamoto, S., Wuerzberger, S. M., Seufzer, B., and Boothman, D. A. (1997) *Proc. Am. Assoc. Cancer Res.* **38,** 624
27. Hsiang, Y. H., and Liu, L. F. (1988) *Cancer Res.* **48,** 1722–1726
28. Giovanella, B. C., Stehlin, J. S., Wall, M. E., Wani, M. C., Nicholas, A. W., Liu, L. F., Silber, R., and Potmesil, M. (1989) *Science* **246,** 1046–1048
29. Liu, L. F. (1989) *Annu. Rev. Biochem.* **58,** 351–375
30. Wang, J. C. (1996) *Annu. Rev. Biochem.* **65,** 635–692
31. Hsiang, Y. H., Hertzberg, R., Hecht, S., and Liu, L. F. (1985) *J. Biol. Chem.* **260,** 14873–14878
32. Covey, J. M., Jaxel, C., Kohn, K. W., and Pommier, Y. (1989) *Cancer Res.* **49,** 5016–5022
33. Hsiang, Y.-H., Lihou, M. G., and Liu, L. F. (1989) *Cancer Res.* **49,** 5077–5082
34. Slichenmyer, W. J., Rowinsky, E. K., Donehower, R. C., and Kaufmann, S. H. (1993) *J. Natl. Cancer Inst.* **85,** 271–291
35. Rothenberg, M. L. (1997) *Ann. Oncol.* **8,** 837–855
36. Miyamoto, S., Seufzer, B., and Shumway, S. (1998) *Mol. Cell. Biol.* **18,** 19–29
37. Poste, G. (1972) *Exp. Cell Res.* **73,** 273–286
38. Cao, Z. D., Xiong, J., Takeuchi, M., Kurama, T., and Goeddel, D. V. (1996) *Nature* **383,** 443–446
39. Chiao, P. J., Miyamoto, S., and Verma, I. M. (1994) *Proc. Natl. Acad. Sci. U. S. A.* **91,** 28–32
40. VanAntwerp, D. J., and Verma, I. M. (1996) *Mol. Cell. Biol.* **16,** 6037–6045
41. Wuerzberger, S. M., Pink, J. J., Planchon, S. M., Byers, K. L., Bornmann, W. G., and Boothman, D. A. (1998) *Cancer Res.* **58,** 1876–1885
42. Lin, J. H., and Castora, F. J. (1995) *Arch. Biochem. Biophys.* **324,** 293–299
43. Baeuerle, P. A., and Baltimore, D. (1988) *Science* **242,** 540–546
44. Fujimori, A., Hoki, Y., Popescu, N. C., and Pommier, Y. (1996) *Oncol. Res.* **8,** 295–301
45. Fujimori, A., Harker, W. G., Kohlhagen, G., Hoki, Y., and Pommier, Y. (1995) *Cancer Res.* **55,** 1339–1346
46. D'Arpa, P., Beardmore, C., and Liu, L. F. (1990) *Cancer Res.* **50,** 6919–6924
47. Brockman, J. A., Scherer, D. C., McKinsey, T. A., Hall, S. M., Qi, X., Lee, W. Y., and Ballard, D. W. (1995) *Mol. Cell. Biol.* **15,** 2809–2818
48. Brown, K., Gerstberger, S., Carlson, L., Franzoso, G., and Siebenlist, U. (1995) *Science* **267,** 1485–1488
49. Traenckner, E. B., Pahl, H. L., Henkel, T., Schmidt, K. N., Wilk, S., and Baeuerle, P. A. (1995) *EMBO J.* **14,** 2876–2883
50. Scherer, D. C., Brockman, J. A., Chen, Z., Maniatis, T., and Ballard, D. W. (1995) *Proc. Natl. Acad. Sci. U. S. A.* **92,** 11259–11263
51. Li, Q., Lu, Q., Hwang, J. Y., Buscher, D., Lee, K. F., Izpisua-Belmonte, J. C., and Verma, I. M. (1999) *Genes Dev.* **13,** 1322–1328
52. Li, Q., Van Antwerp, D., Mercurio, F., Lee, K. F., and Verma, I. M. (1999) *Science* **284,** 321–325
53. Li, Z. W., Chu, W., Hu, Y., Delhase, M., Deerinck, T., Ellisman, M., Johnson,

R., and Karin, M. (1999) *J. Exp. Med.* **189,** 1839–1845
54. Tanaka, M., Fuentes, M. E., Yamaguchi, K., Durnin, M. H., Dalrymple, S. A., Hardy, K. L., and Goeddel, D. V. (1999) *Immunity* **10,** 421–429
55. Hu, Y., Baud, V., Delhase, M., Zhang, P., Deerinck, T., Ellisman, M., Johnson, R., and Karin, M. (1999) *Science* **284,** 316–320
56. Yamaoka, S., Courtois, G., Bessia, C., Whiteside, S. T., Weil, R., Agou, F., Kirk, H. E., Kay, R. J., and Israel, A. (1998) *Cell* **93,** 1231–1240
57. Beg, A. A., and Baltimore, D. (1996) *Science* **274,** 782–784
58. Wang, C. Y., Mayo, M. W., and Baldwin, A. S. (1996) *Science* **274,** 784–787
59. VanAntwerp, D. J., Martin, S. J., Kafri, T., Green, D. R., and Verma, I. M. (1996) *Science* **274,** 787–789
60. Hirano, M., Osada, S., Aoki, T., Hirai, S., Hosaka, M., Inoue, J., and Ohno, S. (1996) *J. Biol. Chem.* **271,** 13234–13238
61. Lee, F. S., Hagler, J., Chen, Z. J., and Maniatis, T. (1997) *Cell* **88,** 213–222
62. Yin, M. J., Christerson, L. B., Yamamoto, Y., Kwak, Y. T., Xu, S., Mercurio, F., Barbosa, M., Cobb, M. H., and Gaynor, R. B. (1998) *Cell* **93,** 875–884
63. Cheng, G., Cleary, A. M., Ye, Z. S., Hong, D. I., Lederman, S., and Baltimore, D. (1995) *Science* **267,** 1494–1498
64. Cheng, G., and Baltimore, D. (1996) *Genes Dev.* **10,** 963–973
65. Ishida, T., Mizushima, S., Azuma, S., Kobayashi, N., Tojo, T., Suzuki, K., Aizawa, S., Watanabe, T., Mosialos, G., Kieff, E., Yamamoto, T., and Inoue, J. (1996) *J. Biol. Chem.* **271,** 28745–28748
66. Rothe, M., Sarma, V., Dixit, V. M., and Goeddel, D. V. (1995) *Science* **269,** 1424–1427
67. Malinin, N. L., Boldin, M. P., Kovalenko, A. V., and Wallach, D. (1997) *Nature* **385,** 540–544
68. Tsukamoto, N., Kobayashi, N., Azuma, S., Yamamoto, T., and Inoue, J. (1999) *Proc. Natl. Acad. Sci. U. S. A.* **96,** 1234–1239
69. Desai, S. D., Liu, L. F., Vazquez-Abad, D., and D'Arpa, P. (1997) *J. Biol. Chem.* **272,** 24159–24164
70. Ryan, A. J., Squires, S., Strutt, H. L., Evans, A., and Johnson, R. T. (1994) *Carcinogenesis* **15,** 823–828
71. Schulze-Osthoff, K., Beyaert, R., Vandevoorde, V., Haegeman, G., and Fiers, W. (1993) *EMBO J.* **12,** 3095–3104
72. Schreck, R., Albermann, K., and Baeuerle, P. A. (1992) *Free Radical Res. Commun.* **17,** 221–237
73. Zandi, E., Chen, Y., and Karin, M. (1998) *Science* **281,** 1360–1363
74. Regnier, C. H., Song, H. Y., Gao, X., Goeddel, D. V., Cao, Z., and Rothe, M. (1997) *Cell* **90,** 373–383
75. Wu, M., Lee, H. Y., Bellas, R. E., Schauer, S. L., Arsura, M., Katz, D., Fitzgerald, M. J., Rothstein, T. L., Sherr, D. H., and Sonenshein, G. E. (1996) *EMBO J.* **15,** 4682–4690
76. Wu, M. X., Ao, S., Prasad, K. V. S., Wu, R., and Schlossman, S. F. (1998) *Science* **281,** 998–1001
77. Chu, Z.-L., McKinsey, T. A., Liu, L., Gentry, J. J., Halim, M. H., and Ballard, D. W. (1997) *Proc. Natl. Acad. Sci. U. S. A.* **94,** 10057–10062
78. Wang, C. Y., Mayo, M. W., Korneluk, R. G., Goeddel, D. V., and Baldwin, A. S. (1998) *Science* **281,** 1680–1683
79. Wang, C. Y., Cusack, J. C. J., Liu, R., and Baldwin, A. S. (1999) *Nat. Med.* **5,** 412–417
80. Huang, T. T., Kudo, N., Yoshida, M., and Miyamoto, S. (2000) *Proc. Natl. Acad. Sci. U. S. A.* **97,** 1014–1019
81. Piret, B., Schoonbroodt, S., and Piret, J. (1999) *Oncogene* **18,** 2261–2271
82. Basu, S., Rosenzweig, K. R., Youmell, M., and Price, B. D. (1998) *Biochem. Biophys. Res. Commun.* **247,** 79–83

Calcium Is a Key Signaling Molecule in β-Lapachone-mediated Cell Death*

Colleen Tagliarino‡§, John J. Pink‡, George R. Dubyak¶, Anna-Liisa Nieminen‖, and David A. Boothman‡**

From the ‡Departments of Radiation Oncology and Pharmacology, ‖Department of Anatomy, and the ¶Department of Physiology and Biophysics, Case Western Reserve University, Cleveland, Ohio 44106-4942

β-Lapachone (β-Lap) triggers apoptosis in a number of human breast and prostate cancer cell lines through a unique apoptotic pathway that is dependent upon NQO1, a two-electron reductase. Downstream signaling pathway(s) that initiate apoptosis following treatment with β-Lap have not been elucidated. Since calpain activation was suspected in β-Lap-mediated apoptosis, we examined alterations in Ca^{2+} homeostasis using NQO1-expressing MCF-7 cells. β-Lap-exposed MCF-7 cells exhibited an early increase in intracellular cytosolic Ca^{2+}, from endoplasmic reticulum Ca^{2+} stores, comparable to thapsigargin exposures. 1,2-Bis-(2-aminophenoxy)ethane-N,N,N',N'-tetraacetic acid-acetoxymethyl ester, an intracellular Ca^{2+} chelator, blocked early increases in Ca^{2+} levels and inhibited β-Lap-mediated mitochondrial membrane depolarization, intracellular ATP depletion, specific and unique substrate proteolysis, and apoptosis. The extracellular Ca^{2+} chelator, EGTA, inhibited later apoptotic end points (observed >8 h, e.g. substrate proteolysis and DNA fragmentation), suggesting that later execution events were triggered by Ca^{2+} influxes from the extracellular milieu. Collectively, these data suggest a critical, but not sole, role for Ca^{2+} in the NQO1-dependent cell death pathway initiated by β-Lap. Use of β-Lap to trigger an apparently novel, calpain-like-mediated apoptotic cell death could be useful for breast and prostate cancer therapy.

β-Lap[1] is a naturally occurring compound present in the bark of the South American Lapacho tree. It has antitumor activity against a variety of human cancers, including colon, prostate, promyelocytic leukemia, and breast (1–3). β-Lap was an effective agent (alone and in combination with taxol) against human ovarian and prostate xenografts in mice, with little host toxicity (4). We recently demonstrated that β-Lap kills human breast and prostate cancer cells by apoptosis, a cytotoxic response significantly enhanced by NAD(P)H:quinone oxidoreductase (NQO1, E.C. 1.6.99.2) enzymatic activity (5).[2] β-Lap cytotoxicity was prevented by co-treatment with dicumarol (an NQO1 inhibitor) in NQO1-expressing breast and prostate cancer cells (5).[2] NQO1 is a cytosolic enzyme elevated in breast cancers (6) that catalyzes a two-electron reduction of quinones (e.g. β-Lap, menadione), utilizing either NADH or NADPH as electron donors. Reduction of β-Lap by NQO1 presumably leads to a futile cycling of the compound, wherein the quinone and hydroquinone form a redox cycle with a net concomitant loss of reduced NAD(P)H (5).

Apoptosis is an evolutionarily conserved pathway of biochemical and molecular events that underlie cell death processes involving the stimulation of intracellular zymogens. The process is a genetically programmed form of cell death involved in development, normal turnover of cells, and in cytotoxic responses to cellular insults. Once apoptosis is initiated, biochemical and morphological changes occur in the cell. These changes include: DNA fragmentation, chromatin condensation, cytoplasmic membrane blebbing, cleavage of apoptotic substrates (e.g. PARP, lamin B), and loss of mitochondrial membrane potential with concomitant release of cytochrome c into the cytoplasm (7–9). Apoptosis is a highly regulated, active process that requires the participation of endogenous cellular enzymes that systematically dismantle the cell. The most well characterized proteases in apoptosis are caspases, aspartate-specific cysteine proteases, that work through a cascade that can be initiated by mitochondrial membrane depolarization leading to the release of cytochrome c and Apaf-1 into the cytoplasm (10), that then activates caspase 9 (11). Non-caspase-mediated pathways are less understood.

We previously showed that apoptosis following β-Lap administration was unique, in that an ~60-kDa PARP cleavage fragment, as well as distinct intracellular proteolytic cleavage of p53, were observed in NQO1-expressing breast or prostate cancer cells (5).[2] These cleavage events were distinct from those observed when caspases were activated by topoisomerase I poisons, staurosporine, or administration of granzyme B (5, 12, 13). Furthermore, β-Lap-mediated cleavage events were blocked by administration of global cysteine protease inhibitors, as well as extracellular Ca^{2+} chelators (12). Based on these data, we concluded that β-Lap exposure of NQO1-expressing breast and prostate cancer cells caused the activation of a Ca^{2+}-dependent protease with properties similar to calpain; in particular, the p53 cleavage pattern of β-Lap-exposed

[1] The abbreviations used are: β-Lap, β-lapachone; MCP, MCF-7:WS8; NQO1, NAD(P)H:quinone oxidoreductase, DT-diaphorase (E.C. 1.6.99.2); PARP, poly(ADP-ribose) polymerase; TUNEL, terminal deoxynucleotidyl transferase-mediated dUTP nick end labeling; ER, endoplasmic reticulum; TG, thapsigargin; STS, staurosporine; BAPTA-AM, 1,2-bis-(2-aminophenoxy)ethane-N,N,N',N'-tetraacetic acid-acetoxymethyl ester.

[2] S. M. Planchon, C. Tagliarino, J. J. Pink, W. G. Bornmann, M. E. Varnes, and D. A. Boothman. *Exp. Cell Res.*, in press.

cells was remarkably similar to the pattern observed after calpain activation (14, 15).

Ca^{2+} is recognized as an important regulator of apoptosis (16–21). The cytoplasmic Ca^{2+} concentration is maintained at ~100 nM in resting cells by relatively impermeable cell membranes, active extrusion of Ca^{2+} from the cell by plasma membrane Ca^{2+}-ATPases, plasma membrane Na$^+$/Ca^{2+} exchangers, and active uptake of cytosolic Ca^{2+} into the endoplasmic reticulum (ER) by distinct Ca^{2+}-ATPases. In contrast, the concentration of Ca^{2+} in the extracellular milieu and in the ER is much higher (in the millimolar range). Evidence for involvement of Ca^{2+} influx into the cytosol as a triggering event for apoptosis has come from studies with specific Ca^{2+} channel blockers that abrogate apoptosis in regressing prostate following testosterone withdrawal (22). Other support for the involvement of Ca^{2+} in apoptosis comes from the observation that agents that directly mobilize Ca^{2+} (*e.g.* Ca^{2+} ionophores or the sarcoplasmic reticulum Ca^{2+}-ATPase pump inhibitor, thapsigargin, TG) can trigger apoptosis in diverse cell types (23–27). Inhibition of the sarcoplasmic reticulum Ca^{2+}-ATPase pump by TG causes a transient increase in cytoplasmic Ca^{2+} from ER Ca^{2+} stores, and a later influx of Ca^{2+} from the extracellular milieu, leading to the induction of apoptotic cell death (24, 27, 28). Consequently, emptying of intracellular Ca^{2+} stores may trigger apoptosis by disrupting the intracellular architecture and allowing key elements of the effector machinery (*e.g.* Apaf-1) to gain access to their substrates (*e.g.* caspase 9). Ca^{2+} has also been shown to be necessary for apoptotic endonuclease activation, eliciting DNA cleavage after many cellular insults (29–31). Buffering intracellular Ca^{2+} released from stored Ca^{2+} pools (*e.g.* ER) with BAPTA-AM, or removal of extracellular Ca^{2+} with EGTA, can protect cells against apoptosis (32, 33). Therefore, increases in intracellular Ca^{2+} levels appear to be important cell death signals in human cancer cells that might be exploited for anti-tumor therapy. Finally, Ca^{2+} may act as a signal for apoptosis by directly activating key proapoptotic enzymes (*e.g.* calpain); however, these proteolytic responses are poorly understood. The role of Ca^{2+} in cell death processes involving caspase activation has been examined in detail (28, 34–36). However, the role of Ca^{2+} in non-caspase-dependent cell death responses is relatively unexplored.

Recent studies have suggested that alterations in mitochondrial homeostasis play an essential role in apoptotic signal transduction induced by cytotoxic agents (37, 38). Various apoptotic stimuli have been shown to induce mitochondrial changes, resulting in release of apoptogenic factors, apoptosis-inducing factor (39), and mitochondrial cytochrome *c* (9) into the cytoplasm. These changes are observed during the early phases of apoptosis in human epithelial cells, and were linked to the initial cascade of events, sending the cell to an irreversible suicide pathway. During high, sustained levels of cytosolic Ca^{2+}, mitochondrial Ca^{2+} uptake is driven by mitochondrial membrane potential to maintain Ca^{2+} homeostasis in the cytosol. In de-energized mitochondria, Ca^{2+} can be released by a reversal of this uptake pathway (40). These data, therefore, linked changes in Ca^{2+} homeostasis and mitochondrial membrane potential to the initiation of apoptosis. Li *et al.* (41) reported that β-Lap caused a decrease in mitochondrial membrane potential with release of cytochrome *c* into the cytoplasm in a number of human carcinoma cell lines, shortly after drug addition. Other alterations in metabolism (*e.g.* ATP depletion) have not been examined in β-Lap-treated cells.

We previously characterized the activation of a novel cysteine protease in various breast cancer cell lines with properties similar to the Ca^{2+}-dependent cysteine protease, calpain, after exposure to β-Lap (12). Using NQO1-expressing breast

cancer cells, we show that β-Lap elicits a rise in intracellular Ca^{2+} levels shortly after drug administration that eventually leads to apoptosis. This paper suggests a critical, but not sufficient, role for Ca^{2+} in the cell death pathway initiated by NQO1-dependent bioactivation of β-Lap. Possible combinatorial effects (*e.g.* NAD(P)H depletion as well as intracellular calcium alterations) that initiate β-Lap-mediated apoptosis in NQO1-expressing breast cancer cells will be discussed.

EXPERIMENTAL PROCEDURES

Reagents—β-Lapachone (3,4-dihydro-2,2-dimethyl-2H-naphtho[1,2b]pyran-5,6-dione) was synthesized by Dr. William G. Bornmann (Memorial Sloan Kettering, New York), dissolved in dimethyl sulfoxide at 10 mM, and the concentration verified by spectrophotometric analysis (2, 5). EGTA, Hoescht 33258, and thapsigargin were obtained from Sigma. BAPTA-AM (1,2-bis-(2-aminophenoxy)ethane-*N,N,N′,N′*-tetraacetic acid tetra-(acetoxymethyl ester)) was obtained from Calbiochem (La Jolla, CA). JC-1 (5,5′6,6′-tetrachloro-1,1′,3,3′-tetraethylbenzimidazolylcarbocyanine iodide) and Fluo-4-AM were obtained from Molecular Probes, Inc. (Eugene, OR).

Cell Culture—MCF-7:WS8 (MCF-7) human breast cancer cells were obtained from Dr. V. Craig Jordan, (Northwestern University, Chicago, IL). MDA-MB-468 cells were obtained from the American Type Culture Collection and transfected with NQO1 cDNA in the pcDNA3 constitutive expression vector as described previously (5). Tissue culture components were purchased from Life Technologies, Inc., unless otherwise stated. MCF-7 cells were grown in RPMI 1640 cell culture medium supplemented with 10% fetal bovine serum, in a 37 °C humidified incubator with 5% CO$_2$, 95% air atmosphere as previously described (2, 5). For all experiments, log-phase breast cancer cells were exposed to 5 μM β-Lap for 4 h (unless otherwise indicated), after which fresh medium was added and cells were harvested at various times post-treatment.

TUNEL Assay—Cells were seeded at 1 × 10^6 cells/10-cm Petri dish and allowed to grow for 24 h. Log-phase cells were then pretreated for 30 min with 10 μM BAPTA-AM, 3 mM EGTA, or 50 μM dicumarol followed by a 4-h pulse of 5 μM β-Lap, as described above, or 24 h treatment of 10 μM ionomycin or 1 μM staurosporine. Medium was collected from experimental as well as control conditions 24 h later, and attached along with floating cells were monitored for apoptosis using TUNEL 3′-biotinylated DNA end labeling via the APO-DIRECT kit (Pharmingen, San Diego, CA) as described (5). Apoptotic cells were analyzed and quantified using an EPICS XL-MCL flow cytometer that contained an air-cooled argon laser at 488 nm, 15 mW (Beckman Coulter Electronics; Miami, Fl), and XL-MCL acquisition software provided with the instrument.

Cell Growth Assays—MCF-7 cells were seeded at 5 × 10^4 cells per well in a 12-well plate and allowed to attach overnight. The following day, log-phase cells were pretreated for 30 min with 5 μM BAPTA-AM, followed by a 4-h pulse of β-Lap (0–5 μM). Drugs were removed and fresh medium added. Cells were allowed to grow for an additional 6 days. DNA content (a measure of cell growth) was determined by fluorescence using Hoechst dye 33258 as described (5) and changes in growth were monitored using a PerkinElmer HTS 7000 Plus Bio Assay Plate Reader (Norwalk, CT) with 360 and 465 nm excitation and emission filters, respectively. Data were expressed as relative growth, T/C (treated/control), using experiments performed at least twice.

Confocal Microscopy—MCF-7 cells were seeded at 2–3 × 10^5 cells per 35-mm glass bottom Petri dishes (MatTek Corp., Ashland, MA) and allowed to attach overnight. Cells were rinsed twice in a Ca^{2+}/Mg^{2+} balanced salt solution (BSS, 130 mM NaCl, 5 mM KCl, 1.5 mM CaCl$_2$, 1 mM MgCl$_2$, 25 mM HEPES, pH 7.5, 5 mM glucose, 1 mg/ml bovine serum albumin) and loaded with the Ca^{2+}-sensitive fluorescent indicator, fluo-4-AM (5 μM), in BSS for ~20–30 min at 37 °C. Cells were rinsed twice in BSS and incubated for an additional 20 min at 37 °C to allow for hydrolysis of the AM-ester. Cells were imaged with a Zeiss 410 confocal microscope (Thornwood, NY) equipped with a ×63 N.A. 1.4 oil immersion planapochromat objective at room temperature (the same results were observed at room temperature and 37 °C). Confocal images of fluo-4 fluorescence were collected using a 488-nm excitation light from an argon/krypton laser, a 560-nm dichroic mirror, and a 500–550 nm band-pass barrier filter. Three basal images were collected before drug addition (8 μM β-Lap, ± 50 μM dicumarol or 200 nM TG). The mean pixel intensity was set to equal one for analyses of fold-increase in fluo-4 fluorescence intensity. Subsequently, images were collected after the indicated treatments at 90-s intervals. BAPTA-AM (20 μM) was co-

loaded with fluo-4-AM where indicated. Mean pixels were determined in regions of interest for individual cells at each time point.

Mitochondrial Membrane Potential Determinations—MCF-7 cells were seeded at $2.5-3 \times 10^5$ cells per 6-well plate, and allowed to grow for 24 h. Log-phase cells were pretreated for 30 min with 10 μM BAPTA-AM, 3 mM EGTA, or 50 μM dicumarol followed by a 4-h pulse of 5 μM β-Lap, unless otherwise indicated. Cells were trypsinized and resuspended in phenol red-minus RPMI medium for analyses. Cells were maintained at 37 °C for the duration of the experiment, including during analyses. Prior to analyses, cells were loaded with 10 μg/ml JC-1 for 9-14 min and samples were analyzed using a Beckman Coulter EPICS Elite ESP (Miami, FL) flow cytometer. JC-1 monomer and aggregate emissions were excited at 488 nM and quantified using Elite acquisition software after signal collection through 525- and 590-nm band pass filters, respectfully. Shifts in emission spectra were plotted on bivariant dot plots, on a cell-by-cell basis, to determine relative mitochondrial membrane potential of treated and control cells.

ATP Measurements—Cells were seeded at 2.5×10^5 cells per well in 6-well dishes and allowed to attach for 24 h. Fresh medium was added to the cells along with Ca²⁺ chelators or dicumarol 30 min prior to β-Lap exposure (4 h unless otherwise indicated). Floating cells were collected, pelleted, and lysed in 1.67 M perchloric acid. Attached cells were lysed directly in 1.67 M perchloric acid. Following a 20-min incubation at room temperature, attached cells were scraped and transferred to corresponding microcentrifuge tube, cooled on ice for several minutes, and spun to pellet protein precipitates. Deproteinized samples were neutralized with 3.5 M KOH and HEPES/KOH (25 mM HEPES, 15 mM KOH, pH 8), and incubated on ice for 15 min. Precipitates were removed by centrifugation and samples stored at -20 °C. Cell extracts were analyzed for ATP and ADP levels using a luciferase-based bioluminescent assay and rephosphorylation protocols, as described (42).

Western Blot Analyses—Whole cell extracts from control or β-Lap-exposed MCF-7 cells were prepared and analyzed by SDS-polyacrylamide gel electrophoresis/Western blot analyses as previously described (2, 5, 12). Loading equivalence and transfer efficiency were monitored by Western blot analyses of proteins that are known to be unaltered by experimental treatments (2), and using Ponceau S staining of the membrane, respectively. Probed membranes were then exposed to x-ray film for an appropriate time and developed. Dilutions of 1:10,000 for the C-2–10 anti-PARP antibody (Enzyme Systems Products, Livermore, CA), and 1:2000 for anti-p53 DO-1 and anti-lamin B (Santa Cruz Biotechnology, Santa Cruz, CA) antibodies were used as described (2, 12).

RESULTS

Ca²⁺ Chelators Prevent β-Lap-induced Apoptotic DNA Fragmentation and Protect against Cell Death—Log-phase MCF-7 cells were treated for 4 h with 5 μM β-Lap, fresh medium was then applied, and cells were harvested 24 h later and analyzed for DNA fragmentation (*i.e.* apoptotic cells staining positive in a TUNEL assay). Treatment of MCF-7 cells with β-Lap resulted in >90% apoptotic cells (Fig. 1, *A* and *B*). However, MCF-7 cells exposed to a 30-min pretreatment with 10 μM BAPTA-AM or 3 mM EGTA, followed by a 4-h pulse of 5 μM β-Lap, exhibited only 20 or 39% apoptotic cells, respectively, in 24 h.

To examine whether BAPTA-AM could affect β-Lap lethality, we measured relative growth of MCF-7 cells with or without exposure to β-Lap, and in the presence or absence of BAPTA-AM. MCF-7 cells were treated for 30 min with 5 μM BAPTA-AM, subsequently exposed to a 4-h pulse of β-Lap (1.5–5 μM), and relative cell growth was measured 6 days later (Fig. 1*C*). The LD$_{50}$ dose of β-Lap in MCF-7 cells was ~2.5 μM in colony forming assays, which correlated well with IC$_{50}$ relative growth inhibition, as measured by DNA content (2, 5). At 1.5 μM β-Lap, cells exhibited little or no toxicity. At β-Lap doses of 3 or 5 μM, cells exhibited considerable toxicity, >90% growth inhibition, as previously reported (2, 5). Toxicity was significantly prevented by 5 μM BAPTA-AM pretreatment. BAPTA-AM pretreated cells exhibit only 44 and 73% growth inhibition after 3 or 5 μM β-Lap treatments, respectively (Fig. 1*C*). BAPTA alone did not affect MCF-7 cell growth compared with untreated controls.

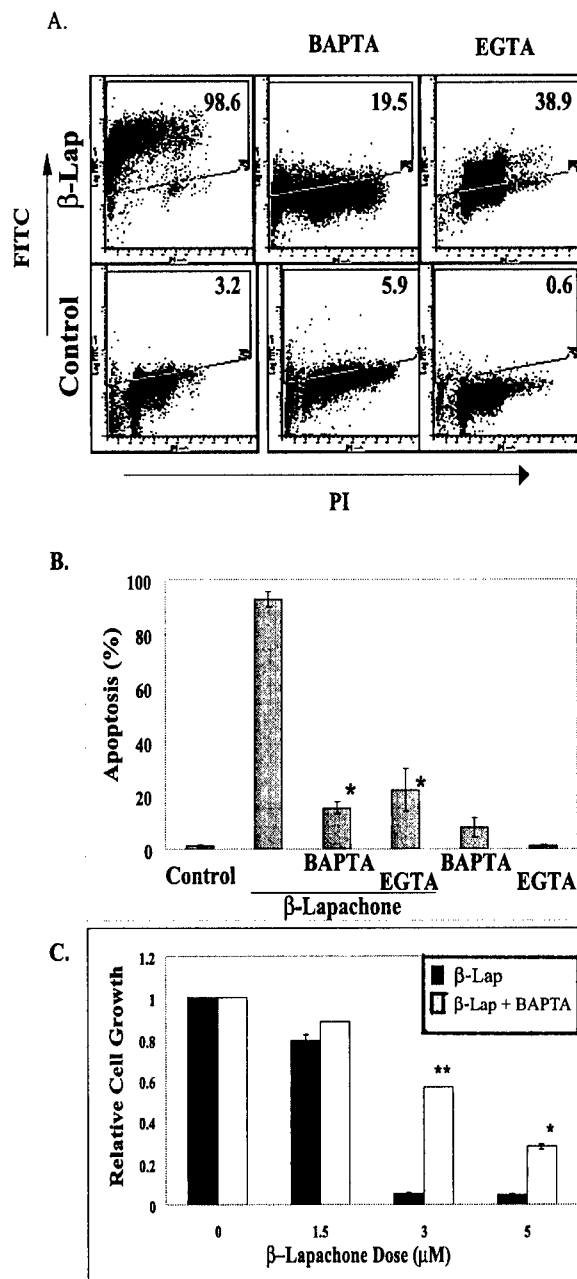FIG. 1. **β-Lap-mediated apoptosis and relative cell growth is Ca²⁺-dependent.** DNA fragmentation was assessed using the TUNEL assay. Log phase MCF-7 cells were treated with the indicated Ca²⁺ chelator for 30 min prior to a 4-h pulse of 5 μM β-Lap. TUNEL assays were performed to monitor apoptosis 24 h after β-Lap addition (*A* and *B*). *A*, shown are the results of any one experiment from studies performed at least three times. The *number* in the *upper right* corner represents percent cells staining positive in the TUNEL assay. Results are graphically summarized in *B* as the average of at three independent experiments, mean $\pm$ S.E. Student's *t* test for paired samples, experimental group compared with MCF-7 cells treated with β-Lap alone are indicated (* $p < 0.01$). *C*, cells were exposed to a 4-h pulse of various concentrations of β-Lap either alone (*closed*), or after a 30-min pretreatment with 5 μM BAPTA-AM (*open*). Relative DNA per well was determined by Hoescht 33258 fluorescence, and graphed as relative growth (treated/control DNA); mean relative DNA per well, $\pm$ S.E. Shown are representative results of experiments performed at least twice. Student's *t* test for paired samples, experimental group compared with MCF-7 cells treated with β-Lap alone are indicated (*, $p < 0.05$; and **, $p < 0.005$).

Ca²⁺ Chelators Do Not Block Apoptosis Induced by Other Agents—It was possible based on the data in Fig. 1 that calcium chelators may block β-Lap-mediated apoptosis by sequestering
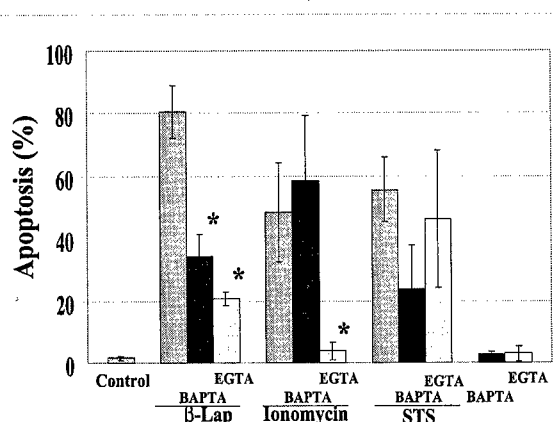
FIG. 2. **Ca²⁺ chelators did not block Ca²⁺-activated endonuclease activation after β-Lap.** NQO1-expressing MDA-468-NQ3 cells (generated from non-expressing human breast cancer cells (5)) were treated with either 3 mM EGTA or 30 μM BAPTA-AM for 30 min prior to drug addition; either a 4-h pulse of 8 μM β-Lap, or 24 h continuous treatment of 10 μM ionomycin or 1 μM STS. Cells were then analyzed using the TUNEL assay for DNA fragmentation. Shown are mean ± S.E. of at least two independent experiments. Student's *t* test for paired samples, experimental group compared with cells treated with drug alone are indicated (*, $p < 0.05$).

calcium required for the activation of apoptotic endonucleases. We, therefore, examined both intra- and extracellular Ca²⁺ chelators for their ability to prevent apoptosis in NQO1-transfected MDA-468 (MDA-468-NQ3) cells induced by β-Lap, ionomycin (which induces Ca²⁺-mediated cell death (36)), and staurosporine (STS, which inhibits protein kinase C and works via a caspase-mediated cell death pathway (43, 44)). We used MDA-468-NQ3 cells to assay for caspase-mediated endonuclease activation and DNA fragmentation since they express the endonuclease-activating caspase 3, unlike MCF-7 cells (45). We previously demonstrated that MDA-468-NQ3 cells responded similarly to β-Lap as MCF-7 cells (Fig. 2 and Ref. 5). EGTA significantly protected MDA-468-NQ3 cells against ionomycin-induced apoptosis, but not against STS-induced apoptosis (Fig. 2). MDA-468-NQ3 cells treated for 24 h with 10 μM ionomycin exhibited 49% apoptotic cells, whereas, MDA-468-NQ3 cells pretreated for 30 min with 3 mM EGTA followed by a 24-h exposure to ionomycin exhibited only 4% apoptotic cells. Cells treated for 24 h with 1 μM STS in the absence or presence of 3 mM EGTA exhibited 56 and 46% apoptosis, respectively. BAPTA-AM (10 μM) did not significantly block apoptosis induced by ionomycin. BAPTA-AM pretreatment of STS-exposed MDA-468-NQ3 cells did not significantly decrease apoptosis ($p < 0.4$) compared with cells exposed to STS alone; the modest effect of BAPTA-AM on STS-induced apoptosis may reflect the Ca²⁺ dependence of the apoptotic endonucleases involved in this response. Neither BAPTA-AM nor EGTA alone elicited apoptotic responses at the doses used in the aforementioned experiments (Figs. 1*B* and 2). Furthermore, preliminary data suggest that DFF45 (ICAD) was cleaved in NQO1-expressing MCF-7 or MDA-468-NQ3 cells at 8 h after β-Lap treatment, in a temporal manner corresponding to the induction of apoptosis (data not shown). Cleavage of DFF45, an endogenous inhibitor of the magnesium-dependent and Ca²⁺-independent apoptotic endonuclease, DFF40 (CAD), suggests that DFF40 is activated following treatment with β-Lap. Taken together with results in Fig. 1, these data strongly suggest that a rise in intracellular Ca²⁺ levels is part of a critical signaling pathway for the induction of apoptosis in NQO1-expressing human breast cancer cells following β-Lap exposure.

Exposure of NQO1-expressing MCF-7 Cells to β-Lap Results in Increased Intracellular Ca²⁺—We next directly examined whether intracellular Ca²⁺ levels were increased in log-phase MCF-7 cells after β-Lap treatment using the cell-permeant intracellular Ca²⁺ indicator dye, fluo-4. Cells were loaded with 5 μM fluo-4-AM, and where indicated, 20 μM BAPTA-AM, incubated for ~25 min to allow for the dye to permeate cells, rinsed, and then incubated for an additional ~20 min for hydrolysis of the AM-ester. Following drug addition, images were collected every 90 s for ~60 min using confocal microscopy. Three basal images were recorded before drug addition and average pixels per cell were determined (indicative of fluo-4 fluorescence and, therefore, basal intracellular Ca²⁺ levels) and used for analyses over time. The fluorescence of basal images were averaged and set to equal one; fold increases were determined from changes in fluo-4 fluorescence over control.

After exposure to 8 μM β-Lap, MCF-7 cells exhibited an ~2-fold increase in fluo-4 fluorescence from 4 to 9 min, after which time Ca²⁺ levels returned to basal levels in a majority of cells examined (43 of 50, 86%) (Fig. 3*A*). The rise in intracellular Ca²⁺ levels in MCF-7 cells following β-Lap exposure was prevented by preloading cells with BAPTA-AM (20 μM) (Fig. 3*B*). Interestingly, not all β-Lap-exposed MCF-7 cells were affected by pretreatment with BAPTA-AM; 3 of 26 cells (12%) exhibited a rise in intracellular Ca²⁺ levels after exposure to β-Lap despite the presence of this Ca²⁺ chelator. However, BAPTA-AM pretreated MCF-7 cells that did exhibit a rise in intracellular Ca²⁺ levels following β-Lap treatment exhibited a similar, but delayed Ca²⁺ increase (10–20 min), as compared with β-Lap-exposed MCF-7 cells in the absence of BAPTA-AM (4–9 min). This may be due to a saturation of the chelator or heterogeneity of the tumor cell population. These results are consistent with previous reports that the buffering capacity of BAPTA-AM may be overwhelmed with time (34, 46). Higher doses of BAPTA-AM were not used due to toxicity caused by the drug alone (data not shown).

Since the ER is a major store of Ca²⁺ in the cell, we tested if the initial rise in intracellular Ca²⁺ levels after exposure of MCF-7 cells to β-Lap was due to release of Ca²⁺ from this organelle. If β-Lap exposure led to release of Ca²⁺ stored in the ER, then TG (a sarcoplasmic reticulum Ca²⁺-ATPase pump inhibitor) administration should not cause additional Ca²⁺ release. Similarly, if the sequence of drug administration were reversed, additional Ca²⁺ release would also not be observed. When β-Lap was added after TG-induced depletion of ER Ca²⁺ stores, no measurable rise in intracellular Ca²⁺ levels occurred in 25 of 27 (93%) cells analyzed (Fig. 3*C*). Similarly, when TG was added to cells after β-Lap, only 1 of 18 (6%) cells that initially responded to β-Lap exhibited a rise in intracellular Ca²⁺ levels following subsequent TG administration (Fig. 3*D*). At the end of the experiment, all cells analyzed remained responsive to ionomycin. Thus, cells exposed to β-Lap and/or TG were still capable of altering Ca²⁺ levels, and the Ca²⁺ indicator dye was not saturated. We noted that the increase in fluo-4 fluorescence (2–3-fold over basal levels, Fig. 3*A*) in MCF-7 cells observed after exposure to β-Lap was comparable to that elicited by TG (1.5–2.5-fold over basal levels, Fig. 3*C*), further suggesting that the two agents mobilized the same ER pool of Ca²⁺. All cells analyzed started with comparable basal levels of Ca²⁺ and appeared to load equal amounts of the indicator dye, as determined by basal fluorescence (measured by pixels per cell) at the beginning of each analysis; relative basal fluo-4 fluorescence for each experiment in Fig. 3 were: A, 56 ± 7; B, 52 ± 7; C, 78 ± 8; D, 79 ± 8 S.E. Untreated or BAPTA-AM-loaded MCF-7 cells did not show any fluctuations in basal Ca²⁺ levels during the time course of the experiment, nor did any of the drugs interfere with the Ca²⁺ indicator dye (data not shown).
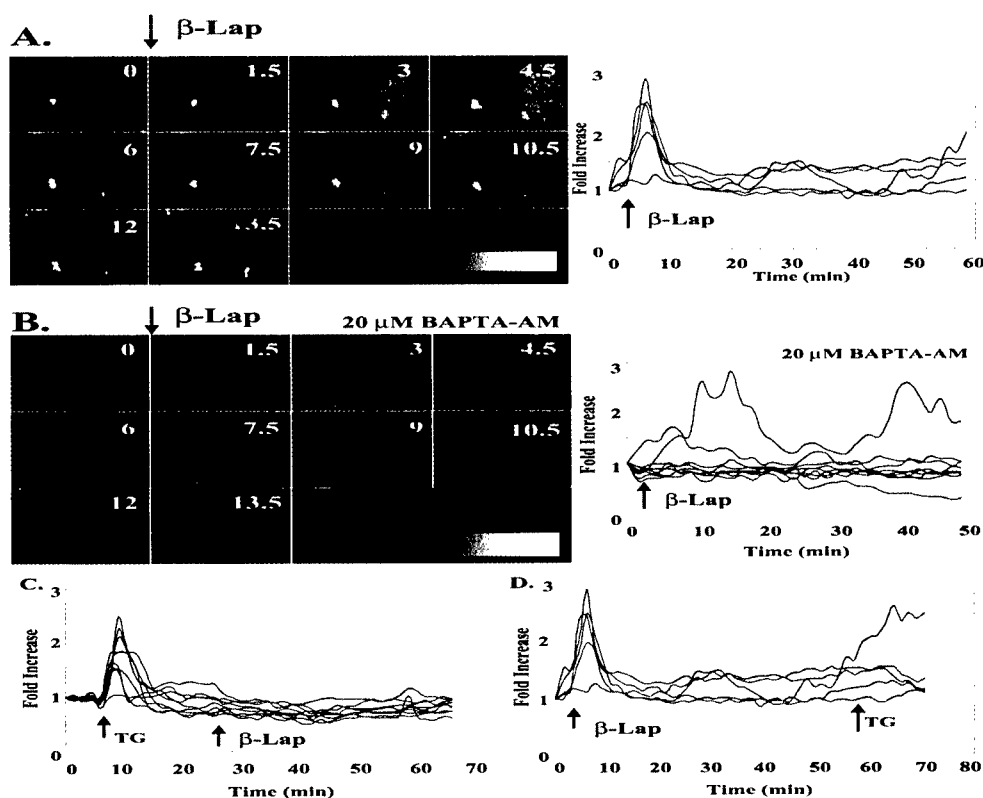
FIG. 3. **Intracellular Ca²⁺ changes after β-Lap.** Intracellular Ca²⁺ levels were measured in live cells via confocal microscopy using the Ca²⁺ indicator dye, fluo-4-AM. MCF-7 cells were loaded with either fluo-4-AM alone (*A, C,* and *D*) or fluo-4-AM and 20 μM BAPTA-AM (*B*). β-Lap (8 μM) was added to cells after basal images were recorded. Images were collected every 90 s for 45–75 min, as indicated. The *number* in the *upper right corner* of each Ca²⁺ image represents the time (min) after β-Lap addition. *A,* representative cells before and after β-Lap treatments are shown as pseudocolored images. These results are also displayed in *graph form* showing fold change (as compared with basal levels) in fluo-4 fluorescence in cells after β-Lap treatment over time, with or without co-loading of BAPTA-AM (*A* and *B*). *C,* TG (200 nM) was added to MCF-7 cells after basal images were recorded. Once fluo-4 fluorescence returned to basal levels, cells were subsequently exposed to β-Lap. *D,* β-Lap was added to MCF-7 cells after basal images were recorded. After fluo-4 fluorescence returned to basal levels, TG was subsequently added to the cells. Each *line* represents the change in fluo-4 fluorescent emission of an individual cell over time; each graph is representative of one of at least three independent experiments.

Loss of Mitochondrial Membrane Potential After β-Lap Is Attenuated by Intracellular, but Not Extracellular, Ca²⁺ Chelation—Mitochondrial membrane potential was previously shown to drop from a hyperpolarized state to a depolarized state after treatment of various human cancer cells with β-Lap (41). A drop in mitochondrial membrane potential in β-Lap-treated cells was accompanied by a concomitant release of cytochrome *c* into the cytosol (41). To explore whether early changes in intracellular Ca²⁺ levels were upstream of mitochondrial changes in NQO1-expressing breast cancer cells, log phase MCF-7 cells were pretreated for 30 min with either 10 μM BAPTA-AM or 3 mM EGTA and then exposed to 5 μM β-Lap for 4 h. Prior to analyses, cells were loaded with JC-1, a cationic dye commonly used to monitor alterations in mitochondrial membrane potential (47, 48). Mitochondrial depolarization measurements using JC-1 were indicated by a decrease in the red/green fluorescence intensity ratio (a movement of events from *upper left* to *lower right*, Fig. 4), as seen following a 10-min treatment with the potassium ionophore, valinomycin (100 nM), which causes a collapse of mitochondrial membrane potential by uncoupling mitochondrial respiration (Fig. 4*e*) (49); cells in the *upper left-hand* quadrant exhibited high mitochondrial membrane potential, whereas, cells in the *lower right-hand* quadrant have low mitochondrial membrane potential and are depolarized. Cells in the *upper right-hand* quadrant exhibited intermediate membrane potential. Mitochondrial membrane potential decreased in MCF-7 cells in a time- and dose-dependent manner following exposure to β-Lap (Figs. 4, *a-d,* and data not shown). By 4 h, the majority of β-Lap-treated MCF-7 cells

exhibited low mitochondrial membrane potential (53%), while the majority of control cells maintained high mitochondrial membrane potential (51%) (Fig. 4, *b, a* and *g, f,* respectively). This drop in mitochondrial membrane potential observed 4 h after treatment with β-Lap (low, 53%) was abrogated by pretreatment with BAPTA-AM (low, 23%), but not by EGTA (low, 48%) (Fig. 4, *g-i,* respectively). Pretreatment with 10 μM BAPTA-AM prevented the decrease in mitochondrial membrane potential (low, 23%); however, BAPTA-AM did not maintain β-Lap-exposed cells in a high-potential state (high, 28%) as observed in control untreated cells (high, 51%). Approximately half of the BAPTA-AM-exposed cells were in an intermediate membrane potential state (45%) (Fig. 4*h*). We noted, however, that BAPTA-AM or EGTA exposures alone caused depolarization of the mitochondria, with a majority of the cells residing in the same intermediate energized state as observed following BAPTA-AM and β-Lap (Fig. 4, *j-k*). Therefore, BAPTA-AM prevented mitochondrial depolarization induced by β-Lap to the same extent as in cells treated with BAPTA-AM alone. Pretreatment with 3 mM EGTA did not affect the loss of mitochondrial membrane potential caused by β-Lap (low 48%), implying that an early rise in intracellular Ca²⁺ levels from intracellular stores was sufficient to cause a drop in mitochondrial membrane potential, and that extracellular calcium was not needed for these effects in β-Lap-treated cells (Fig. 4, *h-i*).

Loss of ATP After β-Lap Is Attenuated by Intracellular Ca²⁺ Chelation—The bioactivation of β-Lap by NQO1 is thought to lead to a futile cycling between quinone and hydroquinone forms of the compound, presumably due to the instability of the
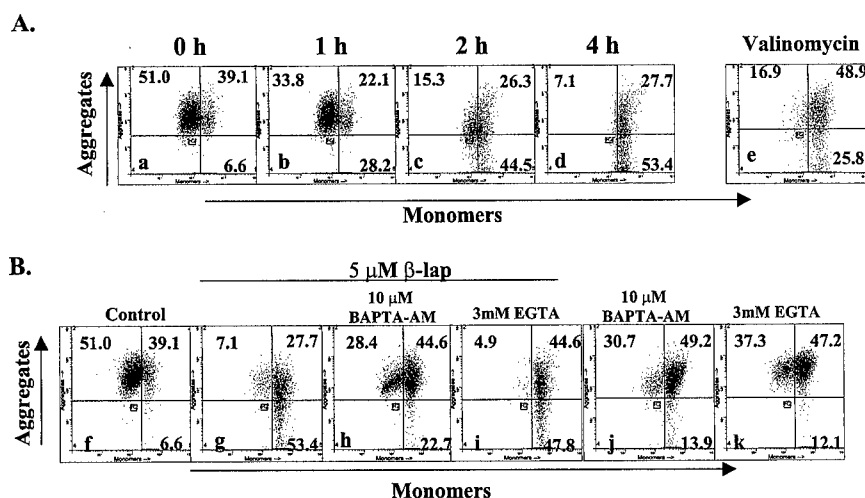
A.

B.

FIG. 4. **β-Lap-induced loss of mitochondrial membrane potential is mediated by alterations in Ca^{2+} homeostasis.** Mitochondrial membrane potential was measured in control or drug-treated MCF-7 cells with the JC-1 dye. *A,* cells were treated with 5 μM β-Lap and assayed for changes in mitochondrial membrane potential at 1, 2, and 4 h post-treatment. Exposure of MCF-7 cells to 100 nM valinomycin for 15 min served as a positive control as described (49). Cells in the *upper left-hand* quadrant exhibit high mitochondrial membrane potential, while cells in the *lower right-hand* quadrant exhibit low mitochondrial membrane potential. *B,* cells were treated for 30 min with either 10 μM BAPTA-AM or 3 mM EGTA prior to a 4-h treatment with 5 μM β-Lap. At 4 h, cells were harvested for analyses of changes in mitochondrial membrane potential using JC-1 as described above. Shown are representative experiments performed at least three times, and *numbers* in each quadrant represent the average of cells in that quadrant of at least three independent experiments. S.E. for any single number was not more than 11%.

hydroquinone form of β-Lap (5). This futile cycling led to depletion of NADH and NADPH, electron donors for NQO1 in *in vitro* assays (5). Exhaustion of reduced enzyme co-factors may be a critical event for the activation of the apoptotic pathway in NQO1-expressing cells following β-Lap exposure. We, therefore, measured intracellular ATP and ADP in log-phase MCF-7 cells after various doses and times of β-Lap (using a luciferase-based bioluminescent assay (42)). Intracellular ATP levels were reduced in MCF-7 cells after treatment with β-Lap in a dose- and time-dependent manner (Fig. 5A). At all doses of β-Lap above the LD_{50} of the drug (~2.5 μM) in MCF-7 cells (2), intracellular ATP levels were reduced by >85% at 4 h, the time at which drug was removed (Fig. 5A, *left*); the loss of ATP correlated well with β-Lap-induced cell death in MCF-7 cells (Fig. 1C). ADP levels remained relatively unchanged after various doses of β-Lap, however, the [ATP]/[ADP][P_i] ratio decreased dramatically. Intracellular ATP levels began to drop to 70% of control levels 2 h after 5 μM β-Lap exposure, the time at which β-Lap began to elicit mitochondrial membrane depolarization (Figs. 5, *A, right,* and 4, *c*). ATP levels continued to drop to 8% of control levels by 4 h after drug exposure (Fig. 5A, *right*). In contrast, ADP levels remained relatively unchanged during the course of the experiment, with an increase at 30 min (172% control levels) that returned to control levels by 1 h post-treatment. Cellular ATP levels in β-Lap-treated cells did not appear to recover to normal levels within the 6–24-h interval after drug removal (data not shown).

Loss of ATP following β-Lap was prevented by a 30-min pretreatment with an intracellular Ca^{2+} chelator, but not an extracellular Ca^{2+} chelator (Fig. 5B). At 4 h, pretreatment with 10 or 30 μM BAPTA-AM elicited only 58 and 43% ATP loss, respectively, compared with β-Lap alone (92% loss). The extracellular Ca^{2+} chelator, EGTA, did not significantly affect the loss of ATP, nor [ATP]/[ADP][P_i] ratio observed in MCF-7 cells after β-Lap treatment (Fig. 5B). Exposure of MCF-7 cells to TG (200 nM) did not elicit decreases in ATP or ADP levels 4 h after drug exposure, compared with untreated control cells.

Ca^{2+} Chelators Prevent β-Lap-induced Proteolysis—We previously showed that apoptosis in various breast cancer cell lines induced by β-Lap was unique, causing a pattern of PARP and p53 intracellular cleavage events distinct from those in-

duced by caspase activating agents (12). After β-Lap treatment, we observed an ~60-kDa PARP cleavage fragment and specific cleavage of p53 in NQO1-expressing breast cancer cells. Furthermore, we showed that this proteolysis in β-Lap-treated cells was the result of activation of a Ca^{2+}-dependent protease with properties similar to μ-calpain (12). PARP and p53 proteolysis in β-Lap-exposed, NQO1-expressing cells was prevented by pretreatment with the extracellular Ca^{2+} chelators, EGTA and EDTA, in a dose-dependent manner (at 8 and 24 h) (Ref. 12, and data not shown). Additionally, PARP, p53, and lamin B proteolysis induced at 24 h in MCF-7 cells following β-Lap treatment were abrogated by pretreatment with 10 or 30 μM BAPTA-AM (Fig. 6). These data strongly suggest that a Ca^{2+}-dependent pathway and potentially a Ca^{2+}-dependent protease are operative in β-Lap-mediated apoptosis.

A simple explanation for the aforementioned results could be that BAPTA blocks bioactivation of β-Lap by NQO1 in a manner similar to that of dicumarol (5). However, BAPTA (free acid) did not affect the enzymatic activities of NQO1 using standard enzymatic assays (data not shown) (5). The free acid (active) form of BAPTA, instead of its −AM ester form, was used in these assays since intracellular accumulation of this Ca^{2+} chelator was not necessary and was physiologically relevant in the *in vitro* enzyme assay. Using β-Lap as a substrate, NQO1 enzymatic activity in the presence of 10 mM BAPTA (a dose of the free acid form of BAPTA that was >1000-fold higher than that used in the experiments of Figs. 1–6) was reduced by <20%. Thus, BAPTA-AM did not affect the activity of NQO1, a two-electron reductase required for β-Lap cytotoxicity (5). We conclude that BAPTA-AM prevents β-Lap-induced apoptosis by blocking Ca^{2+}-mediated signaling events via chelating intracellular Ca^{2+}.

β-Lap Bioactivation by NQO1 Is Critical for Ca^{2+}-mediated Signaling—We previously reported that cells expressing NQO1 are more sensitive to the cytotoxic effects of β-Lap (5).[2] NQO1 is inhibited by dicumarol, which competes with NADH or NADPH for binding to the oxidized form of the enzyme. Dicumarol thereby prevents reduction of quinones (50, 51). We demonstrated that dicumarol attenuates β-Lap-mediated proteolysis of apoptotic substrates (*e.g.* PARP and p53), apoptosis, and survival in NQO1-expressing cells (5).[2] As expected, increases

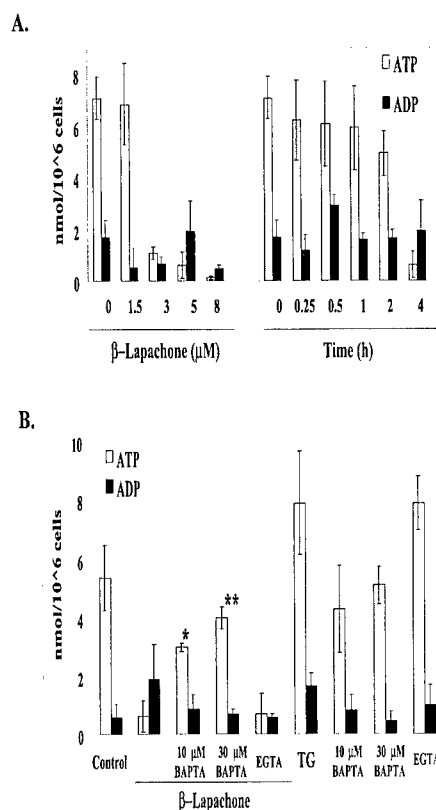*Ca²⁺ Signaling in β-Lap-mediated Apoptosis*

A.

B.

FIG. 5. **ATP depletion after β-Lap treatment is Ca²⁺ dependent.** Intracellular ATP and ADP levels were measured using a luciferase-based bioluminescent assay. *A,* cells were treated with the indicated dose of β-Lap for 4 h or were treated with 5 μM β-Lap for the time indicated, and harvested for ATP analyses. ATP levels were expressed as nanomoles of ATP per 10^6 cells. Purified ATP was used as a standard to determine intracellular ATP concentrations. *B,* cells were either pretreated or untreated with the indicated Ca²⁺ chelators for 30 min prior to drug addition, and β-Lap (5 μM) was then added for 4 h. Cells were harvested for analyses following β-Lap exposure. Results represent the average of at least three independent experiments, ± S.E. Student's *t* test for paired samples, experimental group compared with drug alone are indicated (*, $p < 0.05$; **, $p < 0.01$).

in intracellular Ca²⁺ levels in NQO1-expressing human cancer cells elicited by β-Lap were abrogated by co-treatment with 50 μM dicumarol in 26 of 27 cells (96%) examined (Fig. 7A, *lower panel*). The ability of dicumarol to inhibit increases in intracellular Ca²⁺ levels was greater than that observed with BAPTA-AM, where intracellular Ca²⁺ level increases were prevented in only 89% of cells examined (Fig. 3B). Thus, NQO1 was critical for the rise in intracellular Ca²⁺ levels observed in MCF-7 cells after β-Lap exposure.

Mitochondrial membrane depolarization induced by β-Lap was also abrogated by pretreatment with dicumarol (Fig. 7B). By 4 h, the majority of β-Lap-treated cells exhibited low mitochondrial membrane potential (58%), while very few control cells were depolarized (9%) (Fig. 7B). Pretreatment with dicumarol attenuated this response to β-Lap, with only 34% being depolarized. The inability of dicumarol to prevent mitochondrial depolarization in 34% of β-Lap-treated cells was probably due to the high background of control cells (20%) that were depolarized after exposure to dicumarol alone. In comparison with intracellular Ca²⁺ buffering, BAPTA-AM elicited only a minor depolarization of the mitochondria on its own (low, 14%) and thus was able to elicit a greater protective effect (Fig. 4B); only 23% of cells exposed to BAPTA-AM and β-Lap exhibited low mitochondrial membrane potential as compared with β-Lap exposed cells in the presence of dicumarol (34%).
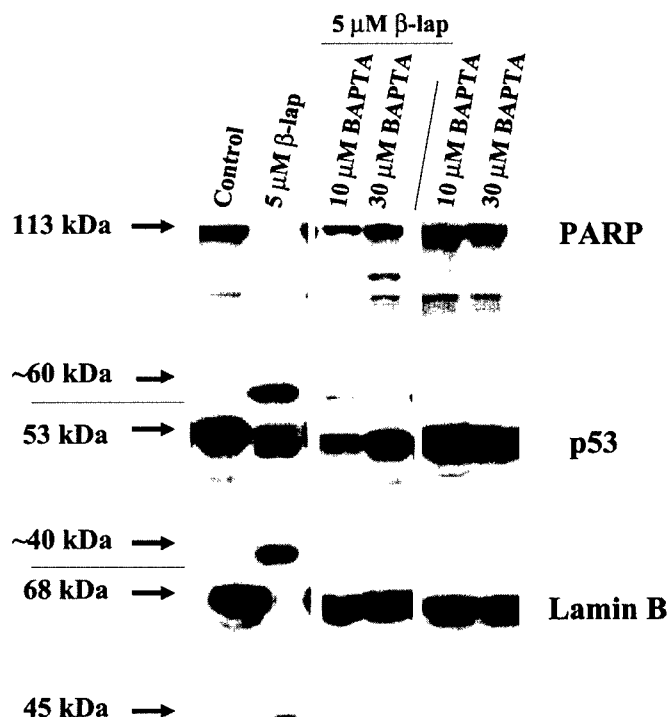

FIG. 6. **Intracellular Ca²⁺ chelators prevent apoptotic proteolysis after β-Lap treatment.** Apoptotic proteolysis was measured in MCF-7 cells exposed to a 4-h pulse of 5 μM β-Lap, with or without a 30-min pretreatment of the indicated dose of BAPTA-AM. Whole cell extracts were prepared 24 h after drug addition, and analyzed using standard Western blotting techniques with antibodies to PARP, p53, and lamin B. Shown is a representative Western blot of whole cell extracts from experiments performed at least three times.

The dramatic loss of intracellular ATP in MCF-7 cells following β-Lap exposure was inhibited by a 30-min pretreatment with 50 μM dicumarol (Fig. 7C). β-Lap-treated MCF-7 cells pretreated with dicumarol exhibited only 34% loss of intracellular ATP, compared with 92% loss after β-Lap treatment alone (Fig. 7C). ADP levels were not altered by any of the treatments used, however, the [ATP]/[ADP][Pᵢ] ratio decreased dramatically in β-Lap-treated cells, and was only partially decreased with dicumarol pretreatment alone, as compared with control untreated cells.

Dicumarol also abrogated DNA fragmentation induced by β-Lap in MCF-7 cells. MCF-7 cells exhibited 94% apoptosis following β-Lap exposure that was prevented by a 30-min pretreatment with 50 μM dicumarol; only 6% of the cells staining positive in a TUNEL assay at 24 h post-treatment (Fig. 7D). These data are consistent with prior results (5), and correlate well with the survival protection afforded by dicumarol to β-Lap-treated cells. Dicumarol did not induce DNA fragmentation on its own. These data are consistent with the protection from apoptosis observed with either intra- and extracellular Ca²⁺ chelators. BAPTA-AM or EGTA protected β-Lap exposed MCF-7 cells from apoptosis (Fig. 1, *A* and *B*). Collectively, these data implicate the bioactivation of β-Lap by NQO1 as a critical step in the rise of intracellular Ca²⁺ levels following β-Lap exposure, and thus β-Lap-mediated downstream apoptotic events.

DISCUSSION

When homeostatic mechanisms for regulating cellular Ca²⁺ are compromised, cells may die, either by necrosis or apoptosis (20, 21, 36). We demonstrated that bioactivation of β-Lap by NQO1 induced cell death in a manner that was dependent upon Ca²⁺ signaling (Figs. 1–6). β-Lap can be reduced by NQO1 and
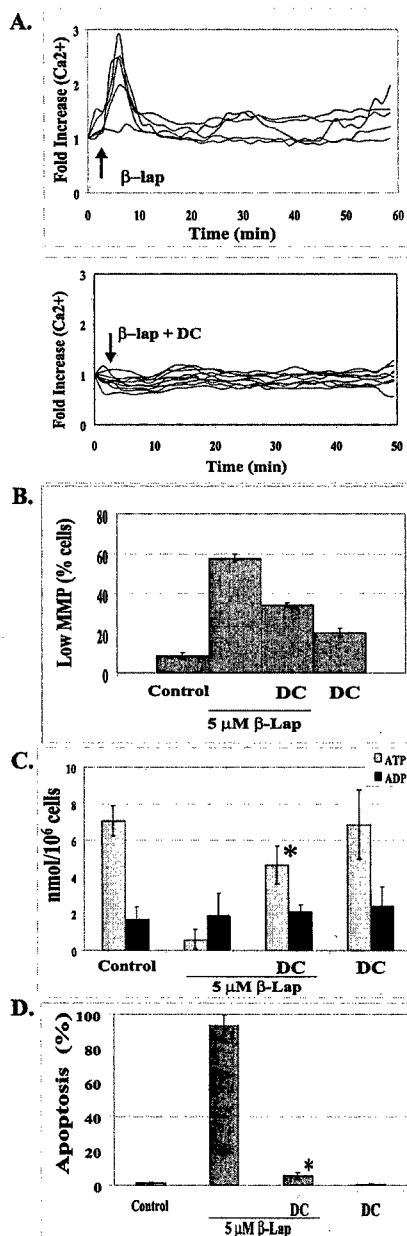
FIG. 8. Proposed model for β-lapachone-mediated apoptosis in NQO1-expressing cells. In cells that express NQO1, β-Lap is reduced from the quinone (*β-lap-Q*) to the hydroquinone (*β-lap-HQ*) form in a futile cycle that results in dramatic losses of NAD(P)H (5). During the metabolism of β-Lap by NQO1, Ca^{2+} is subsequently released from the ER causing a rise in cytosolic Ca^{2+} levels by an as yet unknown mechanism. To maintain low cytoplasmic Ca^{2+} levels, we theorize that mitochondria sequester Ca^{2+} and numerous cellular ATPases probably function to pump Ca^{2+} out of the cytosol. This leads to mitochondrial membrane depolarization and ATP hydrolysis, respectively (Figs. 4 and 5). Sustained depolarization of the mitochondrial membrane leads to further loss of ATP and prevents ATP synthesis by inhibiting respiration. The loss of ATP disrupts ionic homeostasis within the cell and thereby allows extracellular Ca^{2+} to enter the cell down its concentration gradient (see "Discussion"). The secondary rise in cytosolic Ca^{2+} levels leads to protease (presumably activation of calpain or a calpain-like protease) and, thus, endonuclease (DFF40) activation, ultimately resulting in apoptosis.

FIG. 7. NQO1-dependent activation of β-Lap is critical for Ca^{2+} signaling. *A,* intracellular Ca^{2+} was measured on live cells using the Ca^{2+} indicator dye, fluo-4-AM, and confocal microscopy as described in the legend to Fig. 3. Three basal images were recorded before drug treatments. β-Lap (8 μM) was then added to MCF-7 cells, either alone (*upper panel*) or in combination with 50 μM dicumarol (*lower panel*). Images were collected every 90 s for 50–60 min. Shown are representative graphs displaying changes in fluo-4 fluorescence for the duration of the experiment. Each *line* represents the fold change in fluo-4 fluorescent emission (as compared with basal levels) of an individual cell from one experiment, and the graph is representative of experiments performed at least three times. *B,* mitochondrial membrane potential was measured using the JC-1 dye as described in the legend to Fig. 4. MCF-7 cells were treated with 50 μM dicumarol 30 min prior to β-Lap exposure. Four hours later, cells were harvested for analyses of mitochondrial membrane potential. Shown are mean ± S.E. of the percentage of cells with low mitochondrial membrane potential of at least two independent experiments. *C,* ATP and ADP levels were assayed as described in the legend to Fig. 5. Cells were pretreated with dicumarol for 30 min prior to drug addition, 5 μM β-Lap was added for 4 h, and cells were harvested immediately thereafter for analyses. Results represent the mean of at least three independent experiments ± S.E. Student's *t* test for paired samples, experimental groups compared with drug alone are indicated (* $p < 0.05$). *D,* apoptosis, using the TUNEL assay, was assessed as per Fig. 1. MCF-7 cells were treated with 50 μM dicumarol 30 min prior to a 4-h exposure of 5 μM β-Lap. Cells were then harvested for TUNEL analyses at 24 h post-treatment. Shown are
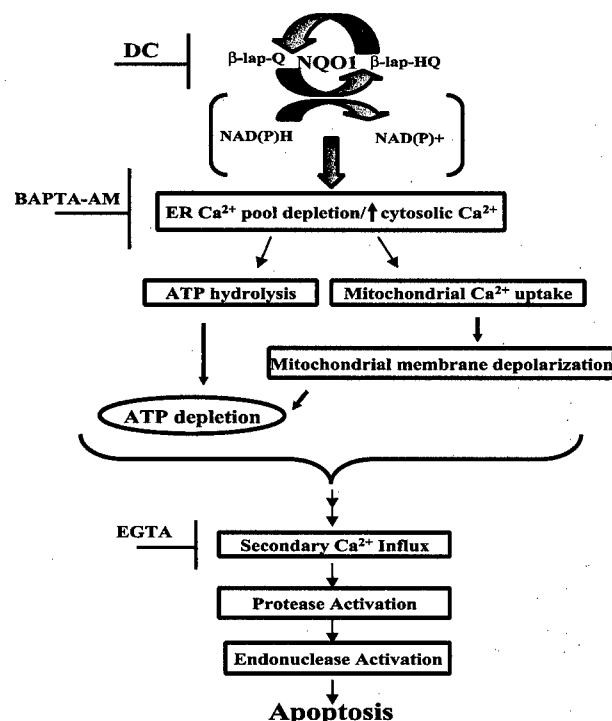
may undergo futile cycling between quinone and hydroquinone forms (β-Lap-Q and β-Lap-HQ, Fig. 8), presumably depleting NADH and/or NADPH in the cell (5). We theorize that depletion of NAD(P)H, along with a rise in intracellular Ca^{2+} levels in response to β-Lap, activate a novel caspase-independent apoptotic pathway, as described in this paper and previously (2, 5, 12). The rise in intracellular Ca^{2+} appears to be dependent upon the bioactivation of β-Lap by NQO1, suggesting a critical and necessary signaling role for Ca^{2+} in the downstream apoptotic pathway induced by this drug. Dicumarol completely abrogated intracellular Ca^{2+} changes (Fig. 7), as well as apoptosis and survival, following β-Lap exposure of NQO1-expressing cells (5).[2] When increases in intracellular Ca^{2+} levels were directly prevented by pretreatment with BAPTA-AM, downstream apoptotic responses, as well as lethality, caused by β-Lap were prevented; when corrected for BAPTA-AM affects alone, β-Lap-induced apoptosis, proteolysis, and lethality were essentially blocked by preventing early Ca^{2+} release from ER stores. Thus, correcting for the BAPTA-AM affects alone, the role of Ca^{2+} in β-Lap-mediated apoptosis may be more significant that that revealed by the data shown. These data strongly

mean ± S.E. of at least three independent experiments. Student's *t* test for paired samples, experimental groups compared with β-Lap exposure alone are indicated (*, $p < 0.005$). *DC*, 50 μM dicumarol.

suggest that DNA fragmentation, mitochondrial membrane depolarization, ATP loss, and apoptotic proteolysis were a consequence of the increase in intracellular Ca^{2+} levels (Figs. 1–6 and 8). Interestingly, the cell death pathway induced by β-Lap was quite distinct from that observed after exposure to TG, an agent known to specifically cause release of Ca^{2+} from ER stores and mediate caspase-dependent apoptosis (24, 28, 33, 52). Thus, Ca^{2+} release was necessary for β-Lap-induced cytotoxicity, but apparently not sufficient for the unique apoptotic responses induced by β-Lap.

β-Lap and TG-induced Similar Ca^{2+} Responses, but Different Patterns of Apoptosis—β-Lap elicited an early rise in intracellular Ca^{2+} levels from the same ER store as released by TG, however, subsequent cell death processes were remarkably different between the two compounds. TG is known to cause transient increases in intracellular Ca^{2+} levels, however, these were insufficient to induce apoptosis. Much like β-Lap, Ca^{2+} was needed from the extracellular milieu, along with a sustained increase in intracellular Ca^{2+} levels, for TG-induced apoptosis (23) in MCF-7 cells (27). Depolarization of the mitochondrial membrane potential and loss of intracellular ATP in cells exposed to β-Lap, may have prevented plasma membrane Ca^{2+} pumps and ER Ca^{2+} pumps from functioning and maintaining Ca^{2+} homeostasis. This, in turn, may have facilitated Ca^{2+} leakage down its concentration gradient into the cytosol, providing a secondary and sustained elevation of Ca^{2+} that initiated a protease cascade(s) and ultimately caused apoptosis after exposure to β-Lap. This is consistent with what we observed in NQO1-expressing cells after β-Lap treatment and co-administration of Ca^{2+} chelators. Buffering intracellular Ca^{2+} with BAPTA-AM partially abrogated all of the downstream events induced in MCF-7 cells by β-Lap (and thus prevented secondary Ca^{2+} entry by buffering the initial rise in cytosolic Ca^{2+}). In contrast, extracellular chelation by EGTA only prevented those events initiated by secondary Ca^{2+} entry (*e.g.* protease activation and DNA fragmentation). Thus, a secondary rise in intracellular Ca^{2+} levels after exposure to β-Lap seems probable, and necessary, for protease activation and DNA fragmentation as was observed for TG-induced caspase-mediated apoptosis (23, 27). However, a secondary influx of Ca^{2+} does not appear to be necessary for reduction in mitochondrial membrane potential or loss of intracellular ATP after β-Lap exposure, since EGTA did not prevent these responses.

Although MCF-7 cells treated with β-Lap had similar calcium responses, as do TG-exposed cells, β-Lap-exposed cells exhibited a very different pattern of apoptosis than TG-treated cells. β-Lap-exposed cells exhibit loss of intracellular ATP and a decrease in the [ATP]/[ADP][P_i] ratio. In contrast, TG-exposed cells did not exhibit loss of ATP (Fig. 5, and as reported by Ref. 53). Our data suggest that in contrast to TG where ATP-dependent caspase activation results in cell death (28, 33, 34, 54), an ATP-independent protease is activated after exposure to β-Lap. Ca^{2+} may regulate apoptosis by activating Ca^{2+}-dependent protein kinases and/or phosphatases leading to alterations in gene transcription. However, with the rapid loss of intracellular ATP after exposure to β-Lap (2–4 h, Fig. 5), β-Lap-mediated cell death unlikely involves stimulated kinases or phosphatases or new protein synthesis. Instead, indirect kinase inhibition, due to ATP depletion, along with continued phosphatase activity is likely. Consistent with this notion, we found dramatic de-phosphorylation of pRb in cells exposed to β-Lap at 3 h (2), a time consistent with loss of ATP following exposure to this drug. Furthermore, loss of ATP at 2 h may also be responsible for inhibition of NF-κB activation induced by tumor necrosis factor-α in β-Lap pre-exposed cells (55), since significant loss of ATP would prevent proteosome-

mediated IκB degradation. Thus, Ca^{2+}-dependent loss of ATP in NQO1-expressing cells following β-Lap treatment may explain the reported pleiotropic effects of this agent.

β-Lap-exposed cells also exhibited a very different pattern of substrate proteolysis compared with that observed after TG (2, 12, 28). We previously showed that β-Lap elicited a unique cleavage of PARP (~60-kDa fragment), compared with the classical caspase-3-mediated fragmentation of the protein (~89 kDa) observed after TG exposure (data not shown and Ref. 28). In a variety of NQO1-expressing cells exposed to β-Lap, atypical PARP cleavage was inhibited by the global cysteine protease inhibitors, iodoacetamide and *N*-ethylmaleimide, as well as the extracellular Ca^{2+} chelators, EGTA and EDTA (12). In addition, β-Lap-mediated apoptotic responses were insensitive to inhibitors of caspases, granzyme B, cathepsins B and L, trypsin, and chymotrypsin-like proteases (12). In contrast, classic caspase inhibitors blocked TG-induced caspase activation and apoptosis (28). Caspase activation, as measured by pro-caspase cleavage via Western blot analyses, does not occur following β-Lap exposures.[3] Thus, protease activation after β-Lap treatment appears to be Ca^{2+}-dependent, or alternatively, is activated by another protease or event that is Ca^{2+}-dependent (Figs. 1–6 and Ref. 12).

Loss of Reducing Equivalents Is Also Necessary for β-Lap-mediated Apoptosis, Similar to Menadione-mediated Apoptosis—Menadione is a quinone that can be detoxified by NQO1 two-electron reduction. However, menadione can also be reduced through two, one-electron reductions via other cellular reductases (56), thus eliciting menadione's toxic effects. Menadione toxicity, elicited via two, one-electron reductions, exhibited many similarities to β-Lap-mediated, NQO1-dependent, toxicity (5). These included: (*a*) elevations in cytosolic Ca^{2+} (57, 58); (*b*) NAD(P)H depletion (5, 59, 60); (*c*) ATP depletion (<0.1% control)[3] (61–63); and (*d*) mitochondrial membrane potential depolarization[3] (64). We previously demonstrated that menadione caused similar substrate proteolysis (p53 and atypical PARP cleavage) in NQO1-deficient cells, or at high doses in cells that express NQO1 where detoxification processes were over-ridden (5).[3] The semiquinone form of menadione can undergo spontaneous oxidation to the parent quinone (59, 63, 65, 66); a pattern similar to the futile cycling observed after β-Lap bioactivation by NQO1 (5). Loss of reducing equivalents, such as NADH, due to the futile cycling of menadione may cause inactivation of the electron transport chain with the concomitant loss of mitochondrial membrane potential, and thus, loss of ATP (67, 68). These responses were also observed in MCF-7 cells exposed to β-Lap (Figs. 4 and 5). Extensive mitochondrial Ca^{2+} accumulation can also mediate mitochondrial depolarization (69, 70). Thus, Ca^{2+} sequestration may elicit mitochondrial membrane depolarization and consequent ATP depletion in cells exposed to β−lap. These data further suggest that Ca^{2+} is necessary for β-Lap-mediated cell death, but other factors are apparently needed for the initiation of the novel execution apoptotic pathway observed in cells treated with this compound.

The rise in intracellular Ca^{2+} appears to be dependent on the bioactivation of β-Lap by NQO1, suggesting a critical and necessary signaling role for Ca^{2+} in the downstream apoptotic pathway induced by this drug. These data suggest that DNA fragmentation, mitochondrial membrane depolarization, ATP loss, and apoptotic proteolysis were a consequence of the increase in intracellular Ca^{2+} levels. Work in our laboratory is focused on elucidating the signaling response(s) that elicits ER Ca^{2+} release following β-Lap bioactivation by NQO1. The cell

---

[3] C. Tagliarino, J. J. Pink, and D. A. Boothman, unpublished results.

death pathway induced by β-Lap is quite distinct from that observed after exposure to TG, and β-Lap-mediated apoptosis exhibited many similarities to menadione-mediated apoptosis. These observations further suggest that early release of Ca^{2+} from ER stores, as well as influx of Ca^{2+} from the extracellular milieu are necessary, but not sufficient for the novel apoptotic execution pathway induced by β-Lap. Thus, changes in Ca^{2+} homeostasis in conjunction with the presumed loss of reducing equivalents are both necessary and sufficient for β-Lap-mediated apoptosis. We propose that development of β-Lap for treatment of human cancers that have elevated NQO1 levels (*e.g.* breast and lung) is warranted (6). Since most clinical agents used to date kill cells by caspase-dependent and p53-dependent pathways, and many cancers evade death by altering these pathways, development of agents that kill by specific targets (NQO1-mediated) and in p53- and caspase-independent manners are needed.

REFERENCES

1. Planchon, S. M., Wuerzberger, S., Frydman, B., Witiak, D. T., Hutson, P., Church, D. R., Wilding, G., and Boothman, D. A. (1995) *Cancer Res.* **55**, 3706–3711
2. Wuerzberger, S. M., Pink, J. J., Planchon, S. M., Byers, K. L., Bornmann, W. G., and Boothman, D. A. (1998) *Cancer Res.* **58**, 1876–1885
3. Li, C. J., Wang, C., and Pardee, A. B. (1995) *Cancer Res.* **55**, 3712–3715
4. Li, C. J., Li, Y. Z., Pinto, A. V., and Pardee, A. B. (1999) *Proc. Natl. Acad. Sci. U. S. A.* **96**, 13369–13374
5. Pink, J. J., Planchon, S. M., Tagliarino, C., Varnes, M. E., Siegel, D., and Boothman, D. A. (2000) *J. Biol. Chem.* **275**, 5416–5424
6. Marin, A., Lopez de Cerain, A., Hamilton, E., Lewis, A. D., Martinez-Penuela, J. M., Idoate, M. A., and Bello, J. (1997) *Br. J. Cancer* **76**, 923–929
7. Patel, T., Gores, G. J., and Kaufmann, S. H. (1996) *FASEB J.* **10**, 587–597
8. Gerschenson, L. E., and Rotello, R. J. (1992) *FASEB J.* **6**, 2450–2455
9. Kluck, R. M., Bossy-Wetzel, E., Green, D. R., and Newmeyer, D. D. (1997) *Science* **275**, 1132–1136
10. Li, P., Nijhawan, D., Budihardjo, I., Srinivasula, S. M., Ahmad, M., Alnemri, E. S., and Wang, X. (1997) *Cell* **91**, 479–489
11. Eguchi, Y., Srinivasan, A., Tomaselli, K. J., Shimizu, S., and Tsujimoto, Y. (1999) *Cancer Res.* **59**, 2174–2181
12. Pink, J. J., Wuerzberger-Davis, S., Tagliarino, C., Planchon, S. M., Yang, X., Froelich, C. J., and Boothman, D. A. (2000) *Exp. Cell Res.* **255**, 144–155
13. Froelich, C. J., Hanna, W. L., Poirier, G. G., Duriez, P. J., D'Amours, D., Salvesen, G. S., Alnemri, E. S., Earnshaw, W. C., and Shah, G. M. (1996) *Biochem. Biophys. Res. Commun.* **227**, 658–665
14. Pariat, M., Carillo, S., Molinari, M., Salvat, C., Debussche, L., Bracco, L., Milner, J., and Piechaczyk, M. (1997) *Mol. Cell. Biol.* **17**, 2806–2815
15. Kubbutat, M. H., and Vousden, K. H. (1997) *Mol. Cell. Biol.* **17**, 460–468
16. Distelhorst, C. W., and Dubyak, G. (1998) *Blood* **91**, 731–734
17. Fang, M., Zhang, H., Xue, S., Li, N., and Wang, L. (1998) *Cancer Lett.* **127**, 113–121
18. Marks, A. R. (1997) *Am. J. Physiol.* **272**, H597–605
19. McConkey, D. J., Hartzell, P., Amador-Perez, J. F., Orrenius, S., and Jondal, M. (1989) *J. Immunol.* **143**, 1801–1806
20. McConkey, D. J., and Orrenius, S. (1997) *Biochem. Biophys. Res. Commun.* **239**, 357–366
21. McConkey, D. J. (1996) *Scanning Microsc.* **10**, 777–793
22. Martikainen, P., and Isaacs, J. (1990) *Prostate* **17**, 175–187
23. Jiang, S., Chow, S. C., Nicotera, P., and Orrenius, S. (1994) *Exp. Cell Res.* **212**, 84–92
24. Kaneko, Y., and Tsukamoto, A. (1994) *Cancer Lett.* **79**, 147–155
25. Levick, V., Coffey, H., and D'Mello, S. R. (1995) *Brain Res* **676**, 325–335
26. Choi, M. S., Boise, L. H., Gottschalk, A. R., Quintans, J., Thompson, C. B., and

Klaus, G. G. (1995) *Eur. J. Immunol.* **25**, 1352–1357
27. Jackisch, C., Hahm, H. A., Tombal, B., McCloskey, D., Butash, K., Davidson, N. E., and Denmeade, S. R. (2000) *Clin. Cancer Res.* **6**, 2844–2850
28. McColl, K. S., He, H., Zhong, H., Whitacre, C. M., Berger, N. A., and Distelhorst, C. W. (1998) *Mol. Cell. Endocrinol.* **139**, 229–238
29. Yakovlev, A. G., Wang, G., Stoica, B. A., Boulares, H. A., Spoonde, A. Y., Yoshihara, K., and Smulson, M. E. (2000) *J. Biol. Chem.* **275**, 21302–21308
30. Gaido, M. L., and Cidlowski, J. A. (1991) *J. Biol. Chem.* **266**, 18580–18585
31. Urbano, A., McCaffrey, R., and Foss, F. (1998) *J. Biol. Chem.* **273**, 34820–34827
32. McConkey, D. J., Nicotera, P., Hartzell, P., Bellomo, G., Wyllie, A. H., and Orrenius, S. (1989) *Arch Biochem. Biophys.* **269**, 365–370
33. Srivastava, R. K., Sollott, S. J., Khan, L., Hansford, R., Lakatta, E. G., and Longo, D. L. (1999) *Mol. Cell. Biol.* **19**, 5659–5674
34. Wertz, I. E., and Dixit, V. M. (2000) *J. Biol. Chem.* **275**, 11470–11477
35. Lotem, J., and Sachs, L. (1998) *Proc. Natl. Acad. Sci. U. S. A.* **95**, 4601–4606
36. Petersen, A., Castilho, R. F., Hansson, O., Wieloch, T., and Brundin, P. (2000) *Brain Res.* **857**, 20–29
37. Green, D. R., and Reed, J. C. (1998) *Science* **281**, 1309–1312
38. Kroemer, G., Dallaporta, B., and Resche-Rigon, M. (1998) *Annu. Rev. Physiol.* **60**, 619–642
39. Susin, S. A., Lorenzo, H. K., Zamzami, N., Marzo, I., Snow, B. E., Brothers, G. M., Mangion, J., Jacotot, E., Costantini, P., Loeffler, M., Larochette, N., Goodlett, D. R., Aebersold, R., Siderovski, D. P., Penninger, J. M., and Kroemer, G. (1999) *Nature* **397**, 441–446
40. Richter, C. (1993) *FEBS Lett.* **325**, 104–107
41. Li, Y. Z., Li, C. J., Pinto, A. V., and Pardee, A. B. (1999) *Mol. Med.* **5**, 232–239
42. Beigi, R. D., and Dubyak, G. R. (2000) *J. Immunol.* **165**, 7189–7198
43. Tang, D., Lahti, J. M., and Kidd, V. J. (2000) *J. Biol. Chem.* **275**, 9303–9307
44. Kim, J. E., Oh, J. H., Choi, W. S., Chang, I. I., Sohn, S., Krajewski, S., Reed, J. C., O'Malley, K. L., and Oh, Y. J. (1999) *J. Neurochem.* **72**, 2456–2463
45. Kurokawa, H., Nishio, K., Fukumoto, H., Tomonari, A., Suzuki, T., and Saijo, N. (1999) *Oncol. Rep.* **6**, 33–37
46. Yao, Y., and Tsien, R. Y. (1997) *J. Gen. Physiol.* **109**, 703–715
47. Cossarizza, A., Baccarani-Contri, M., Kalashnikova, G., and Franceschi, C. (1993) *Biochem. Biophys. Res. Commun.* **197**, 40–45
48. Salvioli, S., Ardizzoni, A., Franceschi, C., and Cossarizza, A. (1997) *FEBS Lett.* **411**, 77–82
49. Inai, Y., Yabuki, M., Kanno, T., Akiyama, J., Yasuda, T., and Utsumi, K. (1997) *Cell Struct. Funct.* **22**, 555–563
50. Hollander, P. M., and Ernster, L. (1975) *Arch. Biochem. Biophys.* **169**, 560–567
51. Hosoda, S., Nakamura, W., and Hayashi, K. (1974) *J. Biol. Chem.* **249**, 6416–6423
52. Distelhorst, C. W., and McCormick, T. S. (1996) *Cell Calcium* **19**, 473–483
53. Waring, P., and Beaver, J. (1996) *Exp. Cell Res.* **227**, 264–276
54. Qi, X. M., He, H., Zhong, H., and Distelhorst, C. W. (1997) *Oncogene* **15**, 1207–1212
55. Manna, S. K., Gad, Y. P., Mukhopadhyay, A., and Aggarwal, B. B. (1999) *Biochem. Pharmacol.* **57**, 763–774
56. Iyanagi, T., and Yamazaki, I. (1970) *Biochim. Biophys. Acta* **216**, 282–294
57. Jewell, S. A., Bellomo, G., Thor, H., Orrenius, S., and Smith, M. (1982) *Science* **217**, 1257–1259
58. Nicotera, P., McConkey, D., Svensson, S. A., Bellomo, G., and Orrenius, S. (1988) *Toxicology* **52**, 55–63
59. Di Monte, D., Bellomo, G., Thor, H., Nicotera, P., and Orrenius, S. (1984) *Arch. Biochem. Biophys.* **235**, 343–350
60. Smith, P. F., Alberts, D. W., and Rush, G. F. (1987) *Toxicol. Appl. Pharmacol.* **89**, 190–201
61. Akman, S. A., Doroshow, J. H., Dietrich, M. F., Chlebowski, R. T., and Block, J. S. (1987) *J. Pharmacol. Exp. Ther.* **240**, 486–491
62. Mehendale, H. M., Svensson, S. A., Baldi, C., and Orrenius, S. (1985) *Eur. J. Biochem.* **149**, 201–206
63. Redegeld, F. A., Moison, R. M., Koster, A. S., and Noordhoek, J. (1989) *Arch. Biochem. Biophys.* **273**, 215–222
64. Saxena, K., Henry, T. R., Solem, L. E., and Wallace, K. B. (1995) *Arch. Biochem. Biophys.* **317**, 79–84
65. Mirabelli, F., Salis, A., Marinoni, V., Finardi, G., Bellomo, G., Thor, H., and Orrenius, S. (1988) *Arch. Biochem. Biophys.* **264**, 261–269
66. Frei, B., Winterhalter, K. H., and Richter, C. (1986) *Biochemistry* **25**, 4438–4443
67. Redegeld, F. A., Moison, R. M., Barentsen, H. M., Koster, A. S., and Noordhoek, J. (1990) *Arch. Biochem. Biophys.* **280**, 130–136
68. Bellomo, G., Jewell, S. A., and Orrenius, S. (1982) *J. Biol. Chem.* **257**, 11558–11562
69. Akerman, K. E. (1978) *Biochim. Biophys. Acta* **502**, 359–366
70. Budd, S. L., Tenneti, L., Lishnak, T., and Lipton, S. A. (2000) *Proc. Natl. Acad. Sci. U. S. A.* **97**, 6161–6166

β-Lapachone-Induced Apoptosis in Human Prostate Cancer Cells: Involvement of NQO1/xip3

Sarah M. Planchon,* John J. Pink,* Colleen Tagliarino,* William G. Bornmann,†
Marie E. Varnes,* and David A. Boothman*,[1]

*Department of Radiation Oncology and Department of Pharmacology, Ireland Comprehensive Cancer Center, Laboratory of Molecular
Stress Responses, Case Western Reserve University, 10900 Euclid Avenue, Cleveland, Ohio 44106-4942; and †Preparative Synthesis
Core Facility, Memorial Sloan-Kettering Cancer Center, New York, New York 10021

β-Lapachone (β-lap) induces apoptosis in various cancer cells, and its intracellular target has recently been elucidated in breast cancer cells. Here we show that NAD(P)H:quinone oxidoreductase (NQO1/xip3) expression in human prostate cancer cells is a key determinant for apoptosis and lethality after β-lap exposures. β-Lap-treated, NQO1-deficient LNCaP cells were significantly more resistant to apoptosis than NQO1-expressing DU-145 or PC-3 cells after drug exposures. Formation of an atypical 60-kDa PARP cleavage fragment in DU-145 or PC-3 cells was observed after 10 μM β-lap treatment and correlated with apoptosis. In contrast, LNCaP cells required 25 μM β-lap to induce similar responses. Atypical PARP cleavage in β-lap-treated cells was not affected by 100 μM zVAD-fmk; however, coadministration of dicoumarol, a specific inhibitor of NQO1, reduced β-lap-mediated cytotoxicity, apoptosis, and atypical PARP cleavage in NQO1-expressing cells. Dicoumarol did not affect the more β-lap-resistant LNCaP cells. Stable transfection of LNCaP cells with NQO1 increased their sensitivity to β-lap, enhancing apoptosis compared to parental LNCaP cells or vector-alone transfectants. Dicoumarol increased survival of β-lap-treated NQO1-expressing LNCaP transfectants. NQO1 activity, therefore, is a key determinant of β-lap-mediated apoptosis and cytotoxicity in prostate cancer cells. © 2001 Academic Press

Key Words: β-lapachone; apoptosis; NQO1; X-ray-inducible protein 3 (xip3); prostate cancer; atypical PARP cleavage; p53 cleavage.

INTRODUCTION

β-Lapachone (β-lap, 3,4-dihydro-2,2-dimethyl-2H-naphtho[1,2-b]pyran-5,6-dione)[2] is a naturally occur-

ring *o*-naphthoquinone present in the bark of the Lapacho tree (*Tabebuia avellanedae*) native to South America. The purified drug has anti-trypanosomal, -fungal, -tumor, and -HIV properties and induces apoptosis in a variety of cell types [1]. The mechanism of action and intracellular target(s) of the compound have, however, remained elusive and prevented the preclinical development of this drug for use as an antitumor or antiviral agent. Using a series of *in vitro* assays, proposed mechanisms of action for this drug have included: (a) activation of topoisomerase (Topo) I [2]; (b) induction of apoptosis [3]; (c) inhibition of Topo I [1, 4, 5]; (d) inhibition of Topo II-α [6]; and (e) suppression of NF-κB activation [7]. β-lap can induce apoptosis in several cell systems, including leukemic (HL-60), prostate, and breast cancer cell lines [1, 3, 5]. The apoptotic response caused by β-lap was independent of both p53 status and androgen dependence in human prostate cancer cell lines [1]. Camptothecin (CPT), a Topo I poison, induces classical caspase-mediated apoptotic responses [3].

We recently showed that the enzymatic activity of NQO1 in breast cancer cell lines is a key determinant for β-lap-mediated cytotoxicity [8]. NAD(P)H:quinone reductase (NQO1, DT diaphorase, xip3, EC 1.6.99.2) is a flavoenzyme that catalyzes the two-electron reduction of quinones into their hydroquinone form, bypassing the often mutagenic semiquinone intermediate and the formation of free radicals [9, 10]. NQO1 detoxifies many quinones [e.g., menadione] [11, 12] and bioactivates other compounds, such as mitomycin C, streptonigrin, or E09 [13–16]. NQO1 gene expression is widespread, with detectable levels in human heart, brain, placenta, lung, skeletal muscle, kidney, and pancreatic tissue, and low or absent in human liver [17]. More

---

importantly, NQO1 levels have been shown to be significantly up-regulated (5- to 20-fold above adjacent normal tissue) in several forms of cancer, including breast and non-small-cell lung tumors [17–19]. Such elevations in certain cancers make NQO1 a potential target for the development of tumor-directed therapies involving β-lap or its derivatives [8, 20].

Apoptosis is a genetically programmed form of cell death, the initiation and execution of which are thought to be the basis of lethality caused by many chemotherapeutic agents [21–23]. Cells undergoing apoptosis exhibit characteristic changes, including cell shrinkage, membrane blebbing, chromatin condensation, internucleosomal DNA cleavage, and cleavage of specific intracellular substrates involved in cell structure, DNA repair [e.g., poly(ADP-ribosyl) polymerase (PARP)], and general homeostasis. These intracellular alterations are often the result of activation of a family of apoptotic proteases, including caspases [24–28] and/or calpains [29–32].

Caspases are activated by multiple signaling pathways during apoptosis and typically result in the cleavage of PARP; the full-length 113-kDa polypeptide is cleaved to diagnostic 89-kDa and 24-kDa proteins [33]. In HL-60 cells, CPT induced an apoptotic pathway that included activation of the caspases, leading to classical PARP cleavage [20, 34]. HL-60 cells treated with β-lap also activated the caspases [20]. However, a different cell death response appeared to be stimulated by the drug in various human breast cancer cells [3, 35]. In many breast cancer (especially MCF-7:WS8) cells, an atypical PARP fragmentation *in vivo* was noted at times and doses correlating with apoptosis. Apoptotic responses induced by β-lap were monitored by DNA fragmentation (cells staining positive in a TUNEL assay), dephosphorylation of pRb, lamin B cleavage, cleavage of p53, and an atypical cleavage of PARP, leading to an ~60-kDa fragment. β-Lap-mediated apoptosis was thought to involve the activation of a calpain-like protease due to the specific calcium-dependent cleavage of both p53 and PARP [8]. Recently, our laboratory discovered that NQO1 was the key determinant of β-lap cytotoxicity in human breast cancer cell lines [8].

In this report, we demonstrate that NQO1 is also a key determinant of β-lap-induced apoptosis and lethality in human prostate cancer cell lines, suggesting a general mechanism of activation for the compound. Variations in NQO1 activity dramatically affected the sensitivity of human prostate cancer cell lines to β-lap, as determined by comparing various cell lines expressing different levels of the enzyme, by transfection of NQO1 expression vectors into enzyme-deficient cells, and/or by the use of the NQO1 inhibitor, dicoumarol. Coadministration of dicoumarol abrogated β-lap-mediated cytotoxicity and downstream apoptotic end points

in NQO1-expressing, but not in NQO1-deficient, human prostate cancer cell lines. Transfection of NQO1-deficient LNCaP cells with NQO1 significantly enhanced sensitivity (apoptosis, substrate proteolysis, and lethality) to β-lap, which was subsequently blocked by dicoumarol coadministration.

MATERIALS AND METHODS

Compounds and drug preparations. β-Lap was synthesized and dissolved in DMSO as described [1]. CPT and dicoumarol were obtained from Sigma Chemical Co. (St. Louis, MO) and prepared in DMSO or water, respectively [3]. zVAD-fmk and zDEVD-fmk were obtained from Enzyme Systems Products (Dublin, CA). Control treatments containing an equivalent percentage of DMSO were included as described [1–3]. The highest DMSO concentration used was 0.2%, which did not affect survival, cell growth, or apoptosis in various human breast or prostate cancer cells examined [1–3].

Cell culture conditions. PC-3, DU-145, and LNCaP human prostate cancer cells were obtained from Dr. George Wilding (University of Wisconsin–Madison) and grown in Dulbecco's minimal essential medium (DMEM) with 5% FBS at 37°C in a humidified 5% CO_2–95% air atmosphere as described [36–38]. Tests for mycoplasma infection, using the Gen-Probe Rapid Detection Kit (Fisher Scientific, Pittsburgh, PA), were performed quarterly and all cell lines were negative.

Drug treatments. For all experiments, cells were plated, allowed at least 24 h to initiate log-phase growth, and then exposed to β-lap or CPT at indicated doses for 4 h. After exposure, drug-containing media were removed and replaced with complete media. Dicoumarol was administered (50 μM) concomitantly with β-lap or CPT for 4 h as described above. For zVAD-fmk exposures, cells were pretreated with 100 μM zVAD-fmk for 30 min or treated with media alone. β-Lap or CPT was then coadministered in the presence or absence of zVAD-fmk for 4 h. All drug-containing media were then removed and replaced with media containing 100 μM zVAD-fmk alone or with fresh, non-drug-containing media.

Stable transfection of LNCaP cells with NQO1. Log-phase LNCaP cells were seeded onto 6-well dishes at 2×10^5 cells/well and allowed to attach overnight. The following day, 1.0 μg of BE8 plasmid DNA, containing human NQO1 cDNA under the control of the CMV promoter in the pcDNA3 constitutive expression vector [39], was added into each of three wells using standard calcium phosphate transfection methodology [40]. After 2 days of growth without selection, cells were exposed to 350 μg/ml geneticin (G418, GIBCO BRL, Gaithersburg, MD). A stable, pooled population was established after approximately 3 weeks of growth in media containing 350 μg/ml G418. Clonal transfectants were finally derived from the pooled population by limiting dilution cloning. Isolated transfectants were then analyzed for NQO1 expression and enzymatic activity as described below and under Results (Table 1).

Colony-forming ability assays. Anchorage-dependent colony-forming ability (CFA) assays were performed [1, 41]. For CFA assays, cells were seeded at 1–2000 viable cells per dish in 35 mm²-tissue culture plates (with grids) and incubated overnight. Plated cells were then treated with equal volumes of media containing β-lap at various concentrations for 4 h. Control cells were treated with DMSO equivalent to the highest dose of β-lap used. β-Lap exposures in the presence or absence of 50 μM dicoumarol were performed as indicated above and under Results. Colonies were allowed to grow for 10–14 days, with one change of medium at day seven. Plates were stained with 1.0% crystal violet in 20% EtOH and destained with water, and colonies of >50 normal-appearing cells were counted [1, 41].

TUNEL assays. Flow cytometric TUNEL analyses were performed to measure DNA fragmentation, sub-G_0/G_1 cell populations, and changes in cell cycle distribution following various drug treatments [1, 35]. TUNEL assays were performed using APO-DIRECT as described by the manufacturer (Pharmingen, San Diego, CA). Samples were analyzed in an EPICS Elite ESP flow cytometer using an air-cooled argon laser at 488 nm, 15 mW (Beckman Coulter Electronics, Miami, FL). Propidium iodide was read with a 640-nm long-pass optical filter. FITC was read with a 525-nm band-pass filter. TUNEL analyses were performed using the Elite acquisition software provided with the instrument. Sub-G_0/G_1 data were analyzed using ModFit (Verity Software House, Inc., Topsham, ME) [1, 3, 35]. Results presented are means ± SD for at least three separate experiments, repeated in duplicate.

Western immunoblot analyses. Control or treated human prostate cancer cells were examined for changes in PARP, p53, and lamin B and for levels of NQO1. Actin was used as a loading control. Briefly, control or treated cells were washed in ice-cold PBS and lysed in loading buffer [62.5 mM Tris, pH 6.8, 6M urea, 10% glycerol, 2% SDS, 0.003% bromophenol blue, 5% 2-mercaptoethanol (freshly added)]. Samples were sonicated with a Fisher Scientific Sonic Dismembrator (model 550) fitted with a microtip probe and stored at −20°C for later analyses as described [35]. Equivalent amounts of protein were incubated at 65°C for 15 min and polypeptides were separated by SDS–PAGE. Separated proteins were then transferred to immobilon-P membranes (Millipore, Danvers, MA), and equivalent protein loading was confirmed by Ponceau S staining [0.2% Ponceau S (w/v) in 3% trichloroacetic acid (w/v) and 3% sulfosalicylic acid (w/v)] (Sigma) using standard techniques. Western immunoblots were incubated with PBS containing 0.2% Tween 20 and 10% FBS for 1 h to prevent nonspecific binding. Membranes were then incubated overnight with primary antibodies diluted in the same blocking buffer at 4°C. Primary antibodies included separate, and sometimes in combination, exposures to anti-PARP C2-10 (Enzyme Systems Products), anti-p53 DO-1 (Santa Cruz Biotechnology, Santa Cruz, CA), anti-lamin B (Calbiochem, San Diego, CA), and anti-actin (Amersham Pharmacia Biotech, Piscataway, NJ). An NQO1 antibody was contained in medium from a mouse hybridoma, clone A180, and used according to previously published procedures [42]. Membranes were washed in PBS containing 0.2% Tween and then incubated with horseradish peroxidase-conjugated secondary antibody (Santa Cruz Biotechnology) for 1 h. Western immunoblots were then washed in PBS containing 0.2% Tween, developed with enhanced chemiluminescence (ECL) substrate (Amersham, Arlington Heights, IL), and exposed to Fuji X-ray film. All Western immunoblots shown below are representative of experiments repeated at least three times.

Preparation of S9 supernatants. Cellular extracts for enzyme assays were prepared from cells in mid- to late-log-phase growth. Cells were harvested by trypsinization (0.25% trypsin and 1 mM EDTA), washed twice in ice-cold, phenol red-free Hank's balanced salt solution, and resuspended in a small volume of PBS, pH 7.2, containing 10 $\mu g/\mu l$ aprotinin. Cell suspensions were sonicated four times on ice using 10-s pulses, then centrifuged at 14,000g for 20 min. S9 supernatants were aliquoted into microfuge tubes and stored at −80°C for later use as described below.

NQO1, cytochrome b5 reductase, and cytochrome P450 reductase enzyme assays. Three general reductase enzyme assays were completed as described [43–46]. Enzyme reactions contained 77 μM cytochrome c (practical grade, Sigma) and 0.14% bovine serum albumin in Tris–HCl buffer (50 mM, pH 7.5). NQO1 activity was measured using NADH (200 μM) as the immediate electron donor and menadione (10 μM) as the intermediate electron acceptor. Each assay was repeated in the presence of 10 μM dicoumarol, and the activity attributed to NQO1 was that inhibited by dicoumarol [44, 47]. NADH:cytochrome b5 reductase (b5R) was measured using NADH (200 μM) as the electron donor, and NADH:cytochrome P-450

TABLE 1

NQO1, Cytochrome b5R, and Cytochrome P450 Reductase Enzyme Activity Levels in Prostate Cancer Cell Lines

Cell line	NQO1	b5R	P450
LNCaP	9.0 ± 2.4	17 ± 3.2	7.0 ± 2.3
DU-145	500 ± 48	39 ± 3.3	6.8 ± 0.6
PC-3	740 ± 100	38 ± 5.1	7.9 ± 1.1
LN-pcDNA3 Clone 5	3.9 ± 0.5	22 ± 1.8	10 ± 2.8
LN-NQ Clone 1	140 ± 22	15 ± 1.9	9.5 ± 0.5
LN-NQ Clone 2	250 ± 61	34 ± 5.4	9.3 ± 4.5
LN-NQ Clone 3	290 ± 30	26 ± 1.5	9.8 ± 1.9
LN-NQ Clone 4	270 ± 30	22 ± 6.3	5.0 ± 1.0
LN-NQ Clone 10	210 ± 24	31 ± 3.3	9.7 ± 2.8

Note. Enzyme levels were measured in S9 supernatent whole cell lysates as described under Materials and Methods. Activities are reported as nmol cytochrome c reduced/min/mg protein.

reductase (P450r) was measured using NADPH (200 μM) as the electron donor [54] in a Beckman DU 640 spectrophotometer (Beckman Instruments, Fullerton, CA). Reactions were performed at 37°C and were initiated by addition of S9 supernatants. Varying amounts (10 to 40 μl) of S9 supernatants were used to ensure linearity of enzyme rates with protein concentration. Enzyme activities were calculated as nmol cytochrome c reduced/min/mg protein, based on the initial rate of change in OD at 550 nm. An extinction coefficient of 21.1 mM/cm was used for cytochrome c.

RESULTS

Expression of NQO1 and p53 in human prostate cancer cells. In examining the apoptotic responses of human prostate cancer cells to β-lap, we noted that LNCaP was resistant to this drug. Since we previously published data that suggested NQO1 expression/activity was a critical determinant in the cytotoxicity of this drug [8], we examined LNCaP, PC-3, and DU-145 cells for expression of this two-electron reductase. DU-145 and PC-3 cells expressed NQO1 protein (Fig. 1) and demonstrated dicoumarol-sensitive enzyme activity (Table 1); enzymatic activity was measured by menadione-mediated, NQO1 reduction of cytochrome c as described under Materials and Methods [43]. In contrast, LNCaP cells did not express NQO1 protein or enzyme activity (Fig. 1 and Table 1).

Dicoumarol enhanced the survival of DU-145 or PC-3, but not LNCaP, cells following β-lap exposure. Since dicoumarol is a relatively specific inhibitor of NQO1, its effects on the survival of β-lap-treated prostate cancer cells were determined. Dicoumarol significantly enhanced the survival of β-lap-treated DU-145 or PC-3 cells (Fig. 2). The LD_{90} values for DU-145 and PC-3 cells were increased (i.e., the drug was less toxic) by three- and two-fold, respectively, compared to β-lap alone. For example, over 95% lethality was noted in DU-145 cells treated with 4.0 μM β-lap, whereas the same β-lap exposure was ineffective (>95% survival)
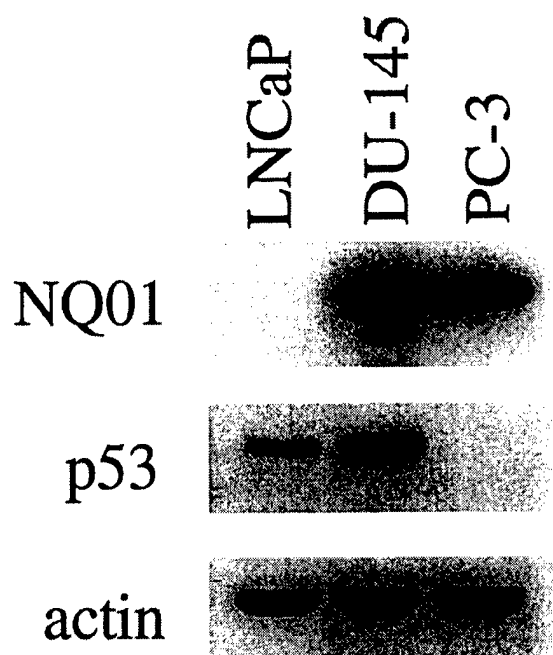
FIG. 1. NQO1 and p53 status of three human prostate cancer cell lines. Western immunoblot analyses of untreated lysates from three human prostate cancer cell lines, DU-145, PC-3, and LNCaP, were performed as described under Materials and Methods. Accurate loading was determined by monitoring actin levels.

when 50 μM dicoumarol was coadministered. In contrast, dicoumarol had no influence on the survival of β-lap-treated LNCaP cells, which also exhibited more intrinsic resistance to β-lap-mediated lethality (LD_{90}, 8.0 μM; LD_{99}, 12 μM) compared to DU-145 (LD_{90}, 3.5 μM; LD_{99}, 5.0 μM) or PC-3 (LD_{90}, 5.0 μM; LD_{99}, 7.5 μM) cells. β-Lap-treated LNCaP cells also exhibited three-fold less apoptosis than either DU-145 or PC-3 cells when exposed to equitoxic concentrations [1]. In contrast, dicoumarol coadministration did not significantly affect the survival of LNCaP, DU-145, or PC-3 cells following CPT exposures (Fig. 2).

Dicoumarol blocked morphologic changes and apoptosis of DU-145 cells after β-lap treatment. In human breast cancer cells, β-lap induced morphologic changes indicative of apoptosis [3]. Similar alterations in morphology, such as chromatin condensation, cell shrinkage, and detachment occurred in DU-145 or PC-3 cells following 4-h β-lap exposures (shown are DU-145 cells, Fig. 3A). Addition of 50 μM dicoumarol significantly blocked β-lap-induced morphologic changes (Fig. 3A), and cells grew normally, consistent with enhanced survival as measured using CFA assays (Fig. 2).

We previously demonstrated the formation of an apoptotic sub-G_0/G_1 peak, representing apoptotic cells
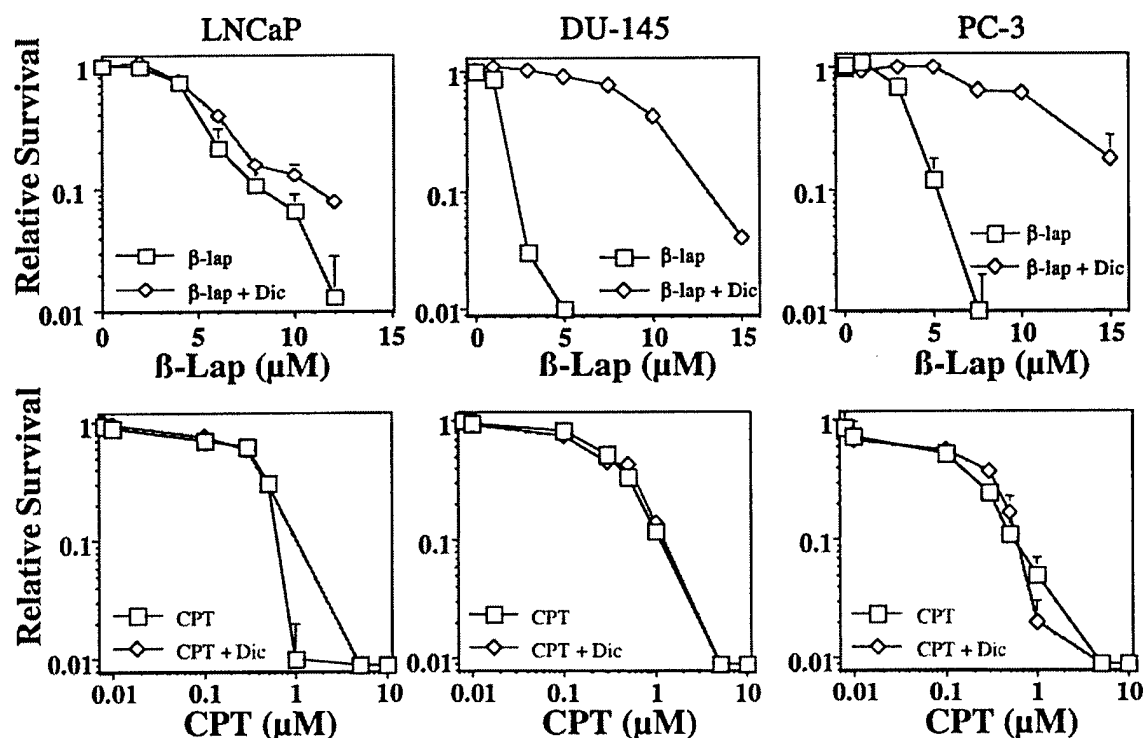

FIG. 2. Dicoumarol protects DU-145 and PC-3, but not LNCaP, human prostate cancer epithelial cell lines from β-lap-induced cytotoxicity. The survival of DU-145, PC-3, and LNCaP human prostate cancer cell lines following β-lap treatment, with or without dicoumarol coadministration, was determined by colony-forming-ability assays as described under Materials and Methods. β-Lap or CPT, with or without 50 μM dicoumarol cotreatments, was given as 4-h pulse treatments as described under Materials and Methods. Shown are the results (means ± SD) of three experiments repeated in duplicate.
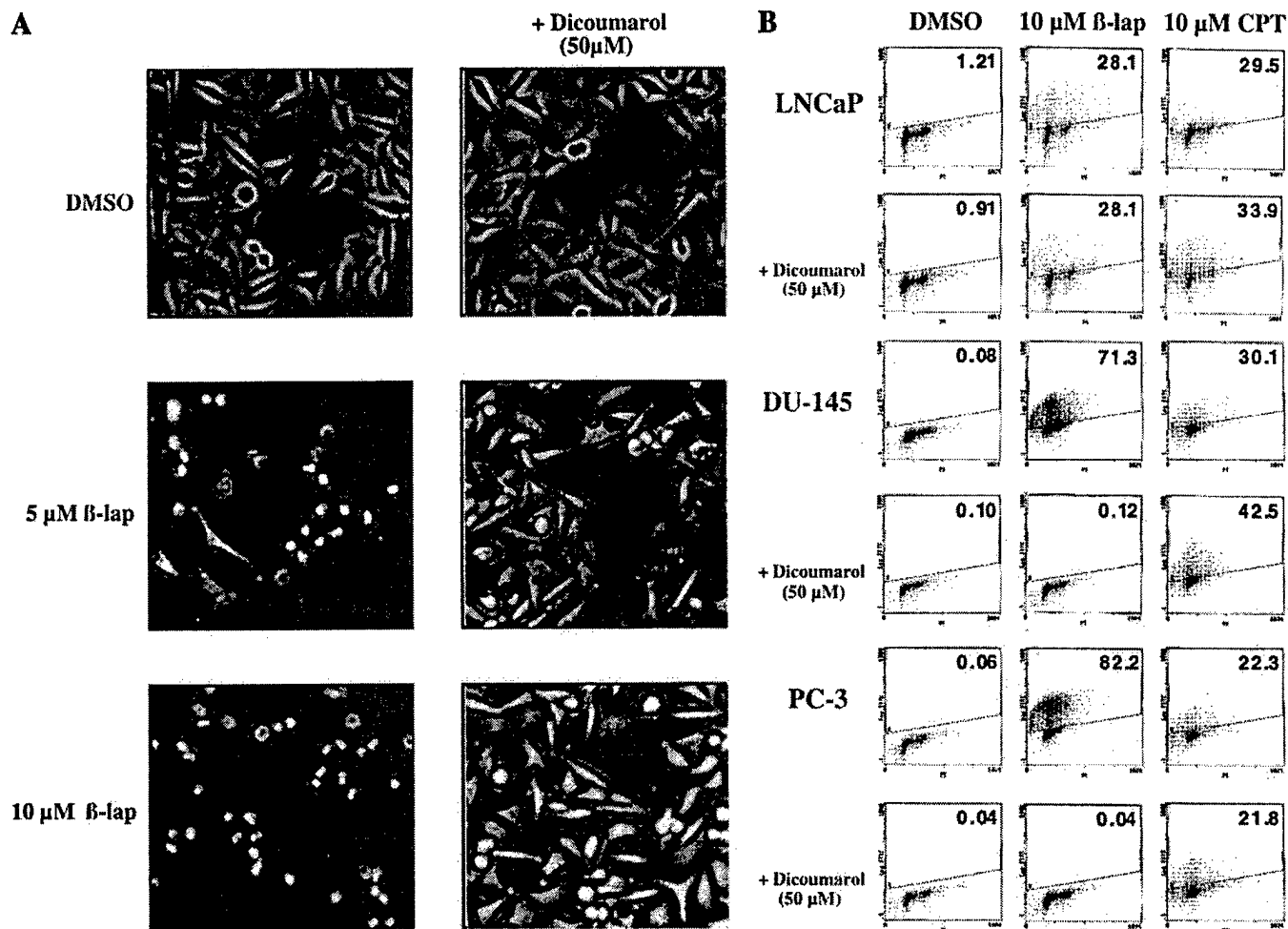
FIG. 3. (A) Dicoumarol blocks morphologic changes in DU-145 cells after β-lap treatment. DU-145 cells were treated with 5 μM or 10 μM β-lap, with or without 50 μM dicoumarol, for 4 h. At 24 h posttreatment, phase-contrast photomicrographs were taken of treated or control cells. Shown are representative photos of experiments repeated three or more times. Magnification, 100×. (B) Dicoumarol prevents apoptosis induced in human prostate cancer cells following β-lap, but not CPT. TUNEL assays to monitor apoptosis in β-lap- or CPT-treated human prostate cancer cells, with or without 50 μM dicoumarol coadministration, were performed 48 h following 4-h drug treatments. The percentage of cells that stained positive by TUNEL assay appears in the top right corner of each panel.

with fractional DNA content, in human prostate or breast cancer cell lines following β-lap treatment. DU-145 or PC-3 cells showed a prominent sub-G_0/G_1 population of cells. In contrast, NQO1-deficient LNCaP cells showed significantly lower levels of sub-G_0/G_1 cells [1]. To further characterize cell death responses in human prostate cancer cell lines after exposure to β-lap or CPT, TUNEL assays were performed to monitor apoptotic-related DNA fragmentation, with or without dicoumarol (Fig. 3B). DU-145 or PC-3 cells were positively stained by TUNEL (71.3 and 82.2%, respectively) after β-lap treatment, and these responses were abrogated by dicoumarol cotreatments. In contrast, β-lap-treated LNCaP cells exhibited a much lower percentage of apoptotic cells (28.1%), consistent with prior data [1]. Coadministration of dicoumarol did not affect β-lap-mediated responses in these

cells. Treatment of each cell line with CPT resulted in only modest apoptosis (i.e., 22–43% apoptotic cells), as previously described [3]. Predictably, CPT-induced apoptosis was not affected by dicoumarol cotreatments (Fig. 3B).

Apoptotic substrate cleavage events in human prostate cancer cells after β-lap exposure. Human prostate cancer cell lines treated with β-lap exhibited the formation of an atypical ~60-kDa PARP polypeptide (Fig. 4A, open arrow), in contrast to classical, CPT-induced, caspase-mediated, 89-kDa PARP cleavage (Fig. 4A, closed arrow). Atypical 60-kDa PARP fragmentation was apparent in DU-145 and PC-3 cells treated with 10 μM β-lap and correlated well with apoptosis (Fig. 3B) [8, 35]. Furthermore, formation of β-lap-induced PARP cleavage was completely blocked by coadministration

of 50 μM dicoumarol (Fig. 4A), consistent with this NQO1 inhibitor's ability to prevent β-lap-mediated apoptosis (Fig. 3B) and lethality (Fig. 2). β-Lap-resistant LNCaP cells required a greater concentration of β-lap (25 μM) to induce an identical atypical PARP cleavage fragment. As with survival responses, coadministration of dicoumarol with β-lap did not affect the formation of the 60-kDa PARP cleavage fragment in β-lap-treated LNCaP cells (Fig. 4A). In contrast, all three human prostate cancer cell lines exhibited the formation of an 89-kDa PARP cleavage fragment (Fig. 4A, closed arrow) after 10 μM CPT exposures, correlating with the level of apoptosis observed (Fig. 3B). Dicoumarol coadministration had no effect on classical, caspase-mediated PARP cleavage after CPT exposures.

Global caspase inhibitors, such as zVAD-fmk, can inhibit the activation of many of the caspases and their downstream events (i.e., substrate proteolysis) [5, 26]. Addition of 100 μM zVAD-fmk completely abrogated the formation of CPT-induced PARP cleavage (89 kDa), (Fig. 4B). In contrast, atypical PARP cleavage noted in β-lap-treated DU-145 cells (open arrow) was not affected by 100 μM zVAD-fmk, suggesting either that β-lap induces a non-caspase-mediated pathway or that zVAD-fmk cannot inhibit this particular caspase-mediated pathway (Fig. 4B).

Cleavage of lamin B (60-kDa full-length protein) to a characteristic 46-kDa polypeptide, typically by caspase 6, is believed to aid in the breakdown of the architecture necessary for apoptosis-related nuclear condensation and membrane blebbing [48–50]. Cleavage of lamin B in β-lap-treated MCF-7:WS8 cells was noted [3]. In DU-145 cells, β-lap but not CPT treatment resulted in lamin B cleavage, possibly due to the relatively poor apoptotic responses induced by CPT compared to those induced by β-lap. Interestingly, 100 μM zVAD-fmk, the pan-caspase inhibitor, did not inhibit β-lap-mediated cleavage of lamin B (Fig. 4B). These data are consistent with prior data from our laboratory that β-lap can stimulate a non-caspase-mediated, cysteine protease-directed apoptotic pathway in certain human cancer cells [35].

We previously showed that p53 was not necessary for β-lap-induced apoptosis [1]. In fact, we reported that the level of p53 *decreased* following treatment of wild-type p53-expressing MCF-7 breast cancer cells following 4–10 μM β-lap [3]. In mutant p53-expressing DU-145 cells, β-lap treatment resulted in the formation of two cleavage fragments (40 kDa and ~20 kDa) that were not inhibited by 100 μM zVAD-fmk coadministration (Fig. 4B). A similar cleavage of p53 was described during calpain-mediated apoptosis, and this protease may be involved in β-lap-mediated cell death responses [35]. Treatment of DU-145 cells with CPT did not result in any changes in the level or cleavage of p53, even

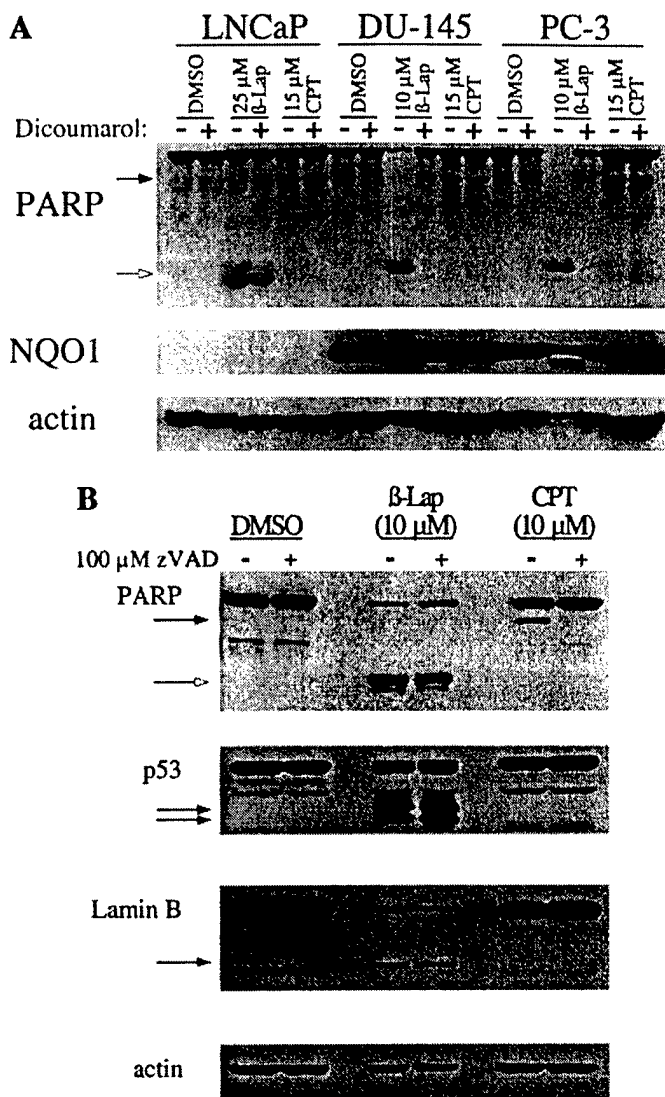FIG. 4. (A) PARP cleavage in human prostate cancer cells following β-lap or CPT exposure. Human prostate cancer cell lines were treated for 4 h with β-lap (10 or 25 μM) or CPT (15 μM), with or without 50 μM dicoumarol. Cells were harvested for analyses 24 h posttreatment and analyzed for specific changes in protein cleavage events by Western blot analyses. Closed arrow; typical 89-kDa PARP cleavage fragment. Open arrow, atypical 60-kDa PARP cleavage fragment. (B) zVAD-fmk blocks CPT-, but not β-lap-, induced apoptotic proteolytic substrate cleavage in DU-145 cells. DU-145 human prostate cancer cells were treated with either 10 μM β-lap or 10 μM CPT, with or without 100 μM zVAD-fmk, for 4 h and specific protein cleavage events were monitored by Western immunoblot analyses. zVAD-fmk treatment began 1 h prior to β-lap addition; treatment was continued throughout the β-lap treatment, and cells were harvest as described under Materials and Methods. PARP: full-length polypeptide, 113 kDa; typical PARP cleavage fragment (closed arrow), 89 kDa; atypical PARP cleavage fragment (open arrow), ~60 kDa. p53: full-length polypeptide, 53 kDa; p53 cleavage fragment, ~40 kDa. Lamin B: full-length polypeptide, 68 kDa; lamin B cleavage fragment, 45 kDa.

though 20% of the cells were apoptotic; DU-145 cells express stable, high levels of mutant p53 protein that are not stabilized by CPT-mediated damage.

Stable transfection of LNCaP cells with NQO1. In order to further characterize the role of NQO1 in β-lap-mediated apoptosis, LNCaP cells were transfected with either pcDNA3 empty vector or pcDNA3 containing full-length NQO1 cDNA, in which expression of this two-electron reductase was controlled by the CMV promoter. Five clonal cell lines containing NQO1 (LN-NQ Clones 1–4, 10) and one vector-alone control (LN-pcDNA3) were isolated. All five NQO1-containing cell lines demonstrated both enzyme activity (15- to 30-fold above nontransfected levels, Table 1) and protein expression (Fig. 7). LNCaP transfectants containing pcDNA3 vector alone exhibited neither NQO1 enzyme activity nor protein expression, similar to nontransfected LNCaP parental cells (Table 1, Fig. 7).

Transfection of NQO1 sensitized human LNCaP prostate cancer cells to β-lap. In clonogenic assays, NQO1-deficient parental LNCaP cells showed moderate resistance to β-lap, relative to DU-145 and PC-3 cells, which express high levels of the enzyme (Fig. 2). Similarly, NQO1-containing LNCaP clones demonstrated significantly increased sensitivity to β-lap relative to NQO1-deficient LNCaP cells containing pcDNA3 vector alone (Fig. 5A). As previously observed with NQO1-expressing DU-145 or PC-3 cells, coadministration of dicoumarol blocked β-lap-mediated cytotoxicity. This resulted in a relatively resistant phenotype, similar to that of NQO1-deficient, pcDNA3 vector-alone, control LNCaP cells. Dicoumarol coadministration had no effect on the sensitivity of NQO1-deficient, LNCaP cells (containing pcDNA3 vector alone) to β-lap treatment (Fig. 5A).

Menadione is detoxified by NQO1 and is thus toxic to cells in the absence of NQO1 activity. In contrast to β-lap-mediated toxicity, NQO1-deficient LNCaP parental or vector-alone transfectants were more sensitive to menadione on an equimolar basis. NQO1-containing LN-NQ clone 10 cells were more resistant to menadione toxicity than NQO1-deficient LN-pcDNA3 cells (Fig. 5B). Thus, the toxicities of menadione and β-lap were reversed. Similar results were found with human NQO1-transfected (or vector-alone-transfected) MDA-MB-468 breast cancer cells treated with β-lap or menadione [8].

To determine whether LNCaP cells compensated for their NQO1 deficiency by increasing the activities of one-electron enzymes, levels of P450 reductase and cytochrome b5R were determined in the three parental cell lines, as well as in the six NQO1-expressing LNCaP clones. No significant differences in P450 reductase or b5R activities were noted (Table 1).

Transfection of LNCaP cells with NQO1 enhanced β-lap-induced apoptosis. Exposure of each NQO1-expressing LNCaP transfectant (LN-NQ Clones 1–4, 10) to 10 μM β-lap resulted in significantly increased apo-
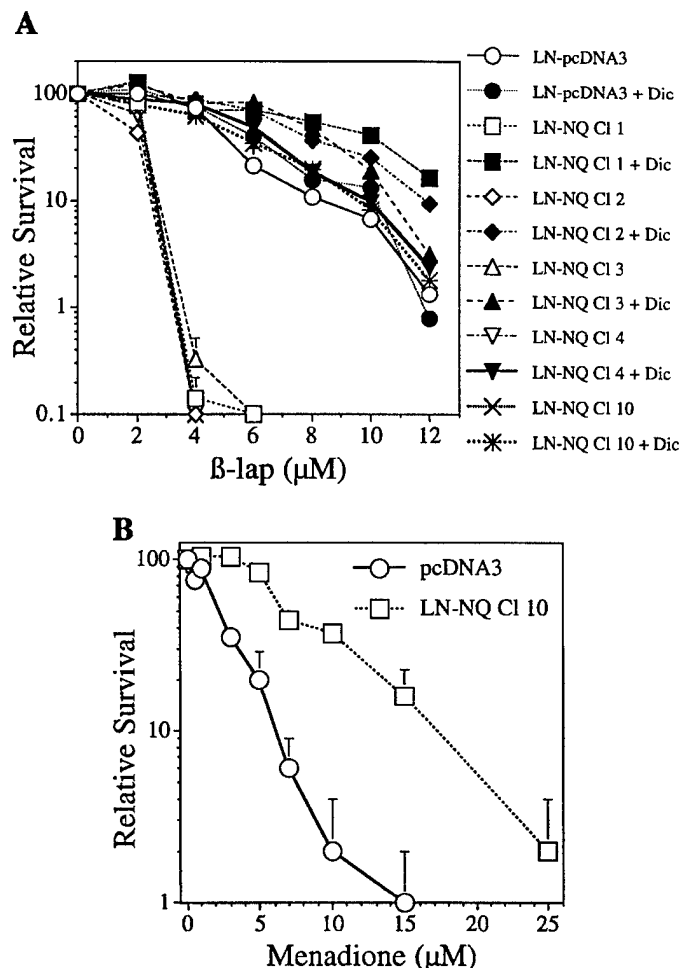
FIG. 5. (A) Transfection of LNCaP cells with NQO1 enhances β-lap-induced lethality. NQO1-containing (LN-NQ Clones 1–4, 10) and -deficient (LN-pcDNA3) LNCaP clonal cell lines were treated with 4-h pulses of various doses of β-lap, with or without concomitant 50 μM dicoumarol coadministration. Survival was then determined by colony-forming-ability assays as described under Materials and Methods. Experiments were performed three times, each in triplicate. Symbols represent means ± SD. Open symbols, β-lap alone. Closed symbols, β-lap with 50 μM dicoumarol coadministration. (B) Transfection of LNCaP cells with NQO1 decreases menadione-induced lethality. One NQO1-transfected LNCaP clonal cell line (LN-NQ Cl 10) and the LNCaP vector-alone clonal isolate (LN-pcDNA3) were treated with 4-h pulses of various doses of menadione, and survival was determined by CFA assays as described under Materials and Methods. Experiments were performed three times, each in triplicate. Symbols represent means ± SD.

ptosis (i.e., 80–90%) compared to that of control LNCaP transfectants containing pcDNA3 vector alone (5%) (Fig. 6). As expected, NQO1-mediated, β-lap-stimulated apoptosis in LN-NQ Clone 1–4 and 10 cell lines were prevented by 50 μM dicoumarol.

Expression of NQO1 in LNCaP cells enhanced atypical PARP cleavage in response to β-lap exposure. Parental LNCaP cells produced an apoptosis-related, atypical cleavage of PARP (formation of a 60-kDa
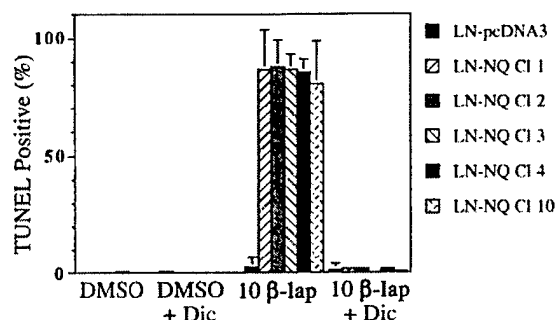
FIG. 6. Stable transfection of LNCaP cells with NQO1 enhances β-lap-induced apoptosis. Stably transfected LNCaP clonal cell lines containing NQO1 or vector alone (from Fig. 5A) were treated for 4 h with various concentrations of β-lap, with or without 50 μM dicoumarol, as described under Materials and Methods. Forty-eight hours posttreatment, cells were monitored for apoptosis-related DNA fragmentation using TUNEL assays. Symbols represent means ± SD of experiments performed three or more times, each in triplicate. LNCaP isolated clonal cell lines examined were pcDNA3, LNCaP stably transfected with vector alone; LN-NQ Cl 1–4 and 10, five separate LNCaP cell lines stably transfected with CMV-controlled NQO1 cDNA, Clones 1–4 and 10.

PARP polypeptide) following 25 μM β-lap, a concentration nearly five times higher than the LD_{50} for the drug (see Figs. 2 and 4A). In contrast, atypical PARP cleavage was apparent in PC-3 or DU-145 cells after 10 μM β-lap, at or near the drug's LD_{90} for these cells. In general, atypical PARP cleavage correlated well with the sensitivities (apoptosis) of each prostate cancer cell line to β-lap exposure (Figs. 2 and 4A), similar to that observed in human breast carcinoma epithelial cells [35]. Empty vector (LN-pcDNA3)- or NQO1-transfected LNCaP (LN-NQ Clones 1–4 and 10) cells were also examined for PARP cleavage following β-lap treatments. Atypical 60-kDa PARP fragmentation was observed in each NQO1-expressing clone following 10 μM β-lap, whereas the parental and vector-alone clones needed significantly greater doses of the compound (≥25 μM) to initiate detectable levels of PARP cleavage (Fig. 7). Thus, PARP fragmentation in NQO1-contain-

ing LNCaP cells, but not in LNCaP parental or empty vector transfectants, following β-lap treatment strongly correlated with overall apoptosis (Fig. 6) and lethality (Fig. 5A). In contrast, altered expression of NQO1 did not influence apoptotic reactions induced by CPT in any of the LNCaP cell lines examined above.

DISCUSSION

NQO1 may be a clinically exploitable target for therapy against certain tumors using β-lap or its derivatives. Our results demonstrate that NQO1 is a key intracellular determinant for β-lap toxicity in human prostate epithelial cancer cells, since dicoumarol prevented β-lap-mediated apoptosis and lethality in DU-145 and PC-3. In contrast, dicoumarol did not affect β-lap-induced apoptosis in NQO1-deficient LNCaP cells. Furthermore, reexpression of NQO1 in deficient LNCaP cells increased their sensitivity to β-lap-mediated apoptosis and lethality. These data suggest that NQO1 activity is a key determinant in β-lap-mediated cytotoxicity, a conclusion also made using human breast cancer cells [8]. Although many laboratories (including our own) have published data supporting other potential targets *in vitro*, including Topo I and Topo II-α, none of these previous studies demonstrated convincing data for an intracellular target for this drug.

We previously showed that β-lap induced a p53-independent apoptotic response in human prostate cancer cells [37]. We now demonstrate that these p53-independent apoptotic responses initiated by this drug are greatly enhanced by NQO1 expression (Fig. 7). Furthermore, we demonstrate that lethality caused by β-lap is opposite to that induced by menadione, wherein NQO1 overexpression increases β-lap lethality but decreases the cytotoxicity of menadione. Similar results were found in human breast cancer cells [8]. Collectively, our data strongly suggest that β-lap is bioactivated in cells expressing NQO1. The possibility of a bioactivated form of β-lap interacting with previ-
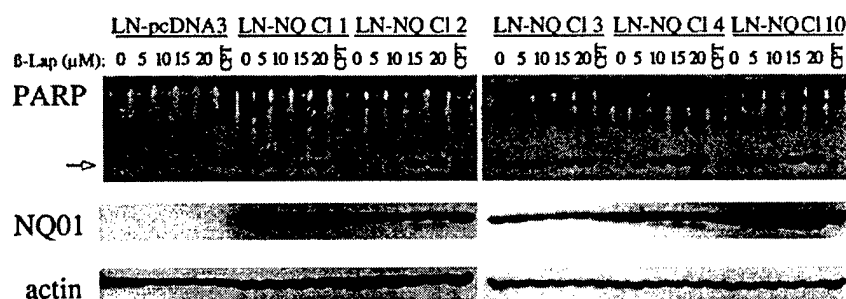

FIG. 7. β-Lap-induced atypical PARP cleavage is enhanced by NQO1 overexpression. NQO1-containing and -deficient LNCaP clonal cell lines (described in the legends to Figs. 5A and 6), were exposed to 4-h treatments with various doses of β-lap or 10 μM CPT. Cells were harvested for Western immunoblot analyses 24 h following drug removal, as previously described. Open arrow, atypical PARP cleavage fragment of ~60-kDa molecular weight by SDS–PAGE.

ously suggested *in vitro* targets, such as Topo I [2], is being explored.

β-Lap induces a unique apoptotic response in epithelial cancer cell lines, such as those of breast or prostate origin. β-Lap stimulates a novel cell death pathway that appears to be caspase-independent (Fig. 4B), calcium-dependent, and NQO1-mediated (Fig. 7) [8, 35]; dicoumarol prevents its activation and cells lacking NQO1 do not demonstrate p53 or PARP proteolytic cleavage events after physiological β-lap exposures (non-supra-lethal doses) (Fig. 4A) [8]. Treatment of human prostate cancer cells with β-lap induced the formation of an atypical PARP cleavage fragment, different from the classical 89-kDa fragment formed during caspase-mediated (via caspases 3, 6, and 7) apoptosis [34]. Production of this atypical 60-kDa PARP fragment correlated well with apoptosis and overall sensitivity of human prostate or breast epithelial cancer cells to β-lap (compare Figs. 5A and 7) [8]. As with β-lap-treated human breast cancer cells, although the overall number of adherent cells was markedly reduced, no evidence of cell *lysis* during β-lap-mediated apoptosis in DU-145 or PC-3 cells was noted, suggesting that cell death was not necrotic in nature. Addition of 100 μM zVAD-fmk, a widely used pan-caspase inhibitor, blocked caspase-induced typical PARP cleavage initiated in DU-145 cells by treatment with 10 μM CPT (Fig. 3B). However, the same concentration of zVAD-fmk had no effect on atypical PARP cleavage or cleavage of other β-lap-induced apoptotic substrates, such as lamin B or p53, in NQO1-expressing human prostate cancer cell lines. Thus, β-lap predominantly stimulates a non-caspase-mediated apoptotic response, which we theorize is directed by the activation of a calcium-dependent cysteine protease with properties similar to calpain [35].

LNCaP cells did exhibit toxicity following nonphysiologically high doses of β-lap, despite their deficiency in NQO1 expression. The observed apoptotic responses in LNCaP parental cells following supralethal doses of β-lap are probably attributed to the lower affinity reduction of this compound by one-electron reducing enzymes, such as p450 reductase, as well as other non-related enzymes (e.g., cytochrome b5 reductase). These enzymes may catalyze two-step, one-electron reductions of quinones (i.e., β-lap) in order to form the hydroquinone, whereas NQO1 mediates one higher affinity, two-electron reduction forming the same byproduct. As a result, a higher dose of β-lap was required (compared to NQO1-containing PC-3, DU-145, or LNCaP transfectants) for a similar apoptotic reaction. Expression of NQO1 in LNCaP cells, via stable transfection with CMV-controlled mammalian NQO1 expression vectors, *significantly* increased their sensitivity to β-lap, a sensitivity ablated by dicoumarol coadministration. These data indicate that while

NQO1 is not the only enzyme capable of activating or metabolizing β-lap, its ability far surpasses the efficiency of other reductases (or other as yet unidentified enzymes) in the cell to bioactivate the drug.

Current dogma states that all apoptotic pathways include caspase activation and that all caspase-independent mechanisms lead exclusively to necrosis. Our data strongly suggest that other non-caspase-mediated apoptotic pathways (e.g., mediated by calpain) are activated after certain drug treatments. Non-caspase-mediated apoptotic pathways have been described in several other cell systems [51–56]. Furthermore, we suggest that there is a spectrum of cell death responses, ranging from caspase-mediated apoptosis to cell lysis during necrosis (i.e., cell plasma membrane rupture and lysis, as observed after sodium azide exposure). Cells treated with β-lap exhibit many characteristics of cells undergoing apoptosis, including morphologic changes (Fig. 3A); chromatin condensation [63]; DNA ladder formation [14, 20]; generation of sub-G_0/G_1 apoptotic cells [1]; cells staining positive with the TUNEL assay, which monitors for endonuclease-specific DNA double-strand breaks (Fig. 3B, 6); specific dephosphorylation of pRb [3]; and specific intracellular cleavage of unique substrates (e.g., Topo I, Topo II, lamin B, and p53), while most other proteins (e.g., cyclins A, B, E and bcl-2) remained intact (Figs. 4A, 4B, and 7) [3, 35]. Yet, concrete evidence of caspase activation is lacking. It was previously reported that β-lap induced apoptosis in some cell systems and necrosis in others, although specific end points for necrosis were not examined [57]. β-Lap-treated breast or prostate cancer cells demonstrated extensive formation of apoptotic cells, as monitored by TUNEL assays, formation of sub-G_0/G_1 cells, morphology changes (i.e., condensed nuclei and rounded cells), and lamin B cleavage (Fig. 4B), as early as 4–8 h following β-lap treatment [8, 35]. Since DNA fragmentation may occur during late-stage necrosis [58], the early (4–8 h) appearance of cells staining positive using a TUNEL assay, concomitant with specific protein cleavage events (e.g., PARP and p53) following β-lap treatment, strongly suggests that an apoptotic, rather than necrotic, cell death mechanism was triggered by β-lap. β-Lap-treated NQO1-expressing cells demonstrate extensive nuclear condensation and unique intracellular substrate cleavages, and the cells detached in a rounded form (Fig. 3). Most importantly, β-lap-treated cells show no visible morphologic hallmarks of necrosis, such as extensive cell debris (Fig. 3). Few cells survive the treatment and the cytotoxic responses have a sharp dose-response curve in which apoptosis and loss of survival are directly correlated in NQO1-expressing cells. All NQO1-containing breast and prostate cancer cells examined thus far respond with identical apoptotic mechanisms to the drug. In contrast, all NQO1-deficient breast or prostate

cancer cells appear to be more resistant to β-lap, showing significantly less apoptosis [8].

We have previously shown that β-lap was a radiosensitizer (after IR exposure) of human cancer cells compared to normal cells [2]. Furthermore, those normal cells that did survive the IR exposures plus β-lap posttreatments demonstrated lower than basal levels of neoplastic transformants [59]. Our laboratory also demonstrated that NQO1 was an X-ray-inducible transcript (i.e., xip3) [10]. The discovery that NQO1 is a major determinant in the sensitivity of human prostate and breast epithelial cancer cells to β-lap [8] may explain the compound's ability to radiosensitize certain cancer cells that express low basal levels of NQO1, but in which the cell's enzyme levels can be dramatically induced by IR pretreatment. We previously found that posttreatments, and not pretreatments, of β-lap sensitized cells to IR [2, 59–61]. A 5-h posttreatment of 4–5 μM β-lap was required, in which IR-treated cells were killed and non-IR-treated cells were spared (<20% lethality). Since NQO1 levels were induced 5- to 20-fold in 3 to 4 h in the same cell line [59], we speculate that the compound's radiosensitizing capacity was due to the exploitation of this damage-inducible, bioactivating (for β-lap) enzyme. Since NQO1 is commonly elevated during early stages of carcinogenesis [62, 63], normal cells that become genetically unstable following IR exposure and later induce stable expression of NQO1 would be rather sensitive to cell death by β-lap posttreatments. We previously demonstrated that post-IR-exposure to 4–5 μM β-lap could dramatically reduce IR-mediated neoplastic transformants [59]. We speculate, therefore, that this compound not only may be useful against NQO1-overexpressing cancer cells (e.g., breast, lung, and possibly prostate cancers), but also could possess great potential as an anti-carcinogenic agent by eliminating genetically unstable, NQO1-overexpressing transformed cells within a normal cell population.

REFERENCES

1. Planchon, S. M., Wuerzberger, S., Frydman, B., Witiak, D. T., Hutson, P., Church, D. R., Wilding, G., and Boothman, D. A. (1995). Beta-lapachone-mediated apoptosis in human promyelocytic leukemia (HL-60) and human prostate cancer cells: A p53-independent response. *Cancer Res.* **55**, 3706–3711.

2. Boothman, D. A., Trask, D. K., and Pardee, A. B. (1989). Inhibition of potentially lethal DNA damage repair in human tumor cells by beta-lapachone, an activator of topoisomerase I. *Cancer Res.* **49**, 605–612.

3. Wuerzberger, S. M., Pink, J. J., Planchon, S. M., Byers, K. L., Bornmann, W. G., and Boothman, D. A. (1998). Induction of apoptosis in MCF-7-WS8 breast cancer cells by beta-lapachone. *Cancer Res.* **58**, 1876–1885.

4. Li, C. J., Wang, C., and Pardee, A. B. (1995). Induction of apoptosis by beta-lapachone in human prostate cancer cells. *Cancer Res.* **55**, 3712–3715.

5. Li, C. J., Averboukh, L., and Pardee, A. B. (1993). beta-Lapachone, a novel DNA topoisomerase I inhibitor with a mode of action different from camptothecin. *J. Biol. Chem.* **268**, 22463–22468.

6. Frydman, B., Marton, L. J., Sun, J. S., Neder, K., Witiak, D. T., Liu, A. A., Wang, H. M., Mao, Y., Wu, H. Y., Sanders, M. M., and Liu, L. F. (1997). Induction of DNA topoisomerase II-mediated DNA cleavage by beta-lapachone and related naphthoquinones. *Cancer Res.* **57**, 620–627.

7. Manna, S. K., Gad, Y. P., Mukhopadhyay, A., and Aggarwal, B. B. (1999). Suppression of tumor necrosis factor-activated nuclear transcription factor-kappaB, activator protein-1, c-Jun N-terminal kinase, and apoptosis by beta-lapachone. *Biochem. Pharmacol.* **57**, 763–774.

8. Pink, J. J., Planchon, S. M., Tagliarino, C., Varnes, M. E., Siegel, D., and Boothman, D. A. (2000). NAD(P)H:quinone oxidoreductase activity is the principal determinant of beta-lapachone cytotoxicity. *J. Biol. Chem.* **275**, 5416–5424.

9. Joseph, P., Xie, T., Xu, Y., and Jaiswal, A. K. (1994). NAD(P)H: quinone oxidoreductase1 (DT-diaphorase): Expression, regulation, and role in cancer. *Oncol. Res.* **6**, 525–532.

10. Boothman, D. A., Meyers, M., Fukunaga, N., and Lee, S. W. (1993). Isolation of X-ray-inducible transcripts from radioresistant human melanoma cells. *Proc. Natl. Acad. Sci. USA* **90**, 7200–7204.

11. Tampo, Y., and Yonaha, M. (1996). Enzymatic and molecular aspects of the antioxidant effect of menadione in hepatic microsomes. *Arch. Biochem. Biophys.* **334**, 163–174.

12. Joseph, P., and Jaiswal, A. K. (1994). NAD(P)H:quinone oxidoreductase1 (DT diaphorase) specifically prevents the formation of benzo[a]pyrene quinone–DNA adducts generated by cytochrome P4501A1 and P450 reductase. *Proc. Natl. Acad. Sci. USA* **91**, 8413–8417.

13. Ross, D., Siegel, D., Beall, H., Prakash, A. S., Mulcahy, R. T., and Gibson, N. W. (1993). DT-diaphorase in activation and detoxification of quinones: Bioreductive activation of mitomycin C. *Cancer Metastasis Rev.* **12**, 83–101.

14. Tedeschi, G., Chen, S., and Massey, V. (1995). DT-diaphorase: Redox potential, steady-state, and rapid reaction studies. *J. Biol. Chem.* **270**, 1198–1204.

15. Smitskamp-Wilms, E., Hendriks, H. R., and Peters, G. J. (1996). Development, pharmacology, role of DT-diaphorase and prospects of the indoloquinone EO9. *Gen. Pharmacol.* **27**, 421–429.

16. Ross, D., Beall, H., Traver, R. D., Siegel, D., Phillips, R. M., and Gibson, N. W. (1994). Bioactivation of quinones by DT-diaphorase, molecular, biochemical, and chemical studies. *Oncol. Res.* **6**, 493–500.

17. Belinsky, M., and Jaiswal, A. K. (1993). NAD(P)H:quinone oxidoreductase1 (DT-diaphorase) expression in normal and tumor tissues. *Cancer Metastasis Rev.* **12**, 103–117.

18. Marin, A., Lopez de Cerain, A., Hamilton, E., Lewis, A. D., Martinez-Penuela, J. M., Idoate, M. A., and Bello, J. (1997).

DT-diaphorase and cytochrome B5 reductase in human lung and breast tumours. *Br. J. Cancer* **76**, 923–929.

19. Rauth, A. M., Goldberg, Z., and Misra, V. (1997). DT-diaphorase: Possible roles in cancer chemotherapy and carcinogenesis. *Oncol. Res.* **9**, 339–349.

20. Planchon, S. M., Wuerzberger-Davis, S. M., Pink, J. J., Robertson, K. A., Bornmann, W. G., and Boothman, D. A. (1999). Bcl-2 protects against beta-lapachone-mediated caspase 3 activation and apoptosis in human myeloid leukemia (HL-60) cells. *Oncol. Rep.* **6**, 485–492.

21. da Silva, C. P., de Oliveira, C. R., da Conceicao, M., and de Lima, P. (1996). Apoptosis as a mechanism of cell death induced by different chemotherapeutic drugs in human leukemic T-lymphocytes. *Biochem. Pharmacol.* **51**, 1331–1340.

22. Decaudin, D., Geley, S., Hirsch, T., Castedo, M., Marchetti, P., Macho, A., Kofler, R., and Kroemer, G. (1997). Bcl-2 and Bcl-XL antagonize the mitochondrial dysfunction preceding nuclear apoptosis induced by chemotherapeutic agents. *Cancer Res.* **57**, 62–67.

23. Cotter, T. G., Glynn, J. M., Echeverri, F., and Green, D. R. (1992). The induction of apoptosis by chemotherapeutic agents occurs in all phases of the cell cycle. *Anticancer Res.* **12**, 773–779.

24. Casiano, C. A., Martin, S. J., Green, D. R., and Eng, M. T. (1996). Selective cleavage of nuclear autoantigens during Cd95 (Fas/Apo-1)-mediated T cell apoptosis. *J. Exp. Med.* **184**, 765–770.

25. Yuan, J. (1997). Transducing signals of life and death. *Curr. Opin. Cell Biol.* **9**, 247–251.

26. Talanian, R. V., Quinlan, C., Trautz, S., Hackett, M. C., Mankovich, J. A., Banach, D., Ghayur, T., Brady, K. D., and Wong, W. W. (1997). Substrate specificities of caspase family proteases. *J. Biol. Chem.* **272**, 9677–9682.

27. Miller, D. K. (1997). The role of the caspase family of cysteine proteases in apoptosis. *Semin. Immunol.* **9**, 35–49.

28. Porter, A. G., Ng, P., and Janicke, R. U. (1997). Death substrates come alive. *Bioessays* **19**, 501–507.

29. Wolf, B. B., Goldstein, J. C., Stennicke, H. R., Beere, H., Amarante-Mendes, G. P., Salvesen, G. S., and Green, D. R. (1999). Calpain functions in a caspase-independent manner to promote apoptosis-like events during platelet activation. *Blood* **94**, 1683–1692.

30. Wood, D. E., and Newcomb, E. W. (1999). Caspase-dependent activation of calpain during drug-induced apoptosis. *J. Biol. Chem.* **274**, 8309–8315.

31. Squier, M. K., Sehnert, A. J., Sellins, K. S., Malkinson, A. M., Takano, E., and Cohen, J. J. (1999). Calpain and calpastatin regulate neutrophil apoptosis. *J. Cell. Physiol.* **178**, 311–319.

32. Squier, M. K., Miller, A. C., Malkinson, A. M., and Cohen, J. J. (1994). Calpain activation in apoptosis. *J. Cell. Physiol.* **159**, 229–237.

33. Lazebnik, Y. A., Kaufmann, S. H., Desnoyers, S., Poirier, G. G., and Earnshaw, W. C. (1994). Cleavage of poly(ADP-ribose) polymerase by a proteinase with properties like ICE. *Nature* **371**, 346–347.

34. Datta, R., Banach, D., Kojima, H., Talanian, R. V., Alnemri, E. S., Wong, W. W., and Kufe, D. W. (1996). Activation of the Cpp32 protease in apoptosis induced by 1-beta-D-arabino-furanosylcytosine and other DNA-damaging agents. *Blood* **88**, 1936–1943.

35. Pink, J. J., Wuerzberger-Davis, S., Tagliarino, C., Planchon, S. M., Yang, X., Froelich, C. J., and Boothman, D. A. (2000). Activation of a cysteine protease in MCF-7 and T47D breast cancer cells during beta-lapachone-mediated apoptosis. *Exp. Cell Res.* **255**, 144–155.

36. Stone, K. R., Mickey, D. D., Wunderli, H., Mickey, G. H., and Paulson, D. F. (1978). Isolation of a human prostate carcinoma cell line (DU 145). *Int. J. Cancer.* **21**, 274–281.

37. Mickey, D. D., Stone, K. R., Wunderli, H., Mickey, G. H., and Paulson, D. F. (1980). Characterization of a human prostate adenocarcinoma cell line (DU 145) as a monolayer culture and as a solid tumor in athymic mice. *Prog. Clin. Biol. Res.* **37**, 67–84.

38. Horoszewicz, J. S., Leong, S. S., Kawinski, E., Karr, J. P., Rosenthal, H., Chu, T. M., Mirand, E. A., and Murphy, G. P. (1983). LNCaP model of human prostatic carcinoma. *Cancer Res.* **43**, 1809–1818.

39. Gustafson, D. L., Beall, H. D., Bolton, E. M., Ross, D., and Waldren, C. A. (1996). Expression of human NAD(P)H:quinone oxidoreductase (DT-diaphorase) in Chinese hamster ovary cells: Effect on the toxicity of antitumor quinones. *Mol. Pharmacol.* **50**, 728–735.

40. Sambrook, J., Fritsch, E. F., and Maniatis, T. (1989). "Molecular Cloning—A Laboratory Manual," Cold Spring Harbor Laboratory Press, Cold Spring Harbor, NY.

41. Rago, R., Mitchen, J., and Wilding, G. (1990). DNA fluorometric assay in 96-well tissue culture plates using Hoechst 33258 after cell lysis by freezing in distilled water. *Anal. Biochem.* **191**, 31–34.

42. Siegel, D., Franklin, W. A., and Ross, D. (1998). Immunohistochemical detection of NAD(P)H:quinone oxidoreductase in human lung and lung tumors. *Clin. Cancer Res.* **4**, 2065–2070.

43. Fitzsimmons, S. A., Workman, P., Grever, M., Paull, K., Camalier, R., and Lewis, A. D. (1996). Reductase enzyme expression across the National Cancer Institute tumor cell line panel: Correlation with sensitivity to mitomycin C and EO9 [see comments]. *J. Natl. Cancer Inst.* **88**, 259–269.

44. Thor, H., Smith, M. T., Hartzell, P., Bellomo, G., Jewell, S. A., and Orrenius, S. (1982). The metabolism of menadione (2-methyl-1,4-naphthoquinone) by isolated hepatocytes: A study of the implications of oxidative stress in intact cells. *J. Biol. Chem.* **257**, 12419–12425.

45. Hollander, P. M., Bartfai, T., and Gatt, S. (1975). Studies on the reaction mechanism of DT diaphorase: Intermediary plateau and trough regions in the initial velocity vs substrate concentration curves. *Arch. Biochem. Biophys.* **169**, 568–576.

46. Strobel, H. W., and Dignam, J. D. (1978). Purification and properties of NADPH-cytochrome P-450 reductase. *Methods Enzymol.* **52**, 89–96.

47. Preusch, P. C., Siegel, D., Gibson, N. W., and Ross, D. (1991). A note on the inhibition of DT-diaphorase by dicoumarol. *Free Radical Biol. Med.* **11**, 77–80.

48. Lotem, J., and Sachs, L. (1996). Differential suppression by protease inhibitors and cytokines of apoptosis induced by wild-type p53 and cytotoxic agents [published erratum appears in (1997) *Proc. Natl. Acad. Sci. USA* **94**, 1603]. *Proc. Natl. Acad. Sci. USA* **93**, 12507–12512.

49. Rao, L., Perez, D., and White, E. (1996). Lamin proteolysis facilitates nuclear events during apoptosis. *J. Cell Biol.* **135**, 1441–1455.

50. Zhivotovsky, B., Gahm, A., and Orrenius, S. (1997). Two different proteases are involved in the proteolysis of lamin during apoptosis. *Biochem. Biophys. Res. Commun.* **233**, 96–101.

51. Margolin, N., Raybuck, S. A., Wilson, K. P., Chen, W., Fox, T., Gu, Y., and Livingston, D. J. (1997). Substrate and inhibitor specificity of interleukin-1 beta-converting enzyme and related caspases. *J. Biol. Chem.* **272**, 7223–7228.

52. Kaiser, N., and Edelman, I. S. (1977). Calcium dependence of glucocorticoid-induced lymphocytolysis. *Proc. Natl. Acad. Sci. USA* **74**, 638–642.

53. Lam, M., Dubyak, G., and Distelhorst, C. W. (1993). Effect of glucocorticosteroid treatment on intracellular calcium homeostasis in mouse lymphoma cells. *Mol. Endocrinol.* **7**, 686–693.

54. Squier, M. K., and Cohen, J. J. (1997). Calpain, an upstream regulator of thymocyte apoptosis. *J. Immunol.* **158**, 3690–3697.

55. Nath, R., Raser, K. J., Stafford, D., Hajimohammadreza, I., Posner, A., Allen, H., Talanian, R. V., Yuen, P., Gilbertsen, R. B., and Wang, K. K. (1996). Non-erythroid alpha-spectrin breakdown by calpain and interleukin 1 beta-converting-enzyme-like protease(s) in apoptotic cells: Contributory roles of both protease families in neuronal apoptosis. *Biochem. J.* **319**, 683–690.

56. Vanags, D. M., Porn-Ares, M. I., Coppola, S., Burgess, D. H., and Orrenius, S. (1996). Protease involvement in fodrin cleavage and phosphatidylserine exposure in apoptosis. *J. Biol. Chem.* **271**, 31075–31085.

57. Li, Y. Z., Li, C. J., Pinto, A. V., and Pardee, A. B. (1999). Release of mitochondrial cytochrome C in both apoptosis and necrosis induced by beta-lapachone in human carcinoma cells. *Mol. Med.* **5**, 232–239.

58. Nishizaki, K., Yoshino, T., Orita, Y., Nomiya, S., and Masuda, Y. (1999). TUNEL staining of inner ear structures may reflect autolysis, not apoptosis. *Hear. Res.* **130**, 131–136.

59. Boothman, D. A., and Pardee, A. B. (1989). Inhibition of radiation-induced neoplastic transformation by beta-lapachone. *Proc. Natl. Acad. Sci. USA* **86**, 4963–4967.

60. Boothman, D. A., Greer, S., and Pardee, A. B. (1987). Potentiation of halogenated pyrimidine radiosensitizers in human carcinoma cells by beta-lapachone (3,4-dihydro-2,2-dimethyl-^{2}H-naphtho[1,2-b]pyran-5,6-dione), a novel DNA repair inhibitor. *Cancer Res.* **47**, 5361–5366.

61. Boothman, D. A., and Pardee, A. B. (1989). Inhibition of radiation-induced neoplastic transformation by beta-lapachone. *Proc. Natl. Acad. Sci. USA* **86**, 4963–4967.

62. Segura-Aguilar, J., Cortes-Vizcaino, V., Llombart-Bosch, A., Ernster, L., Monsalve, E., and Romero, F. J. (1990). The levels of quinone reductases, superoxide dismutase and glutathione-related enzymatic activities in diethylstilbestrol-induced carcinogenesis in the kidney of male Syrian golden hamsters. *Carcinogenesis* **11**, 1727–1732.

63. Leonard, T. B., Dent, J. G., Graichen, M. E., Lyght, O., and Popp, J. A. (1982). Comparison of hepatic carcinogen initiation-promotion systems. *Carcinogenesis* **3**, 851–856.